



iata



CSIC

CONSEJO SUPERIOR DE INVESTIGACIONES CIENTÍFICAS

INSTITUTO DE AGROQUÍMICA Y
TECNOLOGÍA DE LOS ALIMENTOS (IATA-CSIC)



UNIVERSITAT
POLITÈCNICA
DE VALÈNCIA

UNIVERSITAT POLITÈCNICA DE VALÈNCIA
Programa de Doctorado en Ciencia, Tecnología
y Gestión Alimentaria

**Going from digestion to microstructure of
starch-based food products: understanding
the role of polyphenols**

Tesis presentada por:
Andrea Aleixandre Agustín

Tesis supervisada por:
Cristina Molina Rosell

Valencia, noviembre 2021



MINISTERIO
DE CIENCIA
E INNOVACIÓN



CONSEJO SUPERIOR DE INVESTIGACIONES CIENTÍFICAS
CSIC



iata

Dra. Cristina Molina Rosell, Profesora de Investigación del Consejo Superior de Investigaciones Científicas en el Instituto de Agroquímica y Tecnología de Alimentos

Certifica:

Que la presente Tesis Doctoral, titulada “**Going from digestion to microstructure of starch-based food products: understanding the role of polyphenols**” que presenta Andrea Aleixandre Agustín, ha sido realizada bajo su dirección en el Departamento de Ciencia de Alimentos del Instituto de Agroquímica y Tecnología de los Alimentos (IATA-CSIC); y que habiendo revisado el trabajo, considera que reúne las condiciones necesarias para optar al grado de Doctor en Ciencia, Tecnología y Gestión Alimentaria.

Y para que así conste a los efectos oportunos, se expide el siguiente escrito.

Valencia,

MOLINA
ROSELL MARIA
CRISTINA -
20794643K

Firmado digitalmente
por MOLINA ROSELL
MARIA CRISTINA -
20794643K
Fecha: 2021.10.29
11:37:53 +02'00'

Prof. Cristina Molina Rosell

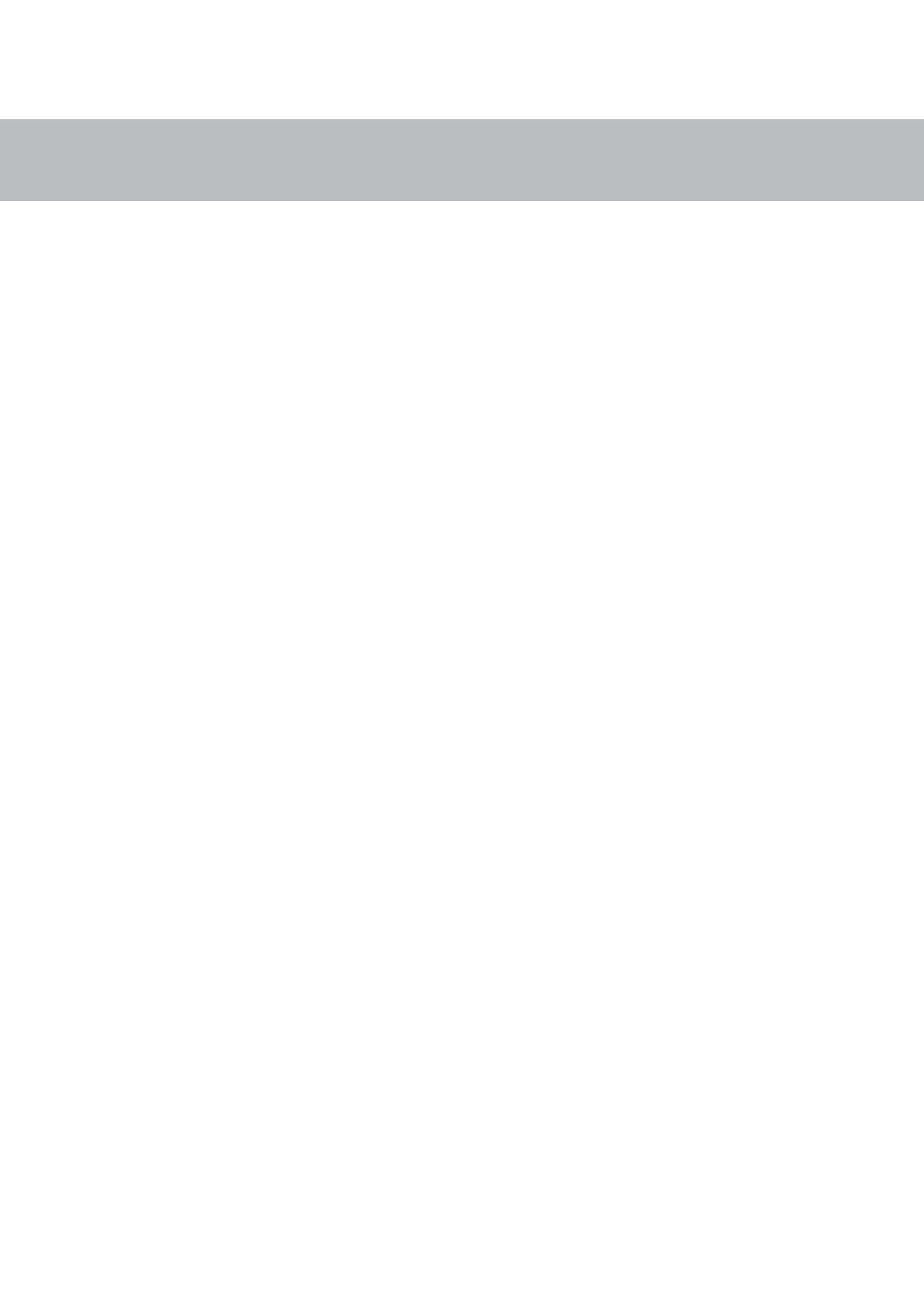
Prof. Cristina Molina Rosell

Este trabajo ha sido financiado por el proyecto RTI2018-095919-B-C2 financiado por MCIN/AEI/10.13039/501100011033, “ERDF A way of making Europe” por la Unión Europea y la Generalitat Valenciana (Proyecto Prometeo 2017/189).

“ You must learn some of my philosophy. Think only of the past as
its remembrance gives you pleasure ”

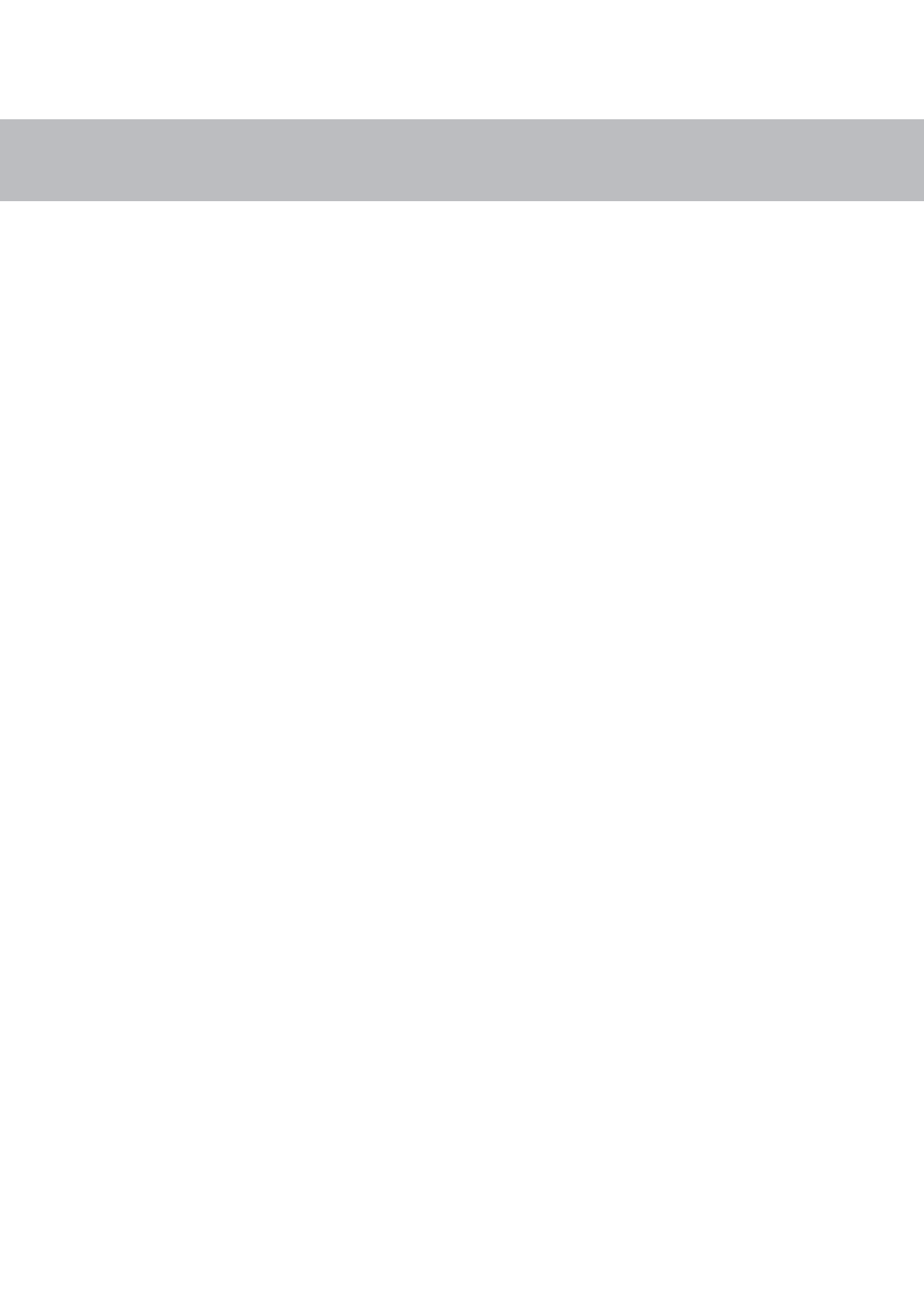
Jane Austen
(Pride and Prejudice, 1813)

A mis padres, mi hermana y Samuel



AGRADECIMIENTOS

- **Gracias** a Cristina por dejarme entrar en su equipo y dedicarme su tiempo para enseñarme y animarme durante estos años. Espero de todo corazón haber estado a la altura de este reto.
- **Gracias** a Yaiza porque como escribí allá por el 2016, me has enseñado, ayudado, aguantado y animado desde entonces. Era todo un presagio de lo que viviríamos juntas después.
- **Gracias** al Lab 109 y en general a toda la gente del IATA que, de una manera u otra (y algunos sin saberlo) me han ayudado a formarme tanto a nivel profesional como personal.
- **Thanks** to Elena and all the people that I met in Skopie: to Elena for help me and to make me feel at home during my stay, a Jana por haber sido tan amable conmigo and to Ivana and Rosana for your kindness.
- **Grazas** a los gallegos por echarme un cable y enseñarme tanto en dos semanas: a Moncho por sus lecciones en el laboratorio y sus visitas turísticas en coche por Santiago y a Mauro por ser un dolor de muelas unas veces y un encanto otras.
- **Gracias** a Samuel: por soportarme en este viaje de altibajos. Tu amor incondicional me ha hecho mucho más llevaderos estos años. Te quiero muchísimo.
- **Gracias** a mi familia: especialmente a mi madre por siempre estar ahí para todo lo que he necesitado y más, a mi padre porque siempre lo llevo conmigo, a mi hermana Clara por estar siempre orgullosa de todo lo que hago, a mi tía Jose por sus ánimos incansables y a mi iaia que, aunque al final no me ha podido ver acabar la tesis, la tengo muy presente.
- **Gracias** a mi lado claro: a Yanni por su apoyo incondicional y su manera de ver la vida, a Claudia por ser una amiga durante estos 3 años y siguiendo, a Yaiza por poner un poco de sensatez al grupo de vez en cuando y a Karina por nuestras infinitas charlas.
- **Gracias** a mis tortus: a Andrea, Belén, Helena, Sheila, Jimena y Noah porque pese a la distancia siempre nos apoyamos en nuestras subidas y bajadas vitales.
- **Gracias** a Eri, Patri y Vera por nuestras charlas dentro y fuera del IATA, y vuestro apoyo y ánimos constantes. Las siguientes sois vosotras, ¡ánimo!
- **Gracias** a Laura, Ana y Hani por aguantarme estos tres años tan ocupados. ¡Japón nos espera!
- **Gracias** a todos mis amigos y conocidos por distraerme durante este periodo con desayuno, comidas, cenas, juegos de mesa, películas, bailes, deportes y un largo etcétera.



ABSTRACT

Due to the increasing importance of diet on health management, it remains of utmost interest to unravel how food is processed in the human digestive system. Food structure can significantly influence food processing, affecting its performance during eating and digestion. Specifically, the digestion of carbohydrate-based foods requires further insight due to their contribution to blood glucose levels. The knowledge of starch digestion kinetics will contribute to designing tailored foods for managing postprandial glucose levels.

The objective of this doctoral thesis was to acquire a better understanding of the impact of microstructure on starch digestion and how digestive enzymes might be modulated by the use of phenolic compounds. With that purpose, the role of bread structure on *in vivo* mastication, and *in vitro* digestion was evaluated. Subsequently, starch gels from different sources were produced and digested in an *in vitro* oro-gastro-intestinal digestion system to analyze the impact of gel microstructure. After the microstructure studies on bread and starch gels, different phenolic acids or seaweed polyphenolic extracts were explored as inhibitors of starch digestive enzymes, and the involvement of starch gel microstructure on the enzymatic digestion was assessed.

Mastication of toasted wheat breads was affected by their different structures, despite no differences in the sensory perception was observed. Bolus texture was also altered by bread structure and texture. The breadmaking process offered the possibility to modify the bread structure. In fact, varying dough shaping led to bread with different crumb structures and texture properties. After stressing the importance of selecting the *in vitro* oral processing method used to simulate mastication, the further digestion of bread with different crumb structures confirmed that they were differently disaggregated yielding variations on posterior starch digestibility. Once stating the importance of crumb microstructure on starch digestion, the focus was shifted to connect starch gels microstructure with its *in vitro* digestion. Gels obtained with a different type of starch, from cereals, pulses, or tubers, showed different digestibility, which was related to their microstructure but also their amylose content. Considering the action of digestive enzymes (α -amylase and α -glucosidase) on starch hydrolysis, different phenolic compounds were studied to understand the interactions between phenolics and either enzymes or substrates. The most effective way to inhibit enzymes was to incubate them with phenolic acids. A higher concentration of the inhibitor was needed when phenolic compounds interacted previously with the substrate, due to their retention within the starch gel. The chemical structure of phenolic acids controlled the enzyme inhibition. Similarly, complex phenolic extracts, like those extracted from *A. nodosum* seaweed could be used to inhibit digestive enzymes, showing greater inhibition effect when they

were previously incubated with the enzyme, owing to the existence of carbohydrate-polyphenol complexes and their different inhibitory capabilities. In addition, phenolic acids affected pasting properties and therefore gel microstructure and gel texture of starches. However, those changes in gel microstructure and texture were not enough to control starch enzymatic hydrolysis, which was related to the specific chemical structure of the phenolic acids and their properties. Overall, crumb or gel microstructure can limit digestive enzymes accessibility, which would reduce starch hydrolysis. Moreover, the inclusion of phenolic acids on starch-based foods might be the alternative to reduce the extent of starch digestion by inhibiting digestive enzymes.

Debido a la creciente importancia de la dieta en el manejo de la salud, sigue habiendo un gran interés en desentrañar como se procesan los alimentos en el sistema digestivo humano. La estructura de los alimentos puede influir significativamente en su procesamiento, afectando al rendimiento durante la alimentación y la digestión. Específicamente, la digestión de alimentos a base de carbohidratos requiere una mayor comprensión debido a su contribución a los niveles de glucosa en sangre. El conocimiento de la cinética de digestión del almidón contribuirá a diseñar alimentos a medida para controlar los niveles de glucosa posprandial.

El objetivo de esta tesis doctoral fue adquirir una mejor comprensión del impacto de la microestructura en la digestión del almidón y cómo las enzimas digestivas podrían ser moduladas por compuestos fenólicos. Con ese propósito, se evaluó el papel de la estructura del pan en la masticación *in vivo* y la digestión *in vitro*. Posteriormente, se produjeron geles de almidón de diferentes fuentes y se digirieron en un sistema de digestión oro-gastro-intestinal *in vitro* para analizar el impacto de la microestructura del gel. Después de los estudios de microestructura en geles de almidón y pan, se exploraron diferentes ácidos fenólicos o extractos polifenólicos de algas como inhibidores de enzimas digestivas de almidón, y se evaluó la participación de la microestructura del gel de almidón en la digestión enzimática.

La masticación y la textura del bolo de panes tostados de trigo se vio afectada por su diferente estructura, a pesar de que no se observaron diferencias en la percepción sensorial. El proceso de panificación también ofreció la posibilidad de modificar la estructura del pan. De hecho, la variación de la forma de la masa dio lugar a panes con diferentes propiedades estructurales y texturales de la miga. La digestión de los panes con diferente estructura de miga confirmó que se disgregaban de manera diferente, produciendo variaciones en la posterior digestibilidad del almidón. Una vez que se estableció la importancia de la microestructura de la miga en la digestión del almidón, se cambió el enfoque para enlazar la microestructura de los geles de almidón con su digestión *in vitro*. Los geles obtenidos con almidones de distintas fuentes botánicas mostraron diferente digestibilidad, lo que se relacionó con su microestructura, pero también con su contenido de amilosa. Considerando la acción de las enzimas digestivas (α -amilasa y α -glucosidasa) sobre la hidrólisis del almidón, se estudiaron diferentes compuestos fenólicos para comprender las interacciones entre los compuestos fenólicos y las enzimas o sustratos. La forma más eficaz de inhibir las enzimas era incubarlas con ácidos fenólicos. Se necesitó una mayor concentración del inhibidor cuando los compuestos fenólicos interactuaban previamente con el sustrato, debido a su retención dentro del gel de almidón. La estructura química de los ácidos fenólicos controlaba

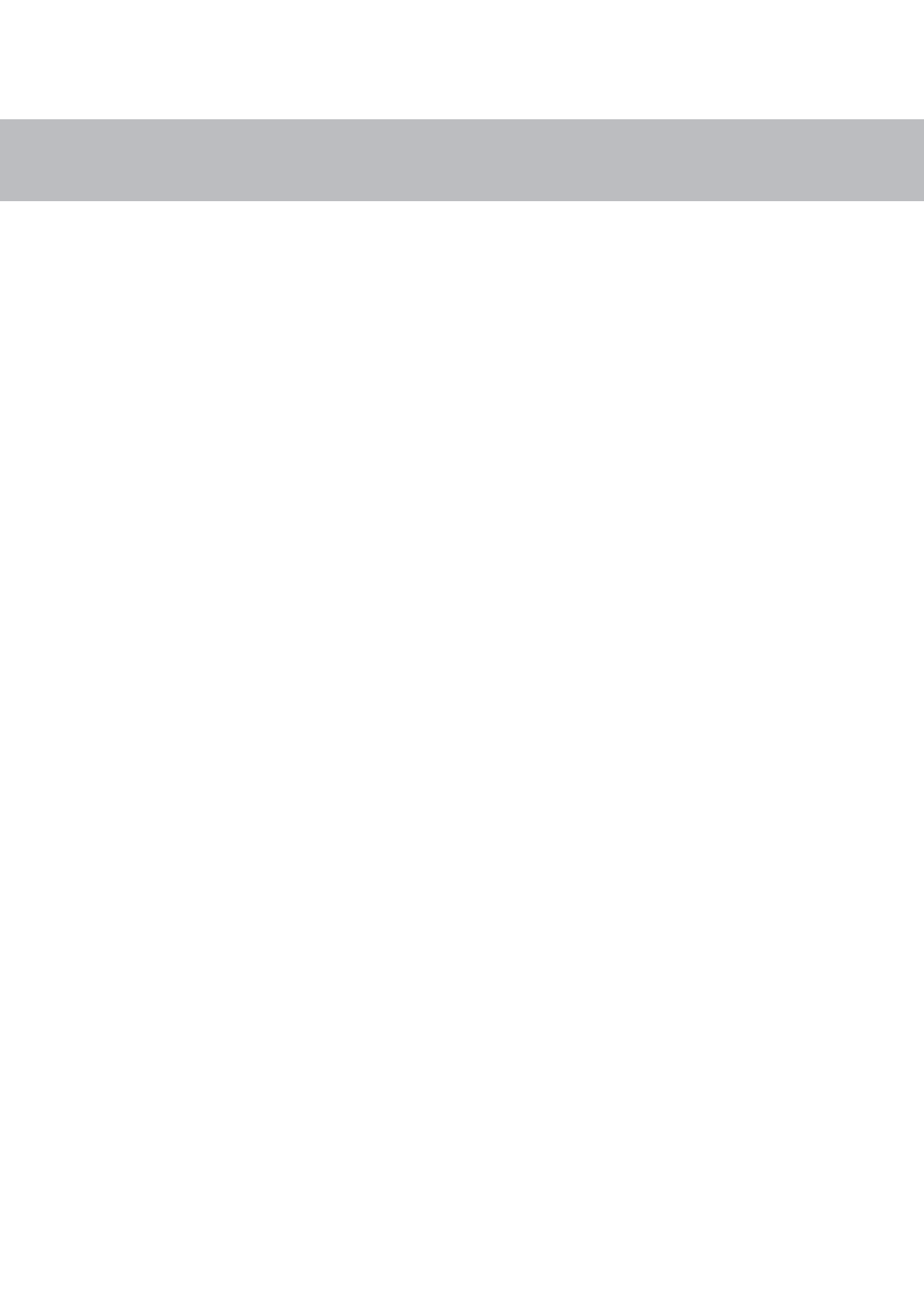
la inhibición de la enzima. Asimismo, los extractos fenólicos complejos, como los extraídos de las algas *A. nodosum*, podrían utilizarse para inhibir las enzimas digestivas, mostrando mayor efecto inhibitorio cuando fueron previamente incubados con la enzima, debido a la existencia de complejos carbohidrato-polifenoles con sus diferentes capacidades inhibitorias. Además, los ácidos fenólicos afectaron las propiedades de pegado y, por lo tanto, a la estructura y textura de geles de almidón. Sin embargo, esos cambios no fueron suficientes para controlar la hidrólisis enzimática del almidón, que estaba relacionada con la estructura química de los ácidos fenólicos y sus propiedades. En general, la microestructura de la miga o del gel puede limitar la accesibilidad de las enzimas digestivas, lo que reduciría la hidrólisis del almidón. Además, la inclusión de ácidos fenólicos en alimentos a base de almidón podría ser la alternativa para reducir el grado de digestión del almidón al inhibir estas enzimas.

A causa de la creixent importància de la dieta en el maneig de la salut, segueix sent de gran interès desentranyar com es processen els aliments en el sistema digestiu humà. L'estructura dels aliments pot influir significativament en el processament dels aliments, afectant al seu rendiment durant l'alimentació i la digestió. Específicament, la digestió d'aliments a base de carbohidrats requereix una major comprensió a conseqüència de la seua contribució als nivells de glucosa en sang. El coneixement de la cinètica de la digestió del midó contribuirà a dissenyar aliments a mesura per controlar els nivells de glucosa postprandial.

L'objectiu d'aquesta tesi doctoral va ser adquirir una millor comprensió de l'impacte de la microestructura en la digestió del midó i com els enzims digestius podrien ser modulats per l'ús de compostos fenòlics. Amb aquest propòsit, es va avaluar el paper de l'estructura del pa en la masticació *in vivo* i la digestió *in vitro*. Posteriorment, es van produir gels de midó de diferents fonts i es van digerir en un sistema de digestió oro-gastrointestinal *in vitro* per analitzar l'impacte de la microestructura del gel. Després dels estudis de microestructura en gels de midó i pa, es van explorar diferents àcids fenòlics o extractes polifenòlics d'algues com inhibidors dels enzims digestius del midó, i es va avaluar la participació de la microestructura del gel de midó en la digestió enzimàtica.

La masticació i la textura de la bitla de pans torrats de blat es va veure afectada per les seues diferències estructurals, tot i que no es van observar diferències en la percepció sensorial. El procés de panificació va oferir la possibilitat de modificar l'estructura del pa. De fet, la variació de la forma de la massa va donar lloc a pans amb diferents propietats d'estructura i textura de la molla. La digestió dels pans amb diferent estructura de molla va confirmar que es disgregaven de manera diferent, produint variacions en la posterior digestibilitat del midó. Una vegada que es va establir la importància de la microestructura de la molla en la digestió del midó, es va canviar l'enfocament per a enllaçar la microestructura dels gels de midó amb la seua digestió *in vitro*. Els gels obtinguts amb midó de diferents fonts botàniques van mostrar diferent digestibilitat, el que es va relacionar amb la seua microestructura, però també amb el seu contingut d'amilosa. Considerant l'acció dels enzims digestius (α -amilasa i α -glucosidasa) sobre la hidròlisi del midó, es van estudiar diferents compostos fenòlics per a comprendre les interaccions entre els fenòlics i els enzims o substrats. La forma més eficaç d'inhibir els enzims era incubar-los amb àcids fenòlics. Es va necessitar una major concentració de l'inhibidor quan els compostos fenòlics interactuaven prèviament amb el substrat, a causa de la seua retenció dins del gel de midó. L'estructura química dels àcids fenòlics controlava la inhibició de l'enzim. Així mateix, els extractes fenòlics complexos, com

els extrems de l'alga *A. nodosum*, podrien utilitzar-se per a inhibir els enzims digestius, mostrant major efecte inhibidor quan van ser prèviament incubats amb l'enzim, a causa de l'existència de complexos carbohidrat-polifenols amb les seues diferents capacitats inhibidores. A més, els àcids fenòlics van afectar les propietats de pegat i, per tant, la estructura i textura dels gels de midó. No obstant, estos canvis en la estructura i textura dels gels no van ser suficients per a controlar la hidròlisi enzimàtica del midó, que estava relacionada amb l'estructura química dels àcids fenòlics i les seues propietats. En general, la microestructura de la molla de pa o gel de midó pot limitar l'accessibilitat dels enzims digestius, la qual cosa reduiria la hidròlisi del midó. A més, la inclusió d'àcids fenòlics en aliments a base de midó podria ser l'alternativa per a reduir el grau de digestió del midó en inhibir aquests enzims.



CONTENTS

I	Introduction	1
	1. Food microstructure and digestion	1
	2. Carbohydrate digestion	2
	2.1. Carbohydrates and diabetes	2
	2.2. <i>In vivo</i> and <i>in vitro</i> digestion studies	4
	2.3. Starch	4
	2.3.1. Structure	4
	2.3.2. Starch digestion	6
	3. Strategies to modulate starch digestion	8
	3.1. Effect of starch characteristics on its digestion	8
3.2. Inhibition of starch digestive enzymes	9	
3.2.1. Dietary fibers	9	
3.2.2. Acidic ingredients	10	
3.2.3. Polyphenols	10	
4. Starch and polyphenol interaction	17	
II	Objectives	27
III	Results	31
CHAPTER 1	Mastication of crisp bread: role of bread texture and structure on texture perception	33
	1.1. Introduction	34
	1.2. Materials and methods	35
	1.2.1. Bread samples and characterization	35
	1.2.2. FOP assessment	36
1.2.3. Characterization of bolus properties	37	

CHAPTER 

1.2.4. Sensory assessment	37
1.2.5. Statistical data analyses	38
1.3. Results and discussion	38
1.3.1. Bread characteristics	38
1.3.2. Sensory evaluation	40
1.3.3. Characterization of FOP and bolus properties	41
1.3.4. Texture, FOP and sensory correlations	43
1.4. Conclusions	44
Effect of bread structure and <i>in vitro</i> oral processing methods in bolus disintegration and glyceimic index	49

2.1. Introduction	50
2.2. Materials and methods	51
2.2.1. Materials	51
2.2.2. Bread preparation	51
2.2.3. Bread characterization	52
2.2.4. <i>In vitro</i> oro-gastro-intestinal digestion	52
2.2.5. Reducing sugars released and <i>in vitro</i> starch digestibility	53
2.2.6. Particle size distribution of the bolus during <i>in vitro</i> digestion	53
2.2.7. Statistical analyses	54
2.3. Results and discussion	54
2.3.1. Variation of bread structure as a consequence of changes in the breadmaking process	54
2.3.2. Bolus particle size throughout <i>in vitro</i> digestion	56
2.3.3. <i>In vitro</i> digestion and expected glyceimic index	59
2.3.4. Multivariable analysis	60
2.4. Conclusions	62

CHAPTER 

<i>In vitro</i> digestibility of gels from different starches: relationship between kinetic parameters and microstructure	67
3.1. Introduction	68
3.2. Materials and methods	69

3.2.1. Materials	69
3.2.2. Chickpea starch isolation	69
3.2.3. Starch gel preparation	69
3.2.4. Chemical composition of starches	70
3.2.5. <i>In vitro</i> oro-gastro-intestinal digestion and reducing sugar analysis	70
3.2.6. Starch digestion modelling	71
3.2.7. Scanning electron microscopy (SEM)	71
3.2.8. Statistical analyses	72
3.3. Results and discussion	72
3.3.1. Starch gels	72
3.3.2. <i>In vitro</i> digestion and modelling	76
3.4. Conclusions	82

CHAPTER

4

Understanding phenolic acids inhibition of α -amylase and α -glucosidase and influence of reaction conditions 89

4.1. Introduction	90
4.2. Materials and methods	91
4.2.1. Materials	91
4.2.2. Inhibition assays of α -amylase	92
4.2.3. Inhibition assays of α -glucosidase	93
4.2.4. Percentage of inhibition and IC_{50}	93
4.2.5. High-performance liquid chromatography analysis	94
4.2.6. Statistical analyses	94
4.2.7. Structure-activity relation	94
4.3. Results and discussion	94
4.3.1. Inhibition of α -amylase	96
4.3.2. Polyphenols inhibition of α -glucosidase	99
4.4. Conclusions	103

CHAPTER

5

***In vitro* inhibition of starch digestive enzymes by ultrasound-assisted extracted polyphenols from *Asco-phyllum nodosum* seaweeds** 109

5.1. Introduction	110
5.2. Material and methods	111

5.2.1. Materials	111
5.2.2. Seaweed sampling	111
5.2.3. Chemical analysis	112
5.2.4. Inhibition assays of α -amylase and α -glucosidase	112
5.2.5. Chromatographic separation	115
5.2.6. $^1\text{H-NMR}$	115
5.2.7. Statistical analyses	116
5.3. Results and discussion	116
5.3.1. Seaweed extracts chemical composition	116
5.3.2. Inhibition effect of seaweed extracts against α -amylase and α -glucosidase enzymes	117
5.3.3. Seaweed freeze-dried extracts characterization: chromatography (RP-HPLC-UV) and nuclear magnetic resonance ($^1\text{H-NMR}$)	120
5.4. Conclusions	124

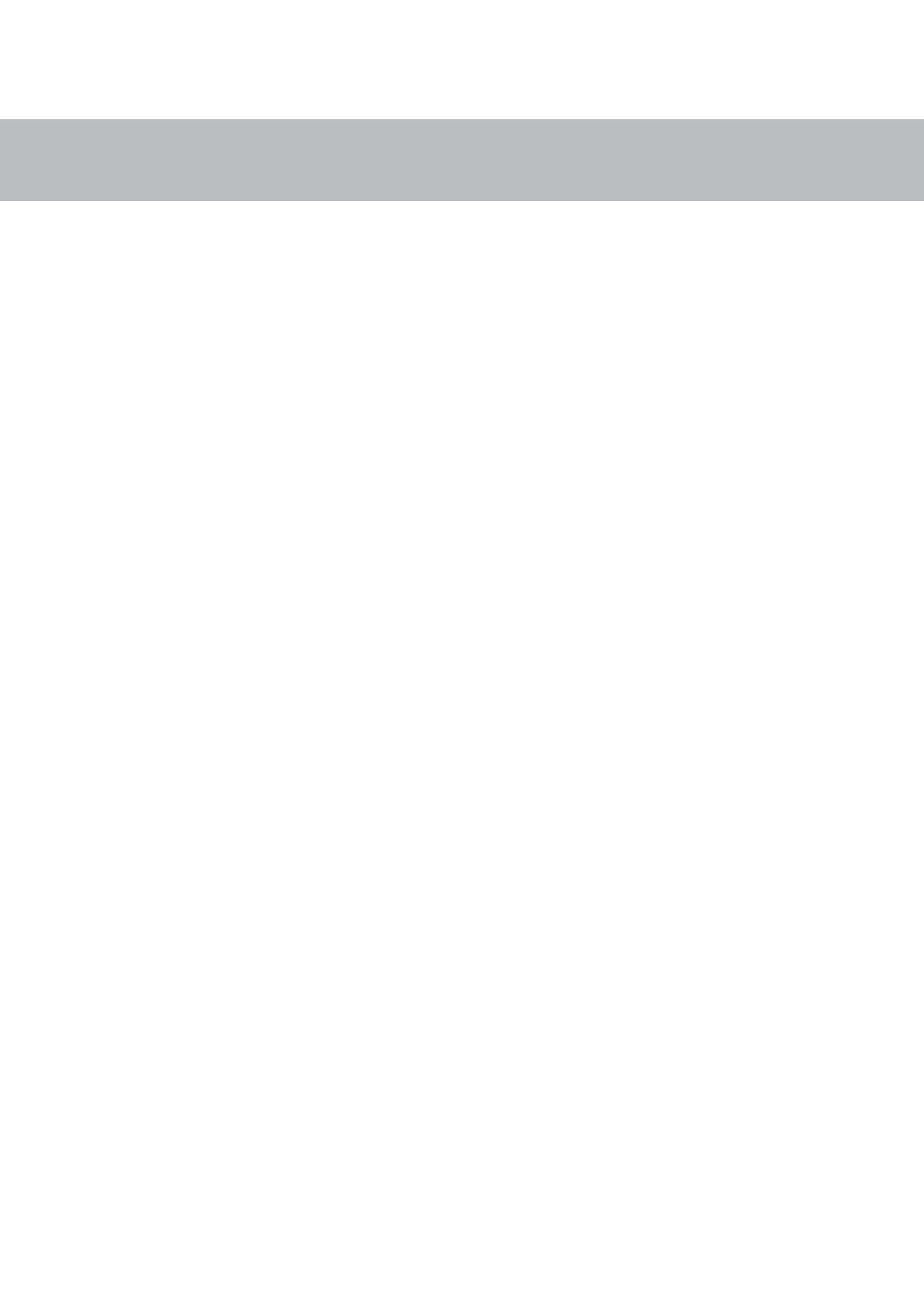
CHAPTER

6

Starch gels enriched with phenolic acids: effects on structure and digestibility	131
6.1. Introduction	132
6.2. Material and methods	133
6.2.1. Materials	133
6.2.2. Starch gels preparation and pasting properties of the slurries	133
6.2.3. High-performance liquid chromatography analysis of phenolic acids	134
6.2.4. Scanning electron microscopy	134
6.2.5. Gel firmness	135
6.2.6. Hydrolysis kinetics	135
6.2.7. Statistical analysis	136
6.3. Results and discussion	136
6.3.1. Starch-polyphenol gels formation	136
6.3.2. Textural and structural characterization of starch gels	140
6.3.3. Digestibility of starch-polyphenol gels	144
6.4. Conclusions	149

IV	General discussion	155
-----------	---------------------------	-----

V	Conclusions	165
----------	--------------------	-----



LIST OF FIGURES

I Introduction

Figure 1. Schematic representation of starch gel formation	5
Figure 2. Scanning electron images of native corn starch granules (left) and gels (right) before (top) and after (bottom) <i>in vitro</i> digestion. Magnifications 300x (left) and 1,500x (right)	6
Figure 3. Schematic representation of enzymes involved in <i>in vivo</i> starch digestion and enzymes used in <i>in vitro</i> starch digestion	7
Figure 4. Basic structure of flavonoids and phenolic acids	11

II Objectives

Figure 1. Overview of the different chapters of the results section	29
--	----

III Results

Chapter 1. Mastication of crisp bread: role of bread texture and structure on texture perception

Figure 1.1. Images of toasted sliced breads. A: WHB: wheat bread; B: WWB: whole wheat bread; C: NSU: non-sugar added wheat bread; D: NSA: non-salt added wheat bread	40
Figure 1.2. Sensory evaluation of texture of toasted sliced bread samples (MEAN \pm SE)	41
Figure 1.3. Correlation loadings plot and scores plot from a principal component analysis (PCA) of the combination of bread moisture, bread texture and structure, mastication, bolus properties, and sensory evaluation	43

Chapter 2. Effect of bread structure and *in vitro* oral processing methods in bolus disintegration and glycemic index

Figure 2.1. Crumb image of wheat breads shaped to conform to the requirements of the loaf bread and bread roll	55
---	----

Figure 2.2. Representative images of bolus particles obtained after oral (a), gastric (b) and intestinal (c) <i>in vitro</i> digestion. Boluses were obtained from loaf bread (1,2) or bread rolls (3,4) using Ultra Turrax (1,3) or Ultra Turrax with crystal balls (2,4) as simulated oral processing methods	57
Figure 2.3. Bolus particle size obtained after the oral (a), gastric (b) and intestinal (c) phase of <i>in vitro</i> digestion. Sample names describe bread type (L-loaf, B-roll bread) followed by letters describing the simulated oral processing method applied (P Ultra Turrax and B Ultra Turrax with crystal balls). Letters on the bars indicate significant differences ($P < 0.05$)	58
Figure 2.4. Effect of bread structure and simulated oral processing method on starch hydrolysis pattern. Sample names describe the shaping method used (L rolling mill process and B balling process) followed by letters describing the simulated oral processing method applied (P Ultra Turrax and B Ultra Turrax with crystal balls)	60
Figure 2.5. Score and loading biplot Dimension 1 \times Dimension 2 of samples and variables obtained by principal component analysis (PCA). Samples are labelled as in the text	61

Chapter 3. *In vitro* digestibility of gels from different starches: relationship between kinetic parameters and microstructure

Figure 3.1. SEM micrographs of starch gels from wheat (A), corn (B), rice (C), potato (D), cassava (E), green pea (F), chickpea (G). Magnification x300	73
Figure 3.2. Boxplots showing the parameters calculated by image analysis of the gel micrographs. A) Wall thickness and B) hole size distribution	75
Figure 3.3. Starch hydrolysis from starch gels during the oro-gastrointestinal <i>in vitro</i> digestion. Vertical lines divided the graph into digestion phases: oral, gastric, and intestinal. Starch gels were grouped according to their source proximity. Scale bar of 100% indicates the value of the graduation marks	77
Figure 3.4. Starch digestibility plots during intestinal <i>in vitro</i> digestion for wheat (A), corn (B), rice (C), potato (D), cassava (E), green pea (F), chickpea (G) gels	78

Figure 3.5. SEM micrographs of digested starch gels after oral (1), gastric (2) and intestinal (3) *in vitro* digestion. Gels were obtained from wheat (A), corn (B), rice (C), potato (D), cassava (E), green pea (F), chickpea (G). Magnification x300

81

Chapter 4. Understanding phenolic acids inhibition of α -amylase and α -glucosidase and influence of reaction conditions

Figure 4.1. Molecular structure of tested phenolic acids 92

Figure 4.2. Inhibitory effect of pure polyphenols against α -amylase. Discontinuous line, M1_{AM} =preincubation PP + enzyme; solid line, M2_{AM} =preincubation PP + substrate; dotted line M3_{AM} =gelatinization PP + starch 95

Figure 4.3. Inhibitory effect of pure polyphenols against α -glucosidase. Discontinuous line, M1_{AG} =preincubation PP + enzyme; solid line, M2_{AG} =preincubation PP + substrate 100

Chapter 5. *In vitro* inhibition of starch digestive enzymes by ultrasound-assisted extracted polyphenols from *Ascophyllum nodosum* seaweeds

Figure 5.1. Methodology scheme of inhibitory assays (M1, M2 and M3) of α -amylase (AM) and α -glucosidase (AG) digestive enzymes against aqueous polyphenols extracts (E70, E80, E90 and P90) from *A. nodosum* seaweed 114

Figure 5.2. Inhibitory capacity of Acarbose, purified and crude seaweed extracts against α -amylase (A= M1_{AM}, B= M2_{AM} and C= M3_{AM}) 118

Figure 5.3. Inhibitory capacity of purified and crude seaweed extracts against α -glucosidase (A= M1_{AG} and B= M2_{AG}) 120

Figure 5.4. RP-HPLC-UV profiles of purified (P90, 50 μ L of 2.5 mgFD/mL) and crude (E90, E80, E70, injected 50 μ L of 5.0 mgFD/mL) aqueous extracts obtained by UAE from *A. nodosum* seaweed 122

Figure 5.5. ¹H-NMR spectra of freeze-dried extracts purified (P90) and crude (E90, E80 and E70) obtained by UAE from *A. nodosum* seaweed 123

Chapter 6. Starch gels enriched with phenolic acids: effects on structure and digestibility

Figure 6.1. Apparent viscosity profiles corn starch gels made with phenolic acids (A), and gels made with phenolic acids adjusting the pH (CpH) (B) obtained with a rapid viscosity analyzer (RVA). Thick solid line indicates temperature settings during the heating-cooling cycle	137
Figure 6.2. SEM micrographs of starch corn gels made with phenolic acid, and gels made with phenolic acids not adjusting and adjusting pH. Magnification $\times 300$	141
Figure 6.3. Boxplots showing the firmness and microstructure parameters calculated by image analysis of the gel micrographs. Different letters on the boxes indicate significant differences ($P < 0.05$)	142
Figure 6.4. Hydrolysis plots of corn starch gels made with phenolic acids (A), and gels made with phenolic acids adjusting the pH (CpH) (B)	145
Figure 6.5. Score and loading biplot of samples and variables obtained by principal component analysis (PCA)	148

LIST OF TABLES

I Introduction

Table 1. Experimental conditions used to evaluate the inhibitory effect of polyphenols against α -amylase	12
Table 2. Experimental conditions used to evaluate the inhibitory effect of polyphenols against α -glucosidase	15

III Results

Chapter 1. Mastication of crisp bread: role of bread texture and structure on texture perception

Table 1.1. Ingredients and nutrition facts (g/100 g) of toasted sliced breads according to producer's labels	36
Table 1.2. Bread characteristics and their performance during FOP (FOP) and the resulting bolus properties of different types of toasted breads (WHB: wheat bread; WWB: whole wheat bread; NSU: non-sugar added wheat bread; NSA: non-salt added wheat bread)	39

Chapter 2. Effect of bread structure and *in vitro* oral processing methods in bolus disintegration and glycemic index

Table 2.1. Moisture, morphological and texture parameters of the wheat bread crumbs	55
Table 2.2. Kinetic constant (k), equilibrium concentration (C_{∞}), area under the hydrolysis curve after 180 min (AUC), hydrolysis index (HI) and estimated glycemic index (eGI) for loaf bread (L) and bread rolls (B) subjected to two different simulating oral processing methods, with Ultra Turrax (P) or crystal balls (B)	59

Chapter 3. *In vitro* digestibility of gels from different starches: relationship between kinetic parameters and microstructure

Table 3.1. Chemical composition of starches from different sources (% DW)	74
Table 3.2. Microstructure characteristics of starch gels from different sources	75

Table 3.3. Statistical parameters for goodness assessment of non-linear fitting with a first-order kinetics-based model (Eq. (1))	77
Chapter 4. Understanding phenolic acids inhibition of α-amylase and α-glucosidase and influence of reaction conditions	
Table 4.1. Effect of different analysis methodologies (M1, M2, M3) on the IC ₅₀ values of pure phenolic acids (PP) against α -amylase	97
Table 4.2. IC ₅₀ values of pure phenolic acids against α -glucosidase of the different analyzed methodologies	102
Chapter 5. <i>In vitro</i> inhibition of starch digestive enzymes by ultrasound-assisted extracted polyphenols from <i>Ascophyllum nodosum</i> seaweeds	
Table 5.1. Chemical composition of freeze-dried (E90, E80 and E70) and purified (P90) extracts obtained by UAE from <i>Ascophyllum nodosum</i> brown edible seaweed	116
Table 5.2. IC ₅₀ values of seaweed extracts against α -amylase and α -glucosidase of the different analyzed methodologies: M1 = preincubation PP+enzyme, M2 = preincubation PP+gelatinized starch, M3 = gelatinized (PP+starch)	117
Chapter 6. Starch gels enriched with phenolic acids: effects on structure and digestibility	
Table 6.1. Pasting properties of starch suspensions containing phenolic acids	138
Table 6.2. <i>In vitro</i> starch hydrolysis and kinetic parameters of gels containing phenolic acids	146

LIST OF ABBREVIATIONS

AG	α -glucosidase
AM	α -amylase
AMG	Amyloglucosidase
ANOVA	One-way analysis of variance
AOAC	International association of analytical communities
AUC	Area under the curve
BNPG7	p-Nitrophenyl maltoheptaoside
C_{∞}	Equilibrium concentration
CHOS	Carbohydrate content
DAD	Photodiode array detector
DNS	3,5-dinitrosalicylic acid
DPPH	2,2-diphenyl-1-picrylhydrazyl
DW	Dry weight
eGI	Expected glycemic index
FOP	Food oral processing
FRAP	Iron cation reduction capacity
GI	Glycemic index
GOD/POD	Glucose oxidase-peroxidase
HbA _{1c}	Glycosylated hemoglobin
HI	Hydrolysis index
¹ H-NMR	Proton nuclear magnetic resonance spectroscopy
HPLC	High-performance liquid chromatography
IC ₅₀	Half-maximum inhibitory concentration
ICC	International association for cereal chemistry
ISO	International organization for standardization
IVSD	In vitro starch digestibility
<i>k</i>	Kinetic constant
LOS	Logarithm of slope plots
LSD	Least significant difference
MGAM	Maltase-glucoamylase
N	Newtons
NSA	Non-added salt bread
NSU	Non-added sugar bread

PCA	Principal Component Analysis
pNPG	4-Nitrophenyl- β -D- glucopyranoside
PP	Polyphenol
PSA	Polar surface area
PVPP	Poly(vinylpolypyrrolidone)
<i>r</i>	Correlation coefficient
RDS	Rapidly digestible starch
RMS	Relative molar sensitivity
RMSE	Root mean square error
RS	Resistant starch
RT	Room temperature
RVA	Rapid visco analyser
SDS	Slowly digestible starch
SEM	Scanning electron microscopy
SGF	Simulated gastric fluid
SSF	Simulated salivary fluid
SI	Sucrose-isomaltase
SIF	Simulated intestinal fluid
TPA	Texture profile analysis
TPC	Total polyphenol content
UA	Uronic acid content
UAE	Ultrasound-assisted extraction
WHB	White bread
WHO	World health organization
WOS	Web of science
WWB	Whole wheat bread



Introduction

1. Food microstructure and digestion

In view of the importance of diet-related health problems around the world, there is a continuing need for more detailed knowledge of food characteristics and how food is processed within the human digestive system. Therefore, a more holistic approach should be considered integrating the relationships between initial food processing, food structure, food composition and food breakdown kinetics (Bornhorst & Singh, 2014), which would be very helpful in the future food design applying reverse engineering.

In the last years, an important topic within the previously mentioned context is food microstructure, a prerequisite to determine how the ingredient compositions and processing conditions are mechanistically related to the product properties (Boland et al., 2014). Food microstructure can be defined as “the spatial arrangements of elements in a food and their interactions” (Golding, 2019). Many foods have defined structure, and it ranges from the complex structures present in plant and animal tissues to the structures of processed foods (Morris & Groves, 2013). Nowadays food structure can be analyzed at almost any dimensional level, even in real time and with minimal intrusion. Three-dimensional imaging techniques (confocal laser scanning microscopy, nuclear magnetic resonance, and so on) have been developed to visualize food microstructure, but two-dimensional imaging techniques such as light or electron microscopy have been mostly used (Devahastin, 2017). In addition, image processing allows quantitative analysis of 2D and 3D images, defining food microstructure in a more objective way. Food structure and the nature of their interactions within a food system can significantly influence their digestion, since it affects the food performance during eating and digestion (Golding, 2019).

Food digestion implies several processes along the oro-gastrointestinal tract, that can be ascribed to four stages in terms of human anatomy, corresponding to mouth (oral processing), stomach (gastric processing), small intestine (intestinal processing) and large intestine or colon (fermentation) (Boland, 2016). Oral processing is the first step, involving physical disruption of food structure that includes cutting, grinding, brought to approximately body temperature, mixing with saliva and tasting (Boland, 2016). Nevertheless, mastication process is much more than the texture and flavour perception, it also influences nutrient bioavailability. Food disruption during chewing is rather variable, depending on food properties and on individuals (Hoebler et al., 2000). In fact, Engelen et al. (2005) analyzed the mastication behavior of different

food structures such as carrot, peanut, cheese, or bread in a group of 266 subjects. Results showed that hard and dry products like carrots and peanuts require more chewing cycles, saliva and higher maximum bite force until swallowing. In addition, oral physiology parameters (saliva flow rate, food fragmentation and bite force) explained less than 10% of the variance in the swallowing threshold.

Food processing continues in the stomach and intestine, which are also affected by structure and composition. Gastric digestion is a complex procedure involving physical and chemical food breakdown (Bornhorst & Singh, 2014), while intestinal digestion is characterized by the enzymatic digestion and absorption of nutrients. All those stages are affected by the physical state of the food. Kong and Singh (2009) studied the disintegration of solid foods like carrots in a model stomach system, demonstrating that the physicochemical structure and properties of cell walls influence digestion breakdown. Mulet-Cabero et al. (2017) affirmed that the gastric behavior was affected by the initial structure of different dairy food structures using a semi-dynamic model. In fact, semi-solid foods (cheese and yogurt mix) showed greater protein and lipid digestion in the early stage of the intestinal phase than liquid sample (oil in water emulsion).

2. Carbohydrate digestion

Dietary carbohydrates are a varied group of molecules that ranged from simple sugars to highly complex polysaccharides, such as starch or dietary fiber (Chambers et al., 2019). Carbohydrates are an essential part of the human diet. World's health agencies recommend a total carbohydrate intake approaching or exceeding half the percentage of total energy intake, being the main energy source in most societies (Buyken et al., 2018). Because of that, there is also a growing interest in evaluating the digestion of carbohydrate-based foods and the factors affecting the kinetics. Hoebler et al. (1998) analyzed wheat bread and pasta, showing the great impact of food structure on mastication process and starch hydrolysis of food bolus. Specifically, particle size after mastication of bread was smaller, than those of the pasta, and bread underwent greater digestion. Conversely, the structural properties of brittle cereal foods affected *in vivo* oral breakdown but not oral digestibility (Alam et al., 2017). Extruded puffs and flakes showed different structures; the porous and softness of puffs require less mastication, and smaller particles are achieved, but they showed similar hydrolysis rate than flakes (Alam et al., 2017).

2.1. Carbohydrates and diabetes

Most carbohydrates are mechanically and enzymatically digested along the human digestive system into glucose and fructose units for absorption, causing a gradual release of glucose to the bloodstream that changes the postprandial glycemia. Glucose provides energy for cell functions, but for that, insulin pancreatic hormone must promote

the absorption of glucose from the blood system into body cells. People with type 1 or type 2 diabetes are, by definition, unable to control their postprandial blood glucose levels in the absence of medical care (Zafar et al., 2019). Diabetes mellitus patients cannot secrete insulin (mostly type 1 diabetes), their insulin action is defective (mostly type 2 diabetes) or both, resulting in hyperglycemia (Punthakee et al., 2018). The chronic hyperglycemia of diabetes is associated with long-term damage, dysfunction, and failure of different organs (American Diabetes Association, 2014), and according to World Health Organization (WHO, 2021) data, in 2019, 1.5 million deaths were directly caused by diabetes. Type 2 diabetes is considered as a lifestyle related disease, and a healthier diet and lifestyle could prevent and improve symptoms of diabetes (Hu et al., 2001).

In 1981, Jenkins et al. defined the glycemic index (GI) of foods as the effect of food carbohydrates on postprandial blood glucose concentrations compared with glucose or white bread. Despite the controversy of GI term in modern nutritional science, low glycemic index diets show a positive effect on glucose control and therefore are recommended for patients with diabetes. Zafar et al. (2019) carried out a systematic review and meta-analysis of low-GI diets as intervention for diabetes patients. 54 randomized controlled trials were evaluated with impaired glucose tolerance, type 1 or type 2 diabetes, proving the effectiveness of low-GI diets on glycemic control and blood lipids content, particularly for type 2 diabetes patients. Nevertheless, due to the lack of studies in type 1 diabetes patients, it was impossible to reach conclusions for this group of people. Conversely, Gilbertson et al. (2001) examine, over 12 months, the effect of a measured carbohydrate exchange diet versus a flexible low-GI diet on glycemic parameters of 104 children with diabetes. Their results suggested that flexible diets, with emphasis on low-GI foods, showed benefits, improving glycosylated hemoglobin (HbA1c) without increasing the risk of hypoglycemia.

On the other hand, the ingestion of foods with higher glycemic index may also be beneficial for hypoglycemic episodes (Jenkins et al., 1981). Hypoglycemia is common in diabetes, and data indicate that 30-40% of people with type 1 diabetes and 24-26% of people with type 2 diabetes experience one to three episodes of severe hypoglycemia each year (International Hypoglycaemia Study Group, 2015). As mentioned previously, some researchers have criticized the use of the GI due to its variability or to disregard the presence of other macronutrients (Pi-Sunyer, 2002; Raheli et al., 2011). But, despite controversies, management of postprandial glucose levels with the diet can be an important strategy to improve people's health. The main approach to modulate the blood glucose absorption rate of high-GI foods is to control carbohydrate's digestion, particularly starch.

2.2. *In vivo* and *in vitro* digestion studies

Considering the impact of food features and composition on human health, there is a growing interest in evaluating the impact of foods on digestion. In fact, a closer examination of research related to digestion using Web of Science (WOS) as search engine, including articles, reviews, or books, from 1990 onwards, reveals higher number of studies on intestinal digestion (21,480) than gastric (11,555) or oral (9,227) digestion. Anyway, the high number of manuscripts published on digestion emphasizes the importance of this line of research, that is carried out by *in vivo* or *in vitro* models.

In vivo digestibility studies are mainly focussed on GI, but many intrinsic and extrinsic factors affect starch nature and therefore the GI (Dona et al., 2010). *In vivo* models (human and animal) are complex to undertake, and expensive due to the countless factors that involve the digestive process. For these reasons, *in vitro* digestion models provide a useful alternative to animal and human models by rapidly screening food ingredients (Jin Hur, 2011). *In vitro* models have several advantages over *in vivo* studies, comprising their low cost, time and labor, and the absence of ethical approval constraints. However, differences are observed between *in vivo* and *in vitro* models. Bohn et al. (2018) reviewed a range of *in vitro* and *in vivo* digestion models investigating the digestion of macronutrients, and bioaccessibility and bioavailability studies of micronutrients and phytochemicals. Their conclusions indicated that *in vitro* models are better predictors of *in vivo* behavior in the case of macronutrient digestion. *In vitro* digestion studies are characterized by the use of human, animal or fungal enzymes in a static, semi-dynamic or dynamic model. Even though semi-dynamic and dynamic *in vitro* digestion methods provide more physiologically relevant data, static models are mostly used (Mulet-Cabero et al., 2020). Nevertheless, significant variations in the use of *in vitro* digestion methods are described in literature, impeding the possibility of results comparison. For this reason, the COST action INFOGEST standardized a static (Minekus et al., 2014), and semi-dynamic (Mulet-Cabero et al., 2020) *in vitro* digestion methods by international consensus. The INFOGEST group proposed this *in vitro* digestion methodology including the oral, gastric, and small intestinal phases, enabling the production of more comparable data.

2.3. Starch

2.3.1. Structure

Starch is a polymeric carbohydrate present in cereals, tubers, and pulses (Olkku & Rha, 1978), and is the basis for many types of foods. Chemically, starch is formed by two polymers of glucose, named amylose and amylopectin, in varying proportions. Starch granules at macrostructural scale show alternate semi crystalline and amorphous growth rings with gradual transition among them (Wang et al., 2015). Heating

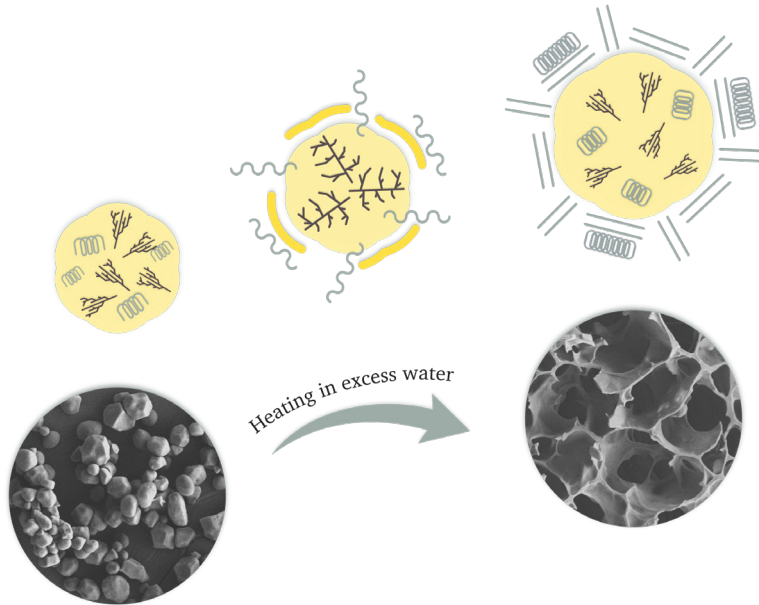


Figure 1. Schematic representation of starch gel formation.

native starches in the presence of excess of water leads to gels, and they are very common in the human diet as a result of cooking or food processing. Starch gelatinization is characterized by starch granules swelling, allowing amylose and amylopectin to leach out into the aqueous phase (Boland et al., 2014). When cooling, disaggregated amylose chains reassociate to form more ordered structures followed by amylopectin, called retrogradation or recrystallization. Starch granules are transformed from ordered semicrystalline granules to an amorphous state, and when retrogradation occurs, the gel is formed (Figure 1).

The chemical composition, structure and properties of starches determined the microstructure of the resulting gels. Starch gels showed a dense structure similar to a sponge due to the loss of the granular structure with spherical or oval cavities surrounded by a gel matrix (Benavent-Gil et al., 2019). Native starches are assembled into relatively ordered granular structures, showing a relatively slow digestion. On the other hand, the open molecular conformation of starch gels makes them accessible to enzymes, increasing their rate of digestion (Pellegrini et al., 2020) (Figure 2).

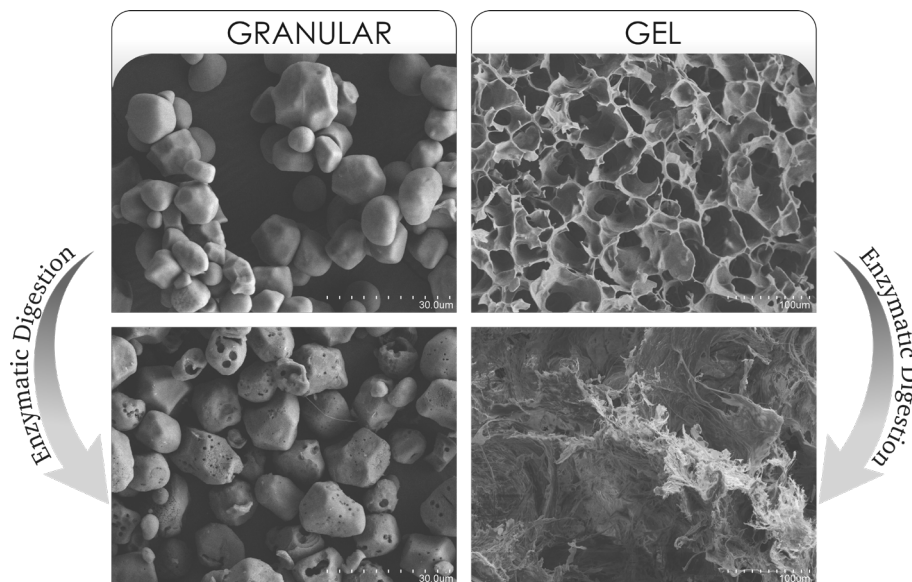


Figure 2. Scanning electron images of native corn starch granules (left) and gels (right) before (top) and after (bottom) *in vitro* digestion. Magnifications 300x (left) and 1,500x (right).

2.3.2. Starch digestion

Starch is mainly digested along the oro-gastrointestinal system by enzymatic action, increasing blood sugar levels after the ingestion of a starch-containing meal (Butterworth et al., 2011). Apart from the mechanical digestion through chewing and gastric churning, starches are digested enzymatically to glucose by the action of two enzymes: α -amylase and α -glucosidase (Figure 3). In humans, two α -amylase enzyme isoforms have been reported, salivary and pancreatic. They hydrolyze α -1,4 internal linkages of starch into oligosaccharides including maltose, maltotriose and limit dextrans with an average size of eight glucose units (Martinez-Gonzalez et al., 2017). Salivary α -amylase provides partial digestion, breaking down starch into shorter oligomers. Upon reaching the gut, starch is extensively digested by pancreatic α -amylase and excreted into the lumen (Brayer et al., 1995). Also, two α -glucosidase isoforms are located at the small intestine: maltase-glucoamylase (MGAM) and sucrose-isomaltase (SI). α -glucosidase hydrolyzes terminal non-reducing α -D-1,4 linkages releasing glucose and oligosaccharides (Martinez-Gonzalez et al., 2017). After α -amylase hydrolysis, the resultant mixture of oligosaccharides passes through the mucous layer to the brush border membrane, and α -glucosidase degrades the oligosaccharides to glucose (Brayer et al., 1995).

The study of the rate and extent of starch digestion catalyzed by enzymes can help

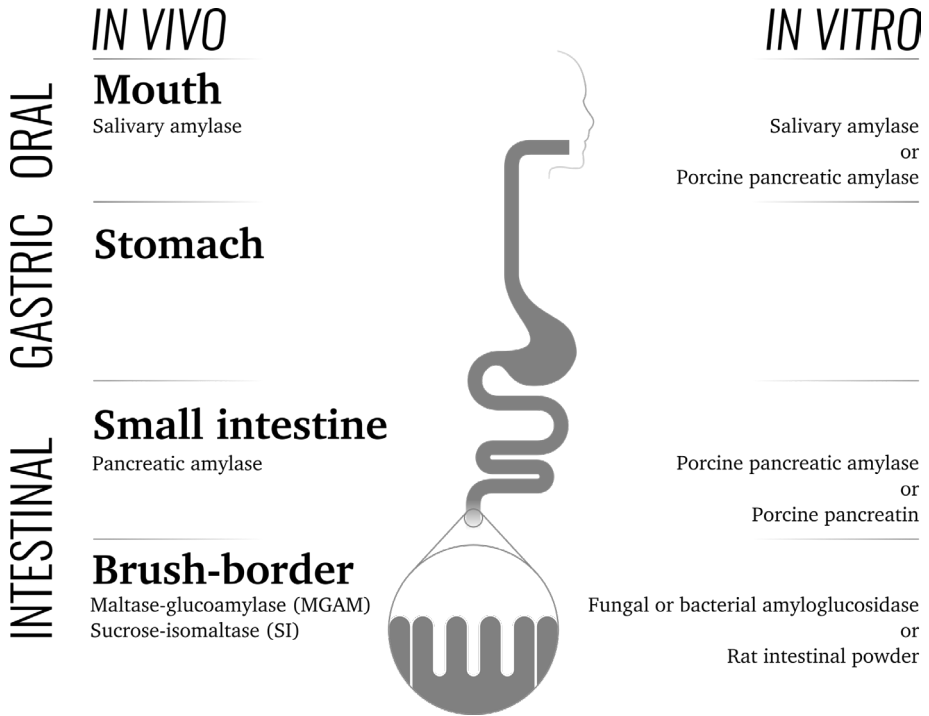


Figure 3. Schematic representation of enzymes involved in *in vivo* starch digestion and enzymes used in *in vitro* starch digestion.

to identify substances or processes that can control the rates of glucose release in the small intestine (Dhital et al., 2017). *In vitro* studies are the best alternative to explore compounds functionality, as well as mechanisms and factors involved in starch hydrolysis. Those methods have been also used for estimating the GI and making a rapid nutritional categorization of starchy foods (Martinez, 2021). Despite the extensive use of *in vitro* methods, there are many discrepancies in the reported methodologies. For instance, regarding the enzymes (Figure 3), some studies use human salivary amylase to simulate *in vitro* starch digestion, but the most frequently used enzyme is porcine pancreatic amylase. Despite the structural differences between human and porcine enzymes substrate and cleavage pattern specificities, porcine pancreatic α -amylase is the most closely related enzyme (Brayer et al., 1995). As regards to α -glucosidase, commercial rat intestinal powder containing MGAM, and SI is used as brush border enzyme. However, fungal or bacterial amyloglucosidase are extensively used, although results cannot be comparable to those with human enzymes (Martinez, 2021).

Several *in vitro* tests have been proposed to measure the starch digestion rate. Granfeldt et al. (1992) proposed a method to measure the rate of starch digestion with the hydrolysis index (HI). HI was calculated as the quotient between the area under

the hydrolysis curve for a food and the area under the curve for white bread. This test assumes that starch is completely digested and absorbed, but the extent of starch digestion is variable. For this reason, Englyst et al. (1992) established an *in vitro* test to classify starch into three types based on its intestinal digestion rate: rapidly digestible starch (RDS), slowly digestible starch (SDS) and resistant starch (RS). RDS was referred to the percentage of total starch hydrolyzed within 30 min of incubation, SDS was the percentage of total starch hydrolyzed within 20 and 100 min, and RS was the starch remaining unhydrolyzed after 120 min of incubation. However, starch digestion mechanism can be better understood by kinetic analysis. Goñi et al. (1997) developed an *in vitro* kinetic procedure to measure the rate of starch digestion in starchy common foodstuffs, being widely used over the years (Goni et al., 2002; Li et al., 2020; Matos & Rosell, 2011). This method fitted starch hydrolysis curves using a mathematical first-order equation and the equilibrium concentration (C_{∞}), kinetic constant (k) and hydrolysis index (HI) were calculated, allowing the estimation of the GI. On the other hand, different methods like logarithm of slope plots (LOS) have been used (Butterworth et al., 2012), in which the logarithm of the LOS of a digestibility curve is plotted against time.

Understanding starch digestibility and its relationship with starch properties is essential for developing starchy foods with desirable glycemic index values. Suitable modeling methods for each sample are necessary, allowing to reduce starch hydrolysis rate into a few parameters that can be correlated with other parameters.

3. Strategies to modulate starch digestion

As described previously, there is great interest in decreasing blood glucose levels after starchy-food ingestion, and the main approach is to reduce starch hydrolysis. According to Dhital et al. (2017), the reduction of starch hydrolysis may be approached from two different points of view: starch features that avoid enzyme action and barriers that prevent the starch-enzyme binding.

3.1. Effect of starch characteristics on its digestion

Concerning starch characteristics, its composition, molecular architecture, surface organization, polymorphic form, granular size, or gelatinization can affect the rate and extent of starch digestibility (Dhital et al., 2017; Dona et al., 2010). Bajaj et al. (2018) analyzed the digestibility of starch granules from different sources (cereals, tubers, and pulses), showing that starches with lower amylose content and smaller granules size had greater enzymatic susceptibility. Concerning starch surface organization, also interferes with starch hydrolysis rate. Benavent-Gil and Rosell (2017) analyzed the *in vitro* digestibility of porous starches obtained with different enzymatic treatment, showing a significant positive correlation of the pore size and total pore area with

the estimated glycemic index. Pore sizes facilitate enzyme accessibility, and therefore starch digestion could be modulated obtaining different pores in the starch surface.

3.2. Inhibition of starch digestive enzymes

The study of α -amylase and α -glucosidase inhibition has ongoing interest in food science. There are oral anti-diabetic drugs used for diabetes treatment that are inhibitors of starch digestive enzymes, like acarbose, voglibose and miglitol. They have high affinity for brush border enzymes, preventing the hydrolysis of disaccharide and oligosaccharide substrates into monosaccharides prior to absorption (Krentz & Bailey, 2005). These anti-diabetic drugs help blood glucose control in diabetes patients, however, their consumption is related with some gastrointestinal disorders (Aoki et al., 2010).

For that reason, the addition of natural ingredients with the capacity to inhibit α -amylase and α -glucosidase enzymes has been further investigated.

3.2.1. Dietary fibers

It is possible to reduce the rate of starch digestion and alter the glucose absorption of foods using soluble and insoluble dietary fibers, and hydrocolloids. Dietary fiber is defined as the plant food part that is resistant to digestion by human digestive enzymes, including polysaccharides, oligosaccharides and resistant starches (Anderson et al., 2009). Food hydrocolloids are carbohydrates capable of creating viscous solutions or gels and they could be considered a component of fiber (Phillips & Williams, 2000). Due to the ability to form gels and alter the viscosity of products, the inhibition of starch digestive enzymes by these compounds has been associated with the modulation of viscosity of the digesta and binding interactions. Nevertheless, the impact on those polysaccharides on starch digestion depends on both the type of fiber and starch. Gularte and Rosell (2011) studied the effect of different hydrocolloids on corn and potato starch digestibility. All tested hydrocolloids increased the *in vitro* digestion of starches except for the blend guar gum and potato starch. Authors attributed the slower rate of potato starch digestion to the high capacity of guar gum to increase the viscosity of the matrix, forming a physical barrier that prevent the enzyme access. Conversely, Sasaki and Kohyama (2011) demonstrated a decrease of *in vitro* rice starch gel digestibility by agar, xanthan gum and Konjac glucomannan. Those divergences might be related to the viscosity of the resulting gels. In fact, Santamaria et al. (2021) recently reported the inhibition of starch hydrolysis in high viscosity gels comprising only starch. Their results demonstrated the real impact of viscosity on starch digestion, where the α -amylase diffusion into the starch gel microstructure could be hampered.

On the other hand, these compounds can also bind starch digestive enzymes, and

therefore inhibit their activity. Nsor-Atindana et al. (2020) demonstrated that starch digestive enzymes might be bound to nanocrystalline cellulose, resulting in inhibition of *in vitro* starch digestion.

The addition of RS as a food ingredient helps to reduce the GI, especially if it is replaced by readily absorbed carbohydrates (Fuentes-Zaragoza et al., 2010). Several *in vivo* and *in vitro* studies had incorporated RS into starchy-foods formulations. Aribas et al. (2020) incorporated chemically modified RS in pasta at 15, 20 and 25% on semolina basis. In addition to the improvement of texture and sensory properties of samples, a decrease in the *in vitro* glycemic index value was observed. On the other hand, Brites et al. (2011) incorporated corn RS granules into wheat and corn bread formulations at 20% of flour basis and analyzed their effects on the postprandial blood glucose response of rats. Their conclusions suggested that the reducing effect on glycemic response by RS was observed in wheat bread, but not in corn bread. Although there are still some discrepancies, and the presence of RS is not probably the only cause for GI differences, it is an important part on glucose metabolism (Sharma et al., 2008).

3.2.2. Acidic ingredients

Acidic ingredients like lemon juice or vinegar induce a reduction of the glycemic response to starch-rich meals. Although the mechanisms are not fully understood, acidic media could inactivate the salivary enzyme in the oral and gastric stage, delaying starch digestion till pancreatic α -amylase action in the intestinal phase (Freitas & Le Feunteun, 2018; Santos et al., 2019). Lemon juice has a remarkable effect on oro-gastric *in vitro* digestion of starch from wheat bread and pasta because of an early acidic-induced inhibition of human salivary α -amylase (Freitas & Le Feunteun, 2018). Furthermore, Santos et al. (2019) discuss the effect of vinegar intake on glycemic index; they hypothesized that vinegar may improve blood sugar levels because of the inhibition of α -amylase action, an improvement in glucose uptake and transcription factors. On the other hand, Rosenblum et al. (1988) demonstrated that at low pH, glucose polysaccharides and purified oligosaccharides can be bound to the active site of human salivary amylases, protecting the enzyme and retarding its inactivation. Therefore, even though acidic medium could be a good inactivation strategy, different circumstances should be taken into consideration.

3.2.3. Polyphenols

Despite all the different compounds used to reduce starch hydrolysis, polyphenols have been largely studied as antioxidants, but also other biological properties such as their hypoglycemic effect (Aryaeian et al., 2017). Polyphenols are plant secondary metabolites with antioxidant properties, present in plant-based foods and an essential part of human diet (Martinez-Gonzalez et al., 2017). These compounds have different

sizes and structures, showing different affinities for enzymes or substrates (Giuberti et al., 2020). Phenolic compounds may be classified into different groups as a function of their structure and the most common polyphenol groups in the diet are flavonoids and phenolic acids (Sun et al., 2019) (Figure 4).

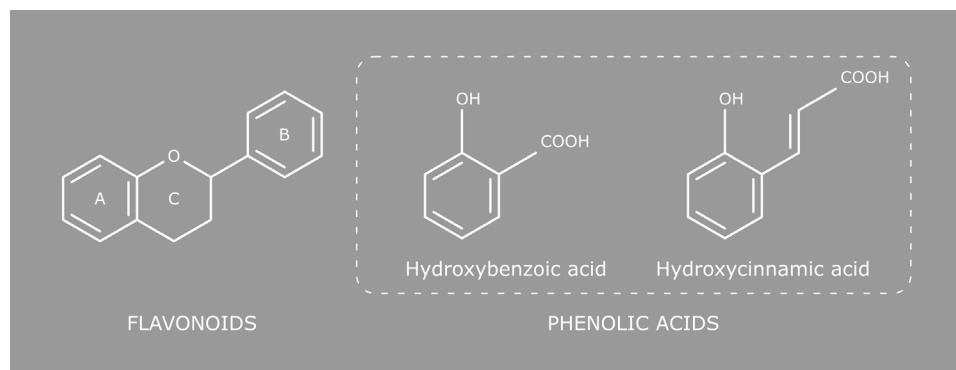


Figure 4. Basic structure of flavonoids and phenolic acids.

Flavonoids are the major polyphenols present in a wide variety of plant sources. Their primary structure consists of two fractions: benzopyran (A and C rings) and phenyl (B ring) groups. According to their chemical structure, flavonoids are classified into anthocyanins, flavan-3-ols, flavanones, flavones, flavonols and isoflavones (Tadera et al., 2006). Phenolic acids are aromatic phenols of secondary plant metabolites with a carboxylic acid functional group. They have one aromatic ring and at least one carboxylic acid moiety in their structure (Kumar et al., 2008). The inhibition of starch digestive enzymes by polyphenols is related with their binding affinity to the enzyme and it is highly related with its molecular structure.

Polyphenols are present in plant foods like fruits, vegetables, tea, coffee, or even seaweeds. Numerous studies have assessed the α -amylase and α -glucosidase inhibition effect of polyphenols from these sources (Williamson, 2013). Nevertheless, the information found in the literature about the inhibitory activity of polyphenols against starch digestive enzymes is disperse and variable. Several methodologies have been used to evaluate the inhibition activity of phenolic compounds, which brings difficulties for comparing among published studies. To simplify the picture of published studies, an analysis of experimental conditions used to analyze the *in vitro* inhibition of pure polyphenols against α -amylase and α -glucosidases is displayed (Table 1 and 2). These different experimental conditions used, such as the source and the concentration of the substrate and the enzyme, the time of incubation, temperature, or pH, make very difficult the comparison and to reach conclusions. Therefore, the reaction conditions should be considered and standardized to better relate results and establish general remarks (Giuberti et al., 2020).

Table 1. Experimental conditions used to evaluate the inhibitory effect of polyphenols against α -amylase.

Polyphenol	Substrate	Substrate concentration	α -amylase source	α -amylase concentration	Time of enzymatic reaction	pH	Temperature (°C)	IC ₅₀	Reference	
Flavonoids										
Flavones	Apigenin	BNPG7	n.d.	Porcine pancreas	0.03 mg/mL	10	6.9	37	>0.5 mM	(Tadera et al., 2006)
	Luteolin								0.36 mM	
	Apigenin	Starch	1 mg/mL	Porcine pancreas	0.1 U/mL	10	7	37	146.8±7.1 μ M	(Zhang et al., 2017)
Luteolin									>400 μ M	
Luteolin	Gelatinized potato starch	n.d.	Human saliva	0.18 μ M	10	6	RT	18.4±3.9 μ M	(Lo Piparo et al., 2008)	
Flavonols	Quercetin	Potato starch	2.5 mg/mL	Porcine pancreas	1 U/mL	3	6.9	25	0.9 μ M	(De Souza et al., 2010)
	Rutin								1.2 μ M	
	Quercetin	Starch	3.33 mg/mL	Porcine pancreas	0.16 mg/mL	10	6.9	25	0.061±0.003 μ M	(Ganiyu Oboh et al., 2015)
Rutin									0.043±0.005 μ M	
Flavones	Hesperidin	Gelatinized potato starch	5 mg/mL	Human pancreas	5 U/mL	20	6	37	6 μ M	(Sahnoun et al., 2017)
	Naringin								8 μ M	
	Poncirin								1 μ M	

Continued on the next page.

Flavan-3-ols	(-)-3-O-galloyl-epicatechin	Gelatinized starch azure	n.d.	10	6.9	37	739 μ M	(Bhandari et al., 2008)
	(-)-3-O-galloyl-catechin						401 μ M	
	(-)-epicatechin-3-gallate	Gelatinized rice starch	0.16 mg/mL	12	n.d.	37	1.5 mM	(Koh et al., 2010)
	(-)-epigallocatechin-3-gallate						1.4 mM	
Theaflavin							67 μ M	
(+)-catechin	Gelatinized corn starch	0.1 mg/mL	0.04 U/mL	n.d.	n.d.	37	9.321 mg/mL	(Sun et al., 2016)
Theaflavin							0.412 mg/mL	
Isoflavones	Daidzein	Starch	1 mg/mL	0.1 U/mL	10	7	>400 μ M	(Zhang et al., 2017)
	Genistein						>400 μ M	
	Cyanidin-3-glucoside	Starch	1 mg/mL	3 U/mL	10	6.9	0.30 mM	(Akkarachivasi et al., 2010)
Anthocyanins	Cyanidin-3.5 diglucoside						>1 mM	
	Cyanidin-3-glucoside	Gelatinized corn starch	n.d.	0.2 mg/mL	15	6.9	0.024 \pm 0.003 mM	(Sui et al., 2016)
	Cyanidin-3.5 glucoside						0.040 \pm 0.007 mM	

Continued on the next page.

Phenolic acids

Caffeic acid	Starch	0.25 mg/mL	Porcine pancreas	5 mg/mL	10	6.9	25	3.68±0.07 μg/mL	(Ganiyu Oboh et al., 2015)
Caffeic acid	Starch	2.5 mg/mL	Porcine pancreas	7.5 U/mL	3	n.d.	25	6.66±0.49 mM	(Tan et al., 2017)
Ferulic acid								31.46±1.29 mM	
Protocatechuic acid								11.45±0.45 mM	
Ferulic acid	Gelatinized potato starch	0.18 mg/mL	Porcine pancreas	n.d.	20	6.9	37	0.622 mg/mL	(Zheng et al., 2020)
Gallic acid	Starch	n.d.	Porcine pancreas	n.d.	3	n.d.	n.d.	57 mM	(Cirillo et al., 2010)
Gallic acid	Starch	5 mg/mL	Porcine pancreas	0.25 mg/mL	10	6,9	25	1.22 μM	(Adefegha et al., 2015)
Protocatechuic acid								1.76 μM	

Table 2. Experimental conditions used to evaluate the inhibitory effect of polyphenols against α -glucosidase.

Polyphenol	Substrate	Substrate concentration	α -amylase source	α -amylase concentration	Time of enzymatic reaction	pH	Temperature (°C)	IC ₅₀	References
Flavonoids									
Flavones									
Apigenin	pNPG	n.d.	<i>Saccharomyces cerevisiae</i>	n.d.	5	6.8	37	82±6 μ M	(Proenca et al., 2017)
Apigenin Luteolin	pNPG	0.625 mM	<i>Saccharomyces cerevisiae</i>	0.05 U/mL	15	6.8	37	21.85 μ M 17 μ M	(H. Li et al., 2009)
Luteolin	pNPG	0.5 mM	<i>Saccharomyces cerevisiae</i>	1000 mM	n.d.	7	37	172±5 μ M	(Yan et al., 2014)
	pNPG	2 mM	<i>Saccharomyces cerevisiae</i>	0.15 U/mL	10	6.8	37	47±1.5 μ M	(Venditti et al., 2015)
Flavonols									
Quercetin	pNPG	1.25 mM	<i>Saccharomyces cerevisiae</i>	5·10 ⁻³ mg/mL	5	6.8	30	7 μ M	(Tadera et al., 2006)
	Maltose	n.d.	Rat intestinal acetone powder	6.6 mg/mL	30	6	37	n.d.	
Quercetin	pNPG	4.16 mM	<i>Saccharomyces cerevisiae</i>	n.d.	5	7	37	0.1 μ M	(De Souza et al., 2010)
Quercetin	pNPG	3.8 mM	n.d.	0.15 U/mL	5	6.9	25	0.038 ± 0.002 μ M	(Ganiyu Oboh et al., 2015)
Flavanones	Naringin	pNPG	n.d.	0.04 U/mL	30	6.9	37	0.55±0.3 μ M	(Sahnoun et al., 2017)

Continued on the next page.

Flavan-3-ols	(+)-catechin	pNPG	4.16 mM	Saccharomyces cerevisiae	n.d.	5	7	37	3.1 μ M	(De Souza et al., 2010)
	(-)-epicatechin-3-gallate	pNPG	2 mM	Mammalian	0.55 mg/mL	15	n.d.	37	1.5 mM	(Koh et al., 2010)
	(-)-epigallocatechin-3-gallate								1.4 mM	
	Theaflavin								67 μ M	
	Theaflavins	pNPG	n.d.	Saccharomyces cerevisiae	n.d.	15	6.8	37	54 μ M	(Jeon et al., 2013)
Isoflavones	Genistein	pNPG	n.d.	Saccharomyces cerevisiae	n.d.	30	6.7	37	50 μ M	(Lee & Lee, 2001)
Anthocyanins	Cyanidin-3-glucoside	Maltose	26 mM	Rat intestinal acetone powder	Maltase: 2.26 U/mL Sucrase: 0.33 U/mL	30	6.9	37	>3 mM	(Akkrachiyasit et al., 2010)
		Sucrose	38 mM						1.42 \pm 0.25 mM	
Phenolic acids										
	Caffeic acid	pNPG	2 mM	Saccharomyces cerevisiae	0.1 U/mL	10	6.8	37	223.3 μ M	(Tan et al., 2017)
	Ferulic acid								460.76 μ M	
	Protocatechuic acid								411.17 μ M	
	Ferulic acid	pNPG	0.18 mM	n.d.	0.18 mg/mL	20	6.9	37	4459 μ M	(Zheng et al., 2020)
	Galllic acid	pNPG	1.25 mM	Saccharomyces cerevisiae	0.5 U/mL	5	6.9	25	0.038 \pm 0.002 μ M	(Obloh et al., 2016)
	Galllic acid	pNPG	1.25 mM	n.d.	0.5 U/mL	10	6.9	25	7,17 μ M	(Adefegha et al., 2015)
	Protocatechuic acid								11,41 μ M	

4. Starch and polyphenol interaction

It has been previously mentioned the interaction between polyphenols and enzymes, but less attention has been pay to potential non-covalent interactions between polyphenols and starch, which may also affect starch digestion kinetics (Giuberti et al., 2020). These interactions involve hydrogen bonds, hydrophobic, electrostatic and ionic interactions, and are categorized into the formation of inclusion and non-inclusion complexes (Zhu, 2015).

Starch-polyphenol interactions and other factors like the pH changes caused by polyphenol addition greatly affected both physical and functional starch characteristics such as rheological, thermal and solubility properties. Wu et al. (2009) described irregular viscosity changes when tea polyphenols were present during rice starch gelatinization, showing a reduction in the final viscosity in comparison with the rice gel. Similarly, the inclusion of caffeic acid change starch gelatinization and retrogradation and exhibited a lower final viscosity (Zheng et al., 2020).

The effect of polyphenol interactions on starch properties are dependent on the chemical composition of the phenolic extract, the phenolic compound, starch structure and the experimental conditions (Zhu, 2015). These changes in the physical and functional properties of the starch affected gel formation, and therefore its textural and structural characteristics. Zhu et al. (2008) studied the addition of 12 phenolic compounds on the hardness and adhesiveness of wheat starch gels. Phenolic compounds reduced hardness and adhesiveness values more than flavonoids, and only chrysin and quercetin flavonoids increased gel hardness. Similar results were described by Karunaratne and Zhu (2016), who analyzed the addition of ferulic acid to corn starch. Some studies describe the starch structural changes caused by starch-polyphenol complexes. Han et al. (2020) characterized the structure of rice starch gels and pure polyphenols complexes. In a similar way, Zhu et al. (2009) observed the effect of polyphenol extract from pomegranate peel on wheat starch gel. Both studies suggested that phenolic compounds caused a looser porous gel matrix. The alteration of starch gel structure might impact the accessibility of the starch to the enzymes, however in these studies, starch digestibility was not evaluated. Miao et al. (2021) studied the structure of rice starch gels containing anthocyanins, and *in vitro* starch digestibility was analyzed. The presence of anthocyanins resulted in a starch gel structure with more and smaller cavities. Digestion results showed an inhibition of starch digestive enzymes by these flavonoids, but the role of the different structure caused by the polyphenols on starch digestion was not identified.

References

- Adefegha, S. A., Oboh, G., Ejakpovi, I. I., & Oyeleye, S. I. (2015). Antioxidant and anti-diabetic effects of gallic and protocatechuic acids: a structure–function perspective. *Comparative Clinical Pathology*, 24(6), 1579-1585.
- Akkrachiyasit, S., Charoenlertkul, P., Yibchok-anun, S., & Adisakwattana, S. (2010). Inhibitory Activities of Cyanidin and Its Glycosides and Synergistic Effect with Acarbose against Intestinal -Glucosidase and Pancreatic -Amylase. *International Journal of Molecular Sciences*, 11(9).
- Alam, S. A., Pentikäinen, S., Närväinen, J., Holopainen-Mantila, U., Poutanen, K., & Sozer, N. (2017). Effects of structural and textural properties of brittle cereal foams on mechanisms of oral breakdown and *in vitro* starch digestibility. *Food Research International*, 96, 1-11.
- American Diabetes Association. (2014). Diagnosis and Classification of Diabetes Mellitus. *Diabetes Care*, 37, S81-S90.
- Anderson, J. W., Baird, P., Davis, R. H., Jr, Ferreri, S., Knudtson, M., Koraym, A., Waters, V., & Williams, C. L. (2009). Health benefits of dietary fiber. *Nutrition Reviews*, 67(4), 188-205.
- Aoki, K., Muraoka, T., Ito, Y., Togashi, Y., & Terauchi, Y. (2010). Comparison of adverse gastrointestinal effects of acarbose and miglitol in healthy men: a crossover study. *Internal Medicine*, 49(12), 1085-1087.
- Aribas, M., Kahraman, K., & Koksels, H. (2020). In vitro glycemic index, bile acid binding capacity and mineral bioavailability of spaghetti supplemented with resistant starch type 4 and wheat bran. *Journal of Functional Foods*, 65, 103778.
- Aryaeian, N., Sedehi, S. K., & Arablou, T. (2017). Polyphenols and their effects on diabetes management: A review. *Medical journal of the Islamic Republic of Iran*, 31, 134.
- Bajaj, R., Singh, N., Kaur, A., & Inouchi, N. (2018). Structural, morphological, functional and digestibility properties of starches from cereals, tubers and legumes: a comparative study. *Journal of Food Science and Technology*, 55(9), 3799-3808.
- Benavent-Gil, Y., Román, L., Gómez, M., & Rosell, C. M. (2019). Physicochemical Properties of Gels Obtained from Corn Porous Starches with Different Levels of Porosity. *Starch - Stärke*, 71(3-4), 1800171.
- Benavent-Gil, Y., & Rosell, C. M. (2017). Performance of granular starch with controlled pore size during hydrolysis with digestive enzymes. *Plant Foods for Human Nutrition*, 72(4), 353-359.

- Bhandari, M. R., Jong-Anurakkun, N., Hong, G., & Kawabata, J. (2008). -Glucosidase and -amylase inhibitory activities of Nepalese medicinal herb Pakhanbhed (*Bergenia ciliata*, Haw.). *Food Chemistry*, 106(1), 247-252.
- Bohn, T., Carriere, F., Day, L., Deglaire, A., Egger, L., Freitas, D., Golding, M., Le Funteun, S., Macierzanka, A., Menard, O., Miralles, B., Moscovici, A., Portmann, R., Recio, I., Rémond, D., Santé-Lhoutelier, V., Wooster, T. J., Lesmes, U., Mackie, A. R., & Dupont, D. (2018). Correlation between *in vitro* and *in vivo* data on food digestion. What can we predict with static *in vitro* digestion models? *Critical Reviews in Food Science and Nutrition*, 58(13), 2239-2261.
- Boland, M. (2016). Human digestion – a processing perspective. *Journal of the Science of Food and Agriculture*, 96(7), 2275-2283.
- Boland, M., Golding, M., & Singh, H. (2014). *Food structures, digestion and health*: Elsevier.
- Bornhorst, G. M. & Singh, R. P. (2014). Gastric Digestion In Vivo and In Vitro: How the Structural Aspects of Food Influence the Digestion Process. *Annual Review of Food Science and Technology*, 5(1), 111-132.
- Brayer, G. D., Luo, Y., & Withers, S. G. (1995). The structure of human pancreatic amylase at 1.8 Å resolution and comparisons with related enzymes. *Protein Science*, 4(9), 1730-1742.
- Brites, C. M., Trigo, M. J., Carrapiço, B., Alviña, M., & Bessa, R. J. (2011). Maize and resistant starch enriched breads reduce postprandial glycemic responses in rats. *Nutrition Research*, 31(4), 302-308.
- Butterworth, P. J., Warren, F. J., & Ellis, P. R. (2011). Human -amylase and starch digestion: An interesting marriage. *Starch - Stärke*, 63(7), 395-405.
- Butterworth, P. J., Warren, F. J., Grassby, T., Patel, H., & Ellis, P. R. (2012). Analysis of starch amylolysis using plots for first-order kinetics. *Carbohydrate Polymers*, 87(3), 2189-2197.
- Buyken, A., Mela, D., Dussort, P., Johnson, I., Macdonald, I., Stowell, J., & Brouns, F. (2018). Dietary carbohydrates: a review of international recommendations and the methods used to derive them. *European journal of clinical nutrition*, 72(12), 1625-1643.
- Chambers, E. S., Byrne, C. S., & Frost, G. (2019). Carbohydrate and human health: is it all about quality? *The Lancet*, 393(10170), 384-386.
- Cirillo, G., Kraemer, K., Fuessel, S., Puoci, F., Curcio, M., Spizzirri, U. G., Altimari, I., & Iemma, F. (2010). Biological Activity of a Gallic Acid–Gelatin Conjugate. *Biom-*

cromolecules, 11(12), 3309-3315.

- De Souza, A., Lajolo, F. M., & Genovese, M. I. (2010). Chemical composition and antioxidant/antidiabetic potential of Brazilian native fruits and commercial frozen pulps. *Journal of Agricultural and Food Chemistry*, 58(8), 4666-4674.
- Devahastin, S. (2017). *Food Microstructure and Its Relationship with Quality and Stability*: Woodhead Publishing.
- Dhital, S., Warren, F. J., Butterworth, P. J., Ellis, P. R., & Gidley, M. J. (2017). Mechanisms of starch digestion by α -amylase—Structural basis for kinetic properties. *Critical Reviews in Food Science and Nutrition*, 57(5), 875-892.
- Dona, A. C., Pages, G., Gilbert, R. G., & Kuchel, P. W. (2010). Digestion of starch: In vivo and *in vitro* kinetic models used to characterise oligosaccharide or glucose release. *Carbohydrate Polymers*, 80(3), 599-617.
- Engelen, L., Fontijn-Tekamp, A., & van der Bilt, A. (2005). The influence of product and oral characteristics on swallowing. *Archives of Oral Biology*, 50(8), 739-746.
- Englyst, H. N., Kingman, S. M., & Cummings, J. (1992). Classification and measurement of nutritionally important starch fractions. *European journal of clinical nutrition*, 46, S33-50.
- Freitas, D., & Le Feunteun, S. (2018). Acid induced reduction of the glycaemic response to starch-rich foods: the salivary α -amylase inhibition hypothesis. *Food & Function*, 9(10), 5096-5102.
- Fuentes-Zaragoza, E., Riquelme-Navarrete, M. J., Sánchez-Zapata, E., & Pérez-Álvarez, J. A. (2010). Resistant starch as functional ingredient: A review. *Food Research International*, 43(4), 931-942.
- Gilbertson, H. R., Brand-Miller, J. C., Thorburn, A. W., Evans, S., Chondros, P., & Werther, G. A. (2001). The Effect of Flexible Low Glycemic Index Dietary Advice Versus Measured Carbohydrate Exchange Diets on Glycemic Control in Children With Type 1 Diabetes. *Diabetes Care*, 24(7), 1137-1143.
- Giuberti, G., Rocchetti, G., & Lucini, L. (2020). Interactions between phenolic compounds, amylolytic enzymes and starch: an updated overview. *Current Opinion in Food Science*, 31, 102-113.
- Golding, M. (2019). Exploring and Exploiting the Role of Food Structure in Digestion. In O. Gouseti, G. M. Bornhorst, S. Bakalis & A. Mackie (Eds.), *Interdisciplinary Approaches to Food Digestion* (pp. 81-128). Springer International Publishing.
- Goñi, I., Valdivieso, L., & Gudiel-Urbano, M. (2002). Capacity of edible seaweeds to

-
- modify *in vitro* starch digestibility of wheat bread. *Nahrung/Food*, 46(1), 18-20.
- Goñi, I., Garcia-Alonso, A., & Saura-Calixto, F. (1997). A starch hydrolysis procedure to estimate glycemic index. *Nutrition Research*, 17(3), 427-437.
- Granfeldt, Y., Björck, I., Drews, A., & Tovar, J. (1992). An *in vitro* procedure based on chewing to predict metabolic response to starch in cereal and legume products. *European Journal of Clinical Nutrition*, 46(9), 649-660.
- Gularte, M., & Rosell, C. (2011). Physicochemical properties and enzymatic hydrolysis of different starches in the presence of hydrocolloids. *Carbohydrate Polymers*, 85(1), 237-244.
- Han, X., Zhang, M., Zhang, R., Huang, L., Jia, X., Huang, F., & Liu, L. (2020). Physicochemical interactions between rice starch and different polyphenols and structural characterization of their complexes. *LWT- Food Science and Technology*, 125, 109227.
- Hoebler, C., Devaux, A., Karinthe, C., Belleville, J., & Barry, C. (2000). Particle size of solid food after human mastication and *in vitro* simulation of oral breakdown. *International Journal of Food Sciences and Nutrition*, 51(5), 353-366.
- Hoebler, C., Karinthe, A., Devaux, M. F., Guillon, F., Gallant, D. J. G., Bouchet, B., Melegari, C., & Barry, J. L. (1998). Physical and chemical transformations of cereal food during oral digestion in human subjects. *British Journal of Nutrition*, 80(5), 429-436.
- Hu, F. B., Manson, J. E., Stampfer, M. J., Colditz, G., Liu, S., Solomon, C. G., & Willett, W. C. (2001). Diet, Lifestyle, and the Risk of Type 2 Diabetes Mellitus in Women. *New England Journal of Medicine*, 345(11), 790-797.
- International Hypoglycaemia Study Group. (2015). Minimizing hypoglycemia in diabetes. *Diabetes care*, 38(8), 1583-1591.
- Jenkins, D. J., Wolever, T., Taylor, R. H., Barker, H., Fielden, H., Baldwin, J. M., Bowling, A. C., Newman, H. C., Jenkins, A. L., & Goff, D. V. (1981). Glycemic index of foods: a physiological basis for carbohydrate exchange. *The American Journal of Clinical Nutrition*, 34(3), 362-366.
- Jeon, S.-Y., Oh, S., Kim, E., & Imm, J.-Y. (2013). -Glucosidase inhibition and antiglycation activity of laccase-catalyzed catechin polymers. *Journal of Agricultural and Food Chemistry*, 61(19), 4577-4584.
- Karunaratne, R., & Zhu, F. (2016). Physicochemical interactions of maize starch with ferulic acid. *Food Chemistry*, 199, 372-379.

- Koh, L. W., Wong, L. L., Loo, Y. Y., Kasapis, S., & Huang, D. (2010). Evaluation of different teas against starch digestibility by mammalian glycosidases. *Journal of Agricultural and Food Chemistry*, 58(1), 148-154.
- Kong, F., & Singh, R. P. (2009). Modes of Disintegration of Solid Foods in Simulated Gastric Environment. *Food Biophysics*, 4(3), 180-190.
- Krentz, A. J., & Bailey, C. J. (2005). Oral Antidiabetic Agents. *Drugs*, 65(3), 385-411.
- Kumar, C. S., Ganesan, P., Suresh, P., & Bhaskar, N. (2008). Seaweeds as a source of nutritionally beneficial compounds-a review. *Journal of Food Science and Technology*, 45(1), 1.
- Lee, D.-S., & Lee, S.-H. (2001). Genistein, a soy isoflavone, is a potent α -glucosidase inhibitor. *FEBS Letters*, 501(1), 84-86.
- Li, C., Gong, B., Hu, Y., Liu, X., Guan, X., & Zhang, B. (2020). Combined crystalline, lamellar and granular structural insights into *in vitro* digestion rate of native starches. *Food hydrocolloids*, 105, 105823.
- Li, H., Song, F., Xing, J., Tsao, R., Liu, Z., & Liu, S. (2009). Screening and structural characterization of α -glucosidase inhibitors from hawthorn leaf flavonoids extract by ultrafiltration LC-DAD-MS n and SORI-CID FTICR MS. *Journal of the American Society for Mass Spectrometry*, 20(8), 1496-1503.
- Lo Piparo, E., Scheib, H., Frei, N., Williamson, G., Grigorov, M., & Chou, C. J. (2008). Flavonoids for controlling starch digestion: structural requirements for inhibiting human α -amylase. *Journal of medicinal chemistry*, 51(12), 3555-3561.
- Martinez-Gonzalez, A. I., Díaz-Sánchez, Á. G., Rosa, L. A. d. l., Vargas-Requena, C. L., Bustos-Jaimes, I., Alvarez-Parrilla, & Emilio. (2017). Polyphenolic Compounds and Digestive Enzymes: In Vitro Non-Covalent Interactions. *Molecules*, 22(4), 669.
- Martinez, M. M. (2021). Starch nutritional quality: beyond intraluminal digestion in response to current trends. *Current Opinion in Food Science*, 38, 112-121.
- Matos, M. E., & Rosell, C. M. (2011). Chemical Composition and Starch Digestibility of Different Gluten-free Breads. *Plant Foods for Human Nutrition*, 66(3), 224.
- Miao, L., Xu, Y., Jia, C., Zhang, B., Niu, M., & Zhao, S. (2021). Structural changes of rice starch and activity inhibition of starch digestive enzymes by anthocyanins retarded starch digestibility. *Carbohydrate Polymers*, 261, 117841.
- Minikus, M., Alminger, M., Alvito, P., Ballance, S., Bohn, T., Bourlieu, C., Carrière, F., Boutrou, R., Corredig, M., & Dupont, D. (2014). A standardised static *in vitro* digestion method suitable for food—an international consensus. *Food & Function*, 5(6), 1113-1124.

- Morris, V., & Groves, K. (2013). *Food microstructures: Microscopy, measurement and modelling*: Elsevier.
- Mulet-Cabero, A.-I., Egger, L., Portmann, R., Ménard, O., Marze, S., Minekus, M., Le Feunteun, S., Sarkar, A., Grundy, M. M.-L., & Carrière, F. (2020). A standardised semi-dynamic *in vitro* digestion method suitable for food—an international consensus. *Food & Function*, *11*(2), 1702-1720.
- Mulet-Cabero, A.-I., Rigby, N. M., Brodtkorb, A., & Mackie, A. R. (2017). Dairy food structures influence the rates of nutrient digestion through different *in vitro* gastric behaviour. *Food hydrocolloids*, *67*, 63-73.
- Nsor-Atindana, J., Yu, M., Goff, H. D., Chen, M., & Zhong, F. (2020). Analysis of kinetic parameters and mechanisms of nanocrystalline cellulose inhibition of α -amylase and α -glucosidase in simulated digestion of starch. *Food & Function*, *11*(5), 4719-4731.
- Oboh, G., Ademosun, A. O., Ayeni, P. O., Omojokun, O. S., & Bello, F. (2015). Comparative effect of quercetin and rutin on α -amylase, α -glucosidase, and some pro-oxidant-induced lipid peroxidation in rat pancreas. *Comparative Clinical Pathology*, *24*(5), 1103-1110.
- Oboh, G., Agunloye, O. M., Adefegha, S. A., Akinyemi, A. J., & Ademiluyi, A. O. (2015). Caffeic and chlorogenic acids inhibit key enzymes linked to type 2 diabetes (*in vitro*): a comparative study. *Journal of Basic and Clinical Physiology and Pharmacology*, *26*(2), 165-170.
- Oboh, G., Ogunsuyi, O., Ogunbadejo, M., & Adefegha, S. (2016). Influence of gallic acid on α -amylase and α -glucosidase inhibitory properties of acarbose. *Journal of food and drug analysis*, *24*(3), 627-634.
- Olkku, J., & Rha, C. (1978). Gelatinisation of starch and wheat flour starch—A review. *Food Chemistry*, *3*(4), 293-317.
- Pellegrini, N., Vittadini, E., & Fogliano, V. (2020). Designing food structure to slow down digestion in starch-rich products. *Current Opinion in Food Science*, *32*, 50-57.
- Phillips, G. O., & Williams, P. A. (2000). *Handbook of hydrocolloids*: CRC press Boca Raton, FL.
- Pi-Sunyer, F. X. (2002). Glycemic index and disease. *The American Journal of Clinical Nutrition*, *76*(1), 290S-298S.
- Proenca, C., Freitas, M., Ribeiro, D., Oliveira, E. F. T., Sousa, J. L. C., Tome, S. M., Ramos, M. J., Silva, A. M. S., Fernandes, P. A., & Fernandes, E. (2017). α -Glucosidase inhibition by flavonoids: an *in vitro* and *in silico* structure-activity relationship study. *Journal of Enzyme Inhibition and Medicinal Chemistry*, *32*(1), 1216-1228.

- Punthakee, Z., Goldenberg, R., & Katz, P. (2018). Definition, Classification and Diagnosis of Diabetes, Prediabetes and Metabolic Syndrome. *Canadian Journal of Diabetes*, 42, S10-S15.
- Rahelić, D., Jenkins, A., Božikov, V., Pavić, E., Jurić, K., Fairgrieve, C., Romić, D., Kokić, S., & Vuksan, V. (2011). Glycemic index in diabetes. *Collegium antropologicum*, 35(4), 1363-1368.
- Rosenblum, J. L., Irwin, C. L., & Alpers, D. H. (1988). Starch and glucose oligosaccharides protect salivary-type amylase activity at acid pH. *American Journal of Physiology-Gastrointestinal and Liver Physiology*, 254(5), G775-G780.
- Sahnoun, M., Trabelsi, S., & Bejar, S. (2017). Citrus flavonoids collectively dominate the α -amylase and α -glucosidase inhibitions. *Biologia*, 72(7), 764-773.
- Santamaria, M., Garzon, R., Moreira, R., & Rosell, C. M. (2021). Estimation of viscosity and hydrolysis kinetics of corn starch gels based on microstructural features using a simplified model. *Carbohydrate Polymers*, 273, 118549.
- Santos, H. O., de Moraes, W. M. A. M., da Silva, G. A. R., Prestes, J., & Schoenfeld, B. J. (2019). Vinegar (acetic acid) intake on glucose metabolism: A narrative review. *Clinical Nutrition ESPEN*, 32, 1-7.
- Sasaki, T., & Kohyama, K. (2011). Effect of non-starch polysaccharides on the *in vitro* digestibility and rheological properties of rice starch gel. *Food Chemistry*, 127(2), 541-546.
- Sharma, A., Yadav, B. S., & Ritika. (2008). Resistant Starch: Physiological Roles and Food Applications. *Food Reviews International*, 24(2), 193-234.
- Sui, X., Zhang, Y., & Zhou, W. (2016). In vitro and in silico studies of the inhibition activity of anthocyanins against porcine pancreatic α -amylase. *Journal of Functional Foods*, 21, 50-57.
- Sun, L., Warren, F. J., & Gidley, M. J. (2019). Natural products for glycaemic control: Polyphenols as inhibitors of alpha-amylase. *Trends in Food Science & Technology*, 91, 262-273.
- Sun, L., Warren, F. J., Netzel, G., & Gidley, M. J. (2016). 3 or 3'-Galloyl substitution plays an important role in association of catechins and theaflavins with porcine pancreatic α -amylase: The kinetics of inhibition of α -amylase by tea polyphenols. *Journal of Functional Foods*, 26, 144-156.
- Tadera, K., Minami, Y., Takamatsu, K., & Matsuoka, T. (2006). Inhibition of α -Glucosidase and α -Amylase by Flavonoids. *Journal of Nutritional Science and Vitaminology*, 52(2), 149-153.

- Tan, Y., Chang, S. K. C., & Zhang, Y. (2017). Comparison of α -amylase, α -glucosidase and lipase inhibitory activity of the phenolic substances in two black legumes of different genera. *Food Chemistry*, 214, 259-268.
- Venditti, A., Maggi, F., Vittori, S., Papa, F., Serrilli, A. M., Di Cecco, M., Ciaschetti, G., Mandrone, M., Poli, F., & Bianco, A. (2015). Antioxidant and α -glucosidase inhibitory activities of *Achillea tenorii*. *Pharmaceutical biology*, 53(10), 1505-1510.
- Wang, S., Li, C., Copeland, L., Niu, Q., & Wang, S. (2015). Starch Retrogradation: A Comprehensive Review. *Comprehensive Reviews in Food Science and Food Safety*, 14(5), 568-585.
- WHO. (2021). Diabetes. In. <https://www.who.int/news-room/fact-sheets/detail/diabetes>.
- Williamson, G. (2013). Possible effects of dietary polyphenols on sugar absorption and digestion. *Molecular Nutrition & Food Research*, 57(1), 48-57.
- Wu, Y., Chen, Z., Li, X., & Li, M. (2009). Effect of tea polyphenols on the retrogradation of rice starch. *Food Research International*, 42(2), 221-225.
- Yan, J., Zhang, G., Pan, J., & Wang, Y. (2014). α -Glucosidase inhibition by luteolin: Kinetics, interaction and molecular docking. *International Journal of Biological Macromolecules*, 64, 213-223.
- Zafar, M. I., Mills, K. E., Zheng, J., Regmi, A., Hu, S. Q., Gou, L., & Chen, L.-L. (2019). Low-glycemic index diets as an intervention for diabetes: a systematic review and meta-analysis. *The American Journal of Clinical Nutrition*, 110(4), 891-902.
- Zhang, B.-W., Li, X., Sun, W.-l., Xing, Y., Xiu, Z.-l., Zhuang, C.-l., & Dong, Y.-s. (2017). Dietary flavonoids and acarbose synergistically inhibit α -glucosidase and lower postprandial blood glucose. *Journal of Agricultural and Food Chemistry*, 65(38), 8319-8330.
- Zheng, Y., Tian, J., Yang, W., Chen, S., Liu, D., Fang, H., Zhang, H., & Ye, X. (2020). Inhibition mechanism of ferulic acid against α -amylase and α -glucosidase. *Food Chemistry*, 317, 126346.
- Zhu, F. (2015). Interactions between starch and phenolic compound. *Trends in Food Science & Technology*, 43(2), 129-143.
- Zhu, F., Cai, Y.-Z., Sun, M., & Corke, H. (2009). Effect of phytochemical extracts on the pasting, thermal, and gelling properties of wheat starch. *Food Chemistry*, 112(4), 919-923.
- Zhu, F., Cai, Y. Z., Sun, M., & Corke, H. (2008). Effect of phenolic compounds on the pasting and textural properties of wheat starch. *Starch-Stärke*, 60(11), 609-616.



Objectives

The overall objective of this research was to gain better understanding of the impact of microstructure on starch digestion and how digestive enzymes might be modulated by the use of phenolic compounds.

To reach the main objective, the following specific objectives and working plan were proposed:

- Understand the effect of bread structure on chewing behavior, bolus formation and sensory perception by consumers.

For that purpose, commercial toast breads were selected to reduce the impact of bread moisture content, and the effect of their structure and texture characteristics was evaluated and related with consumer's mastication and sensory perception.

- Study the influence of bread structure on disintegration along an *in vitro* oro-gastro-intestinal digestion, relating it with starch digestibility.

To reach this goal, two different bread structures were designed by modifying the breadmaking process, and two oral processing methods were compared to analyze the effect on the whole *in vitro* starch digestion.

- Analyze the impact of starch gels microstructures, obtained from different starch sources, on starch digestion.

To achieve this objective, cereal, tuber, and pulse starch gels were produced, analyzing their structure and trying to relate it with their digestibility along an *in vitro* oro-gastric-digestion.

- Evaluate the inhibitory activity of phenolic acids against starch digestive enzymes under different model systems.

To this end, phenolic acids with different structures were used to investigate their interaction with the enzyme or the substrate applying different methodologies, and the capacity to inhibit α -amylase and α -glucosidase enzymes was evaluated.

- Identify the inhibition capacity of *Ascophylum nodosum* aqueous extracts against starch digestive enzymes.

With that purpose, previous described methodologies were employed to evaluate the inhibitory potential of different seaweed extract against α -amylase and α -glucosidase enzymes, trying to identify the different involved compounds.

- Explore the impact of phenolic acids on starch gel microstructure and the effect on starch *in vitro* digestion.

To accomplish this aim, starch gels were prepared in the presence of phenolic acids, and their microstructure and enzymatic intestinal digestion were evaluated.

The results of this thesis have been structured in different chapters that correspond to scientific publications. In Figure 1, a schematic representation of the research performed in this thesis is given.

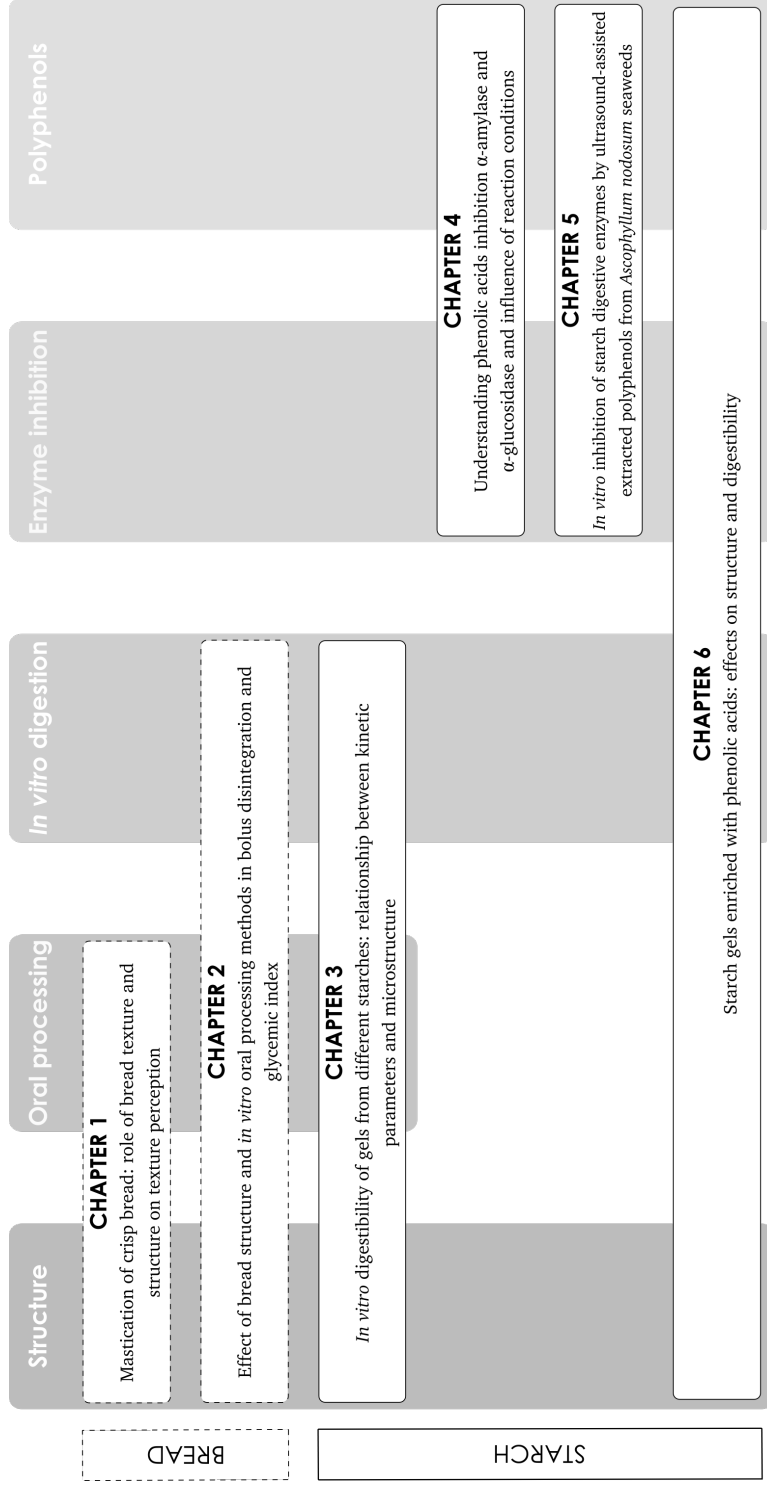


Figure 1. Overview of the different chapters of the results section.





Results

CHAPTER

1



Mastication of crisp bread: role of bread texture and structure on texture perception

Andrea Aleixandre^a, Yaiza Benavent-Gil^a, Elena Velickova^b, Cristina M. Rosell^{a*}

^a Institute of Agrochemistry and Food Technology (IATA-CSIC). C/Agustin Escardino, 7, Paterna 46980, Valencia, Spain.

^b University Ss. Cyril and Methodius, Faculty of Technology and Metallurgy, Rudjer Boskovic 16, Skopje 1000, Macedonia.

*Corresponding author: Cristina M. Rosell (crosell@iata.csic.es)



Abstract

Texture and structure of breads have been related to oral processing (FOP) performance and sensory perceptions, but moisture content might play a significant role. To evaluate the real impact of breads texture and structure, eliminating the possible role of moisture content, different toasted breads were investigated. Four commercial toasted sliced breads (white bread -WHB-, whole wheat bread -WWB-, non-added sugar bread -NSU-, non-added salt bread -NSA-) with similar ingredients but different texture and structure were selected. Texture and structure were instrumentally and sensory evaluated, besides FOP (total chewing time, number of chews until swallowing, chewing frequency, and mouthful) and bolus properties (moisture, saliva to bread ratio, hardness, adhesiveness, and cohesiveness). Toasted breads showed significant differences in hardness, cutting strength, and porosity, but panelists did not discriminate among them. FOP results indicated that harder samples (NSU) required longer mastication and a number of chews, and open crumb structures (WWB, WHB) with higher cell areas required less mastication. Also, bolus characteristics were affected by bread types, and bread with lower crumb hardness (WHB) produced more cohesive bolus. Having toasted breads allowed to eliminate possible influence of moisture content differences on sensory perception, mouthful and bolus water incorporation during mastication.



Keywords

Bread * Texture * Sensory perception * FOP * Mastication * Bolus properties

1.1. Introduction

Digestion performance of foods is becoming of utmost interest due to increasing understanding of the relationship among food-nutrition-health (Lovegrove et al., 2017). Digestion involves very complex processes along the oro-gastrointestinal tract, but all food changes start in the mouth where food is subjected to physical and biochemical changes. Specifically, food oral processing (FOP) involves mastication, salivation, bolus formation, enzyme digestion, and swallowing (Puerta et al., 2021). Considering the importance of bread on the human diet, the study of its oral processing has been the focus of several researches. Particularly, investigations have been centered on bread mastication performance through the duration of chewing or the number and frequency of bites (Mao et al., 2016; Pentikäinen et al., 2014), the textural bolus properties like adhesiveness, hardness, or cohesiveness (Jourden, Panouillé, et al., 2016), the rheological behavior of boluses (Le Bleis et al., 2013), or even the salivary amylase activity during oral digestion (Joubert et al., 2017). Currently, it is known the strong correlation between the mastication parameters of fresh wheat breads having different crumb structures and textures with their oral processing behavior (Alexandre et al., 2019; Gao et al., 2015). Similar relationship was observed with the structural properties and mastication work of different wheat and rye fresh breads (Pentikäinen et al., 2014). Image texture analysis allowed to identify the different degradation underwent by breads depending on their structure and composition (Tournier et al., 2012). Likewise, Jourden, Panouillé, et al. (2016) pointed out the effect of bread structure on oral processing, but stressing the role of bread composition, especially water content, in the bolus properties. That opens a reasonable doubt about the real impact of bread structure on mastication because evaluations have been always carried out in fresh breads, where water plays a crucial role as plasticizer.

Those physical and biochemical processes taking place during mastication are also intimately connected to texture perception, owing to the different stimuli induced by food breakdown and bolus formation. In fact, significant differences in texture perception have been observed among fresh breads with different structures (Gao et al., 2017). Nevertheless, Jourden, Saint-Eve, et al. (2016) found that bolus properties and more specifically bolus hydration and texture had more impact on texture perception than bread structural properties. Considering the high moisture content of the bread and the variability among breads, bolus hydration might be significantly affected by the moisture content of the bread and some texture perception might be hindered due to the water content. Therefore, till now there is no study focused on assessing to what extent the bread texture in absence of water is affecting mastication and texture perception.

The objective of the present study was to better understand the effect of bread properties on consumers' perception and mastication, but to reduce the impact of bread

moisture content, toasted breads were selected. Four commercial toasted sliced breads (white, whole meal, low in salt, low in sugar) with rather similar composition and shape were selected. Relationships between bread properties, sensory and instrumentally analyzed, and sensory perception during oral processing were evaluated.

1.2. Materials and methods

1.2.1. Bread samples and characterization

Four types of commercial toasted sliced breads were purchased from a local Spanish market, including white bread (WHB), whole wheat bread (WWB), no added sugar bread (NSU), and no added salt bread (NSA). Toasted sliced breads were from the same brand to reduce their variability to composition, keeping the breadmaking process.

The ingredient composition and nutrition facts of commercial breads were obtained from the label (Table 1.1). Samples were stored in sealed plastic containers to prevent moisture changes during the study. Characterization of bread samples included moisture content, texture, and structural properties. Moisture content was analyzed following the ICC standard method ICC 110/1 (ICC, 1994). The textural characteristics of toasted bread samples such as hardness and cutting strength were measured using the TA.XT-Plus Texture Analyzer (Stable Micro Systems Ltd., Godalming, UK) equipped with a 5 Kg load cell. A compression test was applied to toasted bread slices, using a 20 mm cylindrical aluminum probe. All bread slices had the same dimensions (10 mm x 6 mm x 1 mm, length x width x thickness). Five compression/slice were performed at a test speed of 0.5 mm/s and compressing up to 50% of the bread slice height. The maximum peak of the force-distance plot was interpreted as hardness. Cutting strength was measured using the 3 mm knife blade at a test speed of 2 mm/s, following the conditions reported for crispy products like biscuits (Hedhili et al., 2021; Prakash et al., 2018). Bread structure analysis was carried out using ImageJ software following the methodology described by Morreale et al. (2018). Bread porosity (%), calculated as total cell area and total slice area ratio in percentage, and mean and median cavities or cells area (mm²) were determined.

Table 1.1. Ingredients and nutrition facts (g/100 g) of toasted sliced breads according to producer's labels.

Sample	Ingredients	Fat	Carbo- hydrate	Sugars	Protein	Salt
WHB	Wheat flour 88%, yeast, vegetal oil (sunflower) 2.5%, glucose and fructose syrup, sugar, salt, malted barley flour, wheat gluten, flour treatment agent: ascorbic acid.	4.6	73	4.9	11	1.2
WWB	Whole wheat flour 58%, wheat flour, yeast, glucose and fructose syrup, vegetal oil (sunflower) 2.9%, wheat gluten, salt, malted barley flour, flour treatment agent: ascorbic acid.	5.6	59	3.8	17	1
NSU	Wheat flour 91%, wheat gluten, yeast, vegetal oil (sunflower) 2.6%, flour treatment agent: ascorbic acid.	5	72	2.9	13	0.05
NSA	Wheat flour 88%, yeast, glucose and fructose syrup, vegetal oil (sunflower) 2.5%, wheat gluten, malted barley flour, flour treatment agent: ascorbic acid.	4.5	71	5.8	13	0.04

1.2.2. FOP assessment

Fourteen healthy subjects (10 females and 4 males), students, and teachers from University participated in the study (30.64 ± 6.73 years, mean \pm SD). Number of subjects in the study is important but the range of participant in similar FOP studies varied between 10 and 20 (Joubert et al., 2017), thus the number selected for this study falls within reported values. Selection criteria were availability for the duration of the study, good dental status, and no reported salivary or masticatory disorders. The participants provided signed consent to their participation in the study, and they did not receive compensation for their participation.

The study was conducted according to Helsinki Ethical Guidelines and adapted for food sensory analysis at the Food Technology and Biotechnology Department at Faculty of Technology and Metallurgy, University Ss Cyril and Methodius in Skopje, Republic of North Macedonia. The study was approved by the Faculty Committee (University Ss

Cyril and Methodius).

For FOP analyses, the participants were instructed to bite bread samples, naturally chew them and, to indicate the swallowing moment. Parameters collected were the total chewing time (s), number of chews until swallowing, chewing frequency, and mouthful (g) as the portion of food ingested for chewing. The total chewing time (s) was calculated as the duration between the first chew and the swallowing time, which was recorded with a digital chronometer (Brannan, S. Brannan & Sons, limited, Cleator Moor, UK). The chronometer was activated after biting the bread slice and stopped when it was swallowed. The number of chews until swallowing were measured as the number of opening and closing movements of the maxilla, and the chewing frequency represents the number of chews per second (Huang et al., 2021). Bread slice was weighed before and after biting and the weight difference between them was referred as mouthful.

1.2.3. Characterization of bolus properties

The participants masticated each sample and spitted it when they felt it was ready to swallow. Chewed samples were immediately analyzed. Bolus moisture (%) and saliva impregnation (g/g bread, W.W.) were determined as previously described by Pentikäinen et al. (2014). Boluses were dried in an oven at 105°C overnight determining their water content, and saliva impregnation was determined by the difference between bolus moisture and the bread moisture. A Texture Profile Analysis (TPA) was used to characterize the bolus, following the procedure described by Jourden, Panouillé, et al. (2016) was performed using a TA.XT-Plus Texture Analyzer (Stable Micro Systems Ltd., Godalming, UK) equipped with a 5 Kg load cell. Bolus was loaded into a 3 cm height poly-methyl methacrylate cup and subjected to compression, with a 20 mm cylindrical aluminum probe, test speed of 0.83 mm/s, and compressing up to 65% of the bolus height and resting time of one second between compressions. Data from three replicates were averaged. Hardness, adhesiveness, and cohesiveness parameters were obtained from the analysis

1.2.4. Sensory assessment

A descriptive sensory evaluation focused on bread texture properties was performed following international standards (ISO, 4121:2003). In one session, participants were presented in a completely randomized way with the samples labeled with 3-digit codes. Participants evaluated successively the toasted breads, rinsing the mouth with water after each sample and leaving 2 minutes between sample analysis. The definition of the texture attributes (hardness, crispness, crunchiness, pastiness, grittiness, dry mouthfeel) was given to the panelists, using the terms previously reported (Callejo,

2011). Specifically, hardness was defined as the force required to break the bread with the incisors. Crispness was referred as the high pitched sound produced when the teeth crack the product during mastication, with multiple fractures at low force loads. Crunchiness was defined as the low-pitched sound produced on bread fracture during mastication. Pastiness was referred as the mouthfeel of ball or paste formation. Grittiness was the presence of small dry particles which tend to scrape off the tongue. Finally, dry mouthfeel was evaluated as the feeling of dryness in the mouth. Hardness, crispness, and crunchiness gave information about bread texture attributes, while pastiness, grittiness, and dry mouthfeel were related to bolus properties. The intensity of all sensory impressions was scored using a 7-point categoric scale (1=extremely low intensity, 2= very low intensity, 3= moderate low intensity, 4= neither intense nor not intense, 5= moderate high intensity, 6= very high intensity, 7= extremely high intensity).

1.2.5. Statistical data analyses

All samples were analyzed in duplicate and results averaged. Statistical analyses were assessed by using Statgraphics Centurion XV (Statistical Graphics Corporation, Rockville, MD, USA). Descriptive statistics and one-way analysis of variance (ANOVA) were performed to evaluate significant differences among bread samples at 95% confidence interval using Fisher's least significant differences (LSD) test. Pearson correlation coefficient (r) and P -value were used to indicate correlations. The data were analyzed by multivariate data analysis in the Principal Component Analysis (PCA) to discriminate among samples.

1.3. Results and discussion

1.3.1. Bread characteristics

Four wheat toasted breads were used to identify possible relationships between instrumental and sensory texture and the effect on mastication without the influence of the moisture content. Breads with very close composition and similar shape were selected: white bread, whole wheat bread, non-added sugar bread, and non-added salt bread. According to their labels (Table 1.1), toasted breads were based on wheat flour, yeast, sunflower oil, wheat gluten, and ascorbic acid. Main differences were the inclusion of whole wheat flour in WWB, the absence of salt and sugar in NSU and NSA, and also the absence of syrup in NSU. Concerning the nutrition facts, as expected WWB bread showed the highest fat and protein values and the lowest carbohydrate content. NSA had the highest sugar content followed by WHB, WWB, and NSU. Salt contents were similar between WHB and WWB (1.2-1 g/g), and NSU and NSA (0.05-0.04 g/g).

As expected, toasted breads had very low moisture content (4.32-5.58%) (Table 1.2), compared to fresh breads (33-37%) (Jourdren, Panouillé, et al., 2016).

Table 1.2. Bread characteristics and their performance during FOP (FOP) and the resulting bolus properties of different types of toasted breads (WHB: wheat bread; WWB: whole wheat bread; NSU: non-sugar added wheat bread; NSA: non-salt added wheat bread).

	WHB	WWB	NSU	NSA
<i>Bread characteristics</i>				
Moisture content (%)	4.32±0.05 ^a	5.58±0.06 ^c	4.55±0.04 ^b	4.38±0.01 ^a
Hardness (N)	22.70±1.99 ^a	36.24±5.24 ^c	47.15±1.65 ^d	29.18±2.31 ^b
Cutting strength (N)	34.80±1.02 ^a	31.02±5.70 ^a	42.64±2.95 ^b	46.10±3.03 ^b
Porosity (%)	30.51±0.70 ^b	33.74±0.41 ^c	21.35±0.83 ^a	30.21±0.95 ^b
Cell area (mm ²)				
Mean	0.54±0.06	0.46±0.04	0.46±0.05	0.53±0.01
Median	0.030	0.012	0.021	0.016
<i>FOP</i>				
Mastication time (s)	14.81±3.02 ^a	13.87±2.83 ^a	17.80±3.71 ^b	15.58±3.18 ^{ab}
Number of chews	14.00±2.86 ^a	16.72±3.34 ^b	19.92±3.91 ^c	18.00±3.75 ^{bc}
Chewing frequency (s ⁻¹)	1.07±0.22 ^a	1.22±0.25 ^b	1.16±0.24 ^{ab}	1.28±0.26 ^b
Mouthful (g)	1.54±0.31	1.38±0.28	1.51±0.30	1.52±0.30
<i>Bolus properties</i>				
Moisture (%)	51.73±5.46	53.87±5.33	52.92±7.03	52.17±5.62
Saliva to bread ratio (g/g bread, W.W.)	0.47±0.09	0.47±0.09	0.48±0.09	0.48±0.09
Hardness (N)	6.20±1.17 ^a	6.93±1.31 ^{ab}	8.17±1.54 ^b	7.42±1.40 ^{ab}
Adhesiveness (N·s)	6.90±1.30 ^b	2.80±0.54 ^a	2.90±0.55 ^a	5.90±1.11 ^b
Cohesiveness	0.48±0.09 ^c	0.32±0.06 ^a	0.39±0.07 ^a	0.43±0.08 ^b

Values followed by different letters within rows are significantly different ($P < 0.05$). Mean±SD (n=3).

Therefore, the low moisture content of these breads would allow assessing the impact of texture and structure without the possible interference of the water plasticizing effect. Despite their similarities in ingredients and composition, they showed significant ($P < 0.05$) differences in hardness and cutting strength (Table 1.2). NSU and WWB had harder structure (47.15 ± 1.65 and 36.24 ± 5.24 N, respectively) than WHB and NSA breads. Cutting strength values were higher in low-salt breads: NSU and NSA samples (42.64 ± 2.95 and 46.10 ± 3.03 N, respectively). Likely, sugar and salt content affected the inner bread structure since a negative relationship was observed between sugar content and hardness ($r = -0.7808$; $P < 0.001$) and salt content and cutting strength ($r = -0.8145$; $P < 0.001$). In fact, Lynch et al. (2009) observed a reduction in bread hardness as the salt content increase when comparing fresh breads with different salt content.

Image analysis of the crumb corroborated their different structure (Figure 1.1).

Crumb porosity (%) was higher in WWB bread ($33.74 \pm 0.41\%$), which also showed



Figure 1.1. Images of toasted sliced breads. A: WHB: wheat bread; B: WWB: whole wheat bread; C: NSU: non-sugar added wheat bread; D: NSA: non-salt added wheat bread.

the lowest median cell area.

1.3.2. Sensory evaluation

Having the focus on texture perception, a sensory evaluation was performed using descriptive sensory analysis (Figure 1.2).

In general terms, attributes related to bread texture perception (hardness, crispiness, and crunchiness) obtained higher scores than attributes related to bolus characteristics (pastiness, grittiness, and dry mouthfeel). In toasted breads, crispiness and

crunchiness are desirable attributes, and high scores are related to freshness. However, differences observed in hardness and cutting strength were not perceived by panelists. The difficulty to perceive differences in crispy products has been previously reported (Saeleaw & Schleining, 2011). Conversely, different oral texture perceptions have been reported in fresh breads and attributed to bread texture and structure (Panouillé et al., 2014). Therefore, the low moisture content of toasted breads led to high hardness and cutting strength, and differences observed when assessing instrumental texture were not perceived and discriminated by panelists.

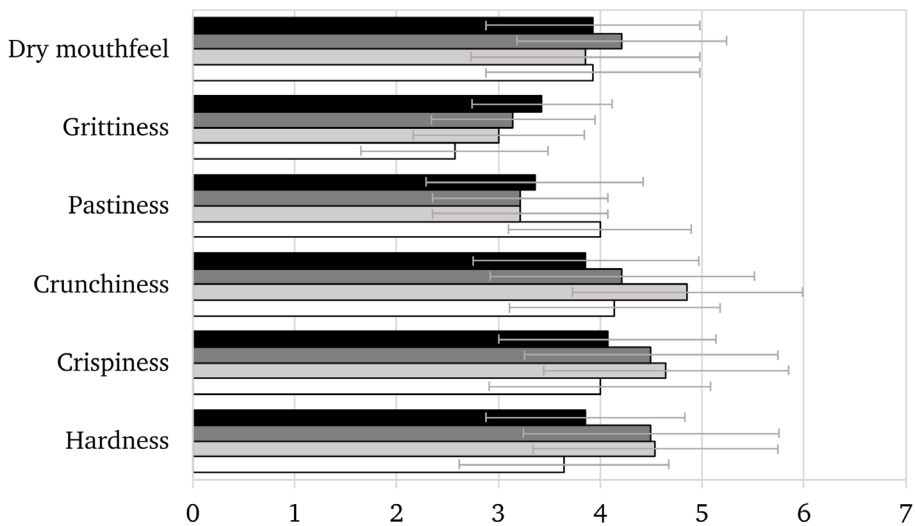


Figure 1.2. Sensory evaluation of texture of toasted sliced bread samples (MEAN \pm SE): ■ WHB: wheat bread; ▒ WWB: whole wheat bread; □ NSU: non-sugar added wheat bread; □ NSA: non-salt added wheat bread.

1.3.3. Characterization of FOP and bolus properties

The statistical analysis of FOP characteristics and bolus properties indicated that both bread type and panelist significantly affected ($P < 0.05$) mastication time, number of chews, and chewing frequency (Table 1.2). Conversely, Tournier et al. (2012) found no differences between bread types but variations between subjects when analyzed the chewing rate of baguette, rye bread, and toasted bread. Nevertheless, the role of the individuality of human beings on FOP had been long described (Chen, 2009). Regarding the mastication time, in general, was lower than the 20 s described for fresh breads (Le Bleis et al., 2016), and similar to the mastication times and the number of chews (13.8 ± 0.5 s with 17.8 ± 0.8 chews) reported for white toasted breads (Van Eck et al., 2019).

Focusing on bread effect, NSU required longer mastication (17.80 ± 3.71 s), being higher the number of chews required to swallow the sample (19.92 ± 3.91 chews). Mastication time was shorter for WHB and WWB, although the number of chews was higher for WWB, likely the bran presence induced this difference. Chewing frequency was lower for WHB (1.07 ± 0.22 chews/s). In fresh breads, a high positive correlation between closed porosity and total mastication work has been reported (Pentikäinen et al., 2014), observing longer mastication time and high number of chews in breads with lower porosity or small pore size. Following that reasoning, a bread structure with lower porosity, like NSU sample, might be related with a denser structure, which is reflected in the major mastication effort required.

Mouthful was significantly ($P < 0.001$) influenced by individuals but no bread type. The average value of mouthful was 1.49 ± 0.07 g, which was lower than values (3-5 g) described in FOP studies with fresh wheat breads (Gao et al., 2015; Hoebler et al., 2000). Very weak ($r < 0.4$) significant correlations were found between FOP results and bread composition or texture properties, revealing that the crumb structure of toasted breads had weak impact on FOP. It has been reported that crumb texture and structure have an important role in FOP (Aleixandre et al., 2019), but present results with toasted breads suggested that crumb moisture content might be responsible for possible differences.

Bolus properties comprising saliva inclusion and texture properties were evaluated (Table 1.2). No significant differences were found among the boluses water content and saliva to bread ratio. But in those parameters, significant differences were found between individuals ($P < 0.001$) (data not shown), which might be expected because salivary flow rate varies within a person over time and among individuals (Ghezzi et al., 2000). Bolus moisture ranged from 51.73 (WHB) to 53.87% (WWB), in agreement with values found for fresh breads (Le Bleis et al., 2016), and close to the values (56-58.5%) obtained by Le Bleis et al. (2013) at swallowing point of diverse commercial white breads. The same trend was described to saliva to bread ratio results, with an average range of 0.47-0.48 g/g bread (W.W.). During mastication, foods required appropriate lubrication and agglomeration to facilitate bolus swallowing. The lower water content of breads, the more mastication time and chews are needed to reach the swallowable state (Mao et al., 2016). Drier products, like cereal flakes, required more saliva than breads to form the bolus keeping the needed hydration level of the bolus (Alam et al., 2017). However, no correlation was found between bolus moisture and mastication frequency, confirming that salivation and chewing cycles are independent (Tournier et al., 2014).

Regarding texture properties of the bolus, significant differences were observed in the hardness of NSU (8.17 ± 1.54 N) and WHB (6.20 ± 1.17 N). About bolus adhesiveness and cohesiveness, WWB and NSU had lower values than WHB and NSA.

Bolus cohesiveness was similar to cracker bolus (Van Eck et al., 2019), but harder and more adhesive. There was no relationship between FOP parameters and the mechanical characteristics of boluses, thus individual mastication performance (chewing times or number of chews during food mastication) did not affect boluses texture. Again, looking to understand the possible role of bread crumb structure, correlations were calculated with bolus properties. Significantly moderate negative correlation was observed between crumb hardness and bolus adhesiveness ($r = -0.4526$; $P < 0.001$). Similarly, crumb structure, specifically mean cell area was positively correlated with bolus adhesiveness ($r = 0.5727$; $P < 0.001$) and cohesiveness ($r = 0.4587$; $P < 0.001$). Therefore, crumb microstructure significantly affected bolus texture, although also initial food composition might affect hardness and adhesiveness of bolus (James et al., 2011).

1.3.4. Texture, FOP and sensory correlations

Bread structure and texture characteristics, mastication properties, and sensory parameters were subjected to statistical analysis, and a principal component analysis was carried out to display the global effect (Figure 1.3).

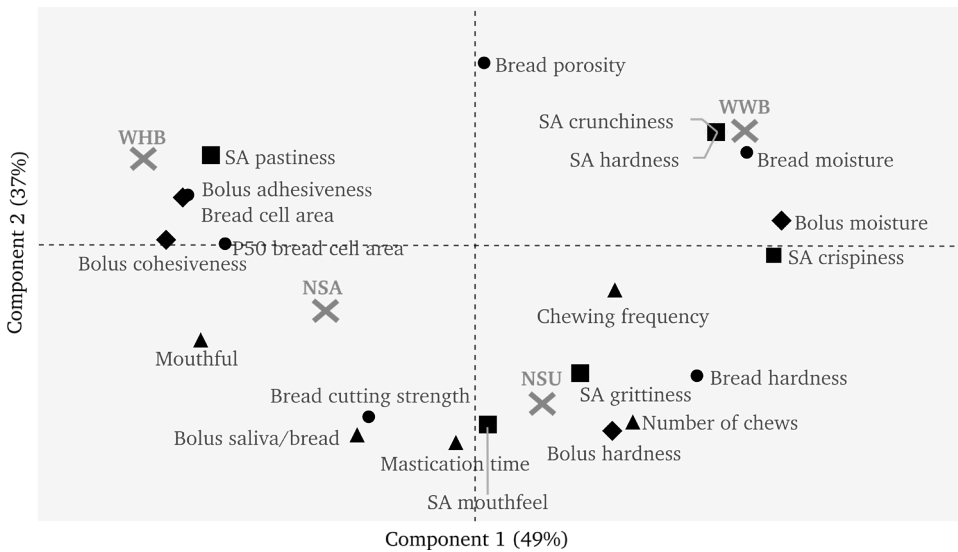


Figure 1.3. Correlation loadings plot and scores plot from a principal component analysis (PCA) of the combination of bread moisture, bread texture and structure ●, mastication ▲, bolus properties ◆, and sensory evaluation ■. WHB: wheat bread; WWB: whole wheat bread; NSU: non-sugar added wheat bread; NSA: non-salt added wheat bread.

Two components explained 86% of the total data variance, describing 49% and 37% of the variation in the principal components 1 and 2, respectively. Component 1 along the x-axis allowed the discrimination among the different types of toasted breads, despite their close structure and composition. Specifically, WHB was located in

the right upper part of the score plot, hence was strongly discriminated by bolus texture, except hardness, pastiness sensation, which was related to the high values of mean and median (P50) cell area. WWB was in the right upper part of the plot, reflecting its higher moisture content. It must be highlighted that even at the low moisture content observed in toasted breads, moisture was correlated with the perceived hardness and crunchiness. NSA and NSU were grouped in the lower part of the score plot, related to bread instrumental texture (hardness and cutting strength), mastication properties (mastication time or the number of chews), and sensory perception of dry mouthfeel and grittiness. Jourden, Saint-Eve, et al. (2016) described how sensory attributes during ingestion of fresh breads were more affected by bolus variations than the initial bread characteristics. Similar conclusions were described by Puerta et al. (2020), correlating perceived sensations at the beginning of consumption with food characteristics, but the remaining sensations were explained by oral attributes. In this study, even though some texture perceptions were impacted by bolus texture or bread moisture, also bread texture and mastication properties contributed to panelist sensations.

1.4. Conclusions

The study carried out with toasted breads allowed to discriminate the impact of bread texture and structure on food oral processing and sensory perceptions, without the possible interference induced by the moisture content. Four different toasted sliced bread made with similar ingredients showed divergences in texture and structure properties. Despite the absence of moisture content in the toasted breads, textural differences among the breads were not perceived by panelists, thus texture differences induced by slight changes in formulations were not sufficient to be detected by panelists. Concerning FOP results, bread structure and texture dominated mastication behavior. Bread crumbs with lower porosity required major mastication efforts. Overall, it can be concluded that crumb bread structure has great impact on bolus adhesiveness, and instrumental bread texture significantly affects mastication performance.

Author Contributions: Credit roles: AA: Conceptualization, Data curation; Formal analysis; Investigation; Methodology, Writing – original draft, YBG: Methodology, EV: Supervision; Writing – review & editing; Funding acquisition, CMR: Conceptualization; Funding acquisition; Investigation; Supervision; Data curation; Writing - review & editing.

Acknowledgments: Authors acknowledge the financial support of the Spanish Ministry of Science, Innovation and Universities (Project RTI2018-095919-B-C21), the European Regional Development Fund (FEDER) and Generalitat Valenciana (Project Prometeo 2017/189). This work is based upon the work from COST Action 18101

SOURDOMICS – Sourdough biotechnology network towards novel, healthier and sustainable food and bioprocesses, where A. Aleixandre was supported by COST (European Cooperation in Science and Technology). COST is a funding agency for research and innovation networks.

Conflicts of Interest: The authors declare that they do not have any conflict of interest.

References

- Alam, S. A., Pentikäinen, S., Närväinen, J., Holopainen-Mantila, U., Poutanen, K., & Sozer, N. (2017). Effects of structural and textural properties of brittle cereal foams on mechanisms of oral breakdown and *in vitro* starch digestibility. *Food Research International*, *96*, 1-11.
- Aleixandre, A., Benavent-Gil, Y., & Rosell, C. M. (2019). Effect of Bread Structure and In Vitro Oral Processing Methods in Bolus Disintegration and Glycemic Index. *Nutrients*, *11*(9), 2105.
- Callejo, M. J. (2011). Present situation on the descriptive sensory analysis of bread. *Journal of Sensory Studies*, *26*(4), 255-268.
- Chen, J. (2009). Food oral processing—A review. *Food hydrocolloids*, *23*(1), 1-25.
- Gao, J., Ong, J. J.-X., Henry, J., & Zhou, W. (2017). Physical breakdown of bread and its impact on texture perception: A dynamic perspective. *Food Quality and Preference*, *60*, 96-104.
- Gao, J., Wong, J. X., Lim, J. C.-S., Henry, J., & Zhou, W. (2015). Influence of bread structure on human oral processing. *Journal of Food Engineering*, *167*, 147-155.
- Ghezzi, E., Lange, L., & Ship, J. (2000). Determination of variation of stimulated salivary flow rates. *Journal of dental research*, *79*(11), 1874-1878.
- Hedhili, A., Lubbers, S., Bou-Maroun, E., Griffon, F., Akinyemi, B. E., Husson, F., & Valentin, D. (2021). Moringa Oleifera supplemented biscuits: Nutritional values and consumer segmentation. *South African Journal of Botany*, *138*, 406-414.
- Hoebler, D., A., Karinithi, C., Belleville, J., & Barry, C. (2000). Particle size of solid food after human mastication and *in vitro* simulation of oral breakdown. *International Journal of Food Sciences and Nutrition*, *51*(5), 353-366.
- Huang, Y.-F., Liu, S.-P., Muo, C.-H., & Chang, C.-T. (2021). The impact of occluding pairs on the chewing patterns among the elderly. *Journal of Dentistry*, *104*, 103511.
- ICC. (1994). International Association for Cereal Chemistry. Standard No 110/1.

ISO. (4121:2003). Sensory Analysis. Evaluation of Food Products by Methods Using Scales. *International Organization for Standardization, Geneva, Switzerland*.

James, B., Young, A., Smith, B., Kim, E., Wilson, A., & Morgenstern, M. P. (2011). Texture changes in bolus to the “point of swallow” - fracture toughness and back extrusion to test start and end points. *Procedia Food Science, 1*, 632-639.

Joubert, M., Septier, C., Brignot, H., Salles, C., Panouillé, M., Feron, G., & Tournier, C. (2017). Chewing bread: impact on alpha-amylase secretion and oral digestion. *Food & Function, 8*(2), 607-614.

Jourdren, S., Panouillé, M., Saint-Eve, A., Déléris, I., Forest, D., Lejeune, P., & Souchon, I. (2016). Breakdown pathways during oral processing of different breads: impact of crumb and crust structures. *Food & Function, 7*(3), 1446-1457.

Jourdren, S., Saint-Eve, A., Panouillé, M., Lejeune, P., Déléris, I., & Souchon, I. (2016). Respective impact of bread structure and oral processing on dynamic texture perceptions through statistical multiblock analysis. *Food Research International, 87*, 142-151.

Le Bleis, F., Chaunier, L., Della Valle, G., Panouillé, M., & Réguerre, A. L. (2013). Physical assessment of bread destructure during chewing. *Food Research International, 50*(1), 308-317.

Le Bleis, F., Chaunier, L., Montigaud, P., & Della Valle, G. (2016). Destructuration mechanisms of bread enriched with fibers during mastication. *Food Research International, 80*, 1-11.

Lovegrove, A., Edwards, C. H., De Noni, I., Patel, H., El, S. N., Grassby, T., Zielke, C., Ulmius, M., Nilsson, L., Butterworth, P. J., Ellis, P. R., & Shewry, P. R. (2017). Role of polysaccharides in food, digestion, and health. *Critical Reviews in Food Science and Nutrition, 57*(2), 237-253.

Lynch, E. J., Dal Bello, F., Sheehan, E. M., Cashman, K. D., & Arendt, E. K. (2009). Fundamental studies on the reduction of salt on dough and bread characteristics. *Food Research International, 42*(7), 885-891.

Mao, Q., Sun, Y., Hou, J., Yu, L., Liu, Y., Liu, C., & Xu, N. (2016). Relationships of image texture properties with chewing activity and mechanical properties during mastication of bread. *International Journal of Food Engineering, 12*(4), 311-321.

Morreale, F., Garzón, R., & Rosell, C. M. (2018). Understanding the role of hydrocolloids viscosity and hydration in developing gluten-free bread. A study with hydroxypropylmethylcellulose. *Food hydrocolloids, 77*, 629-635.

- Panouillé, M., Saint-Eve, A., Déléris, I., Le Bleis, F., & Souchon, I. (2014). Oral processing and bolus properties drive the dynamics of salty and texture perceptions of bread. *Food Research International*, *62*, 238-246.
- Pentikäinen, S., Sozer, N., Närviäinen, J., Ylätaalo, S., Teppola, P., Jurvelin, J., Holopainen-Mantila, U., Törrönen, R., Aura, A.-M., & Poutanen, K. (2014). Effects of wheat and rye bread structure on mastication process and bolus properties. *Food Research International*, *66*, 356-364.
- Prakash, K., Naik, S. N., Vadivel, D., Hariprasad, P., Gandhi, D., & Saravanadevi, S. (2018). Utilization of defatted sesame cake in enhancing the nutritional and functional characteristics of biscuits. *Journal of Food Processing and Preservation*, *42*(9), e13751.
- Puerta, P., Garzón, R., Rosell, C. M., Fiszman, S., Laguna, L., & Tárrega, A. (2021). Modifying gluten-free bread's structure using different baking conditions: Impact on oral processing and texture perception. *LWT- Food Science and Technology*, *140*, 110718.
- Puerta, P., Laguna, L., Villegas, B., Rizo, A., Fiszman, S., & Tarrega, A. (2020). Oral processing and dynamics of texture perception in commercial gluten-free breads. *Food Research International*, *134*, 109233.
- Saeleaw, M., & Schleining, G. (2011). A review: Crispness in dry foods and quality measurements based on acoustic-mechanical destructive techniques. *Journal of Food Engineering*, *105*(3), 387-399.
- Tournier, C., Grass, M., Septier, C., Bertrand, D., & Salles, C. (2014). The impact of mastication, salivation and food bolus formation on salt release during bread consumption. *Food & Function*, *5*(11), 2969-2980.
- Tournier, C., Grass, M., Zope, D., Salles, C., & Bertrand, D. (2012). Characterization of bread breakdown during mastication by image texture analysis. *Journal of Food Engineering*, *113*(4), 615-622.
- Van Eck, A., Hardeman, N., Karatza, N., Fogliano, V., Scholten, E., & Stieger, M. (2019). Oral processing behavior and dynamic sensory perception of composite foods: Toppings assist saliva in bolus formation. *Food Quality and Preference*, *71*, 49.

CHAPTER

2



Effect of bread structure and *in vitro* oral processing methods in bolus disintegration and glycemic index

Andrea Alexandre^a, Yaiza Benavent-Gil^a, Cristina M. Rosell^{a*}

^aInstitute of Agrochemistry and Food Technology (IATA-CSIC). C/Agustin Escardino, 7, Paterna 46980, Valencia, Spain.

*Corresponding author: Cristina M. Rosell (crostell@iata.csic.es)



Abstract

The growing interest in controlling the glycemic index of starchy-rich food has encouraged research about the role of the physical structure of food. The aim of this research was to understand the impact of the structure and the *in vitro* oral processing methods on bolus behavior and starch hydrolysis of wheat bread. Two different bread structures (loaf bread and bread roll) were obtained using different shaping methods. Starch hydrolysis during *in vitro* oro-gastrointestinal digestion using the INFOGEST protocol was analyzed and oral processing was simulated by applying two different disintegration processes (basic homogenizer, crystal balls). The bread structure, and thus the shaping method during breadmaking, significantly affected the bolus particle size during all digestion stages. The different *in vitro* oral processing methods affected the bolus particle sizes after the oral phase in both breads, but they affected the particle size distribution after the gastric and intestinal phase only in the case of loaf bread. Aggregates were observed in the gastric phase, which were significantly reduced in the intestinal phase. When simulated oral processing with crystal balls led to bigger particle size distribution, bread rolls presented the highest *in vitro* starch hydrolysis. The type of *in vitro* oral processing allowed discrimination of the performance of the structures of the two breads during starch hydrolysis. Overall, crumb structure significantly affected texture properties, but also had a significant impact on particle size during digestion and starch digestibility.



Keywords

Bread * Matrix structure * Oral digestion * Bolus particle size * Glycemic index

2.1. Introduction

Dietary guidelines recommend the consumption of carbohydrate-rich foods as an important source of nutrients. During human digestion, carbohydrate-rich foods are broken down, releasing high amounts of sugars, which have been related to metabolic diseases (Jenkins et al., 2002) and are the foundation for several concerns about their long-term consumption (Granfeldt et al., 1992; Singh et al., 2010). However, there is not a direct relationship between food chemical composition and these effects on health because alterations in food matrix structures lead to differences in nutrient bioavailability, rates of absorption and post-prandial outcomes that might modify their potential health risks (Turgeon & Rioux, 2011). Additionally, the breakdown of the food matrix during the digestion process affects the rate at which foods are digested (Gao et al., 2019). Therefore, clear attention should be given to the food matrix structure as well as to the food digestive process in order to understand how to control the glycemic index of carbohydrate-rich foods.

Bread represents one of the principal components of the human diet worldwide. Generally, bread matrix structure has been described as an open-cell foam consisting of highly connected pores. This porosity causes not only the characteristic bread structure but also its classification as a high glycemic index product (Fardet et al., 2007). However, modifications in bread-making process induce quality variations, including texture changes (Gao et al., 2015), and the relationship between wheat bread structure and the postprandial metabolic response has been established (Eelderink et al., 2015). Eelderink et al. (2015) reported that a more compact bread structure, caused by different processing conditions, resulted in a healthier bread. In addition, a review conducted by Björzack et al. (2018) on the glycemic index of wheat bread stated that sourdough fermentation, reduced bread volume or kneading time, and long fermentations resulted in a reduction in glycemic index. From a digestive point of view, food structure can significantly affect the digestibility by modifying the degradation degree (Gao et al., 2019).

In vitro digestion systems have been more than adequate for assessing the rate of carbohydrate digestion and absorption, namely the glycemic index (Borczak et al., 2018). These methods are useful for studying gastrointestinal food degradation without human intervention and provide an alternative to *in vivo* methods (Calvo-Lerma et al., 2018). Because of that, several *in vitro* systems simulating gastrointestinal digestion have been developed and improved (Hur et al., 2011). However, many of the digestion protocols vary depending on the study, so results are often not easily comparable. To overcome this, the INFOGEST cost action recently proposed a consensus document describing a realistic digestion system to simulate food degradation during digestion (Minekus et al., 2014). This method represents a valuable tool for determining the glycemic index. Nevertheless, the evaluation of *in vitro* food degradation is still complicated because both disintegration of food to smaller particles and lubrication of

food mass with simulated fluid should be considered. Previous studies have examined oral bread disintegration using different strategies (Gao et al., 2019), such as cutting, cut-and-pestle, blending and grinding, with the former two methods providing similar physical characteristics to *in vivo* mastication (Gao et al., 2019). Although mastication is a very complex stage, comprising food breakdown and its simultaneous lubrication with saliva, these methods have provided a representative physical measure of the *in vivo* situation. Apart from this first stage breakdown, the disintegration of swallowed food continues during digestion. However, bread disintegration in the stomach and intestine using an *in vitro* model has scarcely been studied.

In the framework of deepening the present knowledge of the influence of bread structure on the bread glycemic index, two different breads were produced using the same ingredients but varying the shaping process. Resulting breads were subjected to an *in vitro* oro-gastro-intestinal digestion, by applying different methods to the disintegrating breads, to determine the impact of the bolus particle size distribution and its influence on the glycemic index. Simultaneously, the textural parameters of the bread were evaluated in order to determine the texture effect on bolus disintegration during digestion, and on the glycemic index.

2.2. Materials and methods

2.2.1. Materials

White wheat flour was purchased from Harinera La Meta S.A (Lleida, Spain). Dry baker's yeast was provided by Lesaffre Group (Valladolid, Spain). The rest of the ingredients were acquired from the local market.

Type VI-B α -amylase from porcine pancreas (EC 3.2.1.1), mucin from porcine stomach Type II (EC 282.010.7), pepsin from porcine gastric mucosa (EC 3.4.23.1), pancreatin from porcine pancreas (EC 232.468.9), bile salts and 3,5-dinitrosalicylic acid (DNS) were purchased from Sigma Aldrich (Sigma Chemical, St. Louis, USA). Solutions and standards were prepared by using deionized water.

2.2.2. Bread preparation

Bread preparation was based on a simple recipe (100% wheat flour, 56.1% water, 1% dry baker's yeast and 1.5% salt). The amount of water used was previously determined and was that required to yield a maximum dough consistency of 1.1 Nm. The mixture was kneaded for 12 min in a mixer (Mahot Labo 25, VMI, Montaigu Vendée, France) at a high speed. After that, the dough was divided into 200 g pieces that were subjected to either automatic sheeting or rolling (L) (Ciberpan, Castellón, Spain) and placed into cardboard pans or bowling (B), to form different matrix structures. The resulting breads were leavened in a proofing chamber (Salva, Gipuzkoa, Spain) at 30

°C for 60 min and were then baked in an electric oven (F106, FM Industrial, Córdoba, Spain) at 185 °C for 25 min. After baking, the breads were cooled down at room temperature for 60 min. The breads were characterized one hour after baking, packed in polyethylene bags and stored at –18 °C for further analysis. Baking was performed by two independent trials.

2.2.3. Bread characterization

Quality parameters including moisture, crumb texture profile analysis (TPA) and crumb image analysis were assayed according to Matos and Rosell (2012). Moisture was determined following the ICC (International Association for Cereal Science and Technology) standard method (ICC 110/1). Hardness, springiness, cohesiveness, chewiness and resilience parameters were recorded from the TA.XT-Plus Texture Analysis (Stable Micro Systems Ltd., Godalming, UK) equipped with a 5 kg load cell. Parameters were measured in 10 mm central vertical slices of the resulting breads with the crust removed. During the test, the center of the crumb was double compressed with a 25 mm aluminum cylindrical probe at a crosshead speed of 1 mm/s and 30 s gap between compressions. Data from five slices per bread were averaged.

Bread crumb structure was analyzed using an image analysis system as previously described Morreale et al. (2018). Data acquired from the crumb structure analysis (slice 2D area (cm²) and surface porosity (%)) were used for comparing the different breads.

2.2.4. In vitro oro-gastro-intestinal digestion

Before digestion, bread samples were defrosted and then subjected to successive oral, gastric and intestinal digestion following the standardized static digestion method developed by Minekus et al. (2014). The selection of this protocol was based on physiologically relevant conditions.

Five grams of bread crumbs were added to 5 mL of simulated salivary fluid (SSF), containing 0.5 mL of α -amylase solution (1500 U/mL), 0.05 mL of mucin solution (0.006 g/mL) and 0.025 mL of 0.3 M CaCl₂ in SSF (prewarmed at 37 °C). Then, the mixture was subjected to two different disintegrating methods, to simulate oral processing, in order to obtain boluses with different degrees of fracturability. The first method (P) was accomplished by using an Ultra Turrax T18 basic homogenizer (IKA-Werke GmbH and Co. KG, Staufen, Germany), while the second one (B) included an Ultra Turrax Tube Drive with crystal balls (IKA-Werke GmbH and Co. KG, Staufen, Germany). For each method, the mix was stirred for 2 min at 37 °C. Gastric digestion was immediately performed by adding 7.5 mL of simulated gastric fluid (SGF) containing 1.6 mL of pepsin solution (25,000 U/mL), 0.005 mL of 0.3 M CaCl₂ and enough volume of

8M HCl to adjust the pH to 3. The mix was then digested in a shaker incubator SKI 4 (ARGO Lab, Carpi, Italy) at 37 °C under constant stirring at 150 rpm. After 2 h of gastric digestion, intestinal digestion was simulated by the addition of 11 mL of simulated intestinal fluid (SIF) containing 5 mL of pancreatic solution (800 U/mL) and 2.5 mL of 160 mM bile extract solution and 0.04 mL of 0.3 M CaCl₂. The pH was adjusted to 7.0 and then, the final mix was digested for 3 h at 37 °C under constant stirring at 150 rpm.

Different aliquots were withdrawn from the reaction vessel at different intervals of each phase of digestion. All aliquots (400 µL) were immediately mixed with 400 µL ethanol (96%) in order to stop enzyme hydrolysis. Then, the aliquots were centrifuged at 10,000 × g and 4 °C for 5 min. The pellet was washed with 200 µL ethanol (50%). The supernatants were collected and stored together at −20 °C until further use.

2.2.5. Reducing sugars released and *in vitro* starch digestibility

Aliquots from intestinal digestion were employed to determine the concentration of released reducing sugar using the DNS method. The amounts of reducing sugars were measured spectrophotometrically ($\lambda = 540$ nm) using an Epoch microplate reader (Biotek Instruments, Winooski, VT, USA). The released reducing sugars were converted into starch and expressed as glucose (mg) × 0.9.

The amount of hydrolyzed starch was plotted against the digestion time (min) after fitting experimental data to a first-order equation (Isabel Goñi et al., 1997):

$$C = C_{\infty} (1 - e^{-kt})$$

C is the percentage of starch hydrolyzed at time t , C_{∞} is the equilibrium percentage of starch hydrolyzed after 180 min, k is the kinetic constant and t is the time (min). The hydrolysis index (HI) was obtained by dividing the area under the hydrolysis curve (0–180 min) of the sample by the area of a standard material (white bread) over the same period of time. The expected glycemic index (*eGI*) was calculated using the equation $eGI = 39.21 + 0.803 HI/90$ (Isabel Goñi et al., 1997).

2.2.6. Particle size distribution of the bolus during *in vitro* digestion

The particle size in the *in vitro* digestion fractions was observed using a digital camera (EVOCam, Vision Engineering Ltd, Surrey, England). Prior to observation, the bolus samples were diluted with 150 mL of glycerol in Petri dishes (9 cm diameter) at room temperature (Le Bleis et al., 2013). Samples were examined with a magnification of 3.78×. Then, high-resolution images of the particles were acquired, and the particle size distribution was analyzed using the image analysis program (ImageJ, UTHSCSA Image Tool software, Barcelona, Spain) and NIS-Elements (Nikon Instru-

ments Inc., Tokyo, Japan) software. Images were saved as an 8-bit tiff format and the MidGrey auto local thresholding was subsequently applied with the ImageJ. Crumbs were analyzed with the NIS-Elements software, removing particles with a mean intensity value less than 150. The scale was initially set using the relationship between pixels and known distance, and then, a box plot displaying the distribution of particle size (corresponding to the particle length) was built.

2.2.7. Statistical analyses

Experimental data were subjected to an analysis of variance (ANOVA) and values were expressed as average \pm confidence interval of at least two individual measurements, using Statgraphics Centurion XV (Statistical Graphics Corporation, city, UK). Fisher's least significant differences (LSD) test was used to describe means with 95% confidence. Pearson correlation coefficient (r) and P -value were used to indicate correlations. Differences of $P < 0.05$ were considered significant. All measurements were performed at least in duplicate. For the particle size distribution analysis, the non-parametric Kruskal–Wallis test was applied to identify possible significant differences between population medians. Furthermore, the data was investigated by multivariate data analysis (principal component analysis (PCA)) with R software version 3.5.0. to determine the differences among the samples.

2.3. Results and discussion

2.3.1. Variation of bread structure as a consequence of changes in the breadmaking process

A simple recipe for wheat bread was used to obtain the dough pieces, which were shaped to conform the requirements of the loaf bread (L) or bread roll (B). The effect of the shaping process on the technological properties of the end-breads are summarized in Table 2.1. The statistical analysis revealed that the method by which dough pieces were shaped induced significant ($P < 0.05$) variations in moisture, volume (slice 2D area), texture, and crumb morphology of bread. The slice 2D area was significantly lower in L bread than in B bread, which might be related to the dough sheeting that forces the partial release of the carbon dioxide produced during bulk leavening. The images of the crumb bread sections can be observed in Figure 2.1. Parameters derived from the image analysis are summarized in Table 2.1.

Table 2.1. Moisture, morphological and texture parameters of the wheat bread crumbs.

	Loaf Bread (L)		Bread Roll (B)	
Moisture (%)	28.18 ± 2.84	a	36.73 ± 3.28	b
Slice 2D Area (cm ²)	30.86 ± 0.68	a	42.06 ± 1.77	b
Cell area (mm ²)	0.26 ± 0.01	b	0.23 ± 0.01	a
Porosity (%)	24.38 ± 1.67	a	33.88 ± 2.06	b
Hardness (N)	1.18 ± 0.10	a	2.69 ± 0.14	b
Cohesiveness	0.95 ± 0.02	b	0.86 ± 0.03	a
Chewiness	1.02 ± 0.02	a	2.74 ± 0.79	b
Resilience	0.54 ± 0.02	b	0.43 ± 0.04	a
Springiness	0.85 ± 0.08	a	0.94 ± 0.04	b

Means within the same row denoted by different superscript letters differ significantly ($P < 0.05$).

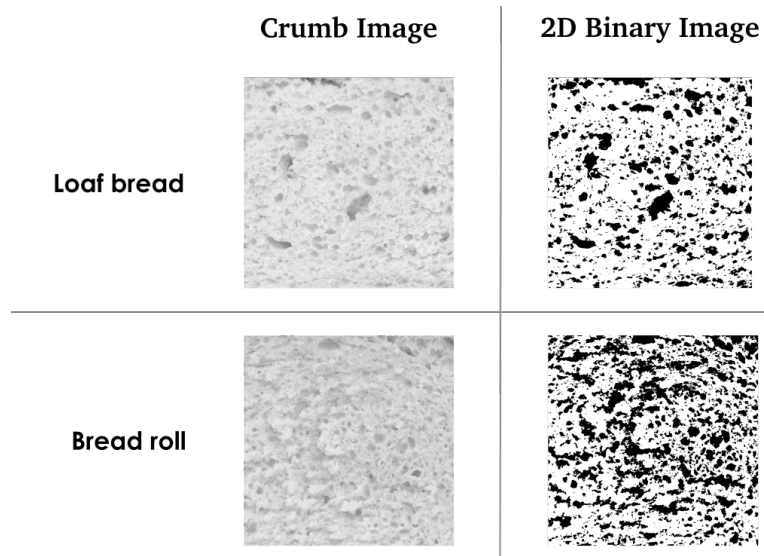


Figure 2.1. Crumb image of wheat breads shaped to conform to the requirements of the loaf bread and bread roll.

The crumb morphology of the end-breads was significantly ($P < 0.05$) influenced by the method applied to shape the dough (Table 2.1). This agrees with previous research reported by Gao et al. (2015), who showed alterations in the matrix structure due to changes in the process conditions. The authors produced three different types of bread (baguette, baked bread and steamed bread) with different structures by changing the mixing and proofing conditions, as well as the proofing and baking times. In the current study, resulting pieces of bread exhibited a highly porous crumb structure with open

pores. The loaf crumb had lower porosity and larger average cell area, in opposition to the roll performance. During shaping, different pressures were applied to the doughs in order to obtain the two types of breads. It has been reported that doughs subjected to different magnitudes of force can undergo modifications in the structure of gluten, which is related to the capacity of the mass to retain gas bubbles (Cauvain, 2015). The distinct cellular structure can be attributed to the different pressures applied during dough shaping, which altered the gas bubble structures.

Owing to the different crumb cell structures, different texture properties were also expected. The variations in the shaping process significantly ($P < 0.05$) influenced the crumb hardness, springiness, cohesiveness, chewiness and resilience (Table 2.1). Loaf bread had softer crumbs with lower chewiness and springiness, but higher cohesiveness and resilience, indicating that its structure was rapidly recovered after compression. According to Cauvain (2015), doughs with different gas retention provide breads with changes in crumb texture, which agrees with the previous observations described in the crumb morphology.

Therefore, variations in the compact degree of bread structure could be obtained by only modifying the shaping of the dough that, in turn, led to changes in texture parameters.

2.3.2. Bolus particle size throughout in vitro digestion

Figure 2.2 shows the visual appearance of L and B bread bolus particles at the final stages of the oral (Figure 2.2a), gastric (Figure 2.2b) and intestinal (Figure 2.2c) phase using a basic Ultra Turrax homogenizer (P) (Figure 2.2, letters followed by 1 or 3) or Ultra Turrax with crystal balls (B) (Figure 2.2, letters followed by 2 or 4) as simulated oral processing methods.

The bolus particles displayed different visual aspects that changed over the *in vitro* digestion. To clearly represent the particle size distribution of each bolus, analysis of the images was carried out to obtain the particle lengths and a boxplot was constructed giving the maximum and minimum values of the particle length for each bolus, as well as the upper and lower quartiles and the median values (Figure 2.3). The ANOVA analysis indicated that the method used to shape the dough significantly affected the particle size distribution. The simulated oral processing methods significantly affected the particle size distribution obtained after the oral phase in both breads, whereas the particle size distribution after the gastric and intestinal phase was significantly affected only in the case of loaf bread.

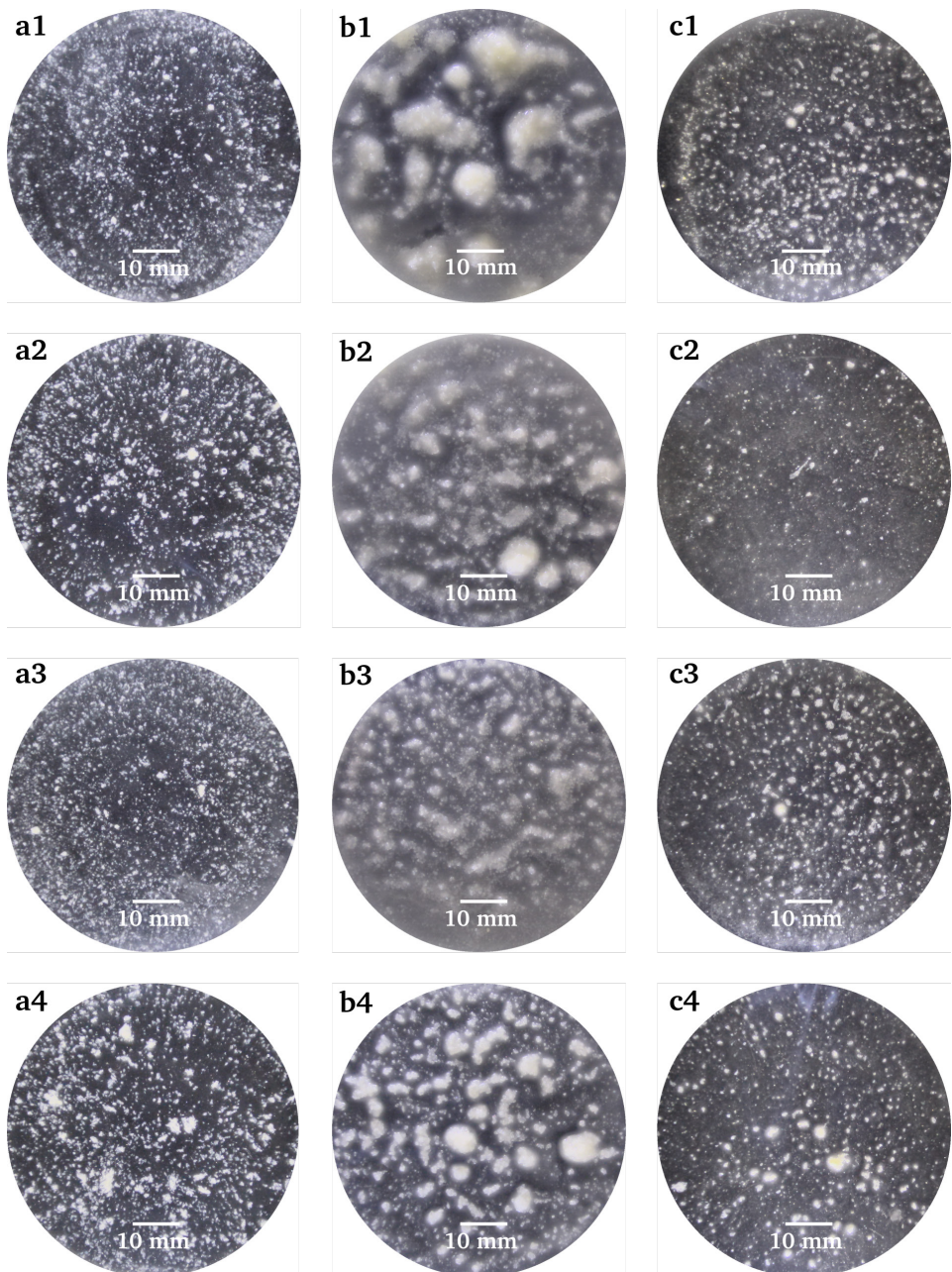


Figure 2.2. Representative images of bolus particles obtained after oral (a), gastric (b) and intestinal (c) *in vitro* digestion. Boluses were obtained from loaf bread (1,2) or bread rolls (3,4) using Ultra Turrax (1,3) or Ultra Turrax with crystal balls (2,4) as simulated oral processing methods.

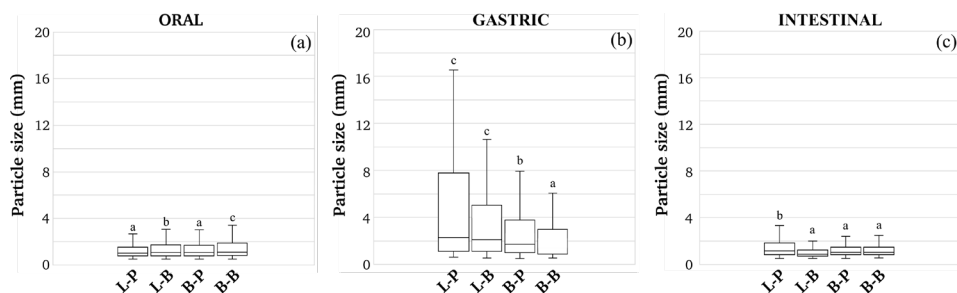


Figure 2.3. Bolus particle size obtained after the oral (a), gastric (b) and intestinal (c) phase of *in vitro* digestion. Sample names describe bread type (L-loaf, B-roll bread) followed by letters describing the simulated oral processing method applied (P Ultra Turrax and B Ultra Turrax with crystal balls). Letters on the bars indicate significant differences ($P < 0.05$).

The first step of food digestion is oral processing. In the oral cavity, the original food structure is transformed by the action of teeth and the tongue (Chen, 2015), leading to the formation of a reduced structure that can be safely swallowed (Mosca & Chen, 2016). In this regard, L-P and B-P pieces of bread were broken down into smaller particles, with a median value of 1.03 mm. A larger particle size was found in the B-B sample (median value of 1.10 mm), followed by the L-B sample (median value of 1.06 mm) (Figure 2.3a). The mean area of the particles for L-P, L-B, B-P, B-B were 0.87, 1.15, 0.77 and 1.56 mm², respectively. These results were lower than those (20–69 mm²) previously reported by Gao et al. (2019), who used different simulated oral processing methods. Nevertheless, the majority of the bolus particles (~90%) that they obtained, with all the tested *in vitro* methods, was larger than the 2 mm recommended by the standardized method (Minekus et al., 2014). It has been also described that after chewing 10 different natural foods, the median particle size (d_{50}) ranged from 0.8 to 3.04 mm, indicating their different fracturability (Jalabert-Malbos et al., 2007). Therefore, both methods used in the present study could be adequate tools to disintegrate foods when using *in vitro* methods. Once the food is swallowed, it is transported to the stomach. Unlike that reported by other authors (Bornhorst & Singh, 2013; Singh et al., 2015; Singh et al., 2010), part of the individual oral particles agglomerated during the gastric phase (Figure 2.2b). As a consequence, an increase in the particle size was observed, along with a wider size distribution in all samples. Among them, the L-P sample exhibited a larger particle size (median value of 2.27 mm), while the B-B sample displayed the lowest one (median value of 1.37 mm). In the stomach cavity, food comes in contact with gastric juice, affecting its physicochemical properties, such as size, surface charge and agglomeration state (Oberdörster et al., 2005). To properly simulate the gastric environment, the commonly suggested medium possesses a pH

around 3. In acidic medium, mucin particles form large, aggregated chains (Sriamornsak et al., 2010). Based on that, the agglomerates and, in turn, the increase in particle size could be attributed to the presence of mucin in the medium. Food digestion ends in the intestinal cavity. In the current study, the intestinal bolus particles appeared to become smaller with more homogeneous sizes (Figure 2c), with medians ranging from 0.87 to 1.16 μm (Figure 2.3c). It is worth noting at this point that mucin particles disperse as a function of pH (Sriamornsak et al., 2010). Therefore, the results obtained in the intestinal phase reinforce the suggestions mentioned for the gastric stage.

2.3.3. *In vitro* digestion and expected glycemic index

The glycemic index has been employed as a reference tool to classify the rate of carbohydrate digestion and absorption of foods (Goñi et al., 1997; Goñi et al., 2002; Granfeldt et al., 1992). Therefore, the glycemic index of L and B bread based on the application of a simulated small intestinal *in vitro* digestion system was measured. In addition, primary and secondary parameters derived from intestinal digestion were analyzed (Table 2.2).

Table 2.2. Kinetic constant (k), equilibrium concentration (C_{∞}), area under the hydrolysis curve after 180 min (AUC), hydrolysis index (HI) and estimated glycemic index (eGI) for loaf bread (L) and bread rolls (B) subjected to two different simulating oral processing methods, with Ultra Turrax (P) or crystal balls (B).

Shaping Method	Oral Processing Method	k	C_{∞} ^A	AUC	HI	eGI ^B
L	P	0.24 ± 0.05	31.94 ± 2.88 a	5600 ± 532 a	70.14 ± 6.67 a	64.86 ± 2.31 a
	B	0.27 ± 0.06	32.66 ± 0.12 a	5736 ± 48 a	71.85 ± 0.6 a	65.44 ± 0.10 a
B	P	0.13 ± 0.01	34.31 ± 2.18 a	5906 ± 355 a	73.98 ± 4.45 a	66.76 ± 1.75 a
	B	0.27 ± 0.14	44.15 ± 0.42 b	7712 ± 42 b	96.6 ± 0.52 b	74.66 ± 0.34 b
P-value						
Shaping method		0.3880	0.0316	0.0436	0.0436	0.0317
Oral processing method		0.2218	0.0738	0.0771	0.0771	0.0712

Values followed by different letters within a column are significantly different ($P \leq 0.05$). ^A C_{∞} and k were determined by the equation, $C = C_{\infty}(1 - e^{-kt})$. ^B eGI was calculated from the equation proposed by Goñi et al. (1997).

In line with previous reports (Björck et al., 1986; Goñi et al., 2002; Woolnough et al., 2010), the quantification of glucose released increased linearly during the first 20 min of intestinal digestion (Figure 2.4), and the kinetic constant (k) for the amylolysis was not significantly affected by the shaping process or simulated oral processing method. After that, a slow release of glucose was observed, reaching a plateau after 40 min of intestinal digestion.

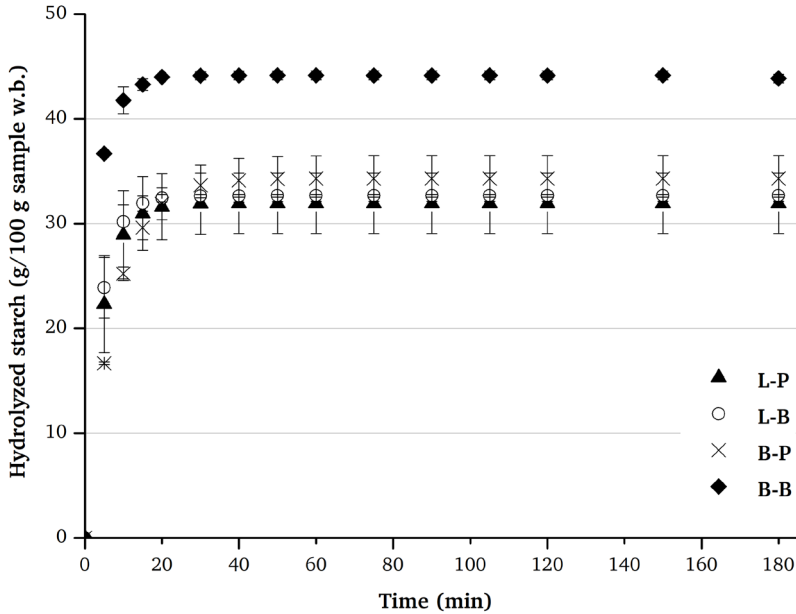


Figure 2.4. Effect of bread structure and simulated oral processing method on starch hydrolysis pattern. Sample names describe the shaping method used (L rolling mill process and B balling process) followed by letters describing the simulated oral processing method applied (P Ultra Turrax and B Ultra Turrax with crystal balls).

The statistical analysis indicated that the shaping method had a significant ($P < 0.05$) effect on the equilibrium concentration of hydrolyzed starch (C_{∞}), the area under the hydrolysis curve after 180 min, hydrolysis index (HI) and estimated glycemic index (eGI) parameters. Results obtained distinguished two different groups. The first group contained the L-P, L-B and B-P bread, which displayed similar values for these parameters. While the second group, containing the B-B sample, showed higher values for the previously mentioned parameters. A deeper statistical analysis carried out for each of the *in vitro* oral processing methods revealed that the bread structure only exerted a significant influence when the simulated oral processing method was B. Therefore, results indicated that the method used to simulate the oral processing process plays a fundamental role in *in vitro* digestion. This makes the settings defined for carrying out *in vitro* oral systems that closely follow the conditions of *in vivo* mastication deeply relevant.

2.3.4. Multivariable analysis

The PCA created from technological characteristics, as well as the digestion para-

meters measured, was used to summarize the relationship between the L and B bread digested with different simulated oral processing methods, providing easier visualization (Figure 2.5). PC1 accounted for 74.8% of the determined variances mainly explaining the variation in textural properties. Whereas the second PC accounted for 19.1% of the determined variances, representing principally the digestion parameters.

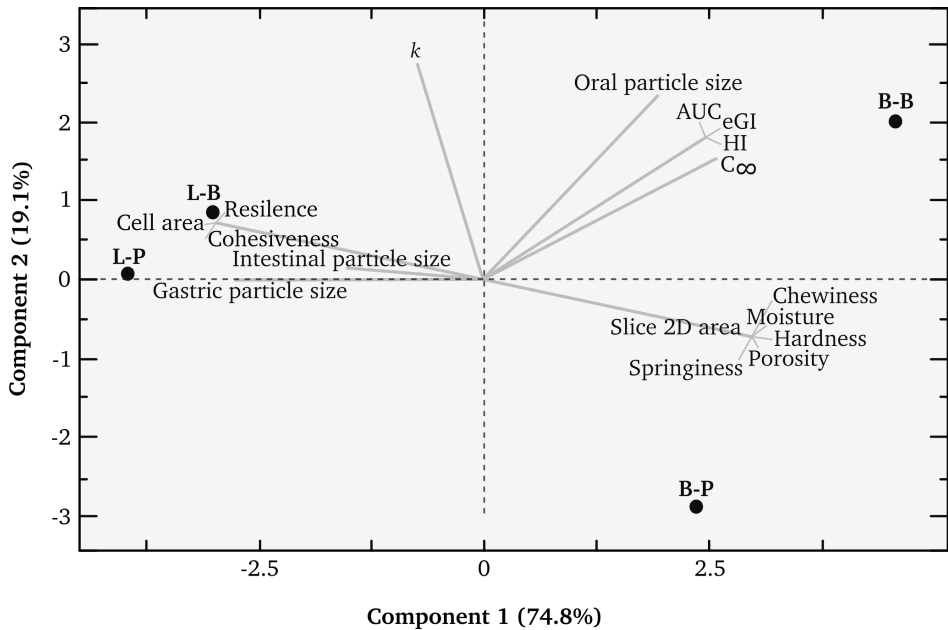


Figure 2.5. Score and loading biplot Dimension 1 \times Dimension 2 of samples and variables obtained by principal component analysis (PCA). Samples are labelled as in the text.

The loadings indicated a weak correlation between the parameters associated with bread structure and glycemic index. Nevertheless, the digestion parameters were strongly related to the oral particle size. In addition, it is important to note the negative relationships observed between structural bread parameters (porosity, hardness, chewiness, springiness, volume) and moisture, with gastric and intestinal particle size distribution, with exception of resilience and cohesiveness. It is assumed that the greater bolus disintegration, the higher glycemic index obtained, which was observed in the PCA, although the correlation obtained with gastric or intestinal particle size distribution and glycemic index was not significant.

The PCA clearly discriminated between loaf bread and bread roll, particularly along PC1. This was a result of the different matrix structures obtained by applying different shaping methods. While L bread was found to the left of the plot, B bread was at the right side, reflecting its higher moisture, volume, hardness and porosity. Similar results were obtained by Bornhorst and Singh (2013) who observed that low moisture content

in the bread promotes a large amount of gastric fluid absorption. The authors also reported that bolus disintegration varied depending on the bread structure, being faster in the bread with the highest hardness. In fact, B bread that showed higher hardness might be quickly disintegrated, giving higher starch hydrolysis. Across PC2, the samples were split between the different simulated oral processing methods used. Hence, the samples digested with Ultra Turrax could be found in the bottom half, which might be due to the low oral particle size distribution and lower glycemic index. Therefore, PCA allowed discrimination between the two crumb bread structures based on their digestibility and physical properties, indicating that breads with higher moisture, porosity, volume and hardness gave higher oral particle size and higher starch digestibility.

2.4. Conclusions

The shaping step in breadmaking played a significant role in bread structure, obtaining breads with different morphological and textural parameters. The different crumb bread structures obtained, and the *in vitro* oral processing method used, affected the bolus behavior along the *in vitro* digestion, achieving different particle sizes.

Starch hydrolysis through the *in vitro* digestion of bread showed a typical trend and it was affected by the bread structure. Bread roll masticated with Ultra turrax with crystal balls showed higher starch hydrolysis, obtaining higher eGI values, but no differences were observed when oral disintegration was carried out with a basic homogenizer. Therefore, the type of oral processing method applied to fractionate bread might allow discrimination of the performance of two bread structures during starch hydrolysis.

Overall, this study indicated that bread structure and simulated oral processing play an important role in bread digestion. Therefore, a gastrointestinal digestion analysis is essential for considering the structure of the food to be digested and the simulated method of oral processing that is carried out.

Author Contributions: Credit roles: AA: Data curation; Formal analysis; Investigation; Roles/Writing – original draft, YBG: Conceptualization; Methodology; Formal analysis; Data curation; Writing – original draft; Writing-Review & Editing; Supervision, CMR: Conceptualization; Methodology; Funding acquisition; Investigation; Supervision; Data curation; Writing - review & editing.

Acknowledgments: Authors acknowledge the financial support of the Spanish Ministry of Science, Innovation and Universities (Project RTI2018-095919-B-C21) and the European Regional Development Fund (FEDER) and Generalitat Valenciana (Project Prometeo 2017/189).

Conflicts of Interest: The authors declare that they do not have any conflict of

interest.

References

- Björck, I., Nyman, M., Pedersen, B., Siljeström, M., Asp, N. G., & Eggum, B. O. (1986). On the digestibility of starch in wheat bread — studies *in vitro* and *in vivo*. *Journal of Cereal Science*, 4(1), 1-11.
- Borczak, B., Sikora, M., Sikora, E., Dobosz, A., & Kapusta-Duch, J. (2018). Glycaemic index of wheat bread. *Starch - Stärke*, 70(1-2), 1700022.
- Bornhorst, G., & Singh, R. (2013). Kinetics of *in Vitro* Bread Bolus Digestion with Varying Oral and Gastric Digestion Parameters. *Food Biophysics*, 8, 50-59.
- Calvo-Lerma, J., Fornés-Ferrer, V., Heredia, A., & Andrés, A. (2018). In Vitro Digestion of Lipids in Real Foods: Influence of Lipid Organization Within the Food Matrix and Interactions with Nonlipid Components. *Journal of Food Science*, 83(10), 2629-2637.
- Cauvain, S. (2015). Breadmaking Processes. In *Technology of Breadmaking* (pp. 23-55). Cham: Springer International Publishing.
- Chen, J. (2015). Food oral processing: Mechanisms and implications of food oral destruction. *Trends in Food Science & Technology*, 45(2), 222-228.
- Eelderink, C., Noort, M. W. J., Sozer, N., Koehorst, M., Holst, J. J., Deacon, C. F., Rehfeld, J. F., Poutanen, K., Vonk, R. J., Oudhuis, L., & Priebe, M. G. (2015). The structure of wheat bread influences the postprandial metabolic response in healthy men. *Food & Function*, 6(10), 3236-3248.
- Fardet, A., Leenhardt, F., Lioger, D., Scalbert, A., & Rémésy, C. (2007). Parameters controlling the glycaemic response to breads. *Nutrition Research Reviews*, 19(1), 18-25.
- Gao, J., Lin, S., Jin, X., Wang, Y., Ying, J., Dong, Z., & Zhou, W. (2019). In vitro digestion of bread: How is it influenced by the bolus characteristics? *Journal of Texture Studies*, 50(3), 257-268.
- Gao, J., Wong, J. X., Lim, J. C.-S., Henry, J., & Zhou, W. (2015). Influence of bread structure on human oral processing. *Journal of Food Engineering*, 167, 147-155.
- Goñi, I., Garcia-Alonso, A., & Saura-Calixto, F. (1997). A starch hydrolysis procedure to estimate glycemic index. *Nutrition Research*, 17(3), 427-437.
- Goñi, I., Valdivieso, L., & Gudiel-Urbano, M. (2002). Capacity of edible seaweeds to modify *in vitro* starch digestibility of wheat bread. *Food / Nahrung*, 46(1), 18-20.

Granfeldt, Y., Björck, I., Drews, A., & Tovar, J. (1992). An *in vitro* procedure based on chewing to predict metabolic response to starch in cereal and legume products. *The American Journal of Clinical Nutrition*, 46(9), 649-660.

Hur, S. J., Lim, B. O., Decker, E. A., & McClements, D. J. (2011). In vitro human digestion models for food applications. *Food Chemistry*, 125(1), 1-12.

International Association for Cereal Science and Technology. ICC-Standard No 110/1. In. (Approved 1960, Revised 1976).

Jalabert-Malbos, M.-L., Mishellany-Dutour, A., Woda, A., & Peyron, M.-A. (2007). Particle size distribution in the food bolus after mastication of natural foods. *Food Quality and Preference*, 18(5), 803-812.

Jenkins, D. J. A., Kendall, C. W. C., Augustin, L. S. A., Franceschi, S., Hamidi, M., Marchie, A., Jenkins, A. L., & Axelsen, M. (2002). Glycemic index: overview of implications in health and disease. *The American Journal of Clinical Nutrition*, 76(1), 266-273.

Le Bleis, F., Chaunier, L., Della Valle, G., Panouillé, M., & Réguerre, A. L. (2013). Physical assessment of bread destructure during chewing. *Food Research International*, 50(1), 308-317.

Matos, M. E., & Rosell, C. M. (2012). Relationship between instrumental parameters and sensory characteristics in gluten-free breads. *European Food Research and Technology*, 235(1), 107-117.

Minekus, M., Alming, M., Alvito, P., Ballance, S., Bohn, T., Bourlieu, C., Carrière, F., Boutrou, R., Corredig, M., Dupont, D., Dufour, C., Egger, L., Golding, M., Karakaya, S., Kirkhus, B., Le Feunteun, S., Lesmes, U., Macierzanka, A., Mackie, A., Marze, S., McClements, D. J., Ménard, O., Recio, I., Santos, C. N., Singh, R. P., Vegarud, G. E., Wickham, M. S. J., Weitschies, W., & Brodtkorb, A. (2014). A standardised static *in vitro* digestion method suitable for food – an international consensus. *Food & Function*, 5(6), 1113-1124.

Morreale, F., Garzón, R., & Rosell, C. M. (2018). Understanding the role of hydrocolloids viscosity and hydration in developing gluten-free bread. A study with hydroxypropylmethylcellulose. *Food Hydrocolloids*, 77, 629-635.

Mosca, A. C., & Chen, J. (2016). Food oral management: physiology and objective assessment. *Current Opinion in Food Science*, 9, 11-20.

Oberdörster, G., Maynard, A., Donaldson, K., Castranova, V., Fitzpatrick, J., Ausman, K., Carter, J., Karn, B., Kreyling, W., Lai, D., Olin, S., Monteiro-Riviere, N., Warheit, D., Yang, H. (2005). Principles for characterizing the potential human health effects from exposure to nanomaterials: elements of a screening strategy. *Particle and Fibre Toxicology*, 2(1), 1-35.

Singh, H., Ye, A., & Ferrua, M. J. (2015). Aspects of food structures in the digestive tract. *Current Opinion in Food Science*, 3, 85-93.

Singh, J., Dartois, A., & Kaur, L. (2010). Starch digestibility in food matrix: a review. *Trends in Food Science & Technology*, 21(4), 168-180.

Sriamornsak, P., Wattanakorn, N., & Takeuchi, H. (2010). Study on the mucoadhesion mechanism of pectin by atomic force microscopy and mucin-particle method. *Carbohydrate Polymers*, 79(1), 54-59.

Turgeon, S. L., & Rioux, L.-E. (2011). Food matrix impact on macronutrients nutritional properties. *Food Hydrocolloids*, 25(8), 1915-1924.

Woolnough, J. W., Bird, A. R., Monro, J. A., & Brennan, C. S. (2010). The Effect of a Brief Salivary α -Amylase Exposure During Chewing on Subsequent in Vitro Starch Digestion Curve Profiles. *International Journal of Molecular Sciences*, 11(8), 2780-2790.

CHAPTER

3



In vitro digestibility of gels from different starches: relationship between kinetic parameters and microstructure

Andrea Aleixandre^a, Yaiza Benavent-Gil^a, Ramón Moreira^b, Cristina M. Rosell^{a,*}

^aInstitute of Agrochemistry and Food Technology (IATA-CSIC). C/Agustin Escardino, 7, Paterna 46980, Valencia, Spain.

^bDepartment of Chemical Engineering, Universidade de Santiago de Compostela. Rúa Lope Gómez de Marzoa, Santiago de Compostela E-15782, Spain.

*Corresponding author: Cristina M. Rosell (crosell@iata.csic.es)



Abstract

Starch performance along digestion is becoming of utmost importance owing to the extensive presence of starch in foods and its association to the foods glycaemic index. However, scarce information exists on the relationship between the digestibility of starch gels and their microstructure. The aim of the study was to identify the rate and degree of digestion of starch gels from different botanical sources and the impact of gels microstructure with the *in vitro* starch digestibility (IVSD) by fitting the hydrolysis kinetics. Starch gels from cereals, tubers, and pulses were structurally analyzed and subjected to a standardized oro-gastrointestinal IVSD. The gel microstructure was significantly different among starches. Cereal gels had thinner walls than tuber and pulses gels, and this discrimination was not evident in the area of the gel cavities. Starches hydrolysis was well fitted to a first-order kinetics model, except for rice starch gel. Potato and chickpea gels showed the slowest digestion, and in the case of potato gel some starch remained undigested at the end of the digestion. The amylose content of gels was correlated with starch hydrolysis rate. Moreover, starch gels with thinner walls and/or bigger cavities seems to facilitate the enzyme action, and therefore, the starch digestibility.



Keywords

Starch gel * In vitro digestion * First-order kinetics * Cereals * Pulses * Tubers

3.1. Introduction

Starch is a polymeric carbohydrate present in cereals, tubers, and pulses, and the most important energy source in the human diet (Chambers et al., 2019). The chemical composition, structure and properties of starches depend on their biological origin (Jayakody & Hoover, 2008), which also determines the microstructure of the resulting gels, particularly regarding shapes and hole sizes (Garzon & Rosell, 2020).

The recent concern about the increase of diabetes prevalence, and its relationship with the consumption of starchy foods, has prompted much research on how to modulate starch hydrolysis and predict the glucose release and absorption following ingestion of starchy foods (Martinez, 2020). The starch digestion rate and absorption determine the postprandial metabolic response after meal ingestion (Goñi et al., 1997). Starch digestion starts in the oral cavity, by the action of the salivary α -amylase enzyme, and continues in the intestine, by the action of pancreatic α -amylase and α -glucosidase enzymes, after being subjected to the stomach conditions. Enzyme-based approach used in the *in vitro* digestion models offers an easier and cheaper alternative to *in vivo* methods (Butterworth et al., 2012). Recently, the international COST INFOGEST network developed a standardized protocol for *in vitro* food digestion (Brodkorb et al., 2019).

When starchy foods are cooked or baked, the starch granules gelatinize, representing more than 90% of the total consumed starch (Lineback & Wongsrikasem, 1980). Most of the enzymatic digestion studies focused their investigation on starch rich food or granular starches (Bustos et al., 2017; Zhang et al., 2006). In those studies, different methods have been used to fit starch-enzyme digestion curves, like first-order kinetics (Goñi et al., 1997), or Log of slope plots (LOS) (Butterworth et al., 2012). Among them, the first-order mathematical equation proposed by Goñi et al. (1997) to fit starch hydrolysis curves ($C=C_{\infty} (1-\exp(-kt))$) has been commonly applied to study the starchy food digestion (Chung et al., 2006; Frei et al., 2003; Segura & Rosell, 2011). Alternatively, first-order model involves two parameters related to the digestion equilibrium (equilibrium concentration, C_{∞}) and the digestion rate (kinetics constant, k). Nevertheless, in those studies, only some of them reported the hydrolysis of gels from starches using the INFOGEST oro-gastro-intestinal standardized method (Feltre et al., 2020; Lavoisier & Aguilera, 2019; Noda et al., 2008). However, despite the applicability of this method to follow the impact of different compounds on digestion, to our best knowledge there is no information about the hydrolysis kinetics of starch gels. Therefore, we initially hypothesize that the oro-gastrointestinal standardized method could be applied to starch gels.

The main purpose of this study was to study the starch hydrolysis kinetics of different starch gels by applying the oro-gastrointestinal standardized method. The particular objectives included: (i) the characterization of the microstructure of starch gels, (ii) the analysis of *in vitro* oro-gastrointestinal digestion of gels and (iii) the experimental

starch hydrolysis data fitting using a first-order kinetic-based model. For that purpose, different starches, three from cereals (wheat, corn, rice), two from pulses (green pea, chickpea), one from potato and other from cassava were selected. Although, cassava is a root tuber, not a tuber like potato, henceforth both starches will be grouped as tuber starches.

3.2. Materials and methods

3.2.1. Materials

The following starches were used: wheat starch (ADM Chamtor, Bazancourt, France), corn starch (Tate & Lyle PLC, London, United Kingdom), rice starch (Sigma Chemical, St. Louis, USA), potato starch (Tereos, Lille, France), cassava starch (local market), and green pea starch (*Pisum sativum*) (Esteve Santiago, Valladolid, Spain). Chickpea was purchased in the local market and used for starch isolation.

Type VI-B α -amylase from porcine pancreas (EC 3.2.1.1), pepsin from porcine gastric mucosa (EC 3.4.23.1), pancreatin from porcine pancreas (EC 232.468.9), bile salts and 3,5-dinitrosalicylic acid (DNS) were purchased from Sigma Aldrich (Sigma Chemical, St. Louis, USA). Other chemicals were of analytical grade. Solutions and standards were prepared using deionized water.

3.2.2. Chickpea starch isolation

Chickpea starch was isolated from the autochthonous chickpea (Pedrosillano variety), due to its higher content in total carbohydrates and lower fat content, compared with other cultivars (Gómez et al., 2008). The isolation was performed using the method described by Demirkesen-Bicak et al. (2018) with minor modifications. Chickpea samples were ground in a Fitzpatrick mill (Fitzmill model, Waterloo, ON, Canada). The powder was mixed with distilled water (1:10) and screened through nylon cloth (170 mesh). Sediment was successively washed with distilled water till it was free of starch. The filtrate slurry was left to rest 1 h and centrifuged at 4,000 x g for 5 min. The upper yellow layer was scrapped off. The white part of the sediment was resuspended in distilled water and recentrifuged for 3-4 times using the settings described above. Isolated starch was dried at 40°C for 12 h in a drying oven and stored at 4°C for further analyses.

3.2.3. Starch gel preparation

Starch samples were mixed with distilled water (1:10) and boiled on a water bath for 15 min, with gentle manual agitation every 2 min. Preliminary analysis were carried out to confirm the homogeneity of the gels using SEM. Gels were immersed in liquid

nitrogen and kept at -80°C till freeze-drying at a pressure between 666 and 133 Pa during 24 h. Two replicates of each gel were prepared. Freeze-dried samples (average moisture content of was $14.52 \pm 4.26\%$) were stored at 4°C till further analysis. The absence of amylopectin retrogradation was verified using a differential scanning calorimetry analysis (data not shown).

3.2.4. Chemical composition of starches

Standard methods were used to determine the native starch physicochemical composition (AOAC, 2000). Total protein content was analyzed according to AOAC Method 992.23. Data were expressed as percentage on a dry weight (DW). Total starch content was determined following the AOAC Method 996.11 using a thermostable α -amylase (Termamyl[®], EC 3.2.1.1) (Novozymes, Bagsværd, Denmark) and amyloglucosidase from *Rhizopus sp.* (EC 3.2.1.3) (Sigma Chemical, St.Louis, USA). Briefly, the starch sample ($0.100 \text{ g} \pm 0.001 \text{ g}$) was suspended in 0.2 mL of 80% ethanol. Then, 2 mL of 1.7 M sodium hydroxide solution were added and tubes vortexed for 15 min before adding 8 mL of 600 mM sodium acetate buffer at pH 3.8. Immediately, α -amylase (280 U) and amyloglucosidase (330 U) were incorporated and samples incubated at 50°C for 30 min. An aliquot of 2 mL was centrifuged for 5 min at $10,000\times \text{g}$ and the supernatant (1 mL) diluted with 10 mL of 100 mM acetate buffer at pH 5. Finally, the glucose content was measured using a glucose oxidase-peroxidase (GODPOD) kit (Megazyme International Ireland Ltd., Bray, Co. Wicklow, Ireland). The absorbance was measured using an Epoch microplate reader (Biotek Instruments, Winooski, USA) at 510 nm. Amylose content of the starches was measured using a commercial amylose/amylopectin assay kit (K-AMYL 06/18, Megazyme International Ireland Ltd., Bray, Co. Wicklow, Ireland) based on Concanavalin A precipitation.

3.2.5. In vitro oro-gastro-intestinal digestion and reducing sugar analysis

Gel samples were subjected to successive oral, gastric and intestinal digestion following the standardized static digestion method developed by Minekus et al. (2014) with minor modifications in the oral step. Portions of freeze-dried starch gels (1.65 g) were used for the digestion evaluation. This amount was selected considering it corresponds to the total starch ingested in 5 g of bread. To simulate oral processing during the oral phase, samples were disintegrated following the methodology described by Aleixandre et al. (2019). Starch was blended with simulated salivary fluid containing α -amylase solution (750 U) in an Ultra Turrax Tube Drive with crystal balls (IKA-Werke GmbH and Co. KG, Staufen, Germany). The gastric and intestinal digestion followed exactly the procedure previously cited (Minekus et al., 2014). Aliquots obtained during

gastric and intestinal *in vitro* digestion (200 μL) were immediately mixed with ethanol (96%) (400 μL) to stop the enzyme hydrolysis. Samples were centrifugated at 10,000 x g and 4°C for 5 min. The pellet was washed with ethanol (50%) (200 μL) and centrifugated again, then supernatants were pooled together. Released reducing sugars were quantified using the DNS method (Miller, 1959). Maltose content was measured in a microplate reader (Epoch Biotek Instruments, Winooski, VT, USA) at 540 nm. Experimental values were the mean of four replicates.

3.2.6. Starch digestion modelling

Several models (first-order kinetics, parallel and sequential kinetics) typically employed for digestion of native starches and starchy foods (Haiteng et al., 2019) were tested to fit the *in vitro* intestinal digestion of starch gels. The first-order kinetics-based model, Eq. (1), was the most suitable to fit experimental pre-gelatinized starch digestion.

$$C = (100 - C_i - C_\infty) \exp(-k t) + C_\infty \quad (1)$$

being C the fraction (%), respect to initial starch, of remnant starch to be digested at time t (min) of digestion, C_i the fraction (%) of starch hydrolyzed in the previous gastric phase ($t=0 \rightarrow C=100-C_i-C_\infty + C_\infty=100-C_i$), k (min^{-1}) and C_∞ (%) are the kinetics constant and the fraction of undigested starch in the intestinal phase at time infinite.

The goodness of fittings was evaluated employing the coefficients of determination (r^2) and root mean square error (RMSE) Eq. (2):

$$\text{RMSE} = \sqrt{\frac{\sum_{i=1}^N (C_{\text{exp}} - C_{\text{mod}})^2}{N}} \quad (2)$$

where N is the number of experimental data and C_{exp} and C_{mod} the experimental data and calculated values by Eq. (1) of starch hydrolysis kinetics during the *in vitro* digestion.

3.2.7. Scanning electron microscopy (SEM)

Microstructure of starch gels, before and during digestion, were analyzed by scanning electron microscopy. Samples were coated with gold using a vacuum evaporator (JEE 400, JEOL, Tokyo, Japan). Observations were done using a SEM (SEM, S-4800, Hitachi, Ibaraki, Japan). All the images were recorded at an accelerating voltage of 10 kV.

Structure analysis of starch gels was carried out using the ImageJ software (National Institutes of Health, Bethesda, MD, USA) as reported Garzon and Rosell (2020). Wall thickness (μm) and hole area (μm^2) were measured. In addition, P10, P50, and P90 were defined to describe that 10%, 50% and 90% of the holes had a lower size or thickness than the ones indicated.

3.2.8. Statistical analyses

All analyses were carried out in duplicate. Mean values and standard deviations are reported. Statistical analyses of experimental results were carried out with Fisher's least significant differences test with 95% confidence. Statgraphics Centurion XV software (Statistical Graphics Corporation, Rockville, MD, USA) was used to calculate Pearson correlation coefficient (r) and P -value. Differences of $P < 0.05$ were considered significant.

3.3. Results and discussion

3.3.1. Starch gels

Gels were prepared from the different starches and their microstructure was analyzed by SEM (Figure 3.1)

Micrographs confirmed the diverse microstructure of the different gels depending on the starch source. Gels did not show any residual starch granules, therefore, heating in water excess resulted in the complete gelatinization of the different starches. All gels displayed a honeycomb or sponge-like structure, typical pictures for gel fractures (Benavent-Gil et al., 2019). Nevertheless, visible differences were observed in the size distribution of the voids and the wall thickness. The micrographs showed that the gels obtained from cereal and tuber starches exhibited well-defined voids or holes with walls separating them. Gels from cassava and potato starches appeared like stronger networks based on the thicker walls separating the cavities. Conversely, pulses gels displayed a more irregular structure with thin and needle-like edges that resembled sub-cavities within the main network, particularly in the case of green pea gel. Li et al. (2007) described a similar irregular structure in gels from corn starch and soy protein concentrate composite. Because of that the chemical composition of starches was assessed (Table 3.1).

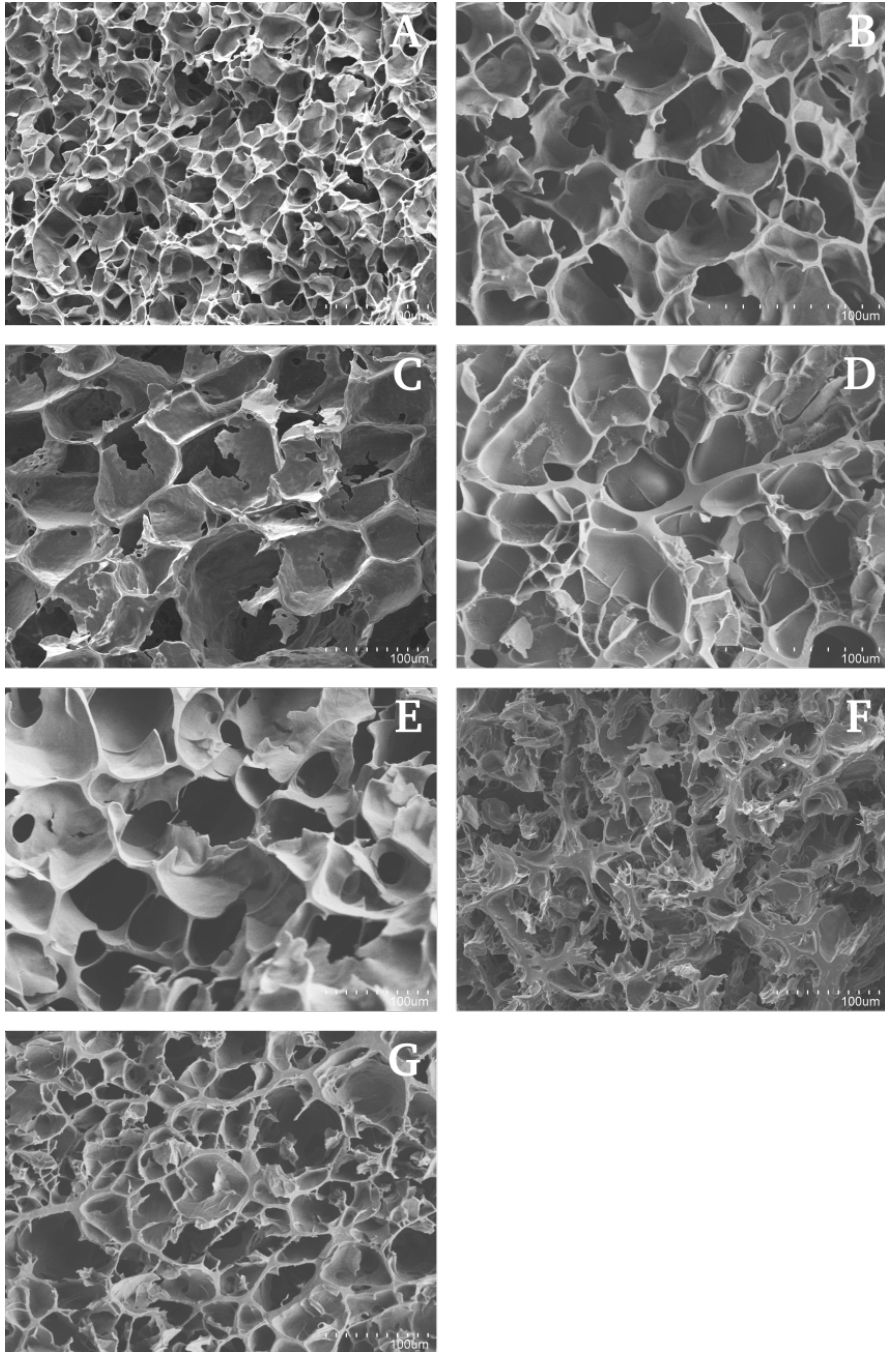


Figure 3.1. SEM micrographs of starch gels from wheat (A), corn (B), rice (C), potato (D), cassava (E), green pea (F), chickpea (G). Magnification x300.

Table 3.1. Chemical composition of starches from different sources (% DW).

Starch source	Protein		Total starch		Amylose	
Wheat	0.64 ± 0.08	a	88.94 ± 2.81	b	27.64 ± 0.25	b
Corn	0.88 ± 0.02	b	94.70 ± 2.06	c	28.13 ± 2.48	b
Rice	0.89 ± 0.11	b	95.63 ± 2.06	c	14.39 ± 0.07	a
Potato	0.58 ± 0.01	a	92.90 ± 0.65	bc	29.38 ± 1.14	bc
Cassava	0.57 ± 0.04	a	92.32 ± 2.49	bc	32.09 ± 0.72	c
Green pea	16.14 ± 0.14	d	74.24 ± 0.50	a	38.49 ± 1.81	d
Chickpea	1.78 ± 0.02	c	91.62 ± 1.54	bc	41.05 ± 0.67	d

Means within a column followed with different letters are significantly different ($P < 0.05$).

All starches presented total starch contents above 90% (DW), except for wheat ($89 \pm 2.81\%$) and green pea ($74 \pm 0.5\%$) samples. These results were within the range of those previously reported (Huang et al., 2007; Mishra & Rai, 2006). Regarding amylose, in general, cereal starches showed lower amylose levels, followed by tuber starches with intermediate values and pulse starches having the highest amylose contents. Therefore, amylose content varied from 14.39% in the case of rice starch to 41.05% exhibited by chickpea starch. These results are in accordance with earlier reports, where pulse starches showed higher amylose content than tubers and cereals (Bajaj et al., 2018; Kaur et al., 2015). The protein content of cereal and tuber starches was rather low, with values ranging from $0.57 \pm 0.04\%$ (cassava) to $0.89 \pm 0.11\%$ (rice). Pulse starches showed significantly higher protein content, especially green pea sample ($16.14 \pm 0.14\%$). Likely, the remarkable presence of proteins in those starches might explain the irregular structure above described for pulse gels. Image analysis was applied to evaluate the wall thickness and the area (hole size) of the different holes or cavities of the gels (Figure 3.2).

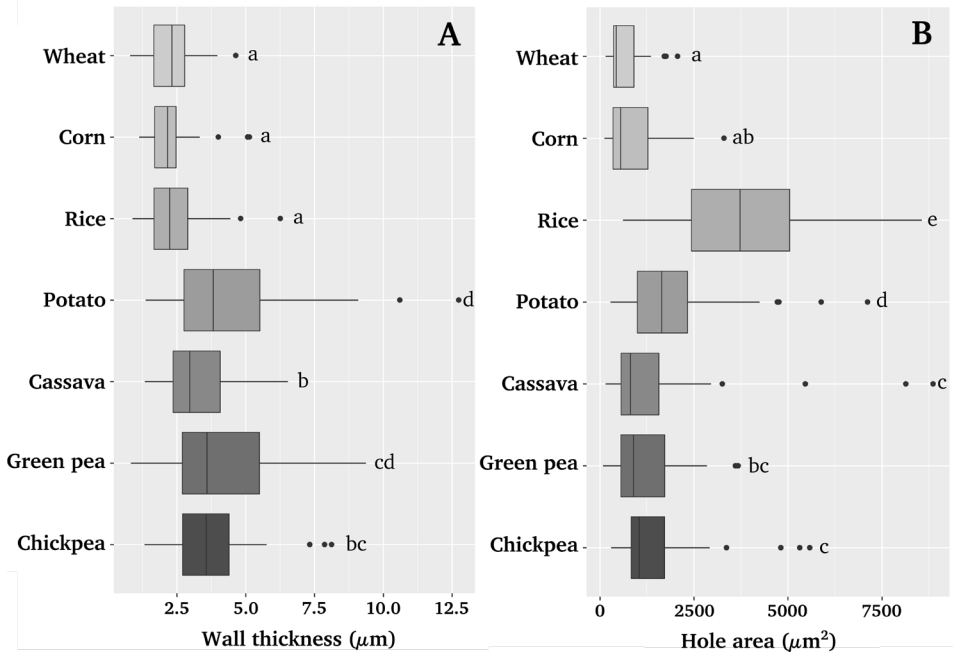


Figure 3.2. Boxplots showing the parameters calculated by image analysis of the gel micrographs. A) Wall thickness and B) hole size distribution.

The analysis confirmed significant differences ($P < 0.001$) among the microstructure of the gels (Table 3.2).

Table 3.2. Microstructure characteristics of starch gels from different sources.

Starch source	Wall thickness (μm)				Hole area (μm ²)					
	Mean ± SD	P10	P50	P90	Mean ± SD	P10	P50	P90		
Wheat	2.32 ± 0.84	a	1.35	2.32	3.55	654.88 ± 452.89	a	212.60	436.71	1298.85
Corn	2.23 ± 0.81	a	1.42	2.16	2.95	874.93 ± 756.07	ab	194.20	550.63	2101.60
Rice	2.39 ± 0.96	a	1.41	2.24	3.36	3882.15 ± 1981.35	e	1431.74	3729.66	6635.78
Potato	4.28 ± 2.20	d	2.00	3.82	6.49	1956.68 ± 1360.75	d	689.22	1647.08	3912.44
Cassava	3.25 ± 1.26	b	1.89	2.89	5.42	1418.11 ± 1644.03	c	356.23	810.66	2725.76
Green pea	4.06 ± 2.03	cd	1.99	3.49	7.21	1284.60 ± 981.65	bc	434.85	891.30	2823.56
Chickpea	3.71 ± 1.43	bc	2.32	3.57	5.43	1449.34 ± 1120.67	c	450.20	1048.42	2754.92
P-value	0.0000				0.0000					

P10, P50 (median), and P90 indicates that 10%, 50% or 90% of the values (wall thickness or hole area) lie to the ones specified.

Regarding wall thickness, despite the outliers observed, cereal-based gels showed thin walls with mean values of 2.32 ± 0.84 , 2.23 ± 0.81 , and $2.39 \pm 0.96 \mu\text{m}$ for wheat, corn, and rice, respectively. Tuber and pulse gels had thicker wall cells than cereal gels, with mean values ranging from 3.25 to 4.28 μm . Green pea gel exhibited bigger data dispersion, which ranged from 0.83 to 9.37 μm , likely due to the sub-cavities having needle-like walls, previously mentioned, intertwined with larger cavities. Maybe its higher protein content might also contribute to its microstructural features.

Data distribution of wall thickness and hole area of cavities was split into P10, P50 (median) and P90 to reflect the 10%, 50% and 90% of the values of those parameters lie below those percentages, respectively. The wall thickness median (P50) also showed that cereal gels had thinner walls than pulses. In the case of tubers, cassava exhibited an intermediate wall thickness median, but potato gels had an even higher median than pulses (Table 3.2). In addition, P90 showed that 90% of the holes exhibited very thin walls in the cereals, but the discrimination between tuber and pulses starches, previously mentioned, did not exist. The analysis of the hole area showed significant differences among starch gels ($P < 0.001$) (Table 3.2). All samples exhibited a right skewed distribution and several outliers. The smallest mean value area was obtained for wheat gel ($654.88 \mu\text{m}^2$), in opposition to the largest mean area obtained for rice gel ($3882.15 \mu\text{m}^2$). Also, rice gel showed the widest distribution of cavity areas.

To identify possible relationships between gels microstructure and proximate composition, correlations were evaluated. A positive correlation was observed between wall thickness P10 and the amylose content ($r = 0.76$, $P < 0.05$). This finding agrees with the reported role of amylose content in structural changes in corn starch gels, making them more resistant to swell and disintegrate (Schirmer et al., 2013). The easier interaction of linear amylose chains may cause higher integrity. Equally, a low amylose matrix, like the one obtained with rice gel, has been related to open structures that tend to disintegrate in water (Biduski et al., 2018).

3.3.2. *In vitro* digestion and modelling

Gels samples were digested following an *in vitro* oro-gastrointestinal digestion, which was recorded by quantifying the reducing sugars released. Figure 3.3 showed the raw starch hydrolysis data during the oro-gastrointestinal digestion to better display the whole *in vitro* digestion.

During the oral stage, slight starch hydrolysis was detected, remaining barely constant during gastric digestion until the beginning of the intestinal phase. Previous studies reported amylase activity in the gastric phase, and they associated to some starch hydrolysis in this phase (Bustos et al., 2017). Those authors studied the gastric digestion of different cereal-based foods, like bread, pasta, and cookies, recording starch hydrolysis during the first 60 min of the gastric phase, likely due to the residual salivary

α -amylase activity. Divergences might be explained by the complexity of the food matrices used by those authors since other polymeric compounds like the gluten network can protect salivary α -amylase in the acidic gastric medium (Bhattarai et al., 2016). In contrast to that, the present research was performed with the unique presence of starch.

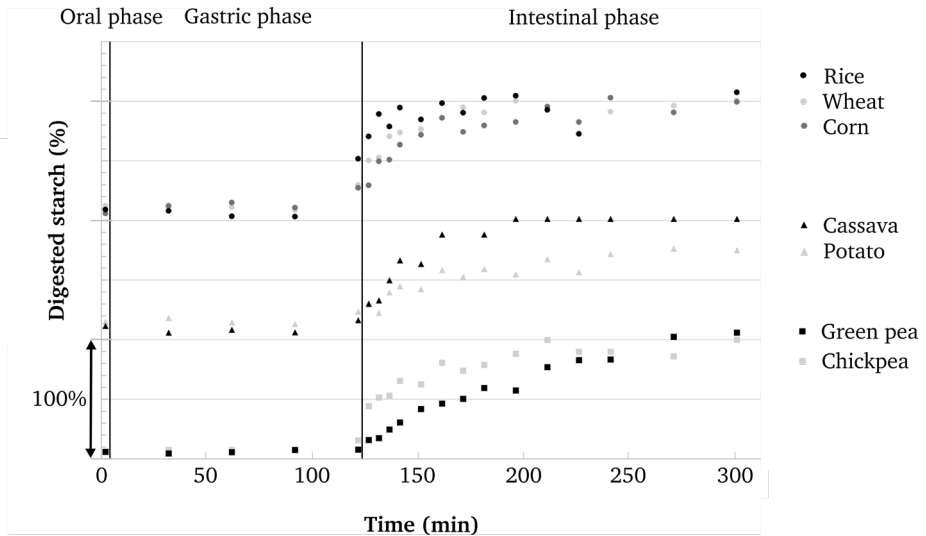


Figure 3.3. Starch hydrolysis from starch gels during the oro-gastrointestinal *in vitro* digestion. Vertical lines divided the graph into digestion phases: oral, gastric, and intestinal. Starch gels were grouped according to their source proximity. Scale bar of 100% indicates the value of the graduation marks.

Starch hydrolysis along the different stages was evaluated following different kinetic models, but only intestinal data were further analyzed. To adjust the experimental data obtained along intestinal starch hydrolysis (Eq. 1), the mean value of the percentage of hydrolyzed starch along the gastric phase (C_i) was used (Table 3.3).

Table 3.3. Statistical parameters for goodness assessment of non-linear fitting with a first-order kinetics-based model (Eq. (1)).

Starch source	C_i (%)	k (min^{-1})	C_∞ (%)	r^2	RMSE	t50 (min)*
Wheat	14.42	0.061	0.00	0.978	5.76	5.7
Corn	15.03	0.039	0.00	0.975	6.40	11.8
Rice	10.37	0.265	0.00	0.876	8.21	0.95
Potato	18.16	0.024	27.70	0.944	5.79	36.5
Cassava	7.32	0.043	0.00	0.987	4.75	14.4
Green pea	9.01	0.064	14.10	0.959	6.27	9.3
Chickpea	7.82	0.013	0.00	0.990	3.85	45.0

*t50, digestion time to reach the 50% of the total starch digestion.

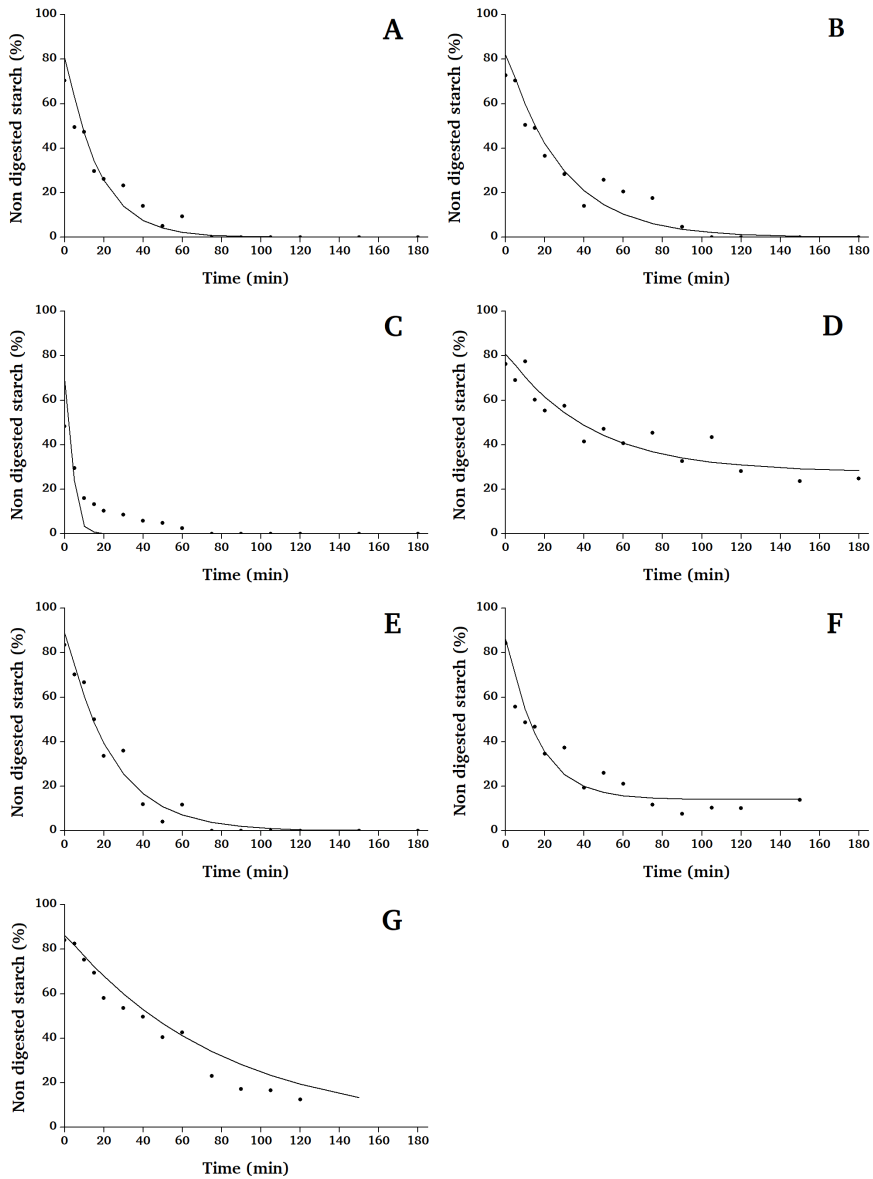


Figure 3.4. Starch digestibility plots during intestinal *in vitro* digestion for wheat (A), corn (B), rice (C), potato (D), cassava (E), green pea (F), chickpea (G) gels.

Values for C_i ranged from 7.32% (cassava) to 18.16% (potato), indicating the significant differences in the extent of starch digestion after oral and gastric digestion, depending on the type of starch. Starch hydrolysis during the intestinal stage was evaluated following different models and first-order kinetics model gave the best fitting (Figure 3.4).

Plots showed the differences in starch hydrolysis depending on the type of starch. Wheat, corn, rice, cassava, and green pea gels showed rapid digestion in the first 120 minutes of the intestinal phase. In fact, 50% of total digestion of wheat, rice, and green pea starches was obtained in less than 12 min (Table 3.3). Rice gel was digested more rapidly, during the first 0.95 min. However, a different behavior was observed for potato and chickpea gels, in which starch was not totally hydrolyzed during the 3 hours of intestine digestion, reaching a plateau (potato) at the end of the intestinal phase or even without apparent equilibrium achievement at that time (chickpea). From the kinetics model (Eq. (1)), it was possible to calculate the hydrolysis rate (k) and the percentage of undigested starch at time infinite (C_∞), and the statistical parameters for goodness assessment (Table 3.3).

Differences among gels could be readily evident when assessing k and C_∞ . Except for rice gel, experimental data were satisfactorily fitted ($r^2 > 0.944$; $RMSE < 6.40$). Rice gel ($r^2 = 0.876$; $RMSE = 8.21$) exhibited the highest k value, suggesting a high enzymatic reaction rate. Lower amylose content starches like waxy starches show easier disruption (Schirmer et al., 2013). Likely the weaker structure of rice gel favored the disappearance of the gel structure and the access of the enzymes to the starch gel, explaining this high digestion rate. Another atypical result was obtained with chickpea gel that had a low k value (0.013 min^{-1}) and null predicted C_∞ , but digestion rate did not achieve the plateau during the 3 h. Maybe the manual isolation method used for chickpea starch can affect gel characteristics. Surely, longer experimental digestion time would allow the achievement of the plateau and a more valid C_∞ could be obtained. Previous studies stated that the digestibility of granular starches from pulses was faster than that of potato or waxy corn starches, but slower than cereal or cassava starches (Srichuwong et al., 2005). Present results with gels confirmed that green pea gel had faster hydrolysis than cassava, potato, wheat, and corn gels but was slower than this observed for rice gels. Nevertheless, chickpea gel showed very low digestion. In the case of granular starch from pulses, this low digestion rate has been explained based on the high amylose content, amylose-lipid, or amylose-protein complexes (Bhattarai et al., 2016; Chung et al., 2008), which might also affect gels digestion, although no trend was observed considering results obtained with green pea gel. Several studies have indicated that the presence of high amylose content decreases starch digestibility due to the formation of double helices during cooling introducing an additional and relevant resistance to enzymatic action (Chung et al., 2010; Zhu et al., 2011). Globally,

a significant negative relationship between k and amylose content ($r = -0.829$) was observed in the present study, where chickpea gels (the highest amylose content) and rice gels (the lowest amylose content) showed the slowest and fastest digestion rates, respectively.

Recent studies have evaluated the effect of structural characteristics (degree of branching, molecular weight, chain lengths, etc.) of amylose and amylopectin on digestibility of native and cooked starches (Syahariza et al., 2013; Yu et al., 2018). These studies suggested that the digestion rate increased with the chain length of amylose and with the low number of long amylopectin branches. To test that hypothesis with the present results, the average chain length of amylose obtained from the bibliography for the tested starches (203, 323, 300, 595, 500, 340, 1420 for wheat, corn, rice, potato, cassava, green pea and chickpea, respectively) (Bertoft, 2017; Charoenkul et al., 2006; Tinay et al., 1983; Yoshimoto et al., 2001) was used to detect possible correlations. It was found an exponential (negative) relationship ($r = -0.787$) between kinetics constant and amylose size, without consideration of the rice results due to its low amylose content and probable different physical and structural resistances to enzymatic activity commented above. These results suggest that the digestion rate of starch gels decreased dramatically with increasing chain length amylose. This fact could be related to the higher recrystallization found in long-chain amylose gels (Baranowska et al., 2020), which makes them more inaccessible to digestive enzymes.

It is important to stress that initial gel microstructure data also showed a correlation with digestion parameters ($P < 0.05$). A highly significant positive correlation was observed for starch gel area cavities with the rate constant ($r = 0.87$), and for wall thickness of starch gel cavities with t_{50} ($r = 0.81$). These results suggest that bigger cavities favored the access of the digestive enzymes on the starch gels and thicker gel walls required longer to be hydrolyzed, although all intrinsic properties of gel networks might not be discarded. The latter occurred except for green pea gel, which showed the thickest cavity walls but low time for hydrolyzing 50% of the total starch. The high protein content of this gel might be responsible for the resulting wall thickness, without affecting the starch hydrolysis. Therefore, an open starch gel microstructure with big holes and thin walls is more susceptible to enzyme activity.

Trying to relate digestion results with gels microstructure, digested gels at the end of the oro-gastric and intestinal phase were microscopically observed (Figure 3.5).

The digested samples underwent centrifugation and freeze-drying to remove gastrointestinal fluids. In the present study, gels kept their structure after the oral phase, except for the cereal gels that lost much of their structures. Baudron et al. (2019) reported that freeze-drying conditions might affect the density and surface area of the starch gels. Even when this methodology may affect starch gel structures, micrographs confirmed different digestion performance of the gels, depending on the starch origin.

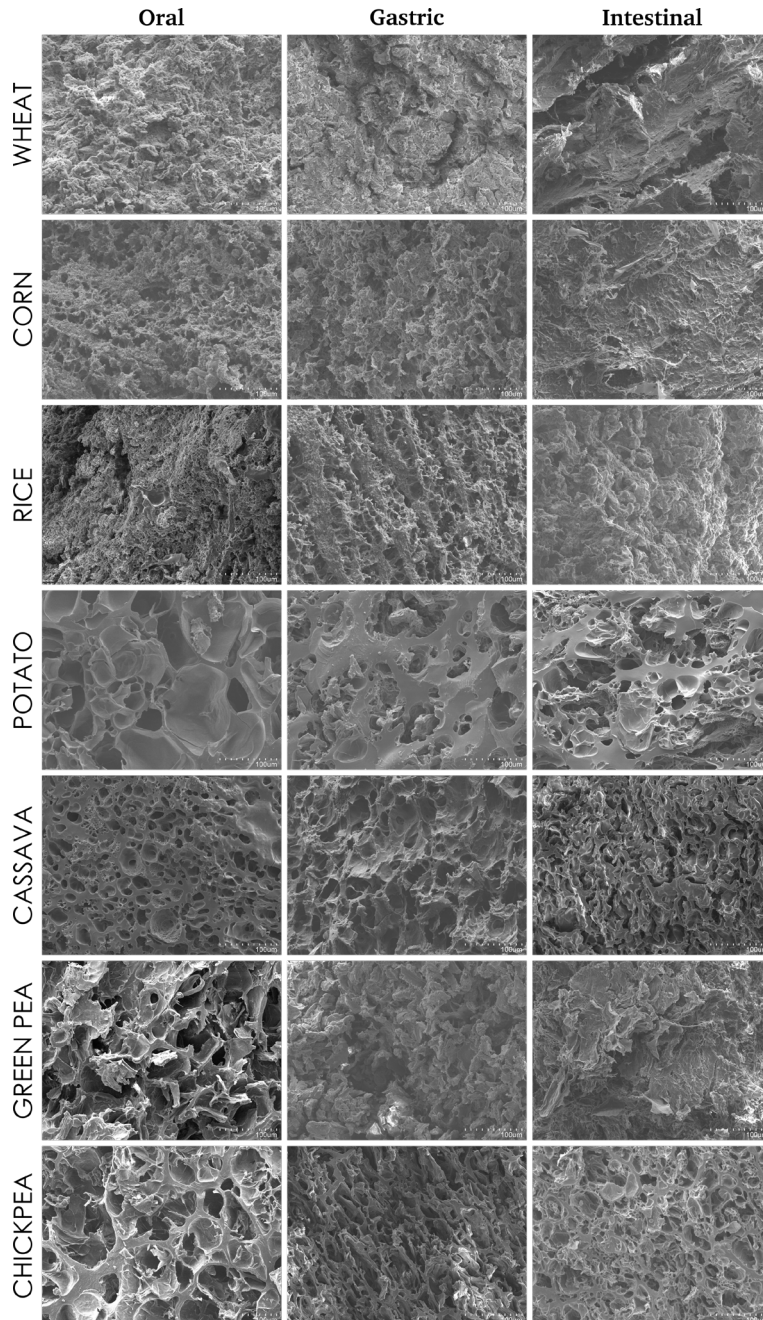


Figure 3.5. SEM micrographs of digested starch gels after oral (1), gastric (2) and intestinal (3) *in vitro* digestion. Gels were obtained from wheat (A), corn (B), rice (C), potato (D), cassava (E), green pea (F), chickpea (G). Magnification x300.

In tubers and pulses gels, the honeycomb structure remained in a certain way after oral digestion. After gastric phase, potato micrographs showed a plane surface with small cavities. Likely, the faster potato hydrolysis indicated by C_i , led to the removal of the fragile parts of the structure, only remaining the compact one with small cavities. Plane structures with small holes are less accessible to intestinal digestive enzymes, hindering starch digestibility, which would explain the lower kinetic constant (k) obtained in the intestinal phase. Conversely, cassava gels revealed a more open structure at the end of gastric digestion, being easier the diffusion of enzymes through starch and digestion fragments. In spite of the low starch hydrolysis of starch gels in the gastric phase, other factors like the acidic pH might explain changes in the gel structure. Great structural changes were observed in the pulse gels after the gastric phase, although starch was barely hydrolyzed. Those changes might be linked to the protease activity of the pepsin added in the stomach phase, which hydrolyze the protein fraction of those gels changing their structure. At the end of the intestinal digestion, in the cereal starches the initial structure was completely lost. Potato and chickpea samples kept the typical structure of starch gels in some way. This observation agrees with digestion results, where potato and chickpea starch gels did not achieve the digestion equilibrium. However, also cassava gel maintained some cavities, but the digestion results showed total starch hydrolysis at 120 min. Probably, digestive enzymes attack the more accessible parts of this gel, keeping the porous structure.

3.4. Conclusions

This study showed significant differences in the structure of starch gels from different sources, particularly, in the gel cavities areas and the thickness of the hole walls. Cereal based gels showed thinner walls, compared to tuber and pulses starches. Some microstructural features with thin and needle-like edges of starch gels from pulses were associated to high protein content. Regarding the area of the cavities, tuber, and pulses gels showed bigger cavities, although rice gel gave the biggest hole area. Starch gel hydrolysis through a standardized oro-gastrointestinal *in vitro* digestion was different for each starch gel, and microscope analyses revealed changes in gel structure from the beginning of *in vitro* digestion. The fitting method was applied to analyze the kinetics of the intestinal stage, and the first-order kinetics model reproduced satisfactorily the starch hydrolysis trend during intestinal *in vitro* digestion, except for rice starch. Differences in starch digestibility were observed depending on the starch source. It was confirmed that the amylose content of starch gels played an important role in their hydrolysis. However, the initial microstructure of gels showed a correlation with digestion parameters, where bigger cavities facilitated the starch hydrolysis.

Author Contributions: Credit roles: AA: Conceptualization; Data curation; Formal analysis; Investigation; Methodology; Writing - original draft; YBG: Methodology; Supervision; RM: Formal analysis; Writing - review & editing; Funding acquisition; CMR: Conceptualization; Funding acquisition; Investigation; Supervision; Data curation; Writing - review & editing.

Acknowledgments: Authors acknowledge the financial support of the Spanish Ministry of Science and Innovation (Project RTI2018-095919-B-C2) and the European Regional Development Fund (FEDER) and Generalitat Valenciana (Project Prometeo 2017/189).

Conflicts of Interest: The authors declare that they do not have any conflict of interest.

References

- Aleixandre, A., Benavent-Gil, Y., & Rosell, M. C. (2019). Effect of Bread Structure and In Vitro Oral Processing Methods in Bolus Disintegration and Glycemic Index. *Nutrients*, *11*(9).
- AOAC. (2000). *Official methods of analysis of the AOAC International*: Association of Analytical Communities.
- Bajaj, R., Singh, N., Kaur, A., & Inouchi, N. (2018). Structural, morphological, functional and digestibility properties of starches from cereals, tubers and legumes: a comparative study. *Journal of Food Science and Technology*, *55*(9), 3799-3808.
- Baranowska, H. M., Sikora, M., Krystijan, M., Dobosz, A., Tomasiak, P., Walkowiak, K., Masewicz, Ł., & Borczak, B. (2020). Analysis of the Retrogradation Processes in Potato Starches Blended with Non-Starchy Polysaccharide Hydrocolloids by LF NMR. *Food Biophysics*, *15*(1), 64-71.
- Baudron, V., Gurikov, P., Smirnova, I., & Whitehouse, S. (2019). Porous Starch Materials via Supercritical- and Freeze-Drying. *Gels (Switzerland)*, *5*(1), 12.
- Benavent-Gil, Y., Román, L., Gómez, M., & Rosell, C. M. (2019). Physicochemical Properties of Gels Obtained from Corn Porous Starches with Different Levels of Porosity. *Starch - Stärke*, *71*(3-4), 1800171.
- Bertoft, E. (2017). Understanding Starch Structure: Recent Progress. *Agronomy*, *7*(3), 56.
- Bhattarai, R. R., Dhital, S., & Gidley, M. J. (2016). Interactions among macronutrients in wheat flour determine their enzymic susceptibility. *Food Hydrocolloids*, *61*, 415-425.

Biduski, B., Silva, W., Colussi, R., Halal, S., Lim, L.-T., Dias, Á., & Zavareze, E. (2018). Starch hydrogels: The influence of the amylose content and gelatinization method. *International Journal of Biological Macromolecules*, *113*, 443-449.

Brodkorb, A., Egger, L., Alming, M., Alvito, P., Assunção, R., Ballance, S., Bohn, T., Bourlieu-Lacanal, C., Boutrou, R., Carrière, F., Clemente, A., Corredig, M., Dupont, D., Dufour, C., Edwards, C., Golding, M., Karakaya, S., Kirkhus, B., Le Feunteun, S., Lesmes, U., Macierzanka, A., Mackie, A. R., Martins, C., Marze, S., McClements, D. J., Ménard, O., Minekus, M., Portmann, R., Santos, C. N., Souchon, I., Singh, R. P., Vegarud, G. E., Wickham, M. S. J., Weitschies, W., & Recio, I. (2019). INFOGEST static *in vitro* simulation of gastrointestinal food digestion. *Nature Protocols*, *14*(4), 991-1014.

Bustos, M. C., Vignola, M. B., Pérez, G. T., & León, A. E. (2017). *In vitro* digestion kinetics and bioaccessibility of starch in cereal food products. *Journal of Cereal Science*, *77*, 243-250.

Butterworth, P. J., Warren, F. J., Grassby, T., Patel, H., & Ellis, P. R. (2012). Analysis of starch amylolysis using plots for first-order kinetics. *Carbohydrate Polymers*, *87*(3), 2189-2197.

Chambers, E. S., Byrne, C. S., & Frost, G. (2019). Carbohydrate and human health: is it all about quality? *The Lancet*, *393*(10170), 384-386.

Charoenkul, N., Uttapap, D., Pathipanawat, W., & Takeda, Y. (2006). Molecular Structure of Starches from Cassava Varieties having Different Cooked Root Textures. *Starch - Stärke*, *58*(9), 443-452.

Chung, H.-J., Lim, H. S., & Lim, S. T. (2006). Effect of partial gelatinization and retrogradation on the enzymatic digestion of waxy rice starch. *Journal of Cereal Science*, *43*(3), 353-359.

Chung, H.-J., Liu, Q., Donner, E., Hoover, R., Warkentin, T. D., & Vandenberg, B. (2008). Composition, molecular structure, properties, and *in vitro* digestibility of starches from newly released Canadian pulse cultivars. *Cereal Chemistry*, *85*(4), 471-479.

Chung, H.-J., Liu, Q., Huang, R., Yin, Y., & Li, A. (2010). Physicochemical Properties and *In Vitro* Starch Digestibility of Cooked Rice from Commercially Available Cultivars in Canada. In *Cereal Chemistry* (Vol. 87, pp. 297-304): John Wiley & Sons, Ltd.

Demirkesen-Bicak, H., Tacer-Caba, Z., & Nilufer-Erdil, D. (2018). Pullulanase treatments to increase resistant starch content of black chickpea (*Cicer arietinum* L.) starch and the effects on starch properties. *International Journal of Biological Macromolecules*, *111*, 505-513.

- Feltre, G., Almeida, F. S., Sato, A. C. K., Dacanal, G. C., & Hubinger, M. D. (2020). Alginate and corn starch mixed gels: Effect of gelatinization and amylose content on the properties and *in vitro* digestibility. *Food Research International*, 132, 109069.
- Frei, M., Siddhuraju, P., & Becker, K. (2003). Studies on the *in vitro* starch digestibility and the glycemic index of six different indigenous rice cultivars from the Philippines. *Food Chemistry*, 83(3), 395-402.
- Garzon, R., & Rosell, C. M. (2020). Rapid assessment of starch pasting using a rapid force analyzer. *Cereal Chemistry*, 98(2), 305-314
- Gómez, M., Oliete, B., Rosell, C. M., Pando, V., & Fernández, E. (2008). Studies on cake quality made of wheat–chickpea flour blends. *LWT - Food Science and Technology*, 41(9), 1701-1709.
- Goñi, I., Garcia-Alonso, A., & Saura-Calixto, F. (1997). A starch hydrolysis procedure to estimate glycemic index. *Nutrition Research*, 17(3), 427-437.
- Haiteng L., Dhital, S., Gidley, M. J., & Gilbert, R. G. (2019). A more general approach to fitting digestion kinetics of starch in food. *Carbohydrate Polymers*, 225, 115244.
- Huang, J., Schols, H. A., van Soest, J. J. G., Jin, Z., Sulmann, E., & Voragen, A. G. J. (2007). Physicochemical properties and amylopectin chain profiles of cowpea, chickpea and yellow pea starches. *Food Chemistry*, 101(4), 1338-1345.
- Jayakody, L., & Hoover, R. (2008). Effect of annealing on the molecular structure and physicochemical properties of starches from different botanical origins – A review. *Carbohydrate Polymers*, 74(3), 691-703.
- Kaur, A., Shevkani, K., Singh, N., Sharma, P., & Kaur, S. (2015). Effect of guar gum and xanthan gum on pasting and noodle-making properties of potato, corn and mung bean starches. *Journal of Food Science and Technology*, 52(12), 8113-8121.
- Lavoisier, A., & Aguilera, J. M. (2019). Effect of a Whey Protein Network Formed by Cold Gelation on Starch Digestibility. *Food Biophysics*, 14(2), 214-224.
- Li, J-Y., Yeh, A.-I., & Fan, K.-L. (2007). Gelation characteristics and morphology of corn starch/soy protein concentrate composites during heating. *Journal of Food Engineering*, 78(4), 1240-1247.
- Lineback, D. R., & Wongsrikasem, E. (1980). Gelatinization of starch in baked products. *Journal of Food Science*, 45(1), 71-74.
- Martinez, M. M. (2020). Starch Nutritional Quality: Beyond Intraluminal Digestion in Response to Current Trends. *Current Opinion in Food Science*, 38, 112-121

Miller, G. (1959). Use of Dinitrosalicylic Acid Reagent for Determination of Reducing Sugar. *Analytical Chemistry*, 31, 426-428.

Minekus, M., Alminger, M., Alvito, P., Ballance, S., Bohn, T., Bourlieu, C., Carrière, F., Boutrou, R., Corredig, M., Dupont, D., Dufour, C., Egger, L., Golding, M., Karakaya, S., Kirkhus, B., Le Feunteun, S., Lesmes, U., Macierzanka, A., Mackie, A., Marze, S., McClements, D. J., Ménard, O., Recio, I., Santos, C. N., Singh, R. P., Vegarud, G. E., Wickham, M. S. J., Weitschies, W., & Brodtkorb, A. (2014). A standardised static *in vitro* digestion method suitable for food – an international consensus. *Food & Function*, 5(6), 1113-1124.

Mishra, S., & Rai, T. (2006). Morphology and functional properties of corn, potato and tapioca starches. *Food Hydrocolloids*, 20(5), 557-566.

Noda, T., Takigawa, S., Matsuura-Endo, C., Suzuki, T., Hashimoto, N., Kottarachchi, N. S., Yamauchi, H., & Zaidul, I. S. M. (2008). Factors affecting the digestibility of raw and gelatinized potato starches. *Food Chemistry*, 110(2), 465-470.

Schirmer, M., Höchstötter, A., Jekle, M., Arendt, E., & Becker, T. (2013). Physico-chemical and morphological characterization of different starches with variable amylose/amylopectin ratio. *Food Hydrocolloids*, 32(1), 52-63.

Segura, M. E. M., & Rosell, C. M. (2011). Chemical composition and starch digestibility of different gluten-free breads. *Plant Foods for Human Nutrition*, 66(3), 224.

Srichuwong, S., Sunarti, T. C., Mishima, T., Isono, N., & Hisamatsu, M. (2005). Starches from different botanical sources I: Contribution of amylopectin fine structure to thermal properties and enzyme digestibility. *Carbohydrate Polymers*, 60(4), 529-538.

Syahriza, Z. A., Sar, S., Hasjim, J., Tizzotti, M. J., & Gilbert, R. G. (2013). The importance of amylose and amylopectin fine structures for starch digestibility in cooked rice grains. *Food Chemistry*, 136(2), 742-749.

Tinay, A. H. E., Hardalou, S. B. E., & Nour, A. M. (1983). Comparative study of three legume starches. *International Journal of Food Science & Technology*, 18(1), 1-9.

Yoshimoto, Y., Matsuda, M., Hanashiro, I., Takenouchi, T., & Takeda, Y. (2001). Molecular structure and pasting properties of legume starches. *Journal of Applied Glycoscience*, 48(4), 317-324.

Yu, W., Tao, K., & Gilbert, R. G. (2018). Improved methodology for analyzing relations between starch digestion kinetics and molecular structure. *Food Chemistry*, 264, 284-292.

Zhang, G., Ao, Z., & Hamaker, B. R. (2006). Slow Digestion Property of Native Cereal Starches. *Biomacromolecules*, 7(11), 3252-3258.

Zhu, L.-J., Liu, Q.-Q., Wilson, J. D., Gu, M.-H., & Shi, Y.-C. (2011). Digestibility and physicochemical properties of rice (*Oryza sativa* L.) flours and starches differing in amylose content. *Carbohydrate Polymers*, 86(4), 1751-1759.

CHAPTER

4



Understanding phenolic acids inhibition of α -amylase and α -glucosidase and influence of reaction conditions

Andrea Alexandre^a, Jose Vicente Gil^{a,b}, Jorge Sineiro^c, Cristina M. Rosell^{a*}

^aInstitute of Agrochemistry and Food Technology (IATA-CSIC). C/Agustin Escardino, 7, Paterna 46980, Valencia, Spain.

^bFood Technology Area, Faculty of Pharmacy, University of Valencia, Avda. Vicent Andrés Estellés s/n, Burjassot 46100, Valencia, Spain.

^cDepartment of Chemical Engineering, Universidade de Santiago de Compostela. Rúa Lope Gómez de Marzoa, Santiago de Compostela E-15782, Spain.

*Corresponding author: Cristina M. Rosell (crostell@iata.csic.es)



Abstract

Phenolic acids are involved in modulating the activity of starch digestive enzymes but remains unclear if their interaction with enzymes or starch is governing the inhibition. The potential inhibition of nine phenolic acids against α -amylase and α -glucosidase was studied applying different methodologies to understand interactions between phenolic acids and either enzymes or substrates. Vanillic and syringic acids were prone to interact with α -amylase requiring low half-maximum inhibitory concentration (IC_{50}) to inhibit starch hydrolysis. Nevertheless, the initial interaction of phenolic acids with starch somewhat obstructed their interaction with starch, requiring 10 times higher IC_{50} , with the exception of chlorogenic and gallic acid. The study demonstrates that 10% of the phenolic acids were retained during starch gelatinization. Those effects were not really evident with α -glucosidase, likely due to the small molecular size of maltose substrate. Phenolic acids with > 1 hydroxyl group like caffeic and protocatechuic acids showed the lowest IC_{50} against α -glucosidase.



Keywords

Digestive enzymes * Starch * Gelatinization * Maltose * In vitro reaction

4.1. Introduction

In the last years, several plant-based products have been reported to inhibit the activity of α -amylase and α -glucosidase, the digestive enzymes that catalyzes the starch breakdown in the digestive tract (Sun et al., 2020). Vinayagam et al. (2016) reviewed the antidiabetic *in vivo* effect of simple phenolic acids such as gallic, protocatechuic, ellagic, syringic or salicylic acids, owing to their role on glucose and insulin receptor function, both of which play an essential role in diabetes. Extracts from different fruits and vegetables (Papoutsis et al., 2021), teas (Kwon et al., 2008) or seaweeds (Lordan et al., 2013) have been investigated for their potential inhibitory action towards α -amylase and α -glucosidase. Most of those studies use crude or purified extracts, and the inhibitory activity has been attributed to polyphenol type compounds. Polyphenols are a large and heterogeneous group of phytochemicals present in plant-based foods and an essential part of human diet (Martinez-Gonzalez et al., 2017). Phenolic acids are one of the most common polyphenols, comprising aromatic phenols of secondary plant metabolites with a carboxylic acid functional group.

Their inhibitory activity against α -amylase and α -glucosidase enzymes has been related with their structure, that allow them to interact with the enzyme or the substrate of the reaction (Sun et al., 2019). Numerous studies have described the *in vitro* inhibition of α -amylase and α -glucosidase induced by phenolic compounds, particularly focusing on characterizing new extract sources like seaweed and black legumes (Lordan et al., 2013; Tan et al., 2017). For instance, different legume fractions from black soybean were able to inhibit α -amylase and α -glucosidase, with IC_{50} from 0.25 to 2 mg/mL and 0.25 to > 1000 μ g/mL, respectively (Tan et al., 2017). It has been previously confirmed the inhibitory action of ferulic acid against α -amylase (IC_{50} of 0.622 mg/mL) and α -glucosidase (0.866 mg/mL) (Zheng, Tian, et al., 2020), and chlorogenic acid inhibition against α -amylase (IC_{50} of 0.498 mg/mL) (Zheng, Yang, et al., 2020).

However, rather different conditions have been used for testing their inhibitory activities. Concerning digestive enzymes, some *in vitro* studies try to simulate the *in vitro* starch hydrolysis using human salivary or pancreatic α -amylase, and rat small intestinal α -glucosidase (Tadera et al., 2006). However, due to the difficulties to employ these enzymes, porcine pancreatic α -amylase and yeast α -glucosidase are mostly used. As regards the substrate of the reaction, chemical compounds can be used such as p-nitrophenyl maltoheptaoside (BPNPG7) and 4-nitrophenyl- β -D- glucopyranoside (PNPG) for α -amylase and α -glucosidase, respectively (Tadera et al., 2006; Zheng, Tian, et al., 2020). Nevertheless, other compounds like starch and maltose are closely resembling human body reactions (Kato-Schwartz et al., 2020; Sun et al., 2020). In fact, starch is the most extensively used substrate to analyze the *in vitro* inhibition induced by rich polyphenol plant-based extracts, generally mixing the polyphenols with the enzyme solution before the addition of the substrate (Sun et al., 2020). However, considering

that polyphenols can either interact with the enzyme or the starch (Zhu, 2015), the order of addition of these components into the reaction might influence the results. Actually, Mkandawire et al. (2013) showed higher inhibitory effect when tannins extracted from sorghum were incubated with α -amylase before adding the substrate, waxy maize starch. Conversely, Camelo-Méndez et al. (2017) showed greater amylase inhibition when polyphenol rich extracts from blue maize flour were incubated with starch before adding α -amylase. Differences encountered among the reported studies might be ascribed to the experimental conditions used, stressing the importance of evaluating the effect of those conditions on the enzymatic activities.

Previous studies for inhibiting α -amylase or α -glucosidase with polyphenols have been reported either using different substrates or extracts as major polyphenol sources, which does not allow to identify and compare the inhibitory ability of each polyphenol on those enzymes. Therefore, the initial hypothesis is that the polyphenols interaction with substrates or enzymes (α -amylase and α -glucosidase) might be associated with the polyphenol chemical structure. Hence, the objective was to study the *in vitro* inhibitory effect of nine pure phenolic acids with diverse chemical structure, against α -amylase and α -glucosidase. For that purpose, different model systems that included: i. incubation of phenolic acids with the enzymes previous to substrate addition, ii. incubation of phenolic acids with the gelatinized starch, iii. Incubation of phenolic acids with the starch previous gelatinization.

4.2. Materials and methods

4.2.1. Materials

Type VI-B α -amylase from porcine pancreas (EC 3.2.1.1) (8 U/mg), type I α -glucosidase from *Saccharomyces cerevisiae* (11 U/mg), D-(+)-maltose, 3,5-dinitrosalicylic acid (DNS), acarbose and native starch from wheat that contained 8.8-11.5% moisture, and <0.3% protein according to product specifications were obtained from Sigma Aldrich (Sigma Chemical, St.Louis, USA). D-glucose Assay Kit (GOD/POD) was obtained from Megazyme (K-GLUC 08/18, Megazyme International Ireland Ltd., Bray, Co. Wicklow, Ireland). Nine phenolic acids were analyzed: caffeic acid, ferulic acid, gallic acid and protocatechuic acid were from Acros Organic (Acros Organic BVBA, Geel, Belgium); p-coumaric acid and syringic acid were from Alfa Aesar (Alfa Aesar Co., Inc., Ward Hill, USA); sinapic acid and vanillic acid were from Fluka (Fluka Analytical, Buchs, Switzerland) and chlorogenic acid were from Sigma Aldrich (Sigma Chemical, St. Louis, USA). The molecular structures of phenolic acids are represented in Figure 4.1.

HYDROXYCINNAMIC ACIDS		HYDROXYBENZOIC ACIDS	
NAME	CHEMICAL STRUCTURE	NAME	CHEMICAL STRUCTURE
Caffeic acid		Gallic acid	
Chlorogenic acid		Protocatechuic acid	
P-coumaric acid		Syringic acid	
Ferulic acid		Vanillic acid	
Sinapic acid			

Figure 4.1. Molecular structure of tested phenolic acids.

Other chemicals were of analytical grade. Solutions and standards were prepared using deionized water.

4.2.2. Inhibition assays of α -amylase

The inhibition assay of α -amylase was adapted from different studies (Tan et al., 2017; Zheng, Tian, et al., 2020). Wheat starch (6.25 mg/mL) was prepared in sodium phosphate buffer (0.02 M, pH 6.9 with 6 mM NaCl), followed by gelatinizing the solution at 100°C for 20 min. Enzymatic reaction contained: 0.05 mL of phenolic compounds dissolved in ethanol (20%, v/v) at different concentrations, 0.05 mL of α -amylase (50 U/mL) and 0.4 mL of gelatinized wheat starch. Three methodologies were carried out varying the order of substrates addition: (M1_{AM}) Enzyme and polyphenol solutions were mixed in a Vortex and preincubated at 37°C for 10 min. Then, gelatinized starch was added, and the mixture was incubated at 37°C for 10 min. (M2_{AM}) Gelatinized starch and polyphenol were mixed in a Vortex and preincubated at 37°C for 10 min. Then, enzyme solution was added, and the mixture incubated at 37°C for 10 min. (M3_{AM}) Polyphenol was mixed with granular starch and subjected to heating for starch gelatinization. After cooling down to room temperature, enzyme solution was added, and the mixture was incubated at 37°C for 10 min.

To stop the reaction, 0.5 mL of 3,5-dinitrosalicylic acid (DNS) color reagent was

added and the mixture was incubated in a boiling water bath for 10 minutes and cooled to room temperature. The reaction mixture was then diluted 1:10 with distilled water, and absorbance was measured at 540 nm in a microplate reader (Epoch Biotek Instruments, Winooski, VT, USA).

4.2.3. Inhibition assays of α -glucosidase

The α -glucosidase assay was performed using maltose as substrate. Maltose (10 mg/mL) was prepared in sodium phosphate buffer (0.1 M, pH 6.9). Enzymatic reaction contained: 0.05 mL of phenolic compounds dissolved in ethanol (20%, v/v) at different concentrations, 0.05 mL of α -glucosidase (10 U/mL) and 0.4 mL of maltose were used. As in the α -amylase assays, to measure the different effect of incubation in enzyme activity, two methodologies were carried out: (M1_{AG}) Enzyme and polyphenol solutions were mixed and preincubated at 37°C for 10 min. Then, maltose was added, and the mixture incubated at 37°C for 10 min. (M2_{AG}) Maltose and polyphenol were mixed and preincubated at 37°C for 10 min. Then, enzyme solution was added, and the mixture incubated at 37°C for 10 min. To stop the reaction, samples were boiled in a water bath for 10 min. Absorbance was measured at 510 nm using a GOD/POD kit. Due to the interference of some colored phenolic acids with the colorimetric GOD/POD method, poly(vinylpyrrolidone) (PVPP) was used to remove polyphenols. In that case, 2% m/v of PVPP was added after ending the enzymatic reaction, samples were vortexed for 5 minutes, and centrifugated at 3,000 xg for 5 min. The absorbance of the supernatant was measured at 510 nm in a microplate reader (Epoch Biotek Instruments, Winooski, VT, USA).

4.2.4. Percentage of inhibition and IC₅₀

The percentage of enzyme inhibition of phenolic acids was calculated by Eq 1:

$$\% \text{ enzyme inhibition} = \left[1 - \left(\frac{Abs_{sample} - Abs_{sample blank}}{Abs_{control} - Abs_{control blank}} \right) \right] \times 100 \quad (1)$$

Where Abs_{sample} is the absorbance value of the sample with substrate solution and enzyme; Abs_{sample blank} is the absorbance of sample and substrate without enzymes; Abs_{control} is the absorbance of buffer (instead of sample), substrate solution and enzyme; Abs_{control blank} is the absorbance of buffer and substrate without enzyme.

The half maximal inhibitory concentration (IC₅₀) is the concentration of sample required for 50% inhibition of the α -amylase or α -glucosidase activity and was calculated from the concentration-by-inhibition plots.

4.2.5. High-performance liquid chromatography analysis

Phenolic acids before and after the enzymatic reactions was quantified using high-performance liquid chromatography (HPLC). Samples preincubated with gelatinized starch (M2_{AG}) and starch gelatinized in presence of polyphenols (M3_{AM}) were dissolved in ethanol, centrifuged and filtered through 0.22 μm mixed cellulose ester filter. The phenolic acid contents were analyzed by HPLC with a Waters liquid chromatography system equipped with a 600E pump and a photodiode array detector (DAD) model 2998. Instrument control, data acquisition and data processing were achieved with Waters and Empower software (Waters Corporation, Milford, USA). A C18 column (150 x 4.6 mm, particle size 2.5 μm) (Waters Corporation, Milford, USA) was used. The mobile phases were 0.1 vol% trifluoroacetic acid in acetonitrile (A) and 0.1 vol% trifluoroacetic acid in water (B). Separation was carried out in 27 min under the following conditions: 0 min 5% A; 20 min 50% A; 21 min 100% A; 23 min 100% A; 27 min 5% A. Chromatographic conditions were: injection volume, 20 μL ; flow rate 1 mL/min; oven temperature 40°C, detection wavelengths, 280 and 320 nm. Calibration curves using phenolic acid standards were constructed to calculate their concentration in the samples. The absorption ratio was defined as the quotient between the concentration of free phenolic acids before and after the enzymatic reaction.

4.2.6. Statistical analyses

The data were expressed as average \pm confidence interval of at least three individual measurements and analyzed through one-way analysis of variance (ANOVA) using Statgraphics Centurion XV software (Statistical Graphics Corporation, Rockville, MD, USA). Mean comparison for significant differences was tested using Fisher's least significant differences test at $P < 0.05$.

4.2.7. Structure-activity relation

To obtain structural parameters that relate molecular structural features and α -glucosidase activity, 3D molecular structure optimization was performed with Allinger's MM2 force field method using software Chem3D version 20.1.0.110, (Perkin-Elmer, Madrid, Spain), minimizing the steric energy to RMS Gradient=0.01.

4.3. Results and discussion

The inhibitory activity of nine phenolic acids against α -amylase and α -glucosidase, was evaluated using different assay conditions: M1= preincubation of the polyphenol with the enzyme; M2= preincubation of the phenolic acid with the substrate, M3= gelatinization of the starch in presence of the phenolic compound. Plots of the enzymatic

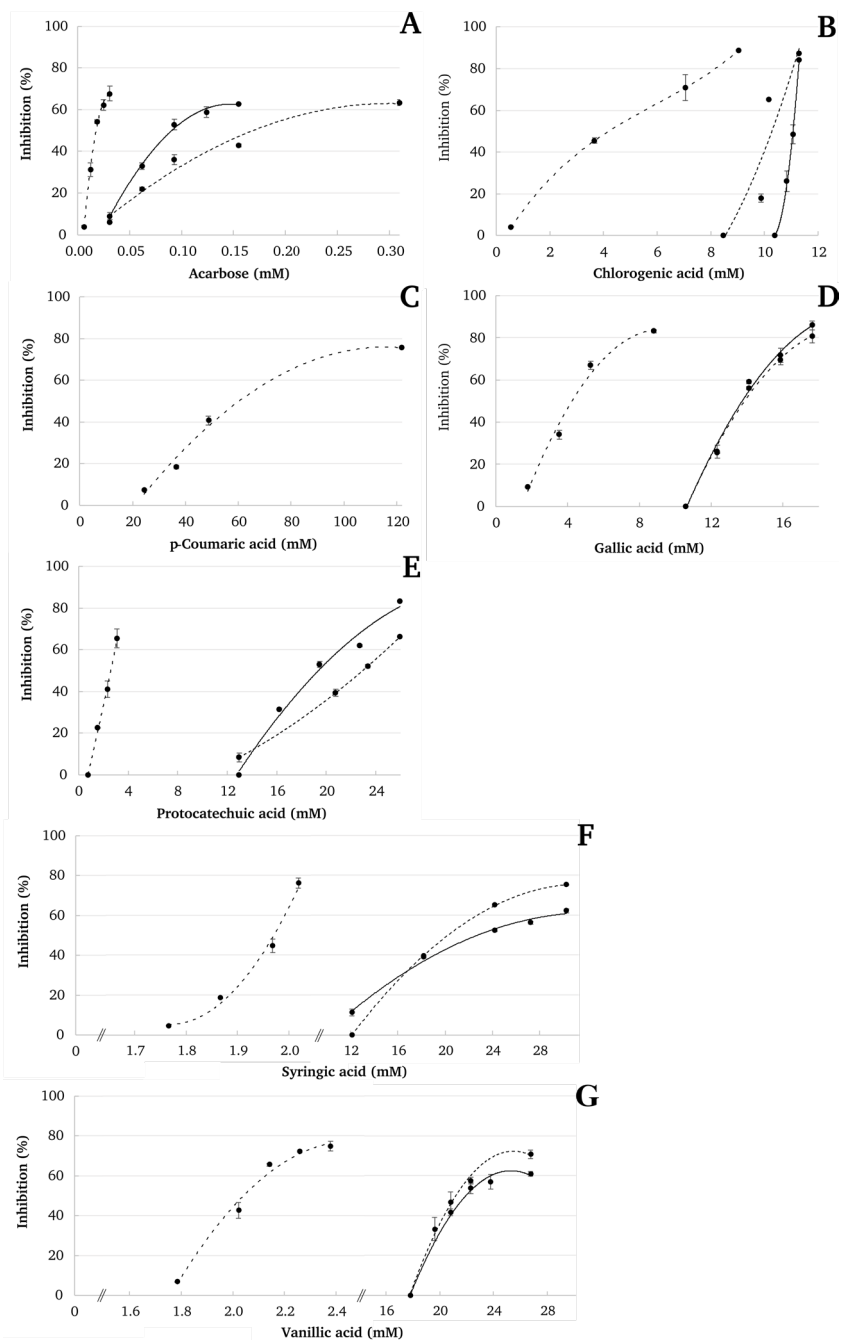


Figure 4.2. Inhibitory effect of pure polyphenols against α -amylase. Discontinuous line, $M1_{AM}$ =preincubation PP + enzyme; solid line, $M2_{AM}$ =preincubation PP + substrate; dotted line $M3_{AM}$ =gelatinization PP + starch.

activities versus concentration of phenolic acids are shown in Figure 4.2 and 4.3.

4.3.1. Inhibition of α -amylase

Concerning α -amylase inhibition (Figure 4.2), as expected, acarbose revealed the highest inhibitory effect.

Preincubating acarbose with α -amylase caused enzyme inhibition in the range 3.95 to 67.72%, on varying its concentration from 0.004 to 0.031 mM. Acarbose is a pseudo-tetra saccharide usually employed as a positive control in inhibition studies of α -amylase and α -glucosidase (Pollini et al., 2020). Also, vanillic and syringic acids showed high inhibitory effect when previously incubated with the α -amylase (M1_{AM}). Both polyphenols gave as result a percentage of inhibition of 4.44 to 76.08% when varying its concentration from 1.77 to 2.38 mM. p-Coumaric acid was the polyphenol tested that displayed the lowest inhibitory activity, needing concentrations of 24.37 to 121.83 mM to obtain an inhibition percentage between 4.1 and 88.74%. Hydroxycinnamic acids (caffeic, chlorogenic, ferulic, p-coumaric and sinapic acids) are characterized by a C=C double bond conjugated with a carbonyl group in their structure that stabilizes the binding forces to the active site of the α -amylase (Giuberti et al., 2020). Likewise, it has been reported the importance of hydroxyl groups of polyphenols on the interaction with amino acid residues at the active site of α -amylase (Glu233) (Sun et al., 2019). In fact, by molecular docking analysis it was suggested that the removal of hydroxyl groups of polyphenols may decrease the inhibition effect (Sun et al., 2019). Chlorogenic acid has the highest number of OH groups (5), followed by gallic acid (3), and protocatechuic and caffeic (2). Nevertheless, inhibitory effect significantly changed when polyphenols were preincubated with the starch instead of the α -amylase (M2_{AM} and M3_{AM}). That change was particularly dramatic in the case of vanillic and syringic acids, which required 10 times higher concentrations to inhibit α -amylase than those obtained when the acids were preincubated with the α -amylase (M1_{AM}). In M2_{AM} and M3_{AM} methodologies, phenolic acids with a greater number of hydroxyl groups (chlorogenic and gallic acid) showed higher inhibition effect against α -amylase than vanillic and syringic acids (Figure 4.2), which have only one hydroxyl group in their structure.

Therefore, results agree with reported statements affirming that phenolic acids and starch digestive enzymes interact by non-covalent interactions, being responsible of their inhibitory activity (Martinez-Gonzalez et al., 2017). Particularly, hydrogen binding, cation- π interactions, salt bridge interactions or electrostatic forces have been described for chlorogenic, caffeic, p-coumaric, vanillic and syringic and the enzyme (Pollini et al., 2020). The differences in the inhibitory concentration observed with the methodologies tested (M1_{AM}, M2_{AM}, M3_{AM}) suggests that starch somewhat hinders the phenolic acids-enzyme interaction, and in consequence greater concentration of phenolic acids are required for the inhibition.

Table 4.1. Effect of different analysis methodologies (M1, M2, M3) on the IC₅₀ values of pure phenolic acids (PP) against α -amylase.

Polyphenol	Treatment	IC ₅₀ (MEAN \pm SD)		Free polyphenols	Absorption ratio	
		mM	mg/mL			
Acarbose	M1 _{AM}	0.018 \pm 0.001	a 0.012 \pm 0.001	a		
	M2 _{AM}	0.087 \pm 0.005	a 0.056 \pm 0.003	a		
	M3 _{AM}	0.300 \pm 0.004	a 0.194 \pm 0.004	b		
Caffeic acid	M1 _{AM}	> 5.55	> 1			
	M2 _{AM}	> 5.55	> 1			
	M3 _{AM}	> 5.55	> 1			
Chlorogenic acid	M1 _{AM}	3.90 \pm 0.08	d 1.41 \pm 0.04	e		
	M2 _{AM}	11.08 \pm 0.04	f 3.92 \pm 0.01	j 3.99 \pm 0.42	de 1.01	
	M3 _{AM}	10.07 \pm 0.00	e 3.57 \pm 0.00	hi 3.21 \pm 0.30	bcd 0.90	
p-Coumaric acid	M1 _{AM}	52.48 \pm 0.89	m 8.62 \pm 0.15	l		
	M2 _{AM}	> 52.48	> 8.62			
	M3 _{AM}	> 52.48	> 8.62			
Ferulic acid	M1 _{AM}	> 5.15	> 1			
	M2 _{AM}	> 5.15	> 1			
	M3 _{AM}	> 5.15	> 1			
Sinapic acid	M1 _{AM}	> 8.92	> 2			
	M2 _{AM}	> 8.92	> 2			
	M3 _{AM}	> 8.92	> 2			
Gallic acid	M1 _{AM}	4.35 \pm 0.07	d 0.75 \pm 0.01	d		
	M2 _{AM}	13.53 \pm 0.07	g 2.30 \pm 0.01	f 2.41 \pm 0.19	ab 1.05	
	M3 _{AM}	13.69 \pm 0.06	g 2.33 \pm 0.01	f 2.30 \pm 0.19	a 0.99	
Protocatechuic acid	M1 _{AM}	2.65 \pm 0.16	c 0.41 \pm 0.02	c		
	M2 _{AM}	18.84 \pm 0.26	h 2.90 \pm 0.04	g 3.05 \pm 0.52	abc 1.05	
	M3 _{AM}	22.94 \pm 0.20	l 3.54 \pm 0.03	h 3.12 \pm 0.35	abc 0.88	
Syringic acid	M1 _{AM}	1.98 \pm 0.01	b 0.39 \pm 0.00	c		
	M2 _{AM}	22.72 \pm 0.17	l 4.50 \pm 0.03	k 4.80 \pm 0.34	e 1.07	
	M3 _{AM}	20.00 \pm 0.02	i 3.98 \pm 0.00	j 3.35 \pm 0.12	cd 0.84	
Vanillic acid	M1 _{AM}	2.05 \pm 0.01	b 0.35 \pm 0.06	c		
	M2 _{AM}	21.73 \pm 0.33	k 3.65 \pm 0.06	i 3.47 \pm 0.76	cd 0.95	
	M3 _{AM}	21.10 \pm 0.49	j 3.55 \pm 0.08	h 3.16 \pm 0.06	bcd 0.89	
P-value						
Polyphenol		0.0000	0.0000	0.0000		
Method		0.0000	0.0000	0.0265		

M1_{AM} = preincubation PP + enzyme, M2_{AM} = preincubation PP + gelatinized substrate, M3_{AM} = gelatinization (PP + starch). Results were expressed as mean \pm SD (n=2) and values followed by different letters within columns are significantly different ($P < 0.05$).

The half-maximum inhibitory concentration (IC_{50}) values of the different analyzed phenolic acids were calculated (Table 4.1).

The ANOVA analysis indicated significant differences ($P < 0.05$) due to the polyphenol acid and the method used. IC_{50} values are specific for the enzyme type, the substrate, and the reaction conditions (Sun et al., 2020), which limit the comparison with other published results. The IC_{50} values of hydroxycinnamic acids such as caffeic, ferulic and sinapic acids could not be determined due to their solubility difficulties (Table 4.1). There were significant differences in the IC_{50} obtained with M1_{AM} and the other two methodologies: preincubating the phenolic acid with the starch (M2_{AM}) and gelatinizing the starch in presence of the polyphenol (M3_{AM}). Acarbose, showed the lowest IC_{50} values (0.012 ± 0.001 , 0.056 ± 0.003 and 0.194 ± 0.004 mg/mL for M1_{AM}, M2_{AM} and M3_{AM}) in all the methodologies tested. In M1_{AM} the enzyme was preincubated with the inhibitory substance, encouraging their binding, which causes the inhibition of the enzymatic activity (Sun et al., 2020). Except for p-coumaric acid, the IC_{50} of phenolic acids obtained when preincubating with the enzyme (M1_{AM}) were < 1.5 mg/mL. Conversely, in M2_{AM} and M3_{AM} the IC_{50} were about 10 times higher, with the exception of chlorogenic and gallic acid which concentration increased around 3 times. When comparing M2_{AM} and M3_{AM}, significantly higher concentrations of phenolic acids were required when they were preincubated with gelatinized starch (M2_{AM}), with exception of protocatechuic acid. Chlorogenic, syringic and vanillic acids presented lower IC_{50} values in M3_{AM} (3.57 ± 0.00 , 3.98 ± 0.00 , 3.55 ± 0.08 mg/mL) than in M2_{AM} (3.92 ± 0.01 , 4.50 ± 0.03 , 3.65 ± 0.06 mg/mL). Differences might be ascribed to the impact of polyphenols on starch gelatinization and the resulting microstructure. In fact, Han et al. (2020) observed changes in the short-range order microstructure of rice gels when ferulic acid, gallic acid or quercetin were present during starch gelatinization. Similarly, Chai et al. (2013) obtained gels from high-amylose maize starch with totally different microstructure when adding 2.5% of tea polyphenols.

The higher concentrations of acids required in M2_{AM} and M3_{AM} to inhibit the enzyme might be attributed to interactions of phenolic acids with amylopectin or amylose chains (Mkandawire et al., 2013). Nevertheless, non-covalent interactions between polyphenols and starch can be influenced by the structure of the phenolic compound, the nature of the starch and/or the different experimental conditions (Giuberti et al., 2020). Considering that α -amylase inhibition still occurred at higher concentrations, results suggest the formation of non-inclusion complexes with weaker binding forces (hydrogen bonds, hydrophobic interactions and/or electrostatic and ionic interactions) (Zhu, 2015).

To explain the possible interaction of starch-polyphenols observed in M2_{AM} and M3_{AM} that might explain the higher concentrations required when preincubated polyphenols with starch, the concentration of free polyphenols was quantified by HPLC

(Table 4.1). No statistical differences were observed in the free polyphenol concentration detected at IC_{50} in M2_{AM} and M3_{AM}. This confirms that the possible interaction between phenolic acids and starch could only involve weaker bonds. Possible absorption of the polyphenol on the starch gel was evaluated by defining the absorption ratio. This parameter for M2_{AM} (absorption ratio ~ 1) suggested that phenolic acids remained free, but for M3_{AM} the absorption ratio was around 0.9, and even lower for gallic acid. Two plausible explanations for the former reduction when applying M3_{AM} could be the thermal degradation of phenolic acids during the heating treatment or the inclusion of the acids into the starch gel structure. However, the analysis of the amount of phenolic acids in the absence of starch confirmed that heat treatment conditions applied for starch gelatinization did not affect the amount of free phenolic acids. Therefore, the absorption ratio results seem to indicate that 10% of the phenolic acids could have been linked to the gelatinized starch, as it has been suggested previously. Moreover, Igoumenidis et al. (2018) described hydrogen bonding or weak van der Waals interactions, no inclusion complexes, between rice starch and caffeic acid after boiling. Similar results were described by Wu et al. (2011) and Liu et al. (2020), who reported hydrogen bonding interaction during gelatinization between phenolic compounds (caffeic acid and tea polyphenols) and rice and maize starch, respectively. Betoret and Rosell (2020) viewed an interaction between corn starch and phenolic compounds from *Brassica napobrassica* leaves powder. In addition, they studied the impact of temperature on polyphenols, describing a thermal degradation, but also a protective effect owing to the starch-phenolic compounds interaction. However, the starch and polyphenol working concentrations were considerably higher than in the present study.

Based on the obtained results, most of the phenolic compounds are present in the reaction medium, apart from the 90% in M3_{AM}. Therefore, all the inhibition effects registered from the different methods cannot be explained by the interaction between starch and phenolic acids, but by different inhibition mechanism of phenolic acids. In the case of acarbose, different studies describe a mixed-type competitive inhibition of porcine pancreatic α -amylase by phenolic acids like caffeic, chlorogenic or ferulic acids, exhibiting both competitive and uncompetitive mechanisms (Kim et al., 1999; Sun et al., 2019; Zheng, Tian, et al., 2020). The existence of different inhibitory mechanisms might explain the lower inhibition effect of phenolic acids in M2_{AM} and M3_{AM} methods. In these cases, the inhibitor did not have a preincubation time with the enzyme and therefore had to compete with the substrate for the enzyme active site during incubation or bind the enzyme-substrate complex.

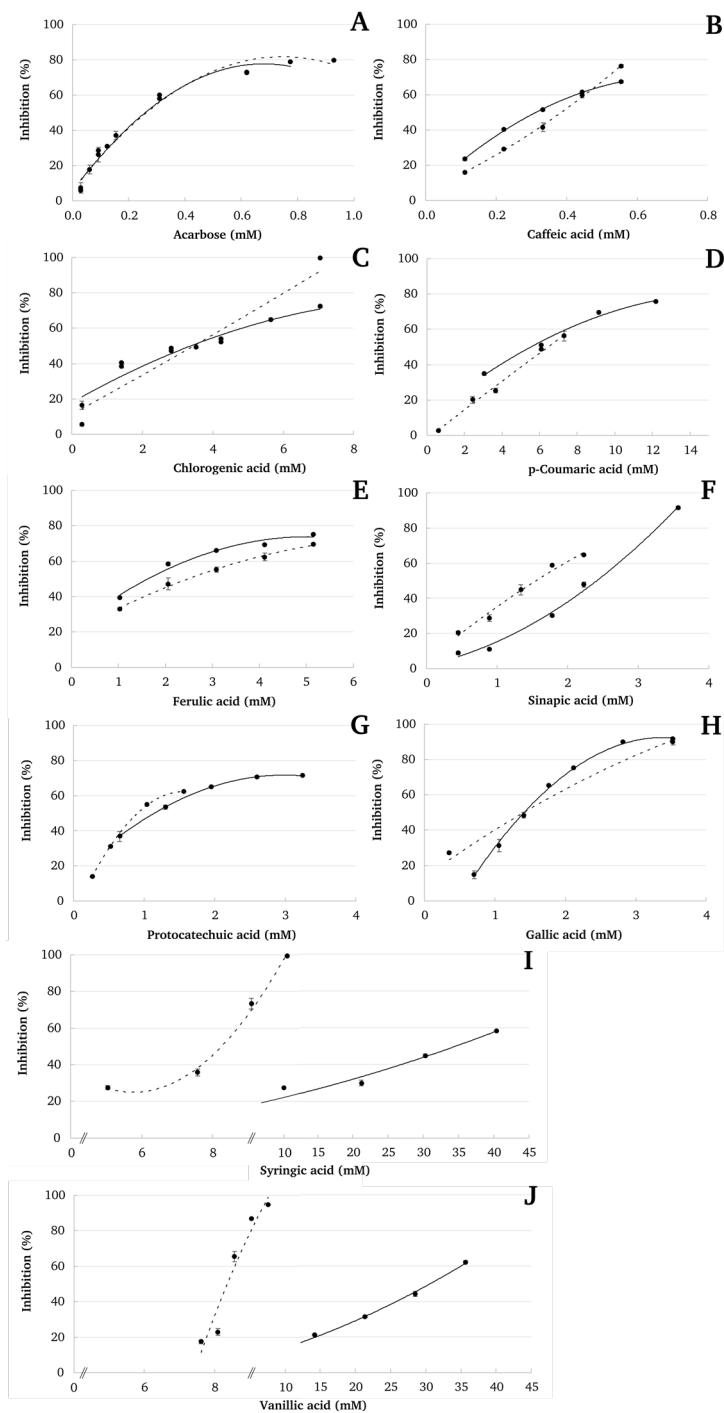


Figure 4.3. Inhibitory effect of pure polyphenols against α -glucosidase. Discontinuous line, M1_{AG} = preincubation PP + enzyme; solid line, M2_{AG} = preincubation PP + substrate.

4.3.2 Polyphenols inhibition of α -glucosidase

Regarding α -glucosidase, two assay conditions (M1_{AG} and M2_{AG}) were tested to identify possible impact of phenolic acid preincubation with enzyme. In M1_{AG} the polyphenol was preincubated with the enzyme and in M2_{AG} the phenolic acid was preincubated with the substrate before the enzymatic reaction. In opposition to α -amylase results, there were minor differences when comparing different methodologies, with exception of syringic and vanillic acids (Figure 4.3).

Likely, there was some interaction between the maltose and their benzoic structure. Considering the inhibitory ability of the acids, 0.1 to 0.5 mM of caffeic acid induced an inhibition percentage of 16.05 to 76.25%, whereas 0.9 mM acarbose was necessary to reach a 79.54% of inhibition (Figure 4.3). Hence, caffeic acid caused greater inhibition than acarbose. Tan et al. (2017) analyzed the effect of commercial polyphenols against α -glucosidase using pNPG as substrate, incubating the polyphenol, substrate, and the enzyme, and also described a high inhibition of caffeic acid compared to other phenolic acids. Syringic and vanillic acids showed the lowest inhibition against α -glucosidase in the M1_{AG} and M2_{AG}. More than 8 mM of these polyphenols were needed to inhibit 50% of the maximum activity of the enzyme. As it was described for α -amylase, hydroxyl groups might play an important role on α -glucosidase inhibition too (Xiao et al., 2013). Phenolic acids with >1 hydroxyl group like caffeic and protocatechuic acids showed higher inhibition effect than some phenolic acids with one hydroxyl group or one hydroxyl group plus one or two methoxy groups in their structure, as p-coumaric, syringic or vanillic acid, which are less polar. A similar result regarding caffeic acid was observed when the activity was on p-nitrophenyl- α -D-glucoside (p-NPG). Oboh et al. (2015) reported lower enzyme affinity for chlorogenic acid than caffeic acid, when using yeast α -glucosidase and pNPG as substrate, not maltose. Likely, the effect of the substitution of an OH group for quinic acid could produce steric constrains for accommodating the structure to the active site of the enzyme.

The IC₅₀ calculated for the α -glucosidase inhibition also revealed differences between the preincubation of the inhibitor with the enzyme or the substrate (M1_{AG} or M2_{AG}) lower than those obtained with α -amylase (Table 4.2).

Only ferulic, sinapic, syringic and vanillic acids showed different IC₅₀ values depending on the method used, showing higher IC₅₀ in M2_{AG} than in M1_{AG}, except for ferulic acid. The preincubation of the ferulic acid with the maltose improved its inhibitory effect (0.45 ± 0.05 and 0.29 ± 0.01 mg/mL for M1_{AG} or M2_{AG}, respectively). These phenolic compounds (ferulic, sinapic, syringic and vanillic acids) present a methoxy group in the aromatic ring that might be responsible of the differences observed in α -glucosidase inhibition, which agrees with the reported inhibition effect of hydroxycinnamic acids with methoxy groups (Malunga et al., 2018).

Although it is known that benzoic acid derivatives are more polar than cinnamic

acids, in general, there was not a difference applicable to the two families of compounds. Analysis of calculated LogP values (available at PubChem and <https://foodb.ca> databases) and first pK_a value did not explain the observed differences for all the compounds (data not shown). In search for an explanation to the high difference between vanillic acid (benzoic acid derivative) and syringic acid (cinnamic derivative) and the rest of the compounds, the molecular features were analyzed. Allinger's force field method MM2 was applied to optimize the molecular structure in Perkin-Elmer Chem3D. The variable found to explain the high observed differences was the molecular dipole/dipole momentum, which was 1.0107 for syringic acid and 1.7444 for

Table 4.2. IC₅₀ values of pure phenolic acids against α -glucosidase of the different analyzed methodologies.

Polyphenol	Treatment	IC ₅₀ (MEAN \pm SD)			
		mM		mg/mL	
Acarbose	M1 _{AG}	0.25 \pm 0.02	a	0.16 \pm 0.01	abcd
	M2 _{AG}	0.21 \pm 0.01	a	0.13 \pm 0.01	abc
Caffeic acid	M1 _{AG}	0.39 \pm 0.02	ab	0.07 \pm 0.00	ab
	M2 _{AG}	0.31 \pm 0.00	ab	0.06 \pm 0.00	a
Chlorogenic acid	M1 _{AG}	3.19 \pm 0.18	e	1.13 \pm 0.07	h
	M2 _{AG}	3.70 \pm 0.05	e	1.31 \pm 0.02	i
p-Coumaric acid	M1 _{AG}	6.20 \pm 0.04	f	1.02 \pm 0.01	gh
	M2 _{AG}	5.95 \pm 0.00	f	0.97 \pm 0.00	g
Ferulic acid	M1 _{AG}	2.32 \pm 0.28	d	0.45 \pm 0.05	f
	M2 _{AG}	1.54 \pm 0.03	c	0.29 \pm 0.01	e
Sinapic acid	M1 _{AG}	1.48 \pm 0.08	c	0.33 \pm 0.02	e
	M2 _{AG}	2.28 \pm 0.04	d	0.51 \pm 0.01	f
Gallic acid	M1 _{AG}	1.53 \pm 0.05	c	0.25 \pm 0.01	de
	M2 _{AG}	1.44 \pm 0.04	c	0.25 \pm 0.01	cde
Protocatechuic acid	M1 _{AG}	0.90 \pm 0.01	bc	0.14 \pm 0.00	abc
	M2 _{AG}	1.15 \pm 0.06	c	0.18 \pm 0.01	bcd
Syringic acid	M1 _{AG}	8.25 \pm 0.09	g	1.63 \pm 0.02	j
	M2 _{AG}	32.36 \pm 0.37	i	6.41 \pm 0.07	l
Vanillic acid	M1 _{AG}	8.38 \pm 0.01	g	1.41 \pm 0.00	i
	M2 _{AG}	30.90 \pm 1.26	h	5.20 \pm 0.21	k
<i>P</i> -value					
Polyphenol		0.0000		0.0000	
Method		0.0112		0.0109	

M1_{AG} =preincubation PP + enzyme, M2_{AG} =preincubation PP + substrate. Results were expressed as mean \pm SD (n=2) and values followed by different letters within columns are significantly different ($P<0.05$).

vanillic acid, whereas it was in the range 3.6582 (caffeic acid) to 5.7429 (ferulic acid) for the rest of the other compounds, excepting chlorogenic acid (dipole-dipole moment = -0.0347). It seems that an association between two molecules of simple phenolic is necessary to fit or block the active site of α -glucosidase and this situation is more likely to happen when the dipolar moment is high, and molecules can form a dipole at the vicinity of active site. The two less polar molecules were less efficient to inhibit the enzyme, probably because this situation does not happen.

It seems that chlorogenic acid, which molecular size is similar to that of the natural substrate (maltose), does not need this interaction to fit in the active site. In summary, simple phenolic acids require a dipole-dipole interaction to effectively block the enzyme.

Acarbose was specifically designed to effectively adsorb onto enzyme, but its N-H link cannot be broken, thus being its IC_{50} value much lower than that of phenolics compounds.

4.4. Conclusions

Different inhibition curves and IC_{50} values were obtained with different phenolic acids, and they were dependent on the previous interaction with the enzyme or the substrate. Results indicated that polyphenol chemical structures affected their capacity to interact with the enzyme. The incubation of the phenolic acid with the enzyme was the most effective way to inhibit α -amylase or α -glucosidase, due to their binding interactions. Conversely, higher concentrations of phenolic acids were needed to inhibit α -amylase when there was previous interaction with starch, which was partially due to the absorption of phenolic acids by starch during gelatinization, but also suggested different inhibition mechanisms. That effect was not observed with small substrates like maltose used for α -glucosidase, in which a dipole-dipole interaction with the phenolic acids is needed to effectively block the enzyme. The presence of methoxyl groups on benzoic acid derivatives showed a high influence in the interaction with the substrates for both α -amylase or α -glucosidase. The present study provides a different approach to explain the α -amylase and α -glucosidase inhibition by polyphenols.

Author Contributions: Credit roles: AA: Conceptualization; Data curation; Formal analysis; Investigation; Methodology; Writing - original draft; JVG: Methodology; Review & editing; JS: Methodology; Funding acquisition; Review & editing; CMR: Conceptualization; Funding acquisition; Investigation; Supervision; Data curation; Writing - review & editing.

Acknowledgments: Authors acknowledge the financial support of the Spanish Ministry of Science and Innovation (Project RTI2018-095919-B-C21, Project RTI2018-

095919-B-C22) and the European Regional Development Fund (FEDER) and Generalitat Valenciana (Project Prometeo 2017/189).

Conflicts of Interest: The authors declare that they do not have any conflict of interest.

References

Betoret, E., & Rosell, C. M. (2020). Effect of particle size on functional properties of Brassica napobrassica leaves powder. Starch interactions and processing impact. *Food Chemistry: X*, 8, 100106.

Camelo-Méndez, G. A., Agama-Acevedo, E., Tovar, J., & Bello-Pérez, L. A. (2017). Functional study of raw and cooked blue maize flour: Starch digestibility, total phenolic content and antioxidant activity. *Journal of Cereal Science*, 76, 179-185.

Chai, Y., Wang, M., & Zhang, G. (2013). Interaction between Amylose and Tea Polyphenols Modulates the Postprandial Glycemic Response to High-Amylose Maize Starch. *Journal of Agricultural and Food Chemistry*, 61(36), 8608-8615.

Giuberti, G., Rocchetti, G., & Lucini, L. (2020). Interactions between phenolic compounds, amylolytic enzymes and starch: an updated overview. *Current Opinion in Food Science*, 31, 102-113.

Han, X., Zhang, M., Zhang, R., Huang, L., Jia, X., Huang, F., & Liu, L. (2020). Physicochemical interactions between rice starch and different polyphenols and structural characterization of their complexes. *LWT- Food Science and Technology*, 125, 109227.

Igoumenidis, P. E., Zoumpoulakis, P., & Karathanos, V. T. (2018). Physicochemical interactions between rice starch and caffeic acid during boiling. *Food Research International*, 109, 589-595.

Kato-Schwartz, C. G., Corrêa, R. C. G., de Souza Lima, D., de Sá-Nakanishi, A. B., de Almeida Gonçalves, G., Seixas, F. A. V., Haminiuk, C. W. I., Barros, L., Ferreira, I. C. F. R., Bracht, A., & Peralta, R. M. (2020). Potential anti-diabetic properties of Merlot grape pomace extract: An *in vitro*, *in silico* and *in vivo* study of α -amylase and α -glucosidase inhibition. *Food Research International*, 137, 109462.

Kim, M.-J., Lee, S.-B., Lee, H.-S., Lee, S.-Y., Baek, J.-S., Kim, D., Moon, T.-W., Robyt, J. F., & Park, K.-H. (1999). Comparative study of the inhibition of α -glucosidase, α -amylase, and cyclomaltodextrin glucanosyltransferase by acarbose, isoacarbose, and acarviosine-glucose. *Archives of Biochemistry and Biophysics*, 371(2), 277-283.

- Kwon, Y.-i., Apostolidis, E., & Shetty, K. (2008). Inhibitory potential of wine and tea against α -Amylase and α -Glucosidase for management of hyperglycemia linked to type 2 diabetes. *Journal of Food Biochemistry*, 32(1), 15-31.
- Liu, B., Zhong, F., Yokoyama, W., Huang, D., Zhu, S., & Li, Y. (2020). Interactions in starch co-gelatinized with phenolic compound systems: Effect of complexity of phenolic compounds and amylose content of starch. *Carbohydrate Polymers*, 247, 116667.
- Lordan, S., Smyth, T. J., Soler-Vila, A., Stanton, C., & Ross, R. P. (2013). The α -amylase and α -glucosidase inhibitory effects of Irish seaweed extracts. *Food Chemistry*, 141(3), 2170-2176.
- Malunga, L. N., Joseph Thandapilly, S., & Ames, N. (2018). Cereal-derived phenolic acids and intestinal alpha glucosidase activity inhibition: Structural activity relationship. *Journal of Food Biochemistry*, 42(6), e12635.
- Martinez-Gonzalez, A. I., Díaz-Sánchez, Á. G., Rosa, L. A. d. l., Vargas-Requena, C. L., Bustos-Jaimes, I., Alvarez-Parrilla, & Emilio. (2017). Polyphenolic Compounds and Digestive Enzymes: In Vitro Non-Covalent Interactions. *Molecules*, 22(4), 669.
- Mkandawire, N. L., Kaufman, R. C., Bean, S. R., Weller, C. L., Jackson, D. S., & Rose, D. J. (2013). Effects of Sorghum (*Sorghum bicolor* (L.) Moench) Tannins on α -Amylase Activity and in Vitro Digestibility of Starch in Raw and Processed Flours. *Journal of Agricultural and Food Chemistry*, 61(18), 4448-4454.
- Oboh, G., Agunloye, O. M., Adefegha, S. A., Akinyemi, A. J., & Ademiluyi, A. O. (2015). Caffeic and chlorogenic acids inhibit key enzymes linked to type 2 diabetes (*in vitro*): a comparative study. *Journal of Basic and Clinical Physiology and Pharmacology*, 26(2), 165-170.
- Papoutsis, K., Zhang, J., Bowyer, M. C., Brunton, N., Gibney, E. R., & Lyng, J. (2021). Fruit, vegetables, and mushrooms for the preparation of extracts with α -amylase and α -glucosidase inhibition properties: A review. *Food Chemistry*, 338, 128119.
- Pollini, L., Riccio, A., Juan, C., Tringaniello, C., Ianni, F., Blasi, F., Mañes, J., Macchiarulo, A., & Cossignani, L. (2020). Phenolic Acids from *Lycium barbarum* Leaves: In Vitro and In Silico Studies of the Inhibitory Activity against Porcine Pancreatic α -Amylase. *Processes*, 8(11), 1388.
- Sun, L., Wang, Y., & Miao, M. (2020). Inhibition of α -amylase by polyphenolic compounds: Substrate digestion, binding interactions and nutritional intervention. *Trends in Food Science & Technology*, 104, 190-207.
- Sun, L., Warren, F. J., & Gidley, M. J. (2019). Natural products for glycaemic control: Polyphenols as inhibitors of alpha-amylase. *Trends in Food Science & Technology*, 91, 262-273.

Tadera, K., Minami, Y., Takamatsu, K., & Matsuoka, T. (2006). Inhibition of α -glucosidase and α -amylase by flavonoids. *Journal of Nutritional Science and Vitaminology*, 52(2), 149-153.

Tan, Y., Chang, S. K. C., & Zhang, Y. (2017). Comparison of α -amylase, α -glucosidase and lipase inhibitory activity of the phenolic substances in two black legumes of different genera. *Food Chemistry*, 214, 259-268.

Vinayagam, R., Jayachandran, M., & Xu, B. (2016). Antidiabetic Effects of Simple Phenolic Acids: A Comprehensive Review. *Phytotherapy Research*, 30(2), 184-199.

Wu, Y., Lin, Q., Chen, Z., & Xiao, H. (2011). The interaction between tea polyphenols and rice starch during gelatinization. *Food Science and Technology International*, 17(6), 569-577.

Xiao, J., Kai, G., Yamamoto, K., & Chen, X. (2013). Advance in Dietary Polyphenols as α -Glucosidases Inhibitors: A Review on Structure-Activity Relationship Aspect. *Critical Reviews in Food Science and Nutrition*, 53(8), 818-836.

Zheng, Y., Tian, J., Yang, W., Chen, S., Liu, D., Fang, H., Zhang, H., & Ye, X. (2020). Inhibition mechanism of ferulic acid against α -amylase and α -glucosidase. *Food Chemistry*, 317, 126346.

Zheng, Y., Yang, W., Sun, W., Chen, S., Liu, D., Kong, X., Tian, J., & Ye, X. (2020). Inhibition of porcine pancreatic α -amylase activity by chlorogenic acid. *Journal of Functional Foods*, 64, 103587.

Zhu, F. (2015). Interactions between starch and phenolic compound. *Trends in Food Science & Technology*, 43(2), 129-143.

CHAPTER

5



Submitted to journal

In vitro inhibition of starch digestive enzymes by ultrasound-assisted extracted polyphenols from *Ascophyllum nodosum* seaweeds

**Andrea Aleixandre^a, Mauro Gisbert^b, Jorge Sineiro^b, Ramón Moreira^b,
Cristina M. Rosell^{a*}**

^aInstitute of Agrochemistry and Food Technology (IATA-CSIC). C/Agustin Escardino, 7, Paterna 46980, Valencia, Spain.

^bDepartment of Chemical Engineering, Universidade de Santiago de Compostela. Rúa Lope Gómez de Marzoa, Santiago de Compostela E-15782, Spain.

*Corresponding author: Cristina M. Rosell (crorell@iata.csic.es)



Abstract

Seaweeds are gaining importance due to their antidiabetic characteristics. The aim of the present study was to investigate the inhibitory effect of different sonicated aqueous polyphenols extracts from *Ascophyllum nodosum* against α -amylase and α -glucosidase enzymes. Different inhibition methodologies were carried out, preincubating the extract either with the enzyme or the substrate. Chemical composition, and polyphenol features were also analysed. Although sonication did not influence their proximal composition, it influenced the antiradical activity. Higher sonication power resulted in higher inhibition capacity against both starch digestive enzymes. The extract purification further reduced the IC₅₀ values. Seaweed extracts showed greater inhibition effect when they were preincubated with the enzyme instead of the substrate. Chromatographic results did not explain the different inhibition ability of the extracts. Nevertheless, the ¹H-NMR spectra showed notorious differences between extracts by the presence of uronic acids-polyphenols complexes and quinones, and hence the inhibitory capacity differences between samples.



Keywords

α -amylase * α -glucosidase * Gelled starch * HPLC * ¹H-NMR * Wheat

5.1. Introduction

In the last decade, carbohydrates digestion has attracted much attention owing its direct relationship with postprandial glycemic response, which in turn has been associated with an increased risk of developing metabolic diseases (Dall'Asta et al., 2020). Digestive carbohydrates are mainly present in human diets as starch, sucrose, free glucose fructose and oligosaccharides. One strategy to manage high blood glucose levels is the inhibition of α -amylase (AM) and α -glucosidase (AG), digestive enzymes involved in the breakdown of starch and disaccharides to glucose (Ríos et al., 2015).

Some antidiabetic drugs such as acarbose are both α -amylase and α -glucosidase enzymes inhibitors and allow the control of postprandial glucose in diabetic patients (Roy et al., 2011). However, current research is focused on discovering natural inhibitors of α -amylase and α -glucosidase enzymes together with the evaluation of anti-diabetic properties involving plant and seaweed derived compounds such as polyphenols because of their safety and health beneficial features (de Paulo Farias et al., 2021).

Polyphenols are secondary metabolites from plants, lichens or seaweeds (Koivikko et al., 2007). Particularly, the commercial interest of brown macroalgae is known, especially for species such as *Ascophyllum nodosum* or *Fucus vesiculosus*, mainly used for extracting alginate, laminarin or fertilizers production (Audibert et al., 2010). Likewise, *A. nodosum* with its high polyphenols content is being considered as a valuable source of extracts to be used in drugs and food (Leandro et al., 2020) industry. In fact, Apostolidis and Lee (2010) showed the pharmaceutical potentiality of *A. nodosum* against hyperglycemia.

Nevertheless, the extraction procedures and conditions employed to produce polyphenols extracts strongly affect their inhibition capacity against α -amylase and α -glucosidase (Yuan et al., 2018). Ultrasound-assisted extraction (UAE) is an efficient method for polyphenols extraction, since is a low-cost equipment and an easy-procedure methodology (Kadam et al., 2015), without affecting heat sensitive polyphenols (Moreira et al., 2016). Usually, aqueous mixtures of methanol, ethanol, acetone, acids among others are employed (Koivikko et al., 2005; Liu et al., 2016). Following the main principle of green chemistry (EPA, 2012), replacement of organo-solvents by water as unique extraction solvent is promoted, hence it has been demonstrated that water is efficient for polyphenols extraction (Leyton et al., 2016) and additionally its use reduces subsequent purification stages and waste residue generation. In fact, several authors have found relevant phytochemical features of aqueous extracts from *A. nodosum* seaweed employing UAE technology (Gisbert et al., 2021; Kadam et al., 2015). Considering the efficiency of this technique, initial hypothesis is that aqueous polyphenolic extracts from UAE might have prominent inhibition capacities against digestive enzymes.

The aim of this study was to analyse and identify the *in vitro* inhibitory effect of different aqueous polyphenolic extracts from UAE of *A. nodosum* against digestive enzymes. For that purpose, seaweed extracts obtained under different sonication conditions were chemically characterized determining the proximate composition and their polyphenols features. To understand the inhibitory mechanism of the extracts against α -amylase or α -glucosidase, studies were conducted adding the polyphenol either to the enzymes or the substrates (starch or maltose, respectively).

5.2. Material and Methods

5.2.1. Materials

Type VI-B α -amylase from porcine pancreatic (EC 3.2.1.1) (8 U/mg), type I α -glucosidase from *Saccharomyces cerevisiae* (EC 3.2.1.20) (11 U/mg), native wheat starch (S5127), D (+)-maltose, acarbose, 3,5-dinitrosalicylic acid (DNS), Amberlite XAD16 resin (surface area 800 m²/g, pore diameter 10 nm), phloroglucinol, resorcinol, glucose and D (+)-glucuronic acid were obtained from Sigma Aldrich (Sigma Chemical, St. Louis, USA). D-glucose assay kit (GOD/POD) was obtained from Megazyme (K-GLUC 08/18, Megazyme International Ireland Ltd., Bray, Co. Wicklow, Ireland). All chemical reagents used were of analytical grade.

5.2.2. Seaweed sampling

Fresh *Ascophyllum nodosum* seaweed from Galicia's coasts (NW of Spain) harvested on November 2019, supplied by Mar de Ardora S.L. company (Ortigueira, Spain), were dried in a hot air convective dryer (Angelantoni, Challenge 250, Massa Martana, Italy) at 50°C, with a constant relative humidity of 30% and air velocity at 2 m/s. Dried algae was grinded in an ultra-centrifugal mill (Retsch GmbH, ZM200, Haan, Germany) and sieved using a vibratory sieve with average particle size of $276 \pm 8 \mu\text{m}$. Milled seaweed were hydrated for 15 min with double distilled water with a liquid-solid ratio of 20 g of water per g of dried seaweed (gW/gDS) before sonication. UAE was carried out with a 1000 W ultrasound processor (Hielscher, UIP-1000 hdT, Teltow, Germany) in a jacketed chamber cooled by a cold-water bath to maintain blend temperature under 30°C. Continuous UAE operation was performed controlling the solid-liquid dispersion flow with a peristaltic pump (Cole Parmer MasterflexTM, USA). Extracts were sonicated for 2 min at 70 (E70), 80 (E80) and 90 W/cm² (E90) of sonication power, conditions previously determined (Gisbert et al., 2021). Solid residue was removed from liquid phase by centrifugation at 12,500 xg for 10 min.

E90 sample was further purified in a (2.5 x 47 cm) Bio-Rad column (Bio-Rad, Hercules, CA, USA) filled with Amberlite XAD16 resin. Working flux was set at 110 mL/h

using a peristaltic pump. Aqueous extract (100 mL) was poured into the column and washed with 300 mL of distilled water. Then, the column was flushed with 200 mL of ethanol 70% (v/v) to obtain a polyphenols-enriched fraction (P90). All extracts and purified fraction were freeze-dried (FD) at -55°C and 50 Pa with a Lyoquest-55 freeze dryer (Telstar Technologies, Terrassa, Spain).

5.2.3. Chemical analysis

Protein and fat content in seaweed extracts were determined by standard AOAC methods (AOAC, 2000). The fat content was determined by Soxhlet extraction and proteins were analysed with a Elementar rapid N exceed nitrogen analyzer (Elementar, Langenselbold, Germany) using 5.0 as a conversion factor of nitrogen into proteins (Angell et al., 2016). Ash content was analysed, by burning a weighed sample in a muffle furnace at 550°C for 6 hours. Data were expressed as percentage on a dry weight (DW). Carbohydrate content (CHOS) was evaluated by Dubois method (Dubois et al., 1956) and results were given in grams of glucose equivalents per gram of lyophilized extract (mgGE/gDW). Total polyphenol content (TPC) was determined following Folin-Ciocalteu reaction, measured spectrophotometrically at 765 nm, and results expressed in grams of phloroglucinol equivalents per gram of DW extract (gPE/gDW). Uronic acid content (UA) determination was carried out at 520 nm (Blumenkrantz & Asboe-Hansen, 1973) and the contents were given in grams of glucose equivalents per gram of DW extract (gGE/gDW). DPPH scavenging activity (%) was determined at 515 nm (Brand-Williams et al., 1995). The iron cation reduction capacity (FRAP) of the extracts was measured at 593 nm after tested samples incubation in darkness for 30 min and results were expressed as μg of trolox equivalents per mg of dry weight of DW extract ($\mu\text{gTE}/\text{mgDW}$).

5.2.4. Inhibition assays of α -amylase and α -glucosidase

The inhibition assay of α -amylase from porcine pancreatic was analyzed following the methodology described by Alexandre et al. (2021), with minor modifications. Briefly, wheat starch solution (6.25 mg/mL) was prepared in sodium phosphate buffer (0.02 M, pH 6.9 containing 6 mM NaCl), followed by a gelatinization in a water bath at 100°C for 20 min. Reaction media included 50 μg of freeze-dried seaweed extracts dissolved in ethanol (20% v/v), 50 μL of α -amylase (50 U/mL) and 400 μL of gelatinized wheat starch. Three methodologies were carried out to evaluate extracts inhibition (Figure 5.1): i. (M1_{AM}) enzyme and polyphenol solutions were mixed and pre-incubated in an Eppendorf Thermomixer Compact at 37°C for 10 min at a speed of 600 rpm. Then, gelatinized starch was added, and reaction mixture incubated at the same conditions. ii. (M2_{AM}) Gelatinized starch and polyphenol extracts were mixed and pre-incu-

bated at 37°C for 10 min before adding the enzyme, and then mixture was incubated at 37°C. iii. (M3_{AM}). Starch was gelatinized in the presence of the extract, and then cooled at rt for 10 min till reaching 37°C. The enzyme solution was then added, and mixture incubated 37°C for 10 min. To stop the reaction in the three methods (M1_{AM}, M2_{AM} and M3_{AM}), 500 μ L of 3,5-dinitrosalicylic acid (DNS) colour reagent was added and the mixture boiled in a water bath for 10 min. Samples were diluted in distilled water (1:10), and their absorbances measured at 540 nm in a microplate reader (Epoch Biotek Instruments, Winooski, VT, USA).

The α -glucosidase from *Saccharomyces cerevisiae* activity was measured using maltose (10 mg/mL) dissolved in sodium phosphate buffer (0.1 M, pH 6.9). Reaction mixture consisted of 50 μ L of seaweed extracts, 50 μ L of α -glucosidase (10 U/mL) and 400 μ L of maltose, but two different methodologies (M1_{AG} and M2_{AG}) were tested (Figure 5.1). In M1_{AG} method, enzyme and polyphenol were initially pre-incubated at 37°C for 10 min and then maltose was added to initiate the enzymatic reaction at 37°C. For M2_{AG} methodology, maltose and seaweed extract were initially pre-incubated at 37°C for 10 min, the enzyme was then added. In both, M1_{AG} and M2_{AG}, enzymatic reaction was stopped by boiling samples in a water bath for 10 min. Absorbance was measured at 510 nm using the above-mentioned GOD/POD kit.

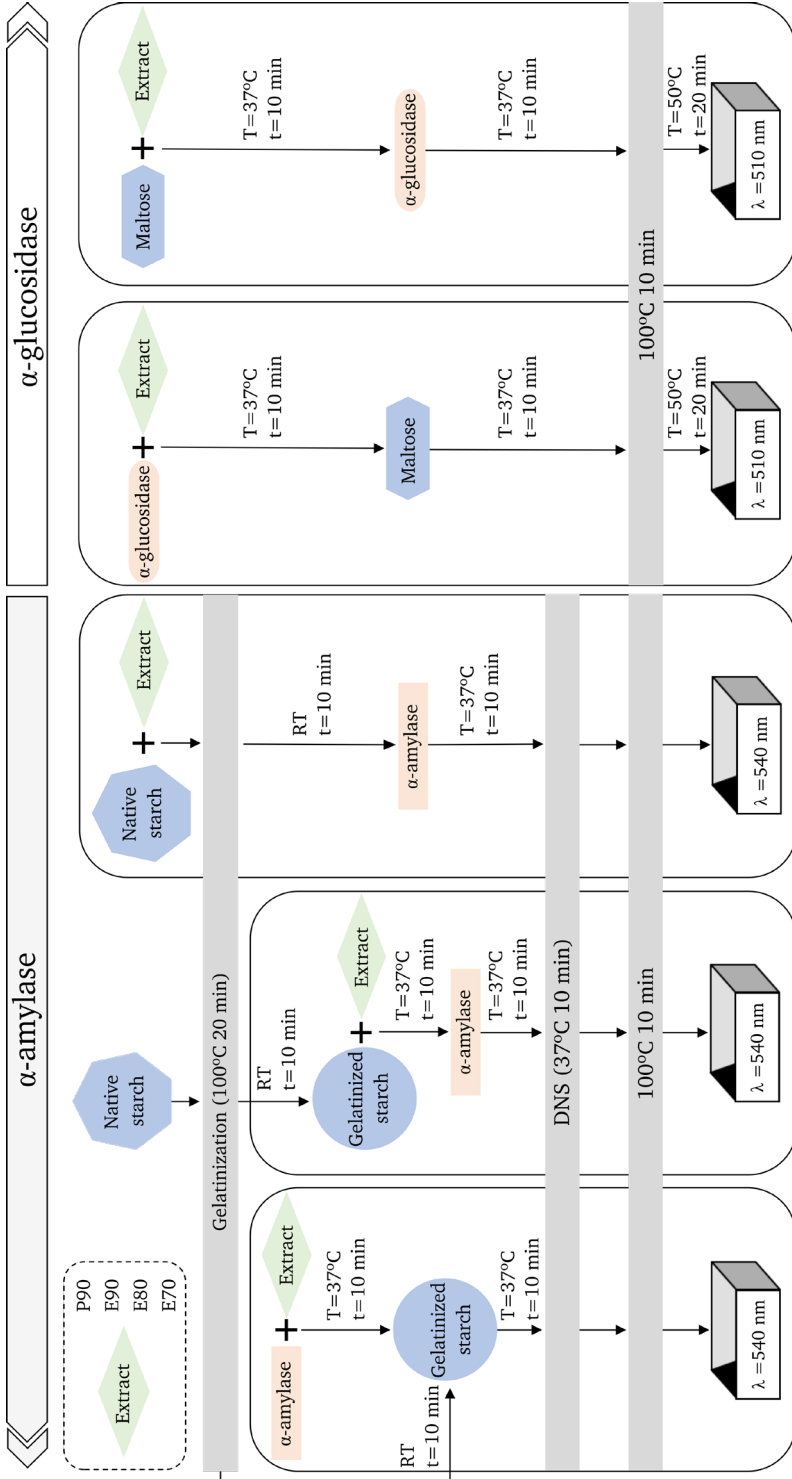


Figure 5.1. Methodology scheme of inhibitory assays (M1, M2 and M3) of α -amylase (AM) and α -glucosidase (AG) digestive enzymes against aqueous polyphenols extracts (E70, E80, E90 and P90) from *A. nodosum* seaweed.

Solutions without seaweed extracts and without enzymes were analyzed as control and blank, respectively. The inhibition rate of seaweed extracts was calculated by Eq 1:

$$\% \text{ enzyme inhibition} = \left[1 - \left(\frac{\text{Abs}_{\text{sample}} - \text{Abs}_{\text{blank sample}}}{\text{Abs}_{\text{control}} - \text{Abs}_{\text{blank control}}} \right) \right] \cdot 100 \quad (1)$$

where, $\text{Abs}_{\text{sample}}$ was the absorbance of sample with substrate and enzyme; $\text{Abs}_{\text{blank sample}}$ was the absorbance obtained without enzyme; $\text{Abs}_{\text{control}}$ was the absorbance without extracts sample; $\text{Abs}_{\text{blank control}}$ was the absorbance of substrate. The IC_{50} value is the sample concentration required for 50% inhibition of the α -amylase or α -glucosidase activity. Acarbose was used as a positive control.

5.2.5. Chromatographic separation

P90, E90, E80 and E70 chromatographic profiles were obtained with an HPLC system (Jasco, Japan) equipped with a PU-980 pump, an UV-1575 detector and a degasser Populaire DP4003. Data were obtained and processed with PowerChrom 2.5 (eDaq Technologies, Australia) software and MATLAB R2019b software (MathWorks Inc., USA). Chromatographic separation was performed on a Kromasil C-18 semi-preparative column (8 x 250 mm) at 30°C. A gradient elution using water (A) and methanol (B) consisted of 0-3 min (99% A, 1% B), 30 min (5% A, 95% B) and 40 (99% A, 1% B). Freeze-dried samples (2 mg/mL) were diluted in EtOH 20% (v/v) and filtered through 0.45 μm syringe filters. Injection volume was 50 μL , detection wavelength 266 nm, and solvent flow rate 0.4 mL/min. Polyphenol content was calculated with standard molecules of phloroglucinol and resorcinol; additionally, glucose and glucuronic acid standards were injected to check for possible interference of uronic acids and sugars (Gonçalves-Fernández et al., 2019). To ensure the reproducibility of the assays, a minimum of 4 injections of each extract were carried out.

5.2.6. $^1\text{H-NMR}$

Proton nuclear magnetic resonance spectroscopy ($^1\text{H-NMR}$) spectra were collected with

Bruker NEO 750 spectrophotometer operated with a 17.61 T (750 MHz resonance ^1H) magnetic field strength. Phenolic extracts were blended with methanol- d_4 . $^1\text{H-RMN}$ spectra treatment was carried out with MestreNova software (Mestrelab Research, Santiago de Compostela, Spain).

5.2.7. Statistical analyses

All measurements were carried out at least in duplicate and presented as mean \pm standard deviation. Statistical analysis was carried out by IBM SPSS statistics 24 (SPSS Inc., USA) software. A one-way analysis of variance (ANOVA) was assessed based on confidence interval of 95% ($p < 0.05$) using a Duncan test.

5.3. Results and discussion

5.3.1. Seaweed extracts chemical composition

Chemical characterisation of *Ascophyllum nodosum* ultrasound-assisted crude extracts (E90, E80 and E70) and purified (P90) sample is summarized in Table 5.1.

Table 5.1. Chemical composition of freeze-dried (E90, E80 and E70) and purified (P90) extracts obtained by UAE from *Ascophyllum nodosum* brown edible seaweed.

	P90	E90	E80	E70	P-value	
					Purification	Sonication
Moisture (% DW)	16.39 \pm 0.12 c	8.78 \pm 0.15 a	8.56 \pm 0.26 a	10.13 \pm 0.59 b	0	0.2383
Protein (% DW)	6.96 \pm 0.30 a	7.48 \pm 0.02 b	7.37 \pm 0.13 b	7.57 \pm 0.11 b	0.0420	0.5649
Mineral (% DW)	8.19 \pm 0.17 a	29.49 \pm 0.20 b	29.78 \pm 0.09 b	29.99 \pm 0.40 b	0	0.2383
Fat (% DW)	3.02 \pm 0.04	4.19 \pm 0.04	3.99 \pm 0.87	4.20 \pm 0.13	0.0577	0.8729
CHOS (mgGE/mg DW)	0.17 \pm 0.04 b	0.11 \pm 0.02 a	0.10 \pm 0.01 a	0.10 \pm 0.02 a	0.0198	0.8193
TPC (mgPE/mg DW)	0.42 \pm 0.04 b	0.20 \pm 0.03 a	0.19 \pm 0.03 a	0.18 \pm 0.03 a	0.0090	0.9131
UA (mgGE/mg DW)	0.05 \pm 0.01 a	0.21 \pm 0.04 b	0.17 \pm 0.02 b	0.17 \pm 0.04 b	0.0205	0.6025
DPPH decay (%)	38.57 \pm 0.34 a	39.59 \pm 0.56 a	39.97 \pm 0.46 a	50.59 \pm 2.16 b	0.5651	0.0041
FRAP (μ gTE/mg DW)	1.79 \pm 0.05 a	1.11 \pm 0.01 b	1.10 \pm 0.11 b	1.12 \pm 0.04 b	0.0017	0.9759

Means within a row followed with different letter are significantly different ($p < 0.05$).

Sonication power did not affect the proximate composition of the extracts and only the further purification had a significant ($p < 0.05$) effect on the moisture, protein, mineral, fat, carbohydrates (CHOS), total polyphenol content (TPC), uronic acids content (UA). Extracts purification with the resin significantly reduced protein content (7%) and particularly ash content (96%) compared to non-purified extracts. Regarding antioxidant activities of the extracts (DPPH and FRAP values), DPPH scavenging activity was significantly reduced by the sonication power, and Fe²⁺ reducing power (FRAP) significantly increased with the purification. Similarly, Kadam et al. (2015) reported TPC and DPPH values of 0.16 mgPE/g and 61.46%, respectively, in aqueous *A. nodosum* extracts obtained by UAE at sonication power of 35.6 W/cm² for 15 min.

UA/TPC ratios of the extracts varied significantly from 0.12 ± 0.02 for P90 up to 0.96 ± 0.08 for E90, E80 and E70. Polyphenols and UA could be partially forming complexes (Wang et al., 2016). The complexation mechanism is not elucidated and is still in discussion. Hydrogen bridges or hydrophobic interactions (Koivikko et al., 2005) and covalent bonds of ether, ester and hemiacetal bonds (Salgado et al., 2009) have been proposed. The bonds of these complexes could affect their structural properties and promote or avoid some chemical interactions. However, the presence of these complexes was not discriminated by common TPC and UA analyses and antioxidant activities (DPPH and FRAP) assays because crude extracts showed not significant differences (Table 5.1). Therefore, results indicate that sonication power had no significant effects on the UA/TPC ratio, but purification dramatically reduced this value. The bonds of these complexes could affect their structural properties and promote or avoid some chemical interactions.

5.3.2. Inhibition effect of seaweed extracts against α -amylase and α -glucosidase enzymes

A comparative study was conducted to determine the capability of the four different *A. nodosum* extracts (P90, E90, E80 and E70) to inhibit α -amylase and α -glucosidase activity. Figures 5.2 and 5.3 showed the α -amylase and α -glucosidase inhibition, respectively, induced by the different extracts compared to acarbose, which was taken as standard inhibitor (Table 5.2).

Table 5.2. IC₅₀ values of seaweed extracts against α -amylase and α -glucosidase of the different analyzed methodologies: M1 = preincubation PP+enzyme, M2 = preincubation PP+gelatinized starch, M3 = gelatinized (PP+starch).

	IC ₅₀ against α -amylase (AM) ($\mu\text{g/mL}$)			IC ₅₀ against α -glucosidase (AG) ($\mu\text{g/mL}$)		
	M1 _{AM}	M2 _{AM}	M3 _{AM}	M1 _{AG}	M2 _{AG}	
Acarbose	11.51±0.63	a 56.07±3.00	a 142.82±12.09	a 0.16±0.01	0.13±0.01	
P90	40.03±1.11	b 74.03±2.58	b 810.48±24.35	b 3.20±0.14	a 3.62±0.23	a
E90	119.55±0.73	c 309.16±4.13	c 4066.32±50.09	c 19.49±0.75	b 26.15±0.76	b
E80	128.81±2.91	d 342.59±0.69	d 4451.00±49.18	d 20.26±0.32	b 28.09±0.04	c
E70	152.97±4.35	e 439.82±9.83	e 4777.66±42.53	e 29.19±0.37	c 30.36±0.70	d
P-value						
Purification	0.0001	0.0001	0.0001	0.0001	0.0001	
Sonication	0.0001	0.0001	0.0003	0.0001	0.0025	

Means within a column followed with different letter are significantly different ($p < 0.05$).

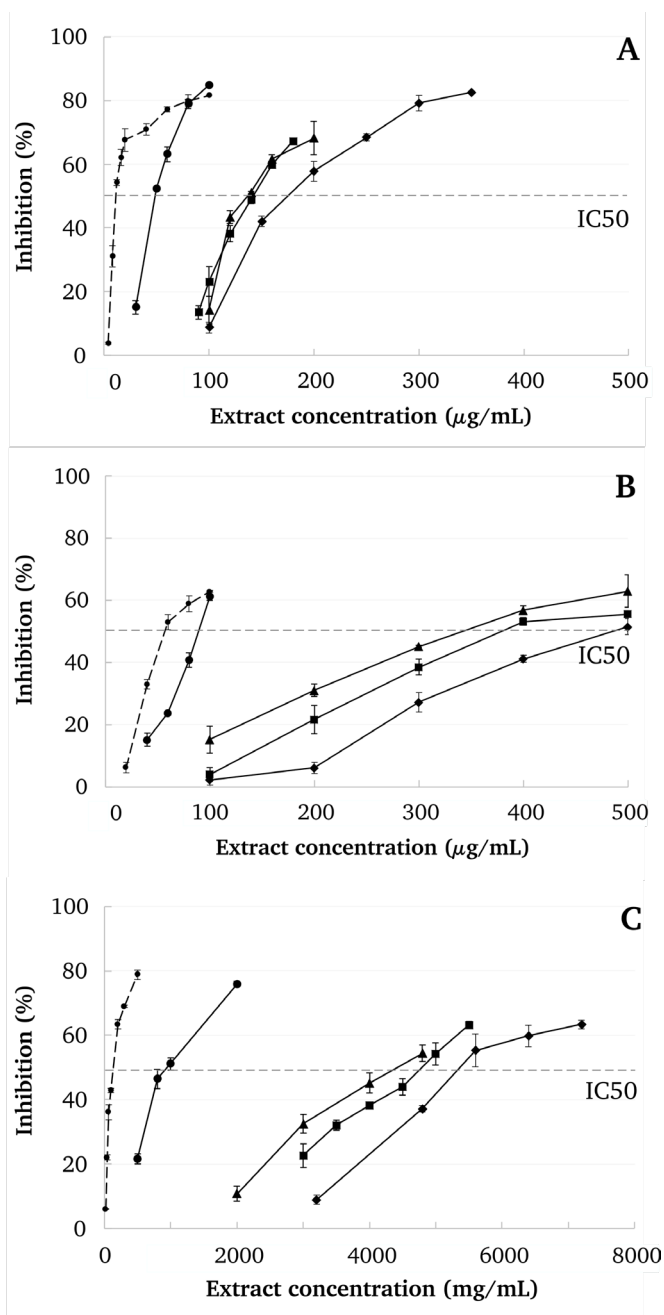


Figure 5.2. Inhibitory capacity of purified (● P90) and crude (▲ E90, ■ E80, ◆ E70) seaweed extracts against α -amylase (A= M1_{AM}, B= M2_{AM} and C= M3_{AM}).

Sonication conditions and purification of polyphenols had significant effect on the IC_{50} ($p < 0.005$) for both starch digestive enzymes. When the extracts were pre-incubated with the enzyme (M1) (Figure 5.2 A, Figure 5.3 A), the UAE sonication power significantly affected the IC_{50} .

The decrease of IC_{50} when increasing the sonication power suggested that the inhibition ability of the extracts increased, despite extracts showed similar total polyphenol contents and DPPH values. The extract purification with Amberlite (P90) largely improved the inhibition efficiency decreasing the IC_{50} of α -glucosidase and α -amylase by 4.4 and 6.3 times, respectively. This result might be explained by its higher polyphenol content (Table 5.1) compared with un-purified extracts. Comparing the effect of tested extracts, higher extract concentrations were required to inhibit α -amylase compared to α -glucosidase. These results support the findings described by Apostolidis and Lee (2010) when analyzing an aqueous extract from AN, observing higher inhibition activity against yeast α -glucosidase than against porcine pancreatic α -amylase. Conversely, Pantidos et al. (2014) found that a tannin-rich fraction of *A. nodosum* obtained with different solvents was more effective inhibiting porcine pancreatic α -amylase than rat intestinal α -glucosidase. Divergences might be ascribed to the different composition of the extracts, which depends on the extraction method. Zhang et al. (2007) determined an $IC_{50} = 77 \mu\text{g/mL}$ against α -glucosidase working with water-ethanol *A. nodosum* extracts. Whereas Liu et al. (2016) determined IC_{50} from 8.9 to 36.3 $\mu\text{g/mL}$ against α -glucosidase from ethanolic extracts of *A. nodosum* in the same range than those found in this work. Nevertheless, discussion of results based on previously published data becomes complicated due to the wide range of experimental conditions used, that makes very difficult to compare IC_{50} values, which are specific for the enzyme type, the substrate used and the reaction conditions.

Given the influence of the procedure carried out to analyze enzyme inhibition, besides the extraction procedure and/or the source of the seaweed, three different methodologies (M1, M2, M3), were used to identify the effect of polyphenols interaction with the enzymes on the level of inhibition. The most effective inhibition was obtained when the extracts were previously incubated with the enzyme (M1) (Figure 5.2 A, Figure 5.3 A), where the interaction between polyphenols and enzyme was favored, before substrate (starch or maltose) addition for α -amylase (M1_{AM}) or α -glucosidase (M1_{AG}), respectively. Conversely, higher IC_{50} values were required with M2, when the extract was previously mixed with gelatinized starch for α -amylase (M2_{AM}) ($IC_{50} = 74.03, 309.16, 342.59$ and $439.82 \mu\text{g/mL}$ for P90, E90, E80 and E70, respectively) or with maltose for α -glucosidase (M2_{AG}) ($IC_{50} = 3.62, 26.15, 28.09$ and $30.36 \mu\text{g/mL}$ for P90, E90, E80 and E70, respectively) (Figure 5.2, B and Figure 5.3, B). These observations suggest that in the M2 method, the substrate hinders the polyphenol accessibility to the enzymes, increasing IC_{50} values. Pantidos et al. (2014) also observed lower effectiveness of a tannin-rich fraction, as porcine pancreatic α -amylase inhibitor,

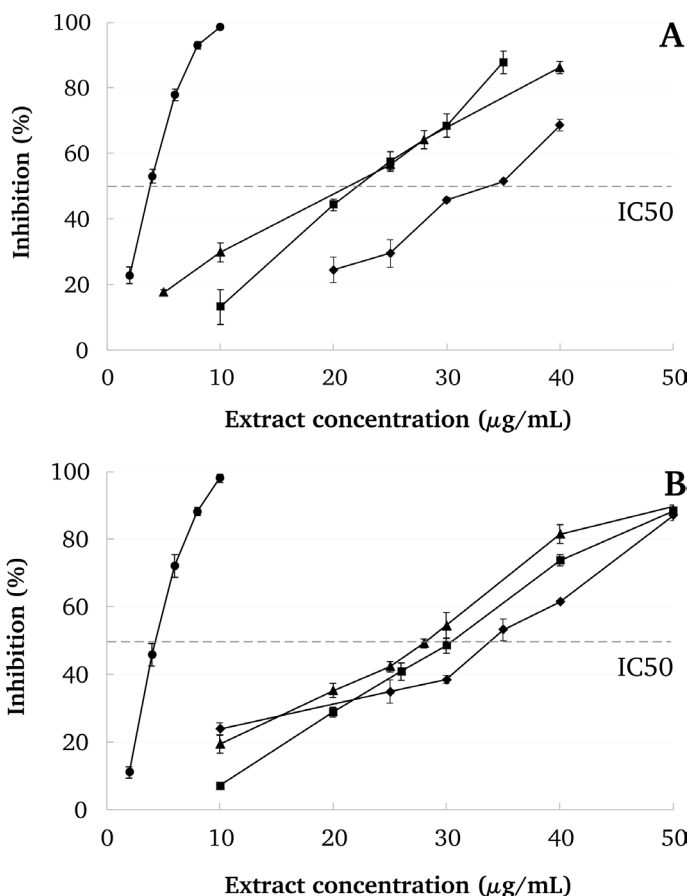


Figure 5.3. Inhibitory capacity of purified (● P90) and crude (▲ E90, ■ E80, ◆ E70) seaweed extracts against α -glucosidase (A= M1_{AG} and B= M2_{AG}).

when it was pre-incubated with gelatinized potato starch. Lordan et al. (2013) described porcine pancreatic α -amylase inhibition ($IC_{50} = 0.05$ mg/mL) with *A. nodosum* extracts obtained from a three-stages process of at least 3 h duration, similar to the one obtained with P90 extract in M2. Like the previously mentioned polyphenol-enzyme binding, phenolic compounds can bind starch by non-covalent interactions, modulating starch digestion kinetics (Giuberti et al., 2020). This lower inhibition effect when the extract was pre-incubated with the starch highlights the significance of the hydrolysis kinetics during *in vitro* analysis and subsequently to the *in vivo* studies, where pancreatic α -amylase and intestinal α -glucosidase are secreted into the gut lumen, where they would meet the seaweed extract and the starch mixture.

Furthermore, the inhibitory effect against α -amylase dramatically decreased when extracts were added to native starch and the blend was subjected to high temperatures to gelatinize the starch ($M3_{AM}$) (Figure 5.2, C). IC_{50} values varied between 810.48 (P90) to 4777.66 (E70) $\mu\text{g/mL}$. Nevertheless, in this case, besides the starch impediment previously mentioned for $M2_{AM}$, polyphenols and starch interaction during the gelatinization process or polyphenols stability might be considered. Wu et al. (2011) described the existence of hydrogen bonding interaction between tea polyphenols and rice starch during gelatinization. On the other hand, high temperature can affect the stability of polyphenols and antioxidant activity (Moreira et al., 2016), and therefore may affect also its ability as enzyme inhibitors. Betoret and Rosell (2020) analyzed the effect of temperature (70, 80 and 90°C for 20 min) on phenolic compounds of *Brassica napobrassica* blended with maize and rice starches. These authors reported the protective role of starch with phenolic compounds, in which the high apparent viscosity might contribute to protect the bioactive compounds. Authors linked the changes of bioactive compounds after thermal treatments with thermal degradation, matrix un-structuring effect and interaction with other ingredients, protecting them from degradation. However, to understand the polyphenol inhibition of the *A. nodosum* extracts, it was necessary to further analyses.

5.3.3. Seaweed freeze-dried extracts characterization: chromatography (RP-HPLC-UV) and nuclear magnetic resonance ($^1\text{H-NMR}$)

Crude (E90, E80 and E70) and purified (P90) polyphenols extracts were chromatographically analysed using phloroglucinol and resorcinol as standards. Chromatograms showed a unique peak (Figure 5.4) around 60 min of retention time, with no signals around 40 min (spectra not shown) that was the retention time of the standards used, concluding that the compounds detected had higher molecular mass than standards.

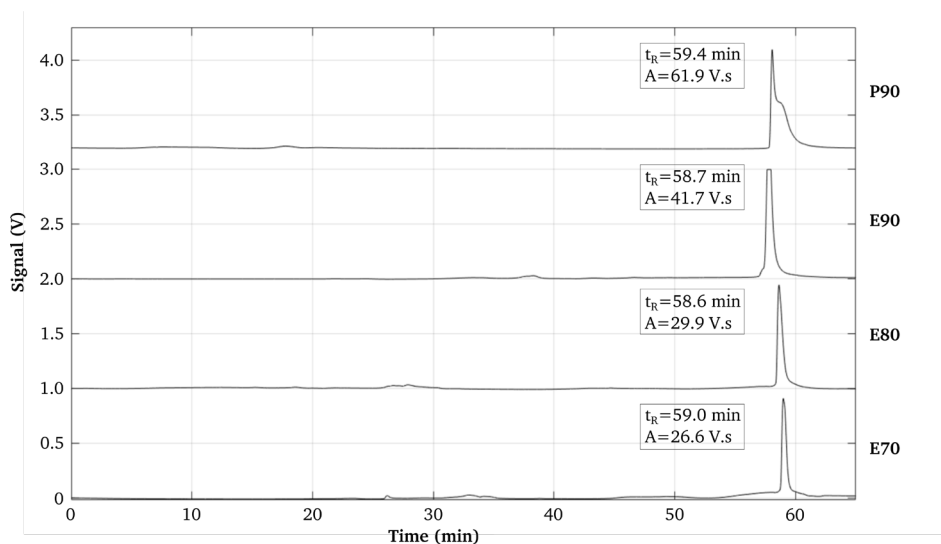


Figure 5.4. RP-HPLC-UV profiles of purified (P90, 50 μ L of 2.5 mgFD/mL) and crude (E90, E80, E70, injected 50 μ L of 5.0 mgFD/mL) aqueous extracts obtained by UAE from *A. nodosum* seaweed.

This result was expected since phloroglucinol does not accumulate in the *A. nodosum* tissues, owing to the rapid polymerisation reactions (Tierney et al., 2014). Standardized phlorotannins chromatographic characterization methodology is limitless since commercial standards are scarce (Koivikko et al., 2007). Very small peak signals located up to 20 to 40 min of retention time show the presence of polysaccharides, in accordance with additional carbohydrates and UA standards (glucose and D (+)-glucuronic acid). No significant differences on chromatographic spectra of crude extracts (E90, E80 and E70) were observed, indicating phlorotannin structure differences were not detectable with RP-HPLC-UV technique. The increase in TPC value of P90, measured by Folin-Ciocalteu, was also confirmed by HPLC analysis, where 50 μ L of 2.5 mgFD/mL of P90 presented a similar peak than 50 μ L of 5.0 mgFD/mL from E90 extract.

Chromatographic results indicated that all UAE extracts contain polyphenols with high polymer size without significant presence of oligomers (expected at shorter times). Hence, differences in enzyme inhibition activities among extracts were not explained by HPLC results. Other authors have previously reported that HPLC method was ineffective separating large polymeric phlorotannins from *A. nodosum* (Tierney et al., 2014), and needs to be complemented with MS and/or NMR techniques (Koivikko et al., 2007).

An adequate method for identifying and quantifying purified polyphenols is $^1\text{H-NMR}$, but it is only qualitative in complex mixtures, since isomers appear at approximately the same chemical shifts. Nonetheless, $^1\text{H-NMR}$ analysis could give a proximate insight

of overall structure of the assayed extracts and understand inhibition results. Figure 5.5 shows $^1\text{H-NMR}$ spectra of purified (P90) and crude UAE (E90, E80 and E70) extracts from *A. nodosum* seaweed.

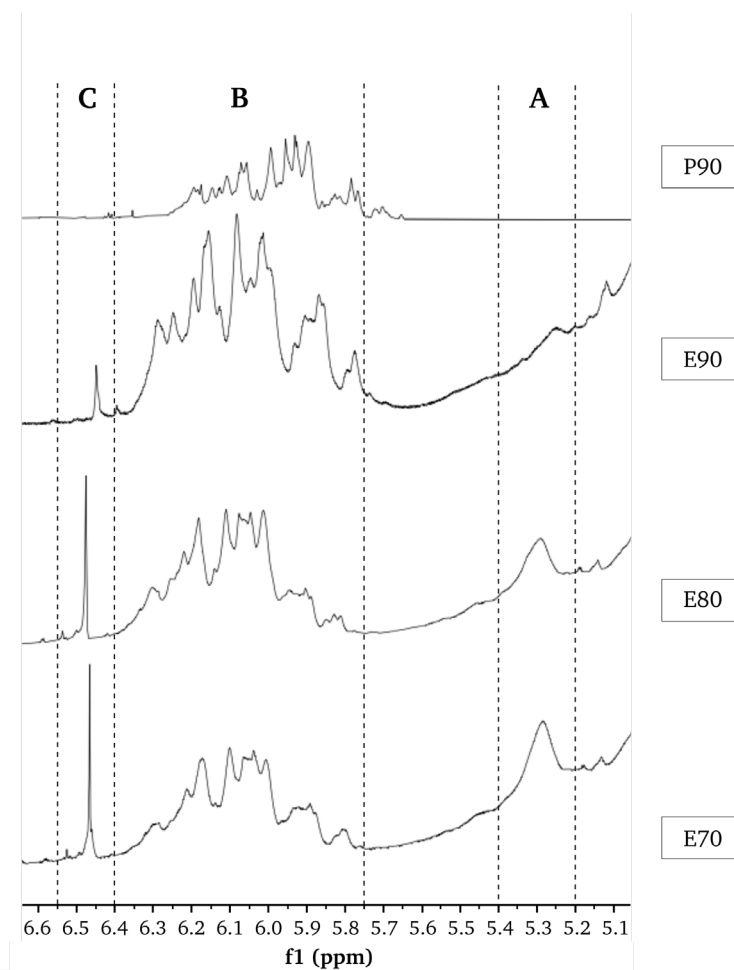


Figure 5.5. $^1\text{H-NMR}$ spectra of freeze-dried extracts purified (P90) and crude (E90, E80 and E70) obtained by UAE from *A. nodosum* seaweed.

Three different ranges could be identified at 5.20-5.40 (A), 5.75-6.40 (B) and 6.40-6.55 (C) ppm in tested samples, which agree with seaweed's polyphenols signals reported between 5.0 and 6.5 ppm (Audibert et al., 2010; Susano et al., 2021). In addition, $^1\text{H-NMR}$ spectra of crude UAE extracts showed below 5.6 ppm a notorious increasing signal associated with the presence of UA and carbohydrates (these last, at low ppm, data not shown) (Zhang et al., 2004).

Polyphenols extracted from brown seaweed are composed of phloroglucinol moieties linked by a mix of aryl-aryl and aryl-ether bonds (Choi et al., 2014). Hydrogens located near to aryl-ether bonds showed values around 6.50 ppm (C-region), meanwhile the aryl-aryl bonds signals around 5.70 to 6.30 ppm (B-region) (Choi et al., 2014; Kim et al., 2019). This was also corroborated by phloroglucinol standard molecule spectra (data not shown) that showed a peak at 5.85 ppm from aryl-aryl bonds. A-region signal has been related to the presence of quinones derived from partial oxidation of polyphenols (Dobado et al., 2011). In fact, this signal dramatically decreased with sonication power (and disappeared in P90). This trend could be associated to the use of high power that increased the lixiviation of less oxidated polyphenols from inner cell-structures (Koivikko et al., 2007) and, oppositely, when low power is employed surface polyphenols from cell-wall (more exposed to oxygen) were mainly extracted. All extracts presented B-region signals and sonication power seemed to only change overall shape. Several peaks observed in this region evidenced the presence of different isomers of phlorotannins extracted during UAE treatment.

Prominent signal in C-region for E70 and E80 was observed in comparison to low signal in E90, meaning that C-region signal decreased with increasing sonication power. After Amberlite purification process (P90), this signal practically disappeared. Chemical composition of extracts (Table 5.1) showed a noticeable reduction of UA/TPC ratio for P90 regarding to E90. Based on these results, it is hypothesized that signals of C-region could be indicative of the presence of some polyphenolic complexes, mainly with uronic acids. The gradual signal reduction with increasing sonication power during UAE could be related to the disruption of these complexes, that could increase polyphenol availability for enzymes inhibition. Then, NMR spectra and *in vitro* inhibitory activities suggested that polyphenols-UA complexes are present on the extracts. The observed trend of digestive enzyme inhibitory activities of the extracts (Table 5.2) could be explained due to the greater presence of “free” polyphenols (not complexed) that interacted more easily with α -amylase and α -glucosidase enzymes during *in vitro* inhibitory assays.

5.4. Conclusions

Aqueous *Ascophyllum nodosum* extracts obtained by ultrasound-assisted extraction have shown to be highly effective inhibitors against α -amylase and particularly, α -glucosidase. Further purification of the UAE extract allowed increasing polyphenol content and reducing uronic acids content. IC₅₀ values of both enzymes progressively decreased with increasing sonication power applied during extraction. Purification of extracts increased inhibition against both digestive enzymes due to its higher polyphenols content. Aqueous seaweeds extracts were more effective inhibitors when they were added

directly to the enzyme previously to the substrates (starch or maltose). The mixing of extracts with substrates (gelatinized or ungelatinized starch, or maltose) prior to the enzymatic reaction reduced the inhibitory effect of the extracts, being especially dramatic for the α -amylase inhibition. Antioxidant activities and chromatographic profiles of *A. nodosum* extracts did not explain the different inhibitions of α -amylase and α -glucosidase enzymes. Relevant differences could be observed in the $^1\text{H-NMR}$ spectra associated to the presence of uronic acids-polyphenols complexes (C-region) and quinones (A-region) that could be related to the measured inhibitory capacities trends of tested extracts. In conclusion, polyphenols-enriched extracts from brown seaweeds with notorious inhibitory capacities against digestive enzymes might be suitable to be used as regulators of postprandial glucose in diabetic patients employing UAE with water (green-solvent).

Author Contributions: Credit roles: AA: Conceptualization; Data curation; Formal analysis; Investigation; Methodology; Writing-original draft; MG: Data curation; Formal analysis; Methodology; Writing-original draft, JS: Formal analysis; Writing-review & editing; Funding acquisition; RM: Formal analysis; Writing-review & editing; Funding acquisition; CMR: Conceptualization; Funding acquisition; Investigation; Supervision; Data curation; Writing-review & editing.

Acknowledgments: Authors acknowledge the financial support of Grant RTI2018-095919-B-C2 funded by MCIN/AEI/10.13039/501100011033, “ERDF A way of making Europe” by the “European Union”, Generalitat Valenciana (Project Prometeo 2017/189) and Xunta de Galicia (ED431B 2019/01).

Conflicts of Interest: The authors declare that they do not have any conflict of interest.

References

- Aleixandre, A., Gil, J. V., Sineiro, J., & Rosell, C. M. (2021). Understanding phenolic acids inhibition of α -amylase and α -glucosidase and influence of reaction conditions. *Food Chemistry*, 131231.
- Angell, A. R., Mata, L., de Nys, R., & Paul, N. A. (2016). The protein content of seaweeds: a universal nitrogen-to-protein conversion factor of five. *Journal of Applied Phycology*, 28(1), 511-524.
- AOAC. (2000). Official methods of analysis of the AOAC International: Association of Analytical Communities.

Apostolidis, E., & Lee, C. M. (2010). In Vitro Potential of *Ascophyllum nodosum* Phenolic Antioxidant-Mediated α -Glucosidase and α -Amylase Inhibition. *Journal of Food Science*, 75(3), H97-H102.

Audibert, L., Fauchon, M., Blanc, N., Hauchard, D., & Ar Gall, E. (2010). Phenolic compounds in the brown seaweed *Ascophyllum nodosum*: distribution and radical-scavenging activities. *Phytochemical Analysis*, 21(5), 399-405.

Betoret, E., & Rosell, C. M. (2020). Effect of particle size on functional properties of Brassica napobrassica leaves powder. Starch interactions and processing impact. *Food Chemistry: X*, 8, 100106.

Blumenkrantz, N., & Asboe-Hansen, G. (1973). New method for quantitative determination of uronic acids. *Analytical Biochemistry*, 54(2), 484-489.

Brand-Williams, W., Cuvelier, M.-E., & Berset, C. (1995). Use of a free radical method to evaluate antioxidant activity. *LWT-Food science and Technology*, 28(1), 25-30.

Choi, J.-S., Lee, K., Lee, B.-B., Kim, Y.-C., Kim, Y., Hong, Y.-K., Cho, K., & Choi, I. (2014). Antibacterial activity of the phlorotannins dieckol and phlorofucofuroeckol-A from *Ecklonia cava* against *Propionibacterium acnes*. *Botanical Sciences*, 92, 425.

Dall'Asta, M., Del Rio, D., Tappy, L., Potì, F., Agostoni, C., & Brighenti, F. (2020). Critical and emerging topics in dietary carbohydrates and health. *International Journal of Food Sciences and Nutrition*, 71(3), 286-295.

de Paulo Farias, D., de Araújo, F. F., Neri-Numa, I. A., & Pastore, G. M. (2021). Antidiabetic potential of dietary polyphenols: A mechanistic review. *Food Research International*, 145, 110383.

Dobado, J., Gómez-Tamayo, J., G. Calvo-Flores, F., Martinez, H., Cardona Villada, W., Weiss-López, B., Ramírez-Rodríguez, O., Pessoa, H., & Araya-Maturana, R. (2011). NMR assignment in regioisomeric hydroquinones. *Magnetic Resonance in Chemistry : MRC*, 49, 358-365.

Dubois, M., Gilles, K. A., Hamilton, J. K., Rebers, P. t., & Smith, F. (1956). Colorimetric method for determination of sugars and related substances. *Analytical Chemistry*, 28(3), 350-356.

EPA. (2012). Basics of Green Chemistry. In: United States Environmental Protection Agency.

Gisbert, M., Barcala, M., Rosell, C. M., Sineiro, J., & Moreira, R. (2021). Aqueous extracts characteristics obtained by ultrasound-assisted extraction from *Ascophyllum nodosum* seaweeds: effect of operation conditions. *Journal of Applied Phycology*, 33(5), 3297-3308.

Giuberti, G., Rocchetti, G., & Lucini, L. (2020). Interactions between phenolic compounds, amylolytic enzymes and starch: an updated overview. *Current Opinion in Food Science*, 31, 102-113.

Gonçalves-Fernández, C., Sineiro, J., Moreira, R., & Gualillo, O. (2019). Extraction and characterization of phlorotannin-enriched fractions from the Atlantic seaweed *Bifurcaria bifurcata* and evaluation of their cytotoxic activity in murine cell line. *Journal of Applied Phycology*, 31(4), 2573-2583.

Kadam, S. U., Tiwari, B. K., Smyth, T. J., & O'Donnell, C. P. (2015). Optimization of ultrasound assisted extraction of bioactive components from brown seaweed *Ascophyllum nodosum* using response surface methodology. *Ultrasonics Sonochemistry*, 23, 308-316.

Kim, J. H., Lee, S., Park, S., Park, J. S., Kim, Y. H., & Yang, S. Y. (2019). Slow-Binding Inhibition of Tyrosinase by *Ecklonia cava* Phlorotannins. *Marine Drugs*, 17(6), 359.

Koivikko, R., Loponen, J., Honkanen, T., & Jormalainen, V. (2005). Contents of soluble, cell-wall-bound and exuded phlorotannins in the brown alga *Fucus vesiculosus*, with implications on their ecological functions. *Journal of Chemical Ecology*, 31(1), 195-212.

Koivikko, R., Loponen, J., Pihlaja, K., & Jormalainen, V. (2007). High-performance liquid chromatographic analysis of phlorotannins from the brown alga *Fucus vesiculosus*. *Phytochemical Analysis: An International Journal of Plant Chemical and Biochemical Techniques*, 18(4), 326-332.

Leandro, A., Pacheco, D., Cotas, J., Marques, J. C., Pereira, L., & Gonçalves, A. M. (2020). Seaweed's bioactive candidate compounds to food industry and global food security. *Life*, 10(8), 140.

Leyton, A., Pezoa-Conte, R., Barriga, A., Buschmann, A., Mäki-Arvela, P., Mikkola, J.-P., & Lienqueo, M. (2016). Identification and efficient extraction method of phlorotannins from the brown seaweed *Macrocystis pyrifera* using an orthogonal experimental design. *Algal Research*, 16, 201-208.

Liu, B., Kongstad, K. T., Wiese, S., Jäger, A. K., & Staerk, D. (2016). Edible seaweed as future functional food: Identification of α -glucosidase inhibitors by combined use of high-resolution α -glucosidase inhibition profiling and HPLC–HRMS–SPE–NMR. *Food Chemistry*, 203, 16-22.

Lordan, S., Smyth, T. J., Soler-Vila, A., Stanton, C., & Ross, R. P. (2013). The α -amylase and α -glucosidase inhibitory effects of Irish seaweed extracts. *Food Chemistry*, 141(3), 2170-2176.

Moreira, R., Chenlo, F., Sineiro, J., Arufe, S., & Sexto, S. (2016). Drying temperature effect on powder physical properties and aqueous extract characteristics of *Fucus vesiculosus*. *Journal of Applied Phycology*, 28(4), 2485-2494.

Pantidos, N., Boath, A., Lund, V., Conner, S., & McDougall, G. J. (2014). Phenolic-rich extracts from the edible seaweed, *Ascophyllum Nodosum*, inhibit α -amylase and α -glucosidase: Potential anti-hyperglycemic effects. *Journal of Functional Foods*, 10, 201-209.

Ríos, J. L., Francini, F., & Schinella, G. R. (2015). Natural products for the treatment of type 2 diabetes mellitus. *Planta Medica*, 81.

Roy, M.-C., Anguenot, R., Fillion, C., Beaulieu, M., Bérubé, J., & Richard, D. (2011). Effect of a commercially-available algal phlorotannins extract on digestive enzymes and carbohydrate absorption *in vivo*. *Food Research International*, 44(9), 3026-3029.

Salgado, L. T., Cinelli, L. P., Viana, N. B., Tomazetto de Carvalho, R., De Souza Mourão, P. A., Teixeira, V. L., Farina, M., & Filho, A. G. (2009). A vanadium bromoperoxidase catalyzed the formation of high-molecular-weight complexes between brown algal phenolic substances and alginates. *Journal of Phycology*, 45(1), 193-202.

Susano, P., Silva, J., Alves, C., Martins, A., Gaspar, H., Pinteus, S., Mouga, T., Goertert, M. I., Petrovski, Ž., & Branco, L. B. (2021). Unravelling the dermatological potential of the brown seaweed *Carpomitra costata*. *Marine Drugs*, 19(3), 135.

Tierney, M. S., Soler-Vila, A., Rai, D. K., Croft, A. K., Brunton, N. P., & Smyth, T. J. (2014). UPLC-MS profiling of low molecular weight phlorotannin polymers in *Ascophyllum nodosum*, *Pelvetia canaliculata* and *Fucus spiralis*. *Metabolomics*, 10(3), 524-535.

Wang, J., Hu, S., Nie, S., Yu, Q., & Xie, M. (2016). Reviews on Mechanisms of In Vitro Antioxidant Activity of Polysaccharides. *Oxidative Medicine and Cellular Longevity*, 2016, 5692852.

Wu, Y., Lin, Q., Chen, Z., & Xiao, H. (2011). The interaction between tea polyphenols and rice starch during gelatinization. *Food Science and Technology International*, 17(6), 569-577.

Yuan, Y., Zhang, J., Fan, J., Clark, J., Shen, P., Li, Y., & Zhang, C. (2018). Microwave assisted extraction of phenolic compounds from four economic brown macroalgae species and evaluation of their antioxidant activities and inhibitory effects on α -amylase, α -glucosidase, pancreatic lipase and tyrosinase. *Food Research International*, 113, 288-297.

Zhang, J., Tiller, C., Shen, J., Wang, C., Girouard, G. S., Dennis, D., Barrow, C. J., Miao, M., & Ewart, H. S. (2007). Antidiabetic properties of polysaccharide-and polyphenolic-enriched fractions from the brown seaweed *Ascophyllum nodosum*. *Canadian Journal of Physiology and Pharmacology*, 85(11), 1116-1123.

Zhang, Q., Li, N., Liu, X., Zhao, Z., Li, Z., & Xu, Z. (2004). The structure of a sulfated galactan from *Porphyra haitanensis* and its *in vivo* antioxidant activity. *Carbohydrate Research*, 339(1), 105-111.

CHAPTER

6



Submitted to journal

Starch gels enriched with phenolic acids: effects on structure and digestibility

Andrea Aleixandre^a, Cristina M. Rosell^{a*}

^aInstitute of Agrochemistry and Food Technology (IATA-CSIC). C/Agustin Escardino, 7, Paterna 46980, Valencia, Spain.

*Corresponding author: Cristina M. Rosell (crostell@iata.csic.es)

“

Abstract

Phenolic compounds affect starch-based gels features and their further hydrolysis with starch digestive enzymes. However, phenolic acids action might be due to either the pH decrease they induce or their specific properties. The aim of this study was to analyze the effect of different phenolic acids (benzoic, protocatechuic, vanillic and veratric acid) on microstructure, texture, and digestion of corn starch gels, discriminating between the effect related to pH decrease and that associated to phenolic acids. Results confirmed that the presence of phenolic acids affected pasting properties, gel microstructure and gel texture of corn starch. Though differences in the pasting properties and gel firmness were significantly reduced when gels of similar pH were compared. Phenolic acids affected gels microstructure, but the area of the cavities and wall thickness increased under pH-controlled conditions. The effect on starch *in vitro* digestibility of gels was dependent on the type of phenolic acids, but when comparing at similar pH all phenolic acids decreased the rate and extent of starch hydrolysis. A principal component analysis indicated that pH adjustment of the gels containing phenolic acids mainly affected pasting performance, firmness, phenolic acid retention, and resistant starch content, but with less impact on starch hydrolysis parameters.

”

Keywords

Corn starch gel * RVA * pH * Texture * Microstructure

6.1. Introduction

Nowadays there is growing interest in evaluating the enzymatic hydrolysis of starches, because starch is the largest source of carbohydrates in human food. Therefore, the control or reduction of the starch digestion rate and subsequent glucose absorption, is a promising strategy for the prevention and treatment of metabolic diseases (Bello-Perez et al., 2020).

One of the principal strategies to reduce starch digestion is to inhibit the digestive enzymes, α -amylase and α -glucosidase, which catalyze the starch breakdown in the digestive tract (Sun & Miao, 2020). In the last years, extracts from different plant sources have been investigated for their inhibitory capacity towards starch digesting enzymes (Papoutsis et al., 2021). This inhibitory activity has been attributed to phenolic compounds, a group of phytochemicals present in plant-based foods and an essential part of the human diet (Martinez-Gonzalez et al., 2017). Phenolic compounds are able to interact with the active site of digestive enzymes, and these binding interactions have been considered the main reason of starch digestion inhibition (Aleixandre, Gil, et al., 2021).

However, there has been surging interest in the potential effect of phenolic compounds on starch, since their interactions might affect starch properties or reduce the amount of polyphenols available for acting on digestive enzymes (Kan et al., 2020). Regarding the impact of phenolic acids on the starch performance, Karunaratne and Zhu (2016) showed that ferulic acid affected corn starch properties such as rheology, gelatinization, retrogradation and gel texture, and the extension of the effect was dependent on the ferulic acid level, but native starch hydrolysis was not affected. Similar results were observed by Han et al. (2020) analyzing the effect of ferulic acid, gallic acid and quercetin on physicochemical properties of rice starch. Microstructure of the starch gels could be also altered by polyphenols, for instance pomegranate peel extract added to wheat starch generates a loose gel matrix (Zhu et al., 2009). Those changes in the starch gel microstructure might have a direct impact on starch digestibility, as lately has been reported (Aleixandre, Benavent-Gil, et al., 2021; Santamaria et al., 2021). Su et al. (2021) described an effect on pasting, thermal, retrogradation and digestive properties when free phenols extracted from purple sweet potato were mixed with native potato starch. On the other hand, Aleixandre, Gil, et al. (2021) evaluate the interaction of different polyphenols with corn starch during its gelatinization, observing that 10% of the polyphenols were absorbed on the starch, reducing its bioavailability for the enzymatic digestion.

Therefore, the interactions between phenolic compounds and starch are influenced not only by the structure of polyphenols, but also by the nature of the starch polymer and/or by the different experimental condition (Giuberti et al., 2020). In fact, the acidification produced by the addition of phenolic acids, might be responsible in some

extent of the effects reported. Guzar et al. (2012) used sodium acetate buffer (pH 5.2) to mitigate the acidification and analyze pasting properties of starches in the presence of tea extracts. Those extract induced changes in pasting properties and the starch hydrolysis was reduced. Also, Beta and Corke (2004) analyzed the addition of ferulic acid and catechin on starch pasting properties adjusting pH levels with HCl or NaOH, observing changes in pasting properties. Specifically, alkaline conditions (pH 11) increased peak viscosity and hot paste viscosity values, while acidic conditions (pH 3) decreased them.

The initial hypothesis of this research was that phenolic acids present during starch gelatinization might modify starch gel structure and hence, affect somewhat their digestibility, but observed effect could be associated either to the pH decrease induced by the acids or their inner properties. The aim of this study was to analyze the impact of pure phenolic acids on the microstructure, texture, and digestibility of corn starch gels, identifying the pH contribution to that effect. In order to reduce the impact of phenolic acid acidification, the pH of the starch slurries was controlled. Therefore, corn starch was gelatinized in the presence of different pure phenolic acids (benzoic, protocatechuic, vanillic and veratric acid), with or without controlling the pH.

6.2. Material and methods

6.2.1. Materials

Four phenolic acids were used: benzoic acid and veratric acid acquired from Sigma Aldrich (Sigma Chemical, St. Louis, USA), protocatechuic acid was from Acros Organic (Acros Organic BVBA, Geel, Belgium) and vanillic acid was from Fluka (Fluka Analytical, Buchs, Switzerland). Food grade native corn starch (purity 95%, amylose 28%) was obtained from Tate&Lyle PLC (London, United Kingdom). Type VI-B α -amylase from porcine pancreas (EC 3.2.1.1) (5 U/mg) was provided by Sigma Aldrich (Sigma Chemical, St. Louis, USA) and amyloglucosidase (AMG) (EC 3.2.1.3) (AMG1100) from Novozymes (Bagsvaerd, Denmark). D-glucose Assay Kit (GOD/POD) was purchased from Megazyme (K-GLUC 08/18, Megazyme International Ireland Ltd., Bray, Co. Wicklow, Ireland). Other chemicals were of analytical grade. Solutions and standards were prepared using deionized water.

6.2.2. Starch gels preparation and pasting properties of the slurries

The starch-phenolic acid slurries and the analysis of the pasting properties were carried out using a Rapid Visco Analyzer (RVA-4, Newport Scientific, Warriewood, Australia). Phenolic acids were separately suspended in 25 mL of distilled water and

corn starch (3 g based on 14% moisture content) was added to reach a final phenolic acid concentration of 5% (w/w, based on the weight of starch in the slurry). Slurries were also prepared adjusting the pH of water-polyphenol mixtures (CpH) previously to RVA analysis. For that purpose, the water polyphenol-mixture was pH-adjusted, using <math><500 \mu\text{L}</math> of NaOH 2 M to bring pH to approximately 6.5, except for benzoic acid and control sample. In the case of benzoic acid, the addition of 500 μL of NaOH allowed to reach pH 6.5. Regarding control or reference sample, very low volume of NaOH was needed. Then, it was proceeded as described above for the non-pH adapted slurries, and corn starch was added. A controlled heating and cooling cycle, from 50 to 95°C in 282 s, holding at 95°C for 150 s and then cooling to 50°C for 344 s was applied. Peak viscosity (maximum viscosity during heating), trough (minimum viscosity during heating), final viscosity at the end of the assay, breakdown (peak viscosity-trough), setback (final viscosity-trough) and onset temperature for pasting formation were evaluated.

6.2.3. High-performance liquid chromatography analysis of phenolic acids

Phenolic acid retention by starch gels was quantified by HPLC following the methodology described by Aleixandre, Gil, et al. (2021). A Waters liquid chromatography system (Waters Corporation, Milford, USA), equipped with a 600E pump and a photodiode array detector (DAD) model 2998 was used. Aliquots of slurries or gels were dissolved in ethanol, centrifuged at 10.000 xg for 10 min, and filtered through 0.22 μm mixed cellulose ester filter. A C18 column (150 x 4.6 mm, particle size 2.5 μm) (Waters Corporation, Milford, USA) was used. The mobile phase consisted of 0.1 vol% trifluoroacetic acid in acetonitrile (A) and 0.1 vol% trifluoroacetic acid in water (B). The gradient profile was 5% A and 95% B (0-18 min), 28,4% A and 71,6% B (18-20 min), 100% A (20-24 min) and 100% B (24-27 min). The flow rate was set at 1 mL/min and a volume of 10 μL was injected. The column was operated at 40°C, and the PDA detector was set at λ 280 nm. Instrument control, data acquisition and data processing were achieved with Waters and Empower software (Waters Corporation, Milford, USA). The polyphenol retention was defined as the quotient between the amount of free polyphenol both before and after the gel formation, expressed in percentage.

6.2.4. Scanning electron microscopy

Microstructure of corn gels prepared in the presence of phenolic acids were analyzed by a Scanning Electron Microscope S-4800 (Hitachi, Ibaraki, Japan). Two replicates of each gel, freshly made in the RVA, were introduced in Eppendorf tubes, immersed in liquid nitrogen and then freeze-dried. Starch was putted onto a silver specimen holder and coated with gold using a vacuum evaporator (JEE 400, JEOL, Tokyo, Japan) with

a coating time of 120 s. Microstructure was examined at an accelerating voltage of 10 kV and 300x magnification. Image analysis was carried out using the ImageJ software (ImageJ, National Institutes of Health, Bethesda, MD, USA). Wall thickness (μm) and hole area (μm^2) were measured.

6.2.5. Gel firmness

To evaluate the texture of polyphenol-starch gels, a TA.XTPlus texture analyzer (Stable Micro Systems, Godalming, UK) equipped with a 5 Kg load cell was used. The gels from RVA were transferred into three glass cups of 3 cm height. These were kept for 30 min at 4°C, before texture measurement. A simple penetration test was made with a 10 mm cylindrical aluminum probe, test speed of 1 mm s⁻¹ and penetrated until a 50% penetration strain. Firmness was measured as the maximum force of penetration in grams. All samples were tested at least six times.

6.2.6. Hydrolysis kinetics

Hydrolysis kinetics of starch gels were determined following the method described by Santamaria et al. (2021). Briefly, one gram of gel was suspended into 4 mL of 0.1 M sodium maleate buffer (pH 6.9) with porcine pancreatic α -amylase (0.9 U/mL), dispersed by using an Ultra Turrax T18 basic homogenizer (IKA-Werke GmbH and Co. KG, Staufen, Germany) and incubated in a shaker incubator SKI 4 (ARGO Lab, Carpi, Italy) at 37°C under constant stirring at 150 rpm during 180 min. Aliquots were withdrawn along hydrolysis and glucose content was quantified.

To quantify the resistant starch fraction (RS), the remnant starch after 24 h hydrolysis was dispersed with 2 mL of 2 M KOH using an Ultra Turrax T18 basic homogenizer (IKA-Werke GmbH and Co. KG, Staufen, Germany) during 5 min at 10,000 rpm. The homogenate was diluted with 8 mL 0.6 M sodium acetate buffer pH 3.8 containing calcium chloride (5mM), incubated with 100 μL AMG (143 U/mL) at 50°C for 30 min and glucose was quantified.

The glucose content was measured using a glucose oxidase-peroxidase (GODPOD) kit (Megazyme, Dublin, Ireland). The absorbance was measured using an Epoch microplate reader (Biotek Instruments, Winooski, USA) at 510 nm. Starch was calculated as glucose (mg) \times 0.9.

The hydrolysis kinetics were calculated fitting experimental data to the first order eq. (1) (Goñi et al., 1997): $C=C_{\infty}(1-e^{-kt})$ where C was the concentration of starch hydrolyzed at t time, C_{∞} was the equilibrium concentration or maximum hydrolysis of starch gels, k was the kinetic constant and t was the time chosen.

The amount of starch fractions based on the hydrolysis rate of starch was calcula-

ted and expressed in amount of glucose released (mg/100 mg) (Englyst et al., 1996). Rapidly digestible starch (RDS) was defined as the starch fraction hydrolyzed within 20 min of incubation, slowly digestible starch (SDS) was the starch fraction hydrolyzed within 20 and 120 min and resistant starch (RS) was defined as the starch fraction that remaining unhydrolyzed after 16 h of incubation.

6.2.7. Statistical analysis

The data were expressed as average \pm confidence interval of at least two individual measurements. Statistical analyses were carried out using Statgraphics Centurion XVIII software (Statistical Graphics Corporation, Rockville, MD, USA). Multivariate analysis of variance (MANOVA) was used to evaluate significant differences among samples at 95% confidence interval using Fisher's least significant differences (LSD) test. Pearson correlation coefficient r and P -value were used to identify correlations. The data were analyzed by multivariate data analysis in the Principal Component Analysis (PCA) to discriminate among samples.

6.3. Results and discussion

6.3.1. Starch-polyphenol gels formation

Starch gels were formed in a Rapid Visco Analyzer (RVA) and the pasting properties were analyzed during heating-cooling cycle to identify the impact of phenolic acids on gel performance (Figure 6.1).

In general, the phenolic acid addition affected the pasting properties of starch. During heating stage, phenolic acids brought forward the pasting formation, showing an early sharp increase of the viscosity. Nevertheless, all pastes featured the same highest viscosity during this stage (peak viscosity). Conversely, during temperature holding at 95°C phenolic acids decreased the viscosity, and that reduction went beyond cooling. The described effect was particularly accentuated in the presence of benzoic acid. A similar profile was described by Beta and Corke (2004), when ferulic acid was added to corn starch and pasting properties were analyzed.

Since part of the effect could be ascribed to the paste acidification, pH of the resulting gels was recorded (Table 6.1).

The addition of phenolic acids significantly ($P < 0.05$) decreased gel pH. Benzoic acid gel yielded the lowest pH value (2.65 ± 0.23), which was expected due to its lower pK_a , and gel containing veratric acid (3.34 ± 0.14) had the minor, although significant, impact on gel pH.

Subsequently, to minimize the impact of pH decrease, water-phenolic acid solutions with pH close to 6.5 were used to prepare the starch slurries and to obtain gels at

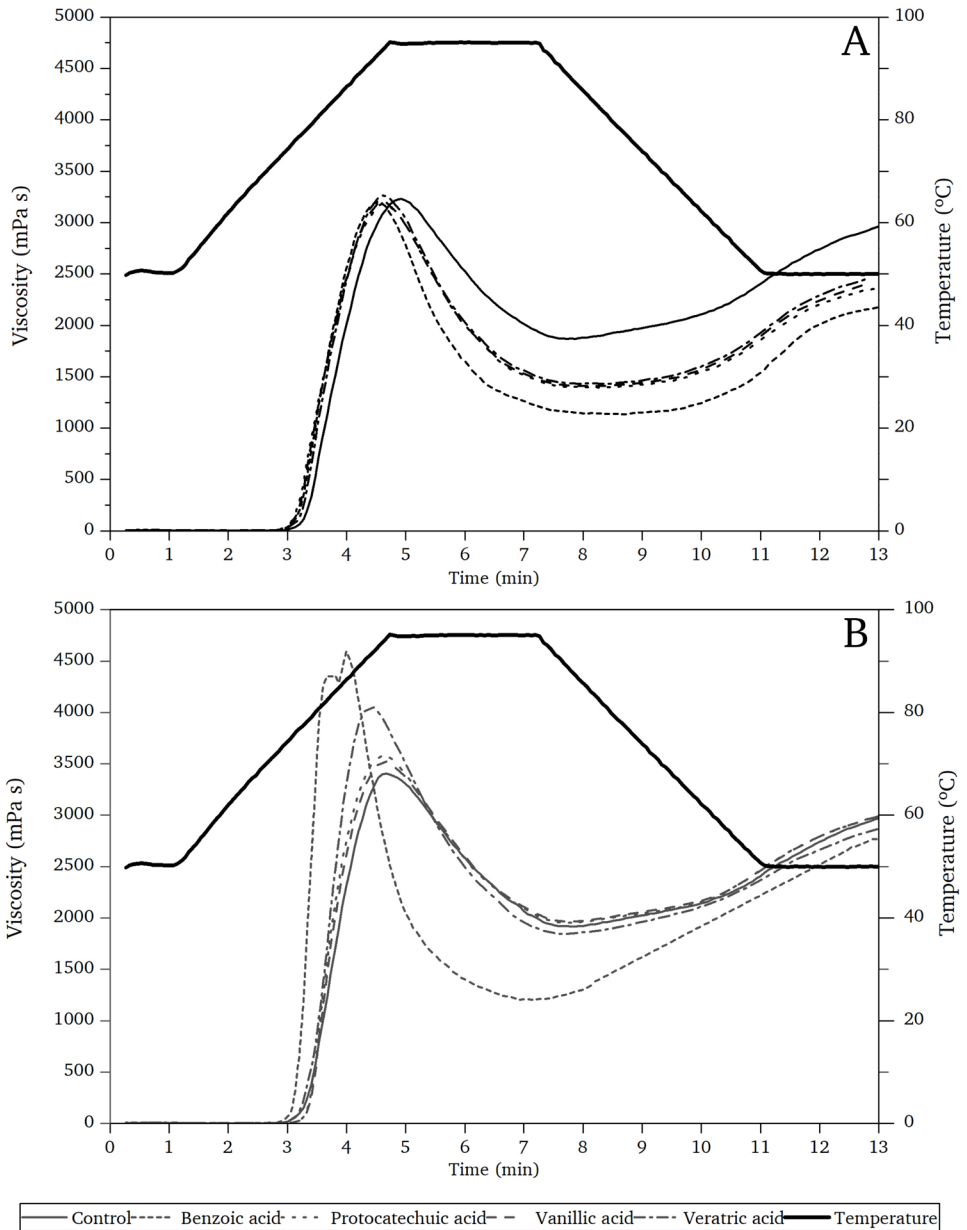


Figure 6.1. Apparent viscosity profiles corn starch gels made with phenolic acids (A), and gels made with phenolic acids adjusting the pH (CpH) (B) obtained with a rapid viscosity analyzer (RVA). Thick solid line indicates temperature settings during the heating-cooling cycle.

Table 6.1. Pasting properties of starch suspensions containing phenolic acids

	pH gel	Onset temperature (°C)	Peak viscosity (mPa s)	Trough (mPa s)	Breakdown (mPa s)	Setback (mPa s)	Final viscosity (mPa s)	Phenolic acid retention (%)							
Control	3.95±0.36	d	3274±172	a	1886±95	cd	1388±92	a	1053±145	ab	2939±85	ef	-		
Benzoic	2.65±0.23	a	73.4±0.9	ab	3185±40	a	1112±35	a	2073±48	d	1064±85	ab	2176±79	a	5.01±2.02
Protocatechuic	2.99±0.24	b	72.7±0.9	a	3186±29	a	1390±44	b	1796±25	c	980±27	a	2370±23	b	23.24±8.49
Vanillic	2.86±0.22	ab	72.8±0.6	a	3205±29	a	1405±35	b	1801±32	c	1013±23	ab	2418±28	bc	21.29±0.72
Veratric	3.34±0.14	c	73.9±0.7	bc	3238±48	a	1386±93	b	1852±64	c	1099±94	b	2484±51	c	21.56±2.72
Control CpH	5.39±0.21	f	74.1±0.8	bcd	3413±90	b	1913±55	cde	1500±134	ab	1057±60	ab	2970±24	f	-
Benzoic CpH	5.02±0.17	e	73.1±0.4	ab	4819±164	e	1116±55	a	3702±160	e	1686±204	c	2802±187	d	30.89±7.97
Protocatechuic CpH	5.85±0.08	h	75.6±1.5	e	3578±28	c	1950±22	de	1628±42	b	1057±50	ab	3007±45	f	37.18±3.44
Vanillic CpH	5.69±0.13	gh	75.5±1.3	e	3541±35	bc	1981±61	e	1559±44	b	1012±58	ab	2993±14	f	34.21±0.20
Veratric CpH	5.50±0.11	fg	75.0±1.0	de	4013±222	d	1847±59	c	2166±247	d	1020±53	ab	2867±21	de	27.70±0.77
P-value															
PP	0	0.1544	0	0	0	0	0	0	0	0	0	0	0	0.0010	
CpH	0	0	0	0	0.0007	0.0028	0	0.0007	0	0	0	0	0	0.0007	

Results were expressed as mean ± SD (n=6) and values followed by different letter within columns are significantly different ($P<0.05$). PP: Phenolic acids, CpH: Adapted pH conditions.

adapted pH (CpH). This pH was selected because it is above the pK_a of all the phenolic compounds, and the pH obtained for the gels was similar to that of the buffer previously reported by Guzar et al. (2012) when added tea extracts to cereal starches (wheat, corn, potato and rice). After the pH adjustment, the pH of the gels ranged from 5.02 (benzoic acid) to 5.85 (protocatechuic acid). It must stress that the pH adjustment of the corn starch slurry in the absence of phenolic acids barely affected the pasting performance of the control, with the exception of the increase in the peak viscosity (Figure 6.1). With the adapted pH different viscosity profiles were obtained (Figure 6.1, B). Control, protocatechuic, vanillic and veratric acid samples showed similar curves, differing only on the peak viscosity, that increase in the presence of the acids, particularly veratric acid. The alteration of the starch pasting properties induced by benzoic acid during heating and holding process was remarkable. Benzoic acid showed the highest peak viscosity, but final viscosity was similar to that of the other gels. Maybe the salt formed when adapting the pH influenced in the pasting properties of starch gel.

The capability of starch to form a viscous gel at cooling was reduced with the incorporation of phenolic acids. Su et al. (2021) and Han et al. (2020) explained the alteration in the pasting properties of starches (sweet potato and rice starch, respectively) when phenolic acids were added due to the restriction of both water availability and mobility for starch gelatinization. The interaction between phenolic acid hydroxyl groups and water molecules, could limit the water molecules required for starch gelatinization. Nevertheless, in the present study, the presence of phenolic acids did not affect the peak viscosity of the starch, which suggest that their impact on pasting was mainly ascribed to pH and no to existing water limitations. In general, the phenolic acid addition affected the pasting properties of starch. During heating stage, phenolic acids brought forward the pasting formation, showing an early sharp increase of the viscosity. Nevertheless, all pastes featured the same highest viscosity during this stage (peak viscosity). Conversely, during temperature holding at 95°C phenolic acids decreased the viscosity, and that reduction went beyond cooling. The described effect was particularly accentuated in the presence of benzoic acid. A similar profile was described by Beta and Corke (2004), when ferulic acid was added to corn starch and pasting properties were analyzed. In fact, when adjusting pH of slurries (CpH) the peak viscosity increased and differences with the control along heating and cooling disappeared, with the exception of benzoic acid. In the former, higher volume of alkali was needed to increase pH, which might affect starch structure. Therefore, results support that the effect of phenolic acids on the starch performance during heating and cooling are related to the acidification of the medium, and not to any direct interference of the acids. The pasting parameters extracted from the plots (Table 6.1), confirmed a significant effect of both the phenolic acid presence and the pH adjustment ($P < 0.05$). Peak viscosity values increased when the pH was augmented using NaOH. This increment obser-

ved in CpH slurries may be attributed either to NaOH addition or pH increase. In fact, concerning NaOH, Lai et al. (2004) evaluated its effect on starch pasting properties under the same experimental conditions, observing even a more significant viscosity increase than in the present study, using a similar NaOH amount (1 g/100 g starch). As regards pH increment, Sriburi and Hill (2000) analyzed the pasting properties of cassava starch extrudates with ascorbic acid at different pH values using HCl, potassium hydrogen phthalate and NaOH. A clear increment of starch peak viscosity when pH increased from 2 to 6.5 was observed. The viscosity decay along holding at 95°C (breakdown) is related to the disintegration degree of starch granules. The significant increase in the breakdown implied that phenolic acids, or the pH drop associated to their addition, induced the starch granules disintegration. But results obtained at adapted pH, where no significant differences were obtained, confirmed that the changes in the starch pasting performance should be ascribed to the pH change induced by the phenolic acids, excepting benzoic acid. This acid addition resulted in the highest breakdown value, independently of the slurry's pH, and also the highest setback, related to amylose retrogradation extent (Villanueva et al., 2018). It should be remarked that a significant positive correlation ($r=0.88$) was found between final viscosity values and gels pH.

After gel formation, the polyphenol retention within the gels was analyzed (Table 6.1). Chromatographic results confirmed the thermal stability of the phenolic acids (data not shown). The acids retention was significantly affected by the phenolic acid and pH. Phenolic acids were retained (~22%) within the gel structure, with the exception of benzoic acid (~5%), but when the pH of the gels was adjusted the retention capacity greatly increased (~32%). Interestingly, a moderate positive correlation was observed between phenolic acids retention and their pK_a ($r=0.75$).

6.3.2. Textural and structural characterization of starch gels

The microstructure of starch-phenolic acid gels was analyzed by SEM (Figure 6.2).

Micrographs confirmed the different structure of gels depending on the phenolic acid and the pH. Analyzing the effect of the addition of phenolic acids, all gels showed a sponge-like structure, typical for gel fractures with well-defined holes and solid walls separating them (Aleixandre, Benavent-Gil, et al., 2021). Nevertheless, the hole sizes and shapes varied among samples depending on the type of phenolic acid. In comparison with the control starch gel microstructure, benzoic and vanillic gels showed similar hole sizes but a less rounded shape.

Conversely, the presence of protocatechuic acid on gel formation, enhanced the cavities size. Conversely, veratric acid greatly reduced the holes size. Therefore, the inclusion of phenolic acids on the starch gels affected the microstructure, which was

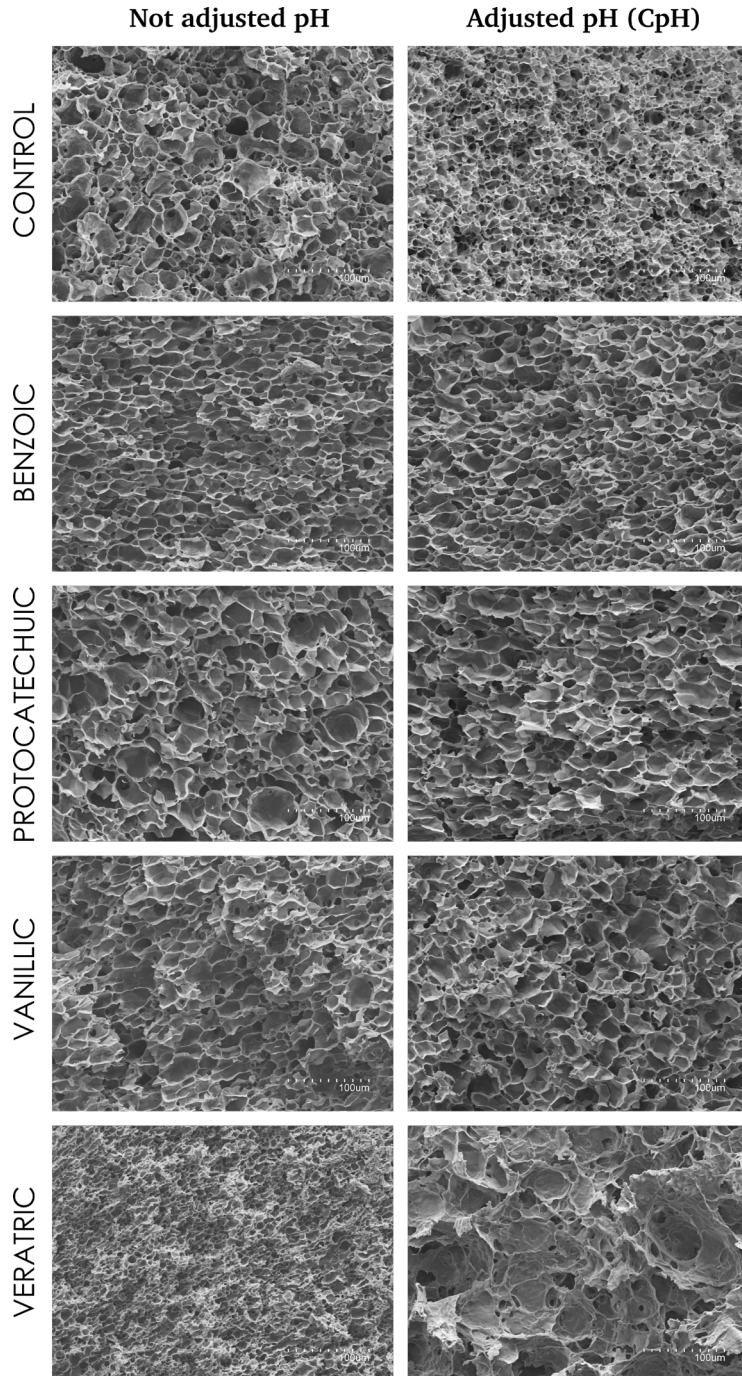


Figure 6.2. SEM micrographs of starch corn gels made with phenolic acid, and gels made with phenolic acids not adjusting and adjusting pH. Magnification $\times 300$.

dependent on the type of phenolic acid. This statement is also supported by previous findings with rice starch gels containing ferulic and gallic acid that resulted in looser porous gel matrix compared to the control (Han et al., 2020).

Regarding CpH gels, the greatest difference was observed between control and veratric acid gels. Control gel showed small and rounded cavities, giving a very porous network. In opposition, veratric acid led to a very open sponge-like structure, showing a smooth surface with uneven big cavities. To objectively evaluate differences among the gels, image analysis was applied to assess the wall thickness and the area of gel cavities, and the texture analysis was performed to evaluate the firmness of fresh gels (Figure 6.3).

Statistical analysis confirmed significant differences ($P < 0.05$) among starch gel microstructures. Hole area results exhibited a positive skewed distribution and some outliers as shown in the box and whisker plots. The smallest holes were obtained for veratric acid starch gel (median $48.46 \mu\text{m}^2$), and the largest area was obtained for protocatechuic acid gel (median $278.83 \mu\text{m}^2$). Zhu et al. (2009) analyzed the structure of wheat starch gels treated with rich phenolic extracts (pomegranate peel) prepared under similar conditions but containing lower amount of phenolic acids, observing big holes in those treated gels, as happened with protocatechuic acid gel in the present study.

Nevertheless, present results confirmed that gels network depended on the type of phenolic acid. The pH adjustment resulted in gels with bigger hole areas, except for the control sample that after increasing the pH (from 3.95 to 5.39) led to a network with smaller cavities. Likewise, Sae-kang and Suphantharika (2006) described a thinner network with bigger porous when tapioca starch gels were prepared at pH 3, whose become more porous with tiny cavities at pH 7 and pH 9. Unexpectedly, veratric acid containing gel presented the highest hole area, but with the greatest distribution of areas.

Regarding wall thickness, protocatechuic acid containing gel showed thicker walls (median $1.13 \mu\text{m}$), but after adapting the pH (CpH gels) differences induced by phenolic acids were reduced and wall thickness median ranged from 1.10 - $1.17 \mu\text{m}$, except for veratric acid ($1.61 \mu\text{m}$). No significant difference was observed on the wall thickness of the control gel due to pH adjustment.

Firmness of starch gels is shown in Figure 6.3. Statistical analysis indicated that both polyphenol presence and the pH had significant effect on gel texture. Without adapting pH, the addition of phenolic acids significantly decreased the gel firmness. That result agrees with previous findings, where the softening effect was related to the presence of phenolic acids and the pH alteration of the system, reducing the formation of the amylose matrix (Karunaratne & Zhu, 2016; Zhu et al., 2008). The introduction of phenolic acids modifies the hydrogen bonds and van der Waals forces involved with the initial retrogradation of amylose and gel firmness (Karunaratne & Zhu, 2016; Zheng et al., 2020). Besides to that, pH decrease results in gel softening, as has been observed

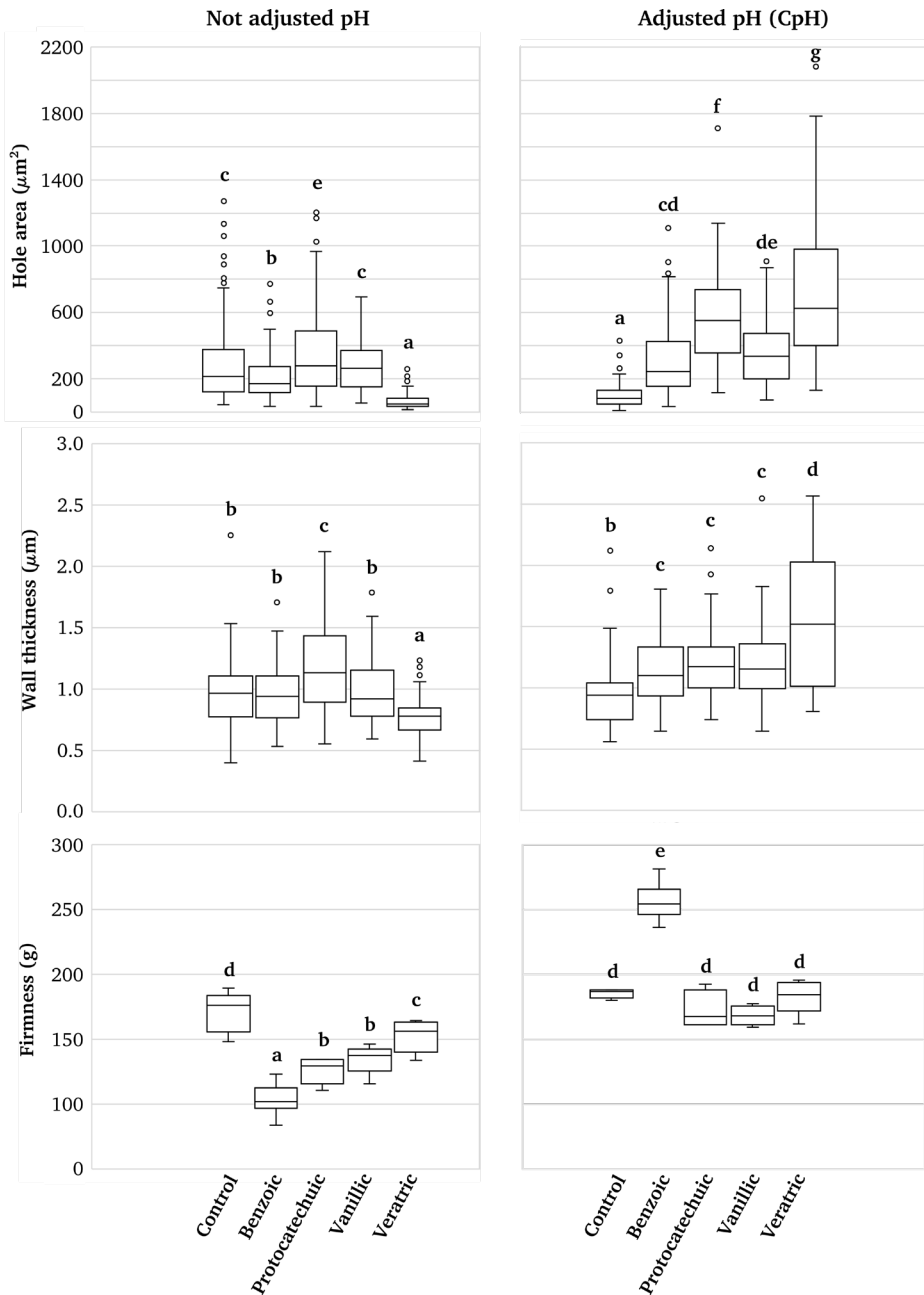


Figure 6.3. Boxplots showing the firmness and microstructure parameters calculated by image analysis of the gel micrographs. Different letters on the boxes indicate significant differences ($P < 0.05$).

with tapioca starch gels (Sae-kang & Supphantharika, 2006). At acid pH, some degree of starch hydrolysis might occur, degrading amylose into low molecular weight molecules, preventing gel retrogradation and decreasing gel strength (Wang et al., 2003).

When adapting pH of the control, increasing the pH from 3.95 to 5.39, the gel firmness did not change (Figure 6.3). But CpH starch gels containing protocatechuic, vanillic or veratric acids, increased their firmness, reaching similar firmness than the control gel. Hence, pH has greater role than phenolic acids on starch gel firmness, excepting benzoic acid pattern. This acid enhanced gel firmness from 104 ± 13 g to 256 ± 15 g after pH adjustment, maybe due to the formation of sodium benzoate. Ofman et al. (2004) observed that the addition of sodium benzoate to tapioca starch before gelatinization increased water sorption and mechanical starch characteristics, which could affect gel texture. It is worthy to note that a strong positive correlation was obtained between gel firmness and peak viscosity ($r=0.83$). Peak viscosity has been related to the water-holding capacity of the starch (Cozzolino, 2016), which could also affect gel firmness.

6.3.3. Digestibility of starch-polyphenol gels

Gels were subjected to enzymatic *in vitro* hydrolysis to simulate starch digestibility. Starch hydrolysis in the gels containing phenolic acids, with and without pH adjustment, was plotted as the percentage of hydrolyzed starch in the gels (Figure 6.4).

Starch hydrolysis plots exhibited a linear increase of hydrolyzed starch and reached a plateau at the final stage of hydrolysis, as a typical starch digestion pattern of gels (Santamaria et al., 2021). With the exception of protocatechuic, gels containing phenolic acids increased the extent of starch hydrolysis. But the opposite effect was observed when gels were obtained adjusting the pH (Figure 6.4B). Control gel showed faster and more extended starch hydrolysis when the pH was increased. All gels containing phenolic acids showed slower and lower starch hydrolysis compared to starch gel.

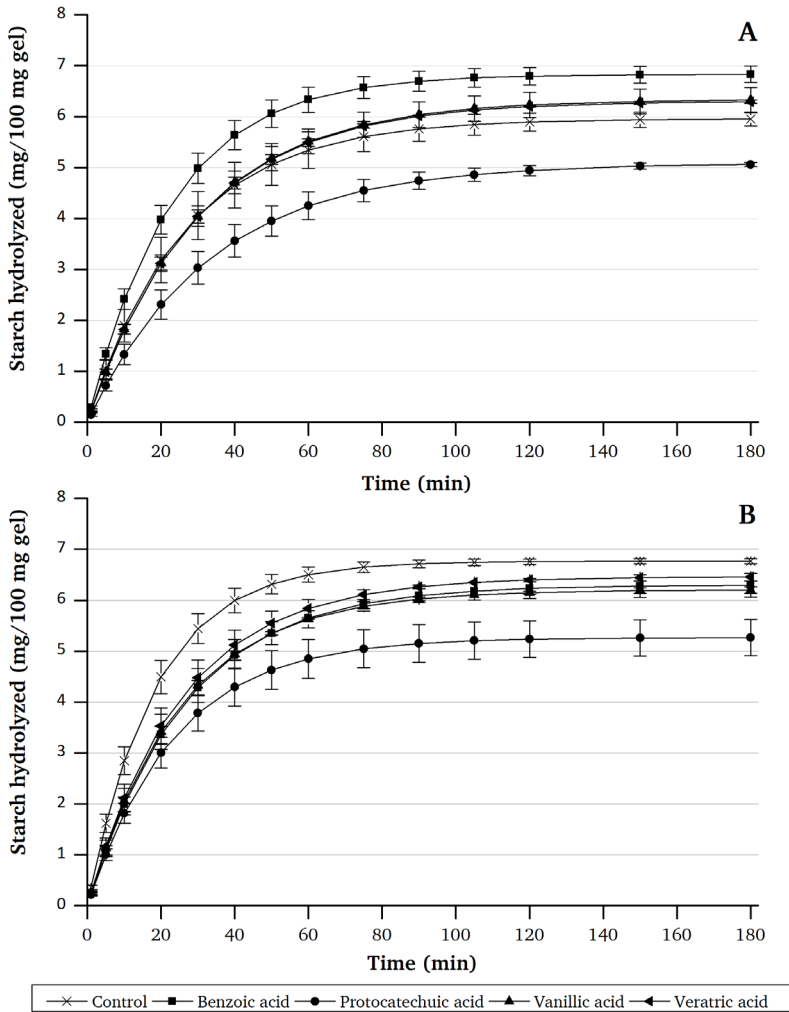


Figure 6.4. Hydrolysis plots of corn starch gels made with phenolic acids (A), and gels made with phenolic acids adjusting the pH (CpH) (B).

Relevant starch fractions related to the rate of starch hydrolysis, including RDS, SDS and RS, were evaluated (Table 6.2).

RDS content were significantly affected by phenolic acids ($P < 0.05$), but not by the pH. Without adjusting pH, benzoic acid induced the largest RDS values, whereas protocatechuic acid led to the lowest value, retarding the starch hydrolysis. SDS and RS fractions were significantly influenced by both phenolic acids and pH. SDS contents mainly decreased when the pH was controlled, while RS contents increased.

Table 6.2. *In vitro* starch hydrolysis and kinetic parameters of gels containing phenolic acids.

	RDS (mg/100 mg)	SDS (mg/100 mg gel)	RS (mg/100 mg gel)	k (min ⁻¹)	C _∞	r ²
Control	3.18±0.45	2.71±0.27	1.76±0.06	0.038±0.007	5.96±0.13	0.93±0.07
Benzoic	3.98±0.28	2.82±0.11	1.65±0.09	0.044±0.003	6.83±0.16	0.96±0.01
Protocatechuic	2.31±0.29	2.64±0.19	1.62±0.07	0.030±0.005	5.09±0.01	0.95±0.02
Vanillic	3.12±0.12	3.11±0.09	1.54±0.06	0.034±0.001	6.34±0.24	0.97±0.01
Veratric	3.12±0.12	3.08±0.14	1.71±0.11	0.034±0.002	6.31±0.04	0.96±0.01
Control CpH	4.49±0.33	2.26±0.27	1.67±0.05	0.055±0.007	6.77±0.05	0.97±0.01
Benzoic CpH	3.36±0.17	2.88±0.26	2.01±0.05	0.038±0.005	6.30±0.24	0.97±0.01
Protocatechuic CpH	3.00±0.30	2.23±0.06	1.70±0.10	0.042±0.002	5.27±0.35	0.93±0.02
Vanillic CpH	3.42±0.34	2.73±0.37	1.74±0.04	0.040±0.007	6.21±0.07	0.97±0.01
Veratric CpH	3.53±0.36	2.87±0.39	1.91±0.10	0.040±0.007	6.46±0.08	0.96±0.02
P-value						
PP	0.0214	0.0159	0	0.4151	0	0.3393
CpH	0.0572	0.0219	0	0.0754	0.4953	0.4361

Results were expressed as mean ± SD (n=2) and values followed by different letter within columns are significantly different ($P < 0.05$)

Lee et al. (2018) did not observe significant differences on RDS, SDS and RS values in potato starch gels obtained at different pH (3.5, 4.5 and 5.5) conditions, probably due to different performance between tuber and cereal starches. SDS fraction of gels containing benzoic, vanillic or veratric acids increased with regard to control gel. The presence of phenolic acids in the gels led to lower RS content. This reduction disagrees with the observations by Gutierrez et al. (2020), who described an increase in RS content in potato starch gels containing gallic acid, perhaps due to the extra hydroxyl groups present in its structure (3). However, CpH gels showed higher RS values in comparison with the control CpH. A significant moderate relationship ($r=0.65$) was found between gel firmness and RS.

From the kinetic model (Eq. (1)), it was possible to obtain the kinetic constant (k) and the equilibrium concentration of hydrolyzed starch (C_{∞}) (Table 6.2). The kinetic constant (k) did not show significant differences among samples, and C_{∞} was significantly affected by the phenolic acids ($P<0.05$) but not by pH (CpH). Protocatechuic acid gels showed the lowest C_{∞} values (5.09 ± 0.01 and 5.27 ± 0.35 , without and with pH adjustment, respectively). Adjustment of pH only increased the extent of hydrolysis (C_{∞}) of control gel (control CpH) and it was reduced when containing benzoic acid. It has been reported that phenolic acids inhibit starch digestive enzyme (Sun, Warren & Gidley, 2019). Tan et al. (2017) described an inhibitory activity of phenolic acids, like protocatechuic and vanillic acid, against porcine pancreatic α -amylase ($IC_{50}=1.78\pm 0.07$ and 4.69 ± 0.21 mg/mL respectively), which agree with the results obtained with protocatechuic acid, even without adjusting pH, but no in the case of vanillic acid. Presumably, protocatechuic acid was better enzyme inhibitor than the other phenolic acids (Guzar et al., 2012). No significant relationships were encountered between structure and texture characteristics of gels and digestion parameters. Conversely, Alexandre, Benavent-Gil, et al. (2021) observed that starch gels with bigger cavities and thinner walls facilitate the enzyme action, increasing starch digestibility. Giuberti et al. (2020) suggested that different factors characterizing the food matrix (composition, structure, starch nature) might be involved in the inhibition of starch-digesting enzymes by phenolic acids. Nevertheless, our findings suggests that the anti-hyperglycemic effect was driven by the effect of phenolic compounds rather than the structure and texture changes in starch gels.

To understand the possible role of polyphenol properties on gel characteristics and digestion parameters, data were subjected to a principal component analysis (PCA). The PCA results showed that four principal components significantly discriminated between starch gels containing phenolic acids, which accounted for 55% of the variability in the original data. This analysis described the 28% and 27% of variation on principal components 1 (PC1) and 2 (PC2), respectively (Figure 6.5).

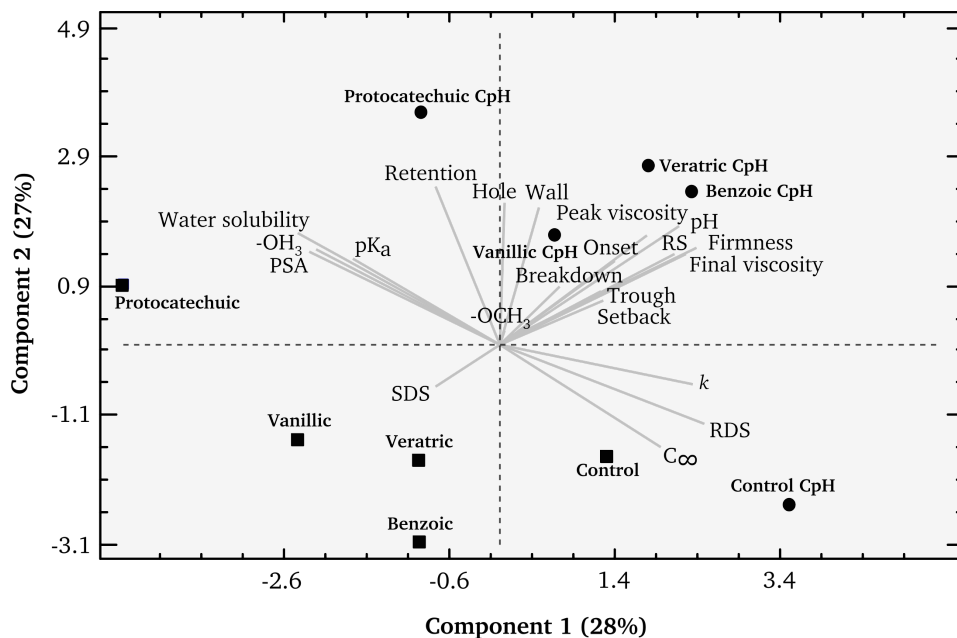


Figure 6.5. Score and loading biplot of samples and variables obtained by principal component analysis (PCA).

Phenolic acids properties like water solubility, pK_a , polar surface area (PSA) values (available at PubChem and <https://foodb.ca> databases), and hydroxyl ($-OH_3$) or methoxy ($-OCH_3$) groups were also included. The PCA clearly discriminated between CpH gels containing phenolic acids along the positive axis of PC2 (Figure 6.5 B), which was associated to pasting performance, gels microstructure, firmness, phenolic acid properties and RS. Whereas, along the negative axis PC2 were located the digestion parameters with the cluster of gels containing phenolic acids and no adjustment of pH, with exception of the protocatechuic acid.

Component 1 discriminates the different phenolic acids. Veratric, benzoic and vanillic acid included in starch gels with adjusted pH were grouped by their pasting performance, microstructure and firmness, whereas protocatechuic acid was discriminated based on its specific properties. The loadings indicated a strong negative correlation between phenolic acid properties like water solubility, PSA and the number of hydroxyl groups, and digestion parameters. Hydroxyl groups have an important role on the interaction of phenolic compounds with amino acid residues at the active site of α -amylase (Sun, Warren & Gidley, 2019). Molecular docking analysis suggested that the less hydroxyl groups the lower enzyme inhibition, and hence higher starch digestion (Sun, Warren, Gidley, et al., 2019). Alexandre, Gil, et al. (2021) reported that phenolic acids with >1 hydroxyl group, like protocatechuic acid, showed higher inhibition effect against α -amylase than other phenolic acids with one hydroxyl group, like vanillic acid,

or one hydroxyl group plus one methoxy groups, like veratric acid. These results are in accordance with the findings of the present research. In fact, protocatechuic was in the negative axis of PC1. Water solubility of phenolic compounds was also negatively correlated with the kinetic parameters of digestion (k and C_{∞}), and RDS values. A greater water solubility can be translated into a greater mobility in the liquid medium to interact with the enzymes (Karunaratne & Zhu, 2016).

6.4. Conclusions

The presence of phenolic acids during corn starch gelatinization affected its pasting properties, particularly heating stability and viscosity during cooling. That effect was ascribed to the pH decreased induced by phenolic acids, since differences faded when setting similar pH conditions. The pH of the slurries also influenced the phenolic acid retention on starch gels, increasing their retention after adjusting the pH close to 6.5. These changes influenced starch gel microstructures, modifying the size and shape of gel cavities, increasing holes area and wall thickness. Phenolic acids presence also changed corn starch gel microstructure, obtaining different cavity areas and wall thickness, that led to softer gels. The addition of phenolic acids to corn starch gels allowed slow down and reduce the enzymatic hydrolysis of starch when proper pH adjustment was conducted. Without that, phenolic acids reduce the gels pH, increasing the extent of starch hydrolysis, with the exception of protocatechuic acid. Regarding the type of phenolic acid, higher inhibition against α -amylase was obtained with phenolic acids with more than one hydroxyl group, like protocatechuic, confirming the importance of the number of hydroxyl groups in the phenolic acids structure on the inhibition of starch digestion.

Author Contributions: Credit roles: AA: Conceptualization; Data curation; Formal analysis; Investigation; Methodology; Writing-original draft; CMR: Conceptualization; Data curation; Supervision; Investigation; Funding acquisition; Writing-review & editing.

Acknowledgments: Authors acknowledge the financial support of Grant RTI2018-095919-B-C2 funded by MCIN/AEI/10.13039/501100011033, “ERDF A way of making Europe” by the “European Union”, and Generalitat Valenciana (Project Prometeo 2017/189).

Conflicts of Interest: The authors declare that they do not have any conflict of interest.

References

Aleixandre, A., Benavent-Gil, Y., Moreira, R., & Rosell, C. M. (2021). In vitro digestibility of gels from different starches: Relationship between kinetic parameters and microstructure. *Food Hydrocolloids*, *120*, 106909.

Aleixandre, A., Gil, J. V., Sineiro, J., & Rosell, C. M. (2021). Understanding phenolic acids inhibition of α -amylase and α -glucosidase and influence of reaction conditions. *Food Chemistry*, 131231.

Bello-Perez, L. A., Flores-Silva, P. C., Agama-Acevedo, E., & Tovar, J. (2020). Starch digestibility: past, present, and future. *Journal of the Science of Food and Agriculture*, *100*(14), 5009-5016.

Beta, T., & Corke, H. (2004). Effect of ferulic acid and catechin on sorghum and maize starch pasting properties. *Cereal Chemistry*, *81*(3), 418-422.

Cozzolino, D. (2016). The use of the rapid visco analyser (RVA) in breeding and selection of cereals. *Journal of Cereal Science*, *70*, 282-290.

Englyst, H. N., Veenstra, J., & Hudson, G. J. (1996). Measurement of rapidly available glucose (RAG) in plant foods: a potential *in vitro* predictor of the glycaemic response. *British Journal of Nutrition*, *75*(3), 327-337.

Giuberti, G., Rocchetti, G., & Lucini, L. (2020). Interactions between phenolic compounds, amylolytic enzymes and starch: an updated overview. *Current Opinion in Food Science*, *31*, 102-113.

Goñi, I., Garcia-Alonso, A., & Saura-Calixto, F. (1997). A starch hydrolysis procedure to estimate glycemic index. *Nutrition Research*, *17*(3), 427-437.

Gutierrez, A. S. A., Guo, J., Feng, J., Tan, L., & Kong, L. (2020). Inhibition of starch digestion by gallic acid and alkyl gallates. *Food hydrocolloids*, *102*, 105603.

Guzar, I., Ragaee, S., & Seetharaman, K. (2012). Mechanism of Hydrolysis of Native and Cooked Starches from Different Botanical Sources in the Presence of Tea Extracts. *Journal of Food Science*, *77*(11), C1192-C1196.

Han, X., Zhang, M., Zhang, R., Huang, L., Jia, X., Huang, F., & Liu, L. (2020). Physicochemical interactions between rice starch and different polyphenols and structural characterization of their complexes. *LWT- Food Science and Technology*, *125*, 109227.

Kan, L., Oliviero, T., Verkerk, R., Fogliano, V., & Capuano, E. (2020). Interaction of bread and berry polyphenols affects starch digestibility and polyphenols bio-accessibility. *Journal of Functional Foods*, *68*, 103924.

- Karunaratne, R., & Zhu, F. (2016). Physicochemical interactions of maize starch with ferulic acid. *Food Chemistry*, *199*, 372-379.
- Lai, L., Karim, A., Norziah, M., & Seow, C. (2004). Effects of Na₂CO₃ and NaOH on pasting properties of selected native cereal starches. *Journal of Food Science*, *69*(4), FCT249-FCT256.
- Lee, S. Y., Lee, K. Y., & Lee, H. G. (2018). Effect of different pH conditions on the *in vitro* digestibility and physicochemical properties of citric acid-treated potato starch. *International Journal of Biological Macromolecules*, *107*, 1235-1241.
- Martinez-Gonzalez, A. I., Díaz-Sánchez, Á. G., Rosa, L. A. d. l., Vargas-Requena, C. L., Bustos-Jaimes, I., Alvarez-Parrilla, & Emilio. (2017). Polyphenolic Compounds and Digestive Enzymes: In Vitro Non-Covalent Interactions. *Molecules*, *22*(4), 669.
- Ofman, M. H., Campos, C. A., & Gerschenson, L. a. N. (2004). Effect of preservatives on the functional properties of tapioca starch: analysis of interactions. *LWT - Food Science and Technology*, *37*(3), 355-361.
- Papoutsis, K., Zhang, J., Bowyer, M. C., Brunton, N., Gibney, E. R., & Lyng, J. (2021). Fruit, vegetables, and mushrooms for the preparation of extracts with α -amylase and α -glucosidase inhibition properties: A review. *Food Chemistry*, *338*, 128119.
- Sae-kang, V., & Suphantharika, M. (2006). Influence of pH and xanthan gum addition on freeze-thaw stability of tapioca starch pastes. *Carbohydrate Polymers*, *65*(3), 371-380.
- Santamaria, M., Garzon, R., Moreira, R., & Rosell, C. M. (2021). Estimation of viscosity and hydrolysis kinetics of corn starch gels based on microstructural features using a simplified model. *Carbohydrate Polymers*, *273*, 118549.
- Sriburi, P., & Hill, S. E. (2000). Extrusion of cassava starch with either variations in ascorbic acid concentration or pH. *International Journal of Food Science & Technology*, *35*(2), 141-154.
- Su, J., Tan, C., Gao, Y., & Feng, Y. (2021). Four phenolic acids from purple sweet potato and their effects on physicochemical, digestive and structural characteristics of starch. *International Journal of Food Science & Technology*, *56*(4), 1896-1904.
- Sun, L., & Miao, M. (2020). Dietary polyphenols modulate starch digestion and glycaemic level: a review. *Critical Reviews in Food Science and Nutrition*, *60*(4), 541-555.
- Sun, L., Warren, F. J., & Gidley, M. J. (2019). Natural products for glycaemic control: Polyphenols as inhibitors of alpha-amylase. *Trends in Food Science & Technology*, *91*, 262-273.

Sun, L., Warren, F. J., Gidley, M. J., Guo, Y., & Miao, M. (2019). Mechanism of binding interactions between young apple polyphenols and porcine pancreatic α -amylase. *Food Chemistry*, *283*, 468-474.

Tan, Y., Chang, S. K. C., & Zhang, Y. (2017). Comparison of α -amylase, α -glucosidase and lipase inhibitory activity of the phenolic substances in two black legumes of different genera. *Food Chemistry*, *214*, 259-268.

Villanueva, M., Pérez-Quirce, S., Collar, C., & Ronda, F. (2018). Impact of acidification and protein fortification on rheological and thermal properties of wheat, corn, potato and tapioca starch-based gluten-free bread doughs. *LWT- Food Science and Technology*, *96*, 446-454.

Wang, Y.-J., Truong, V.-D., & Wang, L. (2003). Structures and rheological properties of corn starch as affected by acid hydrolysis. *Carbohydrate Polymers*, *52*(3), 327-333.

Zheng, Y., Tian, J., Kong, X., Yang, W., Yin, X., Xu, E., Chen, S., Liu, D., & Ye, X. (2020). Physicochemical and digestibility characterisation of maize starch-caffeic acid complexes. *LWT- Food Science and Technology*, *121*, 108857.

Zhu, F., Cai, Y.-Z., Sun, M., & Corke, H. (2009). Effect of phytochemical extracts on the pasting, thermal, and gelling properties of wheat starch. *Food Chemistry*, *112*(4), 919-923.

Zhu, F., Cai, Y. Z., Sun, M., & Corke, H. (2008). Effect of phenolic compounds on the pasting and textural properties of wheat starch. *Starch-Stärke*, *60*(11), 609-616.



IV

General discussion

The current trend in food industry is the design of foods with exceptional health benefits. For that purpose, the investigation of the chemical and physical properties of foods, and their digestion along the oro-gastrointestinal tract is essential to trace technological and physiological processing that could be used in reverse engineering.

Several factors are involved in the digestion of starchy foods. The food matrix microstructure and its oral disruption are probably the principal key points that can facilitate or hamper exchanges with salivary enzymes, nutrient release during mastication and the following digestive processes. Food oral processing (FOP) studies are focused on the destruction and sensory analysis perception by individuals, and all the mechanisms involved are still not understood. There is a clear relationship between food oral processing and food structure, and its understanding is important for improving health-related factors like nutrition or dysphagia.

Gao and Zhou (2021) claimed that chewing effort is related to food density, structure, moisture, and texture. Most of the FOP studies of starchy foods are focus on fresh breads with different structures, showing correlations between the crumb density and the oral processing (Gao et al., 2018; Pentikäinen et al., 2014). However, water content has an important role in the oral processing of starchy foods, requiring lower mastication times and chews those products with higher water content. Consequently, the real impact of structure without the possible interference induced by food moisture must be investigated. Toasted breads with low moisture content and different crumb hardness and porosity were masticated differently. Bread structures with more and bigger porous are slightly related with lower chewing efforts. Maybe bigger cavities allow more saliva absorption, softening the bread, and facilitating the mastication. Nevertheless, the saliva to bread ratio values were not different between samples, so this theory should be discarded. For this reason, the decreased chewing effort should be explained by their softer texture due to a more open structure (Puerta et al., 2021). Mastication not only implies the breakdown of food but also involves the formation of a swallowable bolus. Differences on bolus texture were obtained between breads. But the relation between bolus texture and food structure is unclear. For example, Wada et al. (2017) analyzed the bolus texture of four different starchy foods with great structure differences (cracker, boiled rice and gels), and similar hardness, cohesiveness and adhesiveness values were reported. Also, there is a relationship between bolus characteristics and texture perceptions but is not properly understood. Research involving

many subjects with different physiological conditions would be adequate to clarify it. As regards mastication, it is not possible to modify the chewing pattern, but changing the food structure could be a suitable strategy to improve food digestion.

Replicate oral processing during *in vitro* digestion analysis is a complex and challenging task. Over the years, much less attention has been given to *in vitro* oral digestion as compared to gastric or intestinal, and simple mechanical methods have been used to simulate *in vivo* mastication. The standardized static *in vitro* digestion method, developed by the INFOGEST network (Minekus et al., 2014), recommended to simulate solid food mastication by mincing 2 minutes with α -amylase enzyme, obtaining particle sizes of less than 2 mm. Other processing methods like cutting, cut and pestle or blending have been tested on bread (Gao et al., 2019). However, most of the bolus particles were larger than 2 mm, and some methods do not allow to break the sample and mix it with the enzyme at the same time. Considering the importance of mastication on food digestion, the method used for *in vitro* oral processing should be carefully selected. To use a homogenizer or crystal balls shaker could be a suitable choice to simulate mastication, since they enable to disrupt the sample, mix it with the enzyme, and obtain particle sizes less than 2 mm. It is important to note that some differences in particle size were obtained when the homogenizer or the shaker were employed to simulate mastication, and also in the hydrolyzed starch results. Because of that, when comparing the digestion of different samples, it should be appropriate to use the same *in vitro* oral processing method. Concerning food structure and *in vitro* mastication, results did not show an important difference on disruption results between breads with different structure but using the same oral processing method. This statement does not endorse the evidence of the effect of food microstructure on mastication. That means there might not be enough bread structural differences for these oral processing methods, or these devices did not allow to discriminate between bread structures. Conversely, Blanquet-Diot et al. (2021) showed significant different distribution and bolus median particle size between refined and wholegrain pasta using a specific masticatory apparatus.

Besides the impact of food microstructure on *in vitro* oral processing, the food structure also shows a clear effect on the gastric and intestinal phases. Gastric digestion involves acidic and enzymatic conditions provided by the gastric secretions. *In vitro* gastric digestion of bread was characterized by the increase in bolus particle size as compared to oral phase. This restructuration of particle sizes during gastric digestion was reviewed by Guo et al. (2020). Authors attribute this phenomenon to different mechanisms (pepsin, ions and/or acids), which depend on food characteristics. However, restructuration was described in biopolymers, milk, or emulsions, but not in bread. When gastric digestion was analyzed in a model food system like dried starch gel, a very low starch digestion was detected. This indicates that α -amylase enzyme was not largely involved in the particle size changes of boluses during gastric digestion, pro-

bably due to the enzymatic inactivation. Particle size of digested breads during gastric stage was positively related with some structural and textural bread characteristics, like the area of crumb cavities, and negatively with crumb porosity or hardness. Small cavities provide a denser and harder crumb structure, hampering the absorption of *in vitro* digestive fluids. Lower liquid absorption would be related with lower disruption because the contact between digestive fluids and bread is reduced (Bornhorst & Singh, 2013). Therefore, softening, produced by the liquid permeation, pepsin action or the acidic conditions, influenced by bread structure, affected bolus particle size during gastric phase, and a restructuration was taking place.

The digestion of starchy foods can be further investigated through the analysis of intestinal starch hydrolysis. Although there is some starch digestion in the oral phase due to salivary α -amylase, starch is mainly digested in the intestine by pancreatic enzymes. At that stage, α -amylase digests bread samples, reducing bolus particle size, and likewise, affecting starch gel structure, yielding differences after intestinal digestion.

To further investigate the effect of structure on starch digestion, different starches from cereals, tubers and pulses were analyzed. The use of model food systems like starch gels, allows us examining the role of starch on structure and digestion of starchy foods, eliminating the impact of other components. Different starch gels from several sources were analyzed by SEM after lyophilization, showing different structures. Gels displayed an irregular structure with cavities, and the area of these cavities and the thickness of their walls were measured through image analysis. Wall thickness were similar among cereal starch gels, while there was different distribution of tuber and pulse gels. Regarding the hole area of gels cavities, rice starch showed the highest area, probably due to the lower amylose content, as was described by other authors (Biduski et al., 2018; Jiamjariyatam et al., 2015). As was expected, gel structure affected starch digestibility. The kinetic constant (k), which represents the rate of starch hydrolysis, was positively correlated with the area of gel cavities. Furthermore, wall thickness of gel cavities showed a positive correlation with the digestion time to reach the 50% of the total starch digestion. As was previously described for bread samples, bigger cavities in the structure of the sample were related with greater digestibility, because the enzymatic fluid have better access. Also, amylose had a significant effect on starch hydrolysis, specifically a negative relationship was established between the kinetic constant (k) with the amylose content and the amylose chain size. Other authors have described the control of starch digestion rate by amylose content and chain length distribution (Yu et al., 2018). Perhaps, the effect of amylose on starch digestion could be related with the modification of gel structure, and particularly with the wall thickness, but that hypothesis remains to be explored.

To deepen in the study of starch gel structure and its effect on starch hydrolysis, corn gels were prepared in the presence of phenolic acid. Xu et al. (2021) suggested

the interaction of phenolic acids with starch, even as a way to modify starch. When corn starch was gelatinized in the presence of phenolic acids, differences in both wall thickness and area of gel cavities were observed. The addition of phenolics caused a decrease in the pH of the medium, and consequently affected gel structure. However, it cannot be known if this modification is caused by the phenolic acids or the acidification of the medium. For this reason, pH was fitted to eliminate this interference, and to correctly check the effect of phenolic acids on the structure of corn starch gels. Under these conditions, both area of cavities and wall thickness of gels were bigger than in the absence of acids. This evidence was clear also in the study published by Chen et al. (2020), where the influence of different tea polyphenols concentrations on rice starch gels was analyzed. The starch-phenolic acid interaction through hydrogen bonds can interfere with polymer chains alignment and entanglement, and therefore, affect gel structure. In fact, statistical analysis indicated that the greater phenolic retention, the biggest cavities, and wall thickness of starch gels. Surprisingly, these structural changes did not affect starch gel firmness. It was the acidic pH which decrease gel firmness, maybe due to the degradation of amylose, affecting retrogradation (Wang et al., 2003). Considering the effect of structure on starch digestion, it was expected that the modification of the structure by phenolic acids affected their digestion too. But a correlation between structure and starch hydrolysis parameters was not observed. In order to understand the role of phenolic acid properties on starch digestion parameters, a principal component analysis was carried out. It was noted the effect of phenolic properties like the pK_a , polar surface area, water solubility or structure on starch hydrolysis. Therefore, phenolic acids governed *in vitro* starch digestion, and not the gel structural changes.

Focusing on the analysis of starch digestibility, fitting the starch hydrolysis curves was attempted. Mathematical modeling of *in vitro* starch digestion curves is important to understand the relationship between structure and digestibility. First-order kinetics-based model offers this quantitative relationship between starch structure and starch digestibility (Yu et al., 2021). All the cereal, tuber and pulse starch gels were satisfactorily fitted with the proposed equation except for rice starch probably due to its low amylose content, underlining again the importance of amylose on starch digestibility.

Once confirmed the effect of structural and chemical properties of starch on its digestibility, the inclusion of other components to modulate starch hydrolysis was evaluated. Due to the diverse experimental conditions reported in the literature to measure the inhibition capacity of polyphenols against α -amylase and α -glucosidase, pure phenolic acids were selected, and different experimental conditions were tried. The preincubation of phenolic acids with porcine pancreatic α -amylase was the most effective way to inhibit the enzymes, and also, the most used methodology to analyze the inhibition activity of a compound or an extract. Although it encourages the inhibition,

other scenarios should also be considered. When an enriched food with polyphenols is ingested, starch is previously in contact with the phenolic compound, and finally with the enzyme; thus, usual experimental conditions do not reflect the physiological ones. In those conditions, lower inhibition capacity was registered by pure phenolic acids. While starch can interact with phenolic acids, these compounds have greater affinity for the enzymes (Giuberti et al., 2020). In fact, inhibition is based on the formation of hydrogen bonds between hydroxyl groups of polyphenols and the active site of the enzyme (Sun et al., 2019). Concerning fungal α -glucosidase inhibition, there were no differences between these two methods (preincubation of phenolics with the enzyme or the substrate) except for syringic and vanillic acid, maybe explained by their different molecular dipole/dipole momentum. On the other hand, the gelatinization of starch with phenolic acids also reduced their inhibition capacity. Actually, 10% of phenolic acids content was retained within the gelatinized starch. When wheat starch gels were prepared in the presence of phenolic acids to analyze their structure, the retention was greater. This was largely due to the highest starch concentration (almost 20 times greater), forming a solid gel and thus a major retention (20-30%). The complex formation between starches and polyphenols have been previously studied. On the molecular level, these interactions could be V-type inclusion complex or non-inclusion complex. V-type inclusion complex is characterized by the encapsulation of the polyphenol within the inner hydrophobic helix of the starch (Deng et al., 2021). While the non-inclusion complex resulted in the interaction between starch and hydroxyl and carbonyl groups of phenolic compounds, forming intermolecular aggregates (Deng et al., 2021). When starch is gelatinized in the presence of phenolic acids, the formation of inclusion complexes should be discarded, because a different treatment is needed such as a thermomechanical or coprecipitation method (Liu et al., 2019; Van Hung et al., 2013). Similar studies that boiled phenolic acids with starch, did not reported evidence for the formation of an inclusion complex (Igoumenidis et al., 2018). Therefore, the formation of non-inclusion complexes was expected.

To analyze the effect of these reported methodologies on a more complex matrix, seaweed extracts were selected as a polyphenol source. Seaweed extract consumption has been shown to reduce blood glucose levels *in vivo* (Iwai, 2008; Kang et al., 2013). Even seaweed capsules ingestion decreased the glycemic response to white bread in healthy volunteers (Goñi et al., 2002). Therefore, introducing seaweeds as ingredients might improve the glycemic response. Several *in vitro* studies analyzed the α -amylase and α -glucosidase inhibitory effects of seaweed extracts. Different extraction methodologies have been carried out using mainly water, methanol, acetone, or chloroform, getting extracts with different components like peptides, polysaccharides, or polyphenols. Water is considered in many cases as a green extraction solvent (Castro-Puyana et al., 2017), thus it was the election solvent for the extraction of polyphenolic extracts from

ultrasound-assisted extraction of *Ascophyllum nodosum*. The inhibitory capacity of *A. nodosum* extracts against α -amylase and α -glucosidase showed similar tendency as the previously mentioned for pure phenolic acids. α -glucosidase inhibition was slightly improved when the seaweed extracts were preincubated with the enzyme instead of the substrate. A similar situation happened with the α -amylase inhibition, but higher concentration was required to inhibit the enzyme when the starch was gelatinized in the presence of the extracts. The concentration to inhibit 50% of the enzyme activity was nearly 10 times greater than those required for the other preincubation methods tested. However, it should be noted that the inhibitory activity of *A. nodosum* extracts, particularly the purified one, was remarkable. Actually, seaweed extracts showed higher inhibition capacity than the commercial pure phenolic compounds previously analyzed. Results obtained by proton nuclear magnetic resonance spectroscopy ($^1\text{H-NMR}$) indicated that the greater inhibition of the purified extract could be explained by the presence of not complexed polyphenols, and therefore the interaction with the enzyme was facilitated. Moreover, seaweed extracts are characterized by the presence of several phenolic compounds, and therefore a synergistic effect could increase their inhibition ability (Gao et al., 2013).

References

- Biduski, B., Silva, W. M. F. d., Colussi, R., Halal, S. L. d. M. E., Lim, L.-T., Dias, Á. R. G., & Zavareze, E. d. R. (2018). Starch hydrogels: The influence of the amylose content and gelatinization method. *International Journal of Biological Macromolecules*, *113*, 443-449.
- Blanquet-Diot, S., François, O., Denis, S., Hennequin, M., & Peyron, M. A. (2021). Importance of oral phase in *in vitro* starch digestibility related to wholegrain versus refined pastas and mastication impairment. *Food Hydrocolloids*, *112*, 106277.
- Bornhorst, G. M., & Singh, R. P. (2013). Kinetics of in Vitro Bread Bolus Digestion with Varying Oral and Gastric Digestion Parameters. *Food Biophysics*, *8*(1), 50-59.
- Castro-Puyana, M., Marina, M. L., & Plaza, M. (2017). Water as green extraction solvent: Principles and reasons for its use. *Current Opinion in Green and Sustainable Chemistry*, *5*, 31-36.
- Chen, N., Chen, L., Gao, H.-X., & Zeng, W.-C. (2020). Mechanism of bridging and interfering effects of tea polyphenols on starch molecules. *Journal of Food Processing and Preservation*, *44*(8), e14576.
- Deng, N., Deng, Z., Tang, C., Liu, C., Luo, S., Chen, T., & Hu, X. (2021). Formation, structure and properties of the starch-polyphenol inclusion complex: A review. *Trends in Food Science & Technology*, *112*, 667-675.

Gao, J., Lin, S., Jin, X., Wang, Y., Ying, J., Dong, Z., & Zhou, W. (2019). In vitro digestion of bread: How is it influenced by the bolus characteristics? *Journal of Texture Studies*, 50(3), 257-268.

Gao, J., Tay, S. L., Koh, A. H.-S., & Zhou, W. (2018). Dough and bread making from high- and low-protein flours by vacuum mixing: Part 3. Oral processing of bread. *Journal of Cereal Science*, 79, 408-417.

Gao, J., Xu, P., Wang, Y., Wang, Y., & Hochstetter, D. (2013). Combined Effects of Green Tea Extracts, Green Tea Polyphenols or Epigallocatechin Gallate with Acarbose on Inhibition against α -Amylase and α -Glucosidase in Vitro. *Molecules*, 18(9), 11614-11623.

Gao, J., & Zhou, W. (2021). Oral processing of bread: Implications of designing healthier bread products. *Trends in Food Science & Technology*, 112, 720-734.

Giuberti, G., Rocchetti, G., & Lucini, L. (2020). Interactions between phenolic compounds, amylolytic enzymes and starch: an updated overview. *Current Opinion in Food Science*, 31, 102-113.

Goñi, I., Valdivieso, L., & Gudiel-Urbano, M. (2002). Capacity of edible seaweeds to modify *in vitro* starch digestibility of wheat bread. *Nahrung-Food*, 46(1), 18-20.

Guo, Q., Ye, A., Singh, H., & Rousseau, D. (2020). Deconstructing and restructuring of foods during gastric digestion. *Comprehensive Reviews in Food Science and Food Safety*, 19(4), 1658-1679.

Igoumenidis, P. E., Zoumpoulakis, P., & Karathanos, V. T. (2018). Physicochemical interactions between rice starch and caffeic acid during boiling. *Food Research International*, 109, 589-595.

Iwai, K. (2008). Antidiabetic and antioxidant effects of polyphenols in brown alga *Ecklonia stolonifera* in genetically diabetic KK-A y mice. *Plant Foods for Human Nutrition*, 63(4), 163.

Jiamjariyatam, R., Kongpensook, V., & Pradipasena, P. (2015). Effects of amylose content, cooling rate and aging time on properties and characteristics of rice starch gels and puffed products. *Journal of Cereal Science*, 61, 16-25.

Kang, M.-C., Wijesinghe, W., Lee, S.-H., Kang, S.-M., Ko, S.-C., Yang, X., Kang, N., Jeon, B.-T., Kim, J., & Lee, D.-H. (2013). Dieckol isolated from brown seaweed *Ecklonia cava attenuates* type II diabetes in db/db mouse model. *Food and Chemical Toxicology*, 53, 294-298.

Liu, Y., Chen, L., Xu, H., Liang, Y., & Zheng, B. (2019). Understanding the digestibility of rice starch-gallic acid complexes formed by high pressure homogenization. *International Journal of Biological Macromolecules*, 134, 856-863.

Minekus, M., Alminger, M., Alvito, P., Ballance, S., Bohn, T., Bourlieu, C., Carrière, F., Boutrou, R., Corredig, M., & Dupont, D. (2014). A standardised static *in vitro* digestion method suitable for food—an international consensus. *Food & Function*, 5(6), 1113-1124.

Pentikäinen, S., Sozer, N., Närväinen, J., Ylätaalo, S., Teppola, P., Jurvelin, J., Holopainen-Mantila, U., Törrönen, R., Aura, A.-M., & Poutanen, K. (2014). Effects of wheat and rye bread structure on mastication process and bolus properties. *Food Research International*, 66, 356-364.

Puerta, P., Garzón, R., Rosell, C. M., Fiszman, S., Laguna, L., & Tárrega, A. (2021). Modifying gluten-free bread's structure using different baking conditions: Impact on oral processing and texture perception. *LWT- Food Science and Technology*, 140, 110718.

Sun, L., Warren, F. J., & Gidley, M. J. (2019). Natural products for glycaemic control: Polyphenols as inhibitors of alpha-amylase. *Trends in Food Science & Technology*, 91, 262-273.

Van Hung, P., Phat, N. H., & Phi, N. T. L. (2013). Physicochemical properties and antioxidant capacity of debranched starch–ferulic acid complexes. *Starch-Stärke*, 65 (5-6), 382-389.

Wada, S., Goto, T., Fujimoto, K., Watanabe, M., Nagao, K., Nakamichi, A., & Ichikawa, T. (2017). Changes in food bolus texture during mastication. *Journal of Texture Studies*, 48(2), 171-177.

Wang, Y.-J., Truong, V.-D., & Wang, L. (2003). Structures and rheological properties of corn starch as affected by acid hydrolysis. *Carbohydrate Polymers*, 52(3), 327-333.

Xu, T., Li, X., Ji, S., Zhong, Y., Simal-Gandara, J., Capanoglu, E., Xiao, J., & Lu, B. (2021). Starch modification with phenolics: methods, physicochemical property alteration, and mechanisms of glycaemic control. *Trends in Food Science & Technology*, 111, 12-26.

Yu, W., Tao, K., & Gilbert, R. G. (2018). Improved methodology for analyzing relations between starch digestion kinetics and molecular structure. *Food Chemistry*, 264, 284-292.

Yu, W., Zhou, X., & Li, C. (2021). Application of first-order kinetics modeling to reveal the nature of starch digestion characteristics. *Food & Function*, 12(15), 6652-6663.



V Conclusions

Starch digestion requires enzymes access to the substrate and its subsequent enzymatic hydrolysis. Research conducted through the different chapters is conclusive about the importance of crumb or gel microstructure on the modulation of *in vitro* starch digestion, through controlling the accessibility of the digestive enzymes (α -amylase, α -glucosidase). Likewise, starch digestion could be controlled by inhibiting digestive enzymes with phenolic compounds, although their absorption to starch reduces their inhibitory ability.

The following concluding remarks can be highlighted:

- Low moisture breads were instrumentally differentiated according to their texture and structure characteristics. These differences dominated FOP results, requiring diverse mastication efforts to swallow bread boluses, and affecting bolus texture. Nevertheless, the sensorial perception of panelists did not detect differences between them. Reducing the impact of bread water has allowed underlining the effect of bread texture and structure on mastication behavior and bolus properties.
- Modification of breadmaking, specifically dough shaping, resulted in bread crumbs with different structures, affecting their texture and morphology. Breads with higher porosity but smaller porous areas were more affected by enzymes, showing higher starch digestibility. The oral processing method used during *in vitro* digestion analysis impacted starch hydrolysis results, and therefore it should be carefully selected.
- Starch gels from different sources showed different microstructures, that affected *in vitro* starch gel digestion. Cereals showed smaller cavities than tubers and pulses, having lower *in vitro* starch digestion. Kinetics of starch hydrolysis during intestinal digestion were acceptably reproduced by the first-order kinetics model, except for rice starch gels, maybe due to its low amylose content.
- The inhibition activity of phenolic compounds was different depending on their previous interaction with the substrate, which increased the concentration to inhibit 50% of the α -amylase but did not change α -glucosidase inhibition. The phenolic

acid structure influenced α -amylase inhibition, and hydroxyl groups played an important role in the interaction with the enzyme or the substrate.

- The inhibition capacity of polyphenolic extracts from *A. nodosum* seaweed against α -amylase and α -glucosidase enzymes was significant. Seaweed extracts were more effective against enzymes when they prior interacted with them. The presence of carbohydrate-polyphenols complexes reduced the inhibitory capacity of the extracts, particularly in α -amylase inhibition.

- Phenolic acids influenced the pasting properties of starch gels and their resulting microstructure and firmness, which was partially due to the pH decrease. Nevertheless, those changes in the gels' microstructure were not sufficient to explain the inhibitory ability of phenolic acids against starch digestive enzymes. The specific properties, like chemical structure, of the phenolic acids were responsible for reducing the extent of *in vitro* starch digestion of gels containing phenolic acids.



V Conclusiones

La digestión del almidón requiere que las enzimas tengan acceso al sustrato y posteriormente se produzca la hidrólisis enzimática. La investigación realizada a través de los diferentes capítulos es concluyente sobre la importancia de la microestructura del pan o de los geles en la modulación de la digestión *in vitro* del almidón, mediante el control de la accesibilidad de las enzimas digestivas (α -amilasa y α -glucosidasa). Del mismo modo, la digestión del almidón podría controlarse inhibiendo las enzimas digestivas con compuestos fenólicos, aunque su absorción al almidón reduce su capacidad inhibitoria.

Se pueden destacar las siguientes observaciones finales:

- Los panes con baja humedad se diferenciaron instrumentalmente de acuerdo con sus características texturales y estructurales. Estas diferencias dominaron los resultados de procesamiento oral de los alimentos (FOP), requiriendo esfuerzos de masticación diferentes para tragar los bolos de pan y afectando a la textura del bolo. Sin embargo, la percepción sensorial de los panelistas no detectó diferencias entre ellos. La reducción del impacto de la humedad del pan permitió subrayar el efecto de la textura y estructura del pan sobre el comportamiento de la masticación y las propiedades del bolo.

- La modificación en la panificación, específicamente en el formado del pan, resultó en panes con una estructura de miga diferente, afectando a la textura y morfología. Los panes con una mayor porosidad, pero unas áreas de poro más pequeñas se vieron más afectados por las enzimas, mostrando una mayor digestibilidad del almidón. El método de procesamiento oral utilizado durante el análisis de la digestión *in vitro* afectó a los resultados de hidrólisis del almidón y, por tanto, debe seleccionarse cuidadosamente.

- Los geles de almidón de distintas fuentes mostraron diferentes microestructuras que afectaron a su digestión *in vitro*. Los geles de cereales presentaron cavidades más pequeñas que los de tubérculos y legumbres, mostrando una menor digestión

in vitro del almidón. La cinética de hidrólisis del almidón durante la digestión intestinal se reprodujo adecuadamente mediante el modelo de cinética de primer orden, excepto para los geles de almidón de arroz, tal vez debido a su bajo contenido en amilosa.

- La actividad de inhibición de los compuestos fenólicos fue diferente dependiendo de su interacción previa con el sustrato, aumentando la concentración necesaria para inhibir el 50% de la α -amilasa, pero no modificó la inhibición de la α -glucosidasa. La estructura del ácido fenólico influyó en la inhibición de la α -amilasa, y los grupos hidroxilo desempeñaron un papel significativo en la interacción con la enzima o el sustrato.

- La capacidad de inhibición de los extractos polifenólicos del alga *A. nodosum* frente a las enzimas α -amilasa y α -glucosidasa fue significativa. Los extractos de algas marinas fueron más efectivos contra las enzimas cuando interactuaron previamente con ellas. La presencia de complejos carbohidrato-polifenol redujo la capacidad inhibitoria de los extractos, principalmente en la inhibición de la α -amilasa.

- Los ácidos fenólicos influyeron en las propiedades de pegado de los geles de almidón, en su microestructura y en su firmeza, debido en parte a la disminución del pH. Sin embargo, esos cambios en la microestructura de los geles no fueron suficientes para explicar la capacidad inhibitoria de los ácidos fenólicos frente a las enzimas que digieren el almidón. Las propiedades específicas de los ácidos fenólicos, como su estructura química, fueron las responsables de reducir el grado de digestión *in vitro* de los geles de almidón con ácido fenólicos.



LIST OF PUBLICATIONS

The present thesis is based in the following publications:

Aleixandre, A., Benavent-Gil, Y., & Rosell, C. M. Effect of bread structure and *in vitro* oral processing methods in bolus disintegration and glycemic index. (2019). *Nutrients*, 11(9), 2105.

Aleixandre, A., Benavent-Gil, Y., Velickova, E., & Rosell, C. M. Mastication of crisp bread: Role of bread texture and structure on texture perception. (2021). *Food Research International*, 147, 110477.

Aleixandre, A., Benavent-Gil, Y., Moreira, R., & Rosell, C. M. *In vitro* digestibility of gels from different starches: Relationship between kinetic parameters and microstructure. (2021). *Food Hydrocolloids*, 120, 106909.

Aleixandre, A., Gil, J. V., Sineiro, J., & Rosell, C. M. Understanding phenolic acids inhibition of α -amylase and α -glucosidase and influence of reaction conditions. (2021). *Food Chemistry*, 131231.

Aleixandre, A., Gisbert, M., Sineiro, J., Moreira, R., & Rosell, C. M. *In vitro* inhibition of starch digestive enzymes by ultrasound-assisted extracted polyphenols from *Ascophylum nodosum* seaweeds. *Submitted to journal*.

Aleixandre, A., & Rosell, C. M. Starch gels enriched with phenolic acids: effects on structure and digestibility. *Submitted to journal*.

